The effect of 5-Hydroxytryptamine (5-HT) on neurogenic niches in brainstem and spinal cord region

Nurhafizah binti Ghani

Submitted in accordance with the requirements for the degree of
Doctor of Philosophy

The University of Leeds
School of Biomedical Sciences

December 2021

Intellectual properties

The candidate confirms that the work submitted is his/her own and that appropriate credit has been given where reference has been made to the work of others

.

Acknowledgements

First and foremost I would like to express my deepest thanks and appreciation to my supervisor Professor Susan Deuchars who has provided endless guidance, assistance, kindness and motivation throughout my 4 years study in the UK. A very special thanks to my co supervisor, Professor Jim Deuchars for guidance and advice throughout my study.

My work couldn't have been completed without the support and teaching from Brenda Fraters, Lucy Peers and Dr Nadira Yuldasheva. My appreciation also goes to Kak Nazlah, Norah, Kaisan, Hanan, Lauryn and Pierce who helped me with any technical issues. I highly appreciated the help and friendship of Christian, Catherine, Emily, Claudia, Jess, Aaron and Beatrice.

My love and big hugs to my beloved husband, Ariff for his patience and endless support, my sons, Amsyar and Amirul for being there next to me in hardship and joy. My gratitude to parents, Ghani and Serimpas, my parents-in-law, Zakaria and Che Zawiah for being caring and supportive, even when we are in thousands of miles apart. My appreciation also goes to my siblings, siblings-in-law and all my friends here.

I would like to acknowledge Universiti Sains Malaysia and Ministry of Higher Education Malaysia for providing my PhD funding.

It has been a great experience in my life to study and live here and I owe all of you a sincere thanks from the bottom of my heart.

Abstract

Neurogenesis is the differentiation of neural stem cells into neurones, astrocytes and oligodendrocytes. There is evidence for postnatal neurogenesis in the brainstem and central canal area of the spinal cord. We therefore sought to determine the relationship between 5-HTergic fibres and neural stem cells using nestin-GFP mice and whether modulation of 5-HTergic signalling can influence neurogenesis in the spinal cord and brainstem. In nestin-GFP mice, 5-HTergic fibres formed close proximity with nestin-positive cells in brainstem and spinal cord suggesting that 5-HT may modulate the stem cells. Administration of the 5-HT uptake inhibitor, fluoxetine hydrochloride (flx, 10 mg/kg) promoted greater numbers of proliferating cells in dentate gyrus (DG) of hippocampus (used as a positive control), dorsal vagal complex, raphe nuclei and inferior olives of brainstem and gray matter in thoracic spinal cord. Nevertheless, the proportion of new cells that became astrocytes, oligodendrocytes and neurones were not significant. To determine which 5-HT receptor was involved, *in vitro* experiments revealed that slices treated with cisapride (5-HT4 agonist) had higher numbers of proliferating cells in central canal of spinal cord, while slices treated with another 5-HT4 partial agonist tegaserod maleate had lower numbers compared with control slices. *In vivo,* animals treated with tegaserod had significantly fewer proliferating cells in DG of hippocampus, NTS and ECL of brainstem and selected areas in spinal cord, compared to control. However, there were no significant differences in the proportions of proliferating cells also exhibiting markers for neurones, oligodendrocytes or astrocytes in hippocampus, brainstem and spinal cord

The effects of flx on neurogenesis in animals on high-fat diet was determined, administration of 166 mg/L of flx in drinking water was not able to affect cell proliferation in the hippocampus, selected regions and thoracic spinal cord. Moreover, it did not influence cell differentiation. For metabolic changes, flx did not improve the fasting blood glucose level and did not reverse the increased bodyweight.

In conclusion, this indicated the influence of endogenous 5-HT in promoting high levels of cell proliferation since flx blocks 5-HT transporters, increasing 5-HT levels in the synaptic cleft.

Table of Contents

List of Figures

List of Tables

Abbreviations

%	Percentage
µl	Microliter
µm	Micrometer
µM	MicroMolar
3Rs	Replacement, Reduction and Refinement.
5-CT	5-Carboxamidotryptamine
5-HT	5-Hydroxytryptamine
5-HT-IR	5-HT-Immunoreactive
5-HTRs	5-HT Receptors
5-MeO-DMT	5-Methoxy-N,N-Dimethyltryptamine
8-OH-DPAT	8-Hydroxy-2-(Di-N-Propylamino)Tetralin
aCSF	Artificial Cerebrospinal Fluid
AP	Area Postrema
BDNF	Brain-Derived Neurotrophic Factor
BLBP	Brain Lipid-Binding Protein
BrdU	5-Bromo-2'-Deoxyuridine
CBS	Central Biological Services
CC	Central Canal
CSF	Cerebrospinal Fluid
CSFCc	Cerebrospinal Fluid Contacting Cells
CVO	Circumventricular Organ
DAPI	4′,6-Diamidino-2-Phenylindole
DCX	Doublecortin
dDG	Dorsal Dentate Gyrus

DG	Dentate Gyrus
DH	Dorsal Horn
DMSO	Dimethyl Sulfoxide
DMX	Dorsal Vagal Motor Nucleus
DNA	Deoxyribonucleic Acid
DVC	Dorsal Vagal Complex
EC	Ependymal Cells
ECL	Ependymal Cell Layer
EdU	5-Ethynyl-2'-Deoxyuridine
ELISA	Enzyme-Linked Immunosorbent Assay
Flx	Fluoxetine
GFAP	Glial Fibrillary Acidic Protein
GFP	Green Fluorescent Protein
GIT	Gastrointestinal System
gm	Gram
GM	Gray Matter
GRK	G-Couple Protein Receptor Kinases
GTT	Glucose Tolerance Test
HF	High-Fat Diet
i.p	Intraperitoneal
IML	Intermediolateral Cell Column
IO	Inferior Olives
IPC	Intermediate Progenitor Cells
ITT	Insulin Tolerance Test
LF	Low-Fat Diet
M	Molar
mg/kg	Milligram/Kilogram
ml	Mililiter

mM	Milimolar
MR	Median Raphe
MS	Multiple Sclerosis
N	Numbers of animals
n	Numbers of sections
NaCl	Normal Saline (Sodium Chloride)
NPC	Neural Progenitor Cell
NSPC	Neural Stem/Progenitor Cells
NTS	Nucleus Tractus Solitarius
PB	Phosphate Buffer
PBS	Phosphate Buffered Saline
PFA	Paraformaldehyde
pK_i	Binding Affinity
PSA-NCAM	Polysialylated-Neural Cell Adhesion
ROI	Regions of Interest
SCI	Spinal Cord Injury
SEM	Standard Error of Mean
SGZ	Subgranular Zone
SSRI	Selective Serotonin Reuptake Inhibitor
SVZ	Subventricular Zone
TBI	Traumatic Brain Injury
TrkB	Tropomyosin Receptor Kinase
WHO	World Health Organisation
WM	White Matter
α-methyl-5HT-maleate	Alpha-Methyl-5-Hydroxytryptamine-Maleate

Chapter 1

GENERAL INTRODUCTION

1.1 Introduction

The adult nervous system was originally thought to be stable in terms of no generation of new neurons in the brain. This was based on a study using radiolabelling showed that tritium-labelled thymidine (which would be taken up by dividing cells) injected into adult rhesus monkey brain was not found in neurones, even after six years post-injection (Rakic, 1985). However, as far back as the 1960s, using similar thymidine incorporation studies, Altman and Das (1965) had observed new cells in the adult dentate gyrus in rats and over recent years, it was proven that adult brains showed more regenerative potential than previously thought in terms of neurogenesis and neural plasticity (Eriksson *et al.*, 1998, Eriksson, 2003). This has led to a resurgence of interest in harnessing or enhancing adult neurogenesis in treating conditions where neurones are lost, such as Alzheimer's disease (Llorens-Martín, 2018). It appears that there are two main neurogenic niches in the brain, the dentate gyrus of the hippocampus and the subventricular zone (Lledo *et al.*, 2006) but neural stem cells exist in other regions such as the brainstem and spinal cord, and it is these regions that are of interest here.

It is also necessary to consider new approaches to reverse damage to, and loss of other critical cells such as astrocytes and oligodendrocytes. Most current treatments for many conditions such as multiple sclerosis or spinal cord injury tend to focus on reducing inflammation or increasing plasticity in existing circuits. However, as our knowledge of the regenerative capacity of the central nervous system changes, this may be an important therapeutic avenue to consider, since neurogenesis also covers production of

these glial cells. Therefore, research into the recruitment of adult neural stem cells through neurogenesis is significant to improve the mode of treatment and management of the neuronal-related problems.

One way in which this is possible is by intrinsic or extrinsic modulation of the neural stem cells to trigger them to proliferate and differentiate into the cells that are required, for example neurones or oligodendrocytes to help with remyelination.

There is a growing volume of research considering the importance of 5-hydroxytryptamine (5-HT, also known as serotonin) in the modulation of neurogenesis in the brain neurogenic niches. 5-HT is produced in the raphe nuclei of the brainstem (Palkovits *et al.*, 1974) and these neurones send projections throughout the central nervous system by forming ramifications and anastomosis plexi (Takeuchi *et al.*, 1983).

To date, there is little known about how the spinal cord and brainstem neurogenic niches can be modulated by 5-HT in order to produce new neurones, oligodendrocytes or astrocytes, yet this could be an important therapeutic avenue in aid in recording after brain or spinal cord injury or in situations such as MS. This introduction will consider neurogenesis in general then focus on what is known about the neural stem cell capacity of the brainstem and spinal cord. It will then consider factors such as 5-HT in promoting neurogenesis and whether such factors can be harnessed to restore function.

1.2 Neurogenesis

1.2.1 Neurogenesis in established neurogenic niches of the brain

Neurogenesis is a process by which new neurons are formed whereas neural plasticity is the ability of neural circuits to undergo changes in the function or organisation due to its previous activity. Both neurogenesis and neural plasticity occur in the foetal and adult brain, but these are more pronounced in foetal brains (Eriksson, 2003). In most parts of

the brain, neurogenesis only occurs during intrauterine life. However, it was shown that this process persists in some parts of the brains of certain species throughout the postnatal and adult period. Researchers have studied neurogenesis using a technique that exploits the mechanism of incorporation of nucleosides into newly synthesised DNA of dividing cells during the S phase of the cell cycle. Thymidine analogues such as 5-bromo-2'-deoxyuridine (BrdU) or 5-Ethynyl-2′-deoxyuridine (EdU) can be injected into animals or added to cultures to label proliferating cells, although this does not differentiate between cell types.

Therefore, to consider generation of new neurones, BrdU or EdU labelling is often accompanied with immunolabelling using antibodies for immature neurones. The two prominent brain regions that have been identified to be neurogenic in adult rodents (and indeed in other animals such as adult primates) are the subventricular zone (SVZ) and the subgranular zone (SGZ) of the hippocampal dentate gyrus (Seaberg and van der Kooy, 2002). In the SVZ, the newly formed neuroblasts migrate along the rostral migratory stream to the olfactory bulb where they become integrated into the local circuitry, many becoming GABAergic interneurons or glomerular cells (Lledo *et al.*, 2006). A study on post-mortem tissue of adult human hippocampus also proved that neurogenesis persists throughout human life (Eriksson *et al.*, 1998). Other regions have also been considered as having neurogenic potential, for example, Gould *et al.* (2001) reported the presence of new cells with neuronal characteristics in the neocortex of adult rats and macaques but with lower rates of proliferation compared to the dentate gyrus. Furthermore, in the amygdala of adult primates, cells labelled with BrdU and also for markers of new neurons, such as β-tubulin-III were reported (Bernier *et al.*, 2002). However, for both of these studies, it was suggested that the origin of these cells was the SVZ and that different migratory streams may exist for these to follow to their final destination. This suggests therefore that rather than proliferation occurring throughout the neuroaxis, there are specific niches where higher levels of neurogenesis occur.

In these brain niches, neurogenesis has different phases - precursor phase, early survival phase, early post-mitotic maturation phase and a late post-mitotic maturation phase (Figure 1.1) (Kempermann *et al.*, 2015).

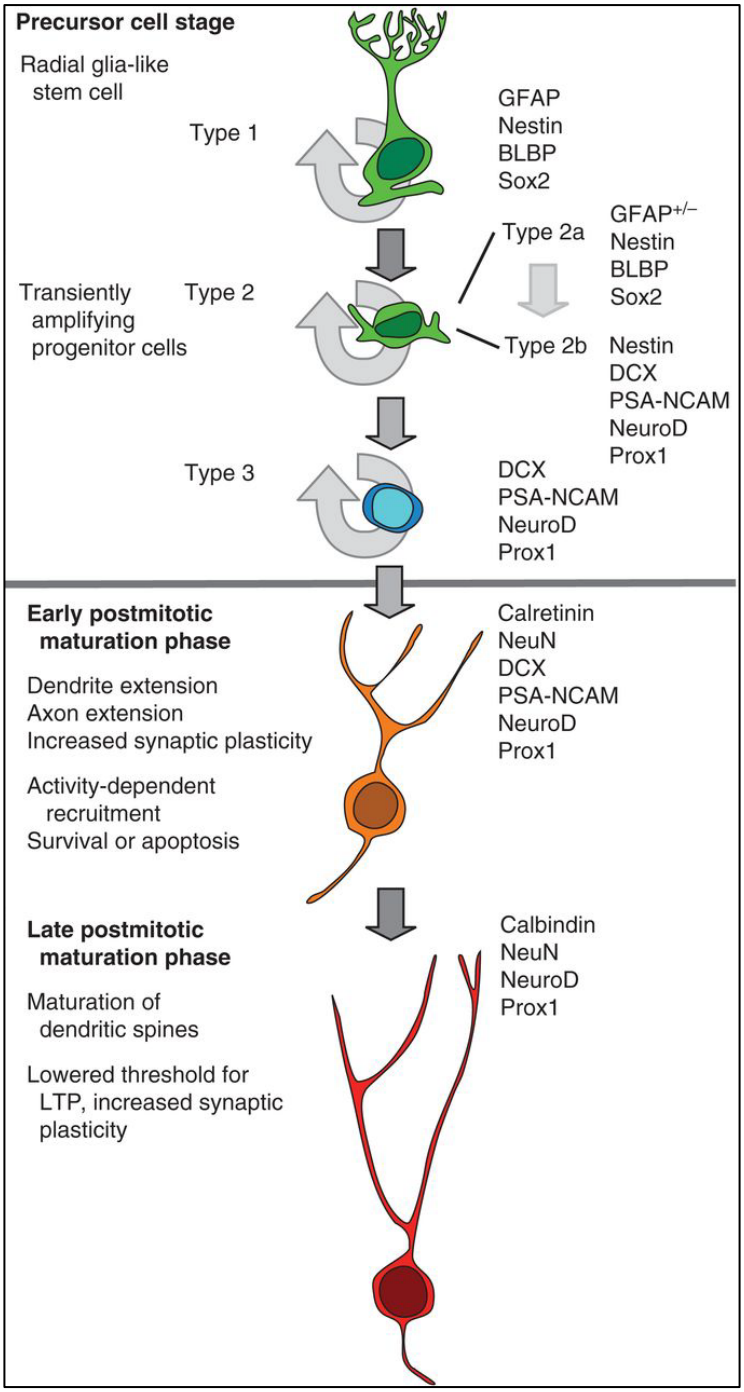

Figure 1.1 Stages of the neurogenic process in brain. A diagrammatic picture showing the stages of neurogenesis and markers expressed at every stage. Adapted from (Kempermann *et al.*, 2015).

In these stages, there are different markers expressed by cells that can be used to indicate the degree of development, although a degree of caution is needed since there is overlap in expression of these at different time periods. In the brain, neurogenesis starts from the neural progenitor cells (NPC) that have astrocytic properties. At this stage, it can be detected by nestin which is a specific marker for neural progenitor cells and glial fibrillary acidic protein (GFAP) for the glial properties.

After this stage, there are three identifiable progenitors of precursor cells that have different morphology at the earlier stage of neurogenesis. In hippocampus, Type 1 cells have one single thick process that extends into the granular layer. Then the single process branches out to become processes that extend to the inner molecular layer (Wang *et al.*, 2005). However, the Type 2 cells have a different morphology compared to the Type 1 cells. They possess short horizontal processes or lack of processes and these cells are most highly proliferative and capable of migration. The Type 2 cells can be further divided into Type 2a and Type 2b (Steiner *et al.*, 2006). Type 2a expresses cell markers, such as GFAP, nestin, brain lipid-binding protein (BLBP) and Sox2. Therefore, from the cell markers, it gives some clue regarding the type of cell these Type 2a cells are. The presence of GFAP is consistent with identification as an astrocytic cell, Sox2 shows stem cell properties, and BLBP is a radial glial marker. Therefore, the Type 2a are stem cells that have astrocytic properties. While nestin is present in both types, the Type 2b cell expresses different markers, including doublecortin (DCX), polysialylated-neural cell adhesion (PSA-NCAM), Neuro-D and Prox-1. Doublecortin (DCX) is a marker for new neurones and research on DCX shows the importance of this marker for the survival of the neurone (Rao and Shetty, 2004). PSA-NCAM is a marker for developing and migrating neurones (Quartu *et al.*, 2008). Neuro-D is important in postnatal neurogenesis with a role in the differentiation of the neurone. Miyata *et al.* (1999) found neuronal cell death in mice that were totally lacking Neuro-D. Prox-1 is important in the middle and late stages of neurogenesis. Its function is to maintain the intermediate progenitor cells (IPCs), and it is also important for granule cell maturation.

IPCs help in amplifying the division of cells and the progenitor itself (Pontious *et al.*, 2008).

The Type 3 cells do not express astrocyte-like cell markers. The cells present as a “clump cell” without any processes or extension of cytoplasmic processes. The Type 3 cells express immature neurone markers and give some clue that at this stage, they prepare themselves for proliferation and further differentiation to form mature neurones.

Therefore, the early phases of neurogenesis (precursor cell stage) are mainly for the proliferation and differentiation of the neuronal cells, and this is very important for survival of neurones and the capability to enter the next stage for maturation process. Besides that, these phases act to provide stem cell pools that are highly proliferative to increase the rate of neurogenesis (the amplification process).

The next process is the postmitotic maturation process that can be divided into early phase and late phase. This phase is mainly more on the survival of the neurone and the final maturation into functional neurones. The presence of calretinin indicates the early phase of postmitotic maturation in the neurogenic process, although it is important to note that calretinin is expressed by many groups of mature neurones in both the brain and spinal cord (Ren *et al.*, 1993, Brandt *et al.*, 2003). The cells keep growing by extension of the axon and dendrites and the formation of synapses (Kempermann *et al.*, 2015). The late postmitotic maturation phase is more on the refining process. The cells express the marker for mature neurones, calbindin (Gage *et al.*, 1995). It represents the final establishment of neurones as mature, stable and fully functioning. The estimation of whole cycle of neurogenesis may take place for about 7 weeks in humans while the estimation for rats and mice is still unknown. These markers may be useful in studies of adult neurogenesis since they help in identifying the stage of the neurogenesis cycle at which our newly born cells are found.

Most of our understanding of postnatal neurogenesis is based on these two neurogenic niches however, it is clear that there is neurogenic potential in other regions and my interest lies particularly in the brainstem and the spinal cord so I will cover these in turn.

1.2.2 Neurogenesis in brainstem

The brainstem is located in between the cerebrum and the spinal cord. It is like a ‘bridge' that brings these two regions together and where some of the ascending and descending tracts decussate. Motor and sensory neurones travel through the brainstem for relaying signals between higher centres and spinal cord. It has a crucial function since it also controls non-voluntary actions especially regulation of cardiovascular and respiratory function (Joynt, 2015). The brainstem is also associated with nuclei of all cranial nerves except the olfactory and optic nerves. Furthermore, it has important nuclei involved in sympathetic and parasympathetic autonomic function.

The brainstem consists of three main regions, from rostral to caudal, midbrain, pons and medulla oblongata. The most caudal region of the brainstem is the medulla oblongata that has a continuation with the cervical spinal cord. The dorsal medulla makes up the ventral floor of the fourth ventricle. The regions of interest in this study are mainly in medullary areas where the dorsal vagal complex area (DVC) resides.

The DVC consists of three collections of nuclei that are close to each other and located dorsomedially within the medulla oblongata - these are the nucleus tractus solitarius (NTS), area postrema (AP) and dorsal vagal motor nucleus (DMX) (Binder *et al.*, 2009). The DVC area is very complex; every level from caudal to rostral has a different position and coverage area (Figure 1.2).

Every region that forms the DVC has an important role. The NTS is a mainly comprised of sensory nuclei that primarily integrates information from visceral organs such as those

in the gastrointestinal, cardiovascular and urinary systems. A variety of different stimuli directly activate NTS neurones which in turn innervate parasympathetic preganglionic neurones, premotor autonomic centres, thalamus and limbic systems. Therefore, the NTS is a major processing station for ascending visceral information and also plays a role in autonomic reflexes (Travagli, 2009). The AP region is a circumventricular organ (CVO) that protrudes into the fourth ventricle. The region enables detection of changes in circulating chemical messengers in blood and is also responsible as a chemoreceptor zone that controls vomiting. The AP also integrates neuronal inputs from other brainstem regions and sends projections to the NTS region (D.Binder, 2009). The DMX is located ventral to the NTS and has mainly a parasympathetic vagal function innervating regions such as the gastrointestinal tract, lungs and other abdominal regions. It also receives projections from many other brain regions such as hypothalamus, NTS. The main innervation of the heart is provided by the cell bodies of the preganglionic parasympathetic neurones residing in the nucleus ambiguus (Geis and Wurster, 1980).

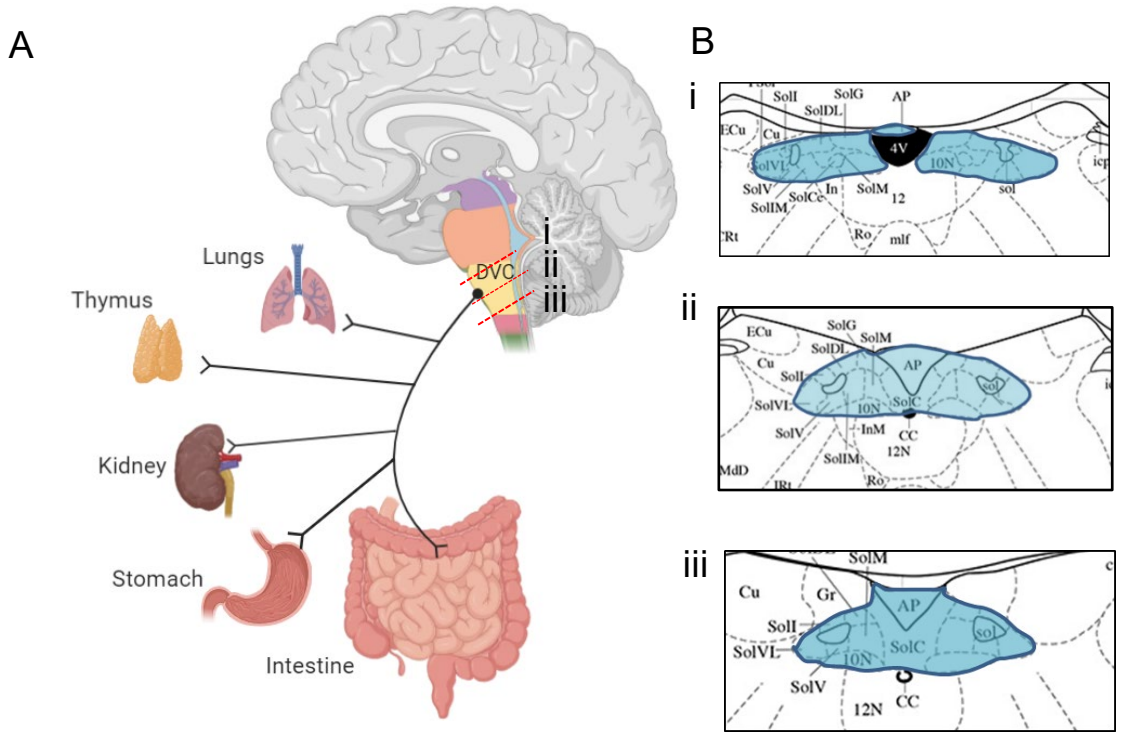

Figure 1.2 Location of dorsal vagal complex and outputs from DMX. (A) The outputs from the DMX to gastrointestinal, respiratory, system, urinary system and immune system. (Bi-iii) Cross-sections of medulla oblongata where the DVC area resides showing differences in shape and location of the 3 regions. Note that the DMX is labelled as 10N.

Neurogenesis studies in the brainstem are relatively small in number, potentially due to the extent of neurogenesis that is observed. However, it is clear that this process does exist and therefore it is important to consider where and how it occurs. The first study that was reported by Bauer *et al.* (2005) showed that, in intact brainstem, the proliferating cells were pronounced in the dorsal vagal complex area (DVC) which is comprised of the nucleus tractus solitarii (NTS), area postrema (AP) and dorsal vagal motor nucleus (DMX). Proliferating cells labelled with BrdU were seen mainly in the AP (16%) and medio-dorsal and lateral NTS (75%). Surrounding areas of the brainstem lacked any labelling. Newly generated cells differentiated equally into either neurones or astrocytes.

Thus in basal conditions, the proliferating cells were mainly in the DVC area compared to other regions in the brainstem. Further investigation was carried out by creating injury conditions by unilateral vagotomy. The injury triggered an ipsilateral increase of BrdU labelled cells and microglial proliferation in the DMX and an increase in neurones and astrocytes in the NTS. Thus, neurogenesis in the DVC can be stimulated by an injury (Bauer *et al.*, 2005).

Another study by Charrier *et al.* (2006) showed in intact rat, Ki-67^{+} labelled proliferating cells and these were given as a percentage of total cell proliferation in the different regions - 54% in NTS, 25% in AP and 21% in DMX. These percentages were considered as basal level of cell proliferation. In vagotomised rats, the number of proliferating cells was elevated at three days after the procedure and returned towards basal levels by day 7 (Charrier *et al.*, 2006). However, they did not observe whether these proliferating cells were differentiated into astrocytes, neurones or oligodendrocytes in *in vivo*. Thus there are not too many proliferation studies in this area, yet the DVC has the potential to promotes neurogenesis, so it is worth exploring the effect of 5-HT on neurogenesis in the brainstem area.

1.2.3 Neurogenesis in the spinal cord

The region of the spinal cord that is considered as the neurogenic niche is Lamina X, which surrounds the central canal and includes the dorsal and ventral gray commisures and the substantia gelatinosa centralis. Within lamina X is an area immediately adjacent to the central canal or ependymal region. The central canal is lined by simple columnar epithelial cells with cilia known as ependymal cells (EC). The ependymal region consists of several cell types with specific markers, morphology and function. The ependymal cells form the wall of the central canal of the spinal cord in a tube-like structure that contains cerebrospinal fluid. The different types of ependymal cells in central canal

indicate a capability to maintain the cell pools and withstand the mechanical forces that happen during vertebral column bending. The ependymal cells include cuboidal ependymal cells, radial ependymal cells, tanycytes, and biciliated ependymal cells (Johansson *et al.,* Meletis *et al.*, 2008). The most common type that can be seen through ultrastructural analysis is the cuboidal ependymal cell followed by tanycytes, with the least numerous being the radial ependymal cells whose morphology is similar to cuboidal ependymal cells but with the addition of a long basal process. Furthermore, these radial ependymal cells are located mainly at the dorsal and ventral poles of the ependymal layer (Figure 1.3).

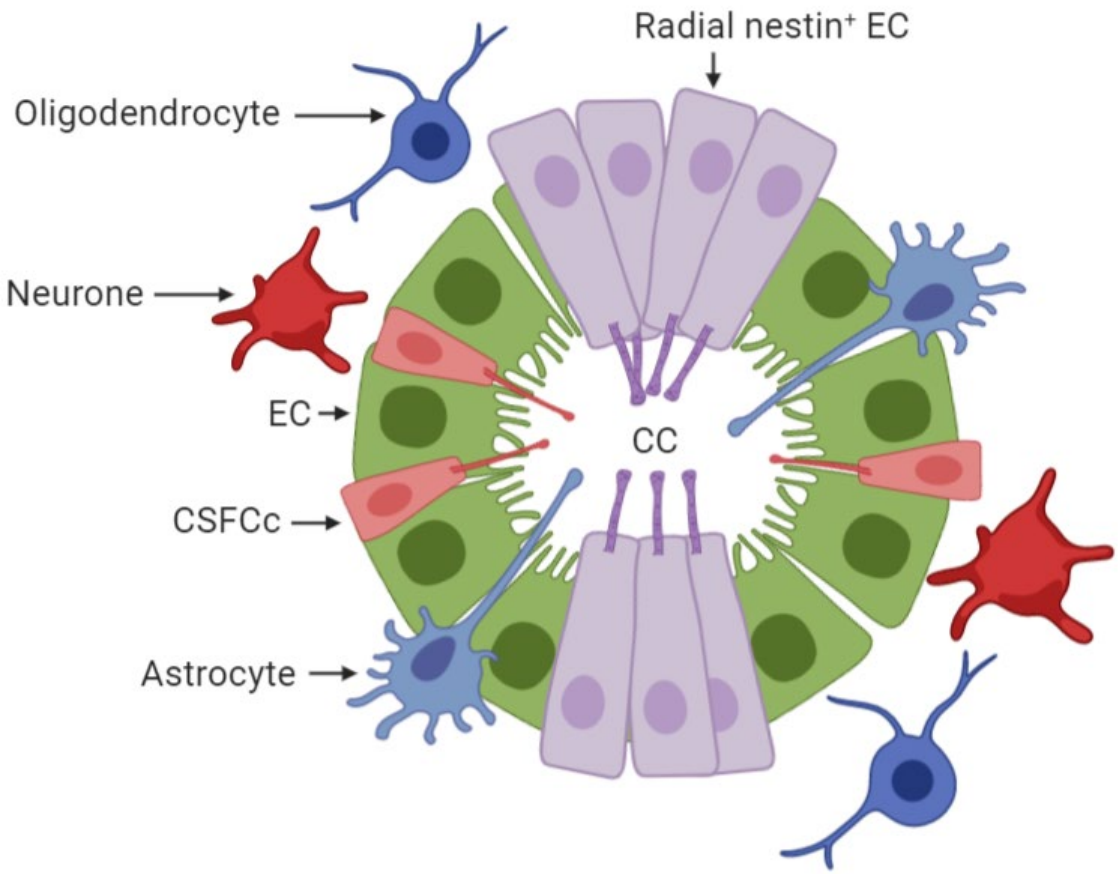

Figure 1.3 Arrangement of cells around the central canal. The epithelium that surrounds the central canal (CC) are ependymal cells (EC) with nestin$^+$ ependymal cell are located mainly at the dorsal and ventral pole. The oligodendrocytes and neurones are mainly located at subependymal layer. There also cerebrospinal fluid contacting cells (CSFCc) located in between ependymal cells. Produced using BioRender.

Neurogenesis in the spinal cord has unique characteristics. In early 80's Nornes and Carry (1978) reported the mosaic pattern of neurogenesis in the embryonic spinal cord which referred to the proliferation, migration and establishment of neurones using autoradiographic analysis. However, the research was confined to the embryonic time points when early development of the neurones occurs, showing the role that the spinal cord plays in neurogenesis. People are in doubt whether spinal cords are capable of postnatal neurogenesis despite knowing that there is a second wave of neurogenesis in the brain. Therefore, ongoing research on spinal cord postnatal neurogenesis is very crucial and important.

1.2.3.1 Evidence that ependymal cells are the neural stem cells.

There is growing evidence that ependymal cells around the central canal region may proliferate and differentiate or mature to fully functioning cells (depending on cell type) in both physiological and pathological conditions. One of the first studies cultured dissociated ependymal cells using conditions previously found to support the growth of adult neural stem cells (Johansson *et al.*, 1999). They showed that these cells formed spheroids of tightly clustered cells, which could be induced to differentiate into neurones, astrocytes and oligodendrocytes, suggesting that the ependymal cells could not only proliferate but were multipotent. Since the spinal cord does not have a defined subventricular zone, unlike the brain, this study then injected BrdU into the intact spinal cord and found that the labelled ependymal cells were mainly confined to the layer lining the central canal with few immediately outside that layer. An important study, Barnabé-Heider *et al.* (2010) concluded that the cells involved as progenitor cells are ependymal cells, astrocytes and oligodendrocytes but only ependymal cells show the ability of proliferation and differentiation to different cell types under both pathological and physiological conditions. Using transgenic mice expressing tamoxifen-dependent Cre

recombinase (CreER) under different cell type-specific promoters to identify the different cell types (ependymal cells (FoxJ1), astrocytes (Connexin 30), or oligodendrocyte lineage cells (Olig2), they showed that in the normal state, ependymal cells and astrocytes proliferate and differentiate to their own-cell type (self-duplicate) in order to maintain the cell population or to compensate the cell loss while the oligodendrocyte progenitors also self-duplicate and also generate new cells which become mature oligodendrocytes (Barnabé-Heider *et al.*, 2010).

Since there are multiple cell types in the ependymal cell layer, it is important to establish which may have stem cell capacity. The heterogeneous morphology of ependymal cells in the central canal region of spinal cord was determined and is believed to be related with the function and the molecular protein expression of the cells (Johansson *et al.*, 1999, Meletis *et al.*, 2008). Since the subventricular zone is a well-known neural stem cell niche, Hamilton *et al.* (2009) made comparisons between these two regions using immunohistochemical staining (Table 1.1). They observed the distribution of stem cells and the associated cells within the ependymal region and subependymal layer. Interestingly, in the spinal cord they found nestin-immunoreactivity was prominent in cells at the dorsal pole of the ependymal layer with the fibres extending to the dorsal midline, together with GFAP staining that was also located at the dorsal region. They also found nestin-positive fibres at the ventral pole of the central canal however, the nestin staining at the ventral pole is less prominent when compared to dorsal pole. It suggested that ependymal cells located at the dorsal pole and potentially ventral pole of central canal are neural stem cells, and not all ependymal cells can become stem cells. There are also other cells present, the immature oligodendrocytes ($NG2^+$) and oligodendrocyte progenitor cells ($Olig2^+$), which are mainly located in the subependymal region and also proliferate and mature but cannot differentiate into other cell types.

These researchers also determined the level of cell proliferation using Ki-67 as marker for proliferating cells as this marker is endogenous and expressed at all stages of proliferating cells. They found the asymmetrical distribution of proliferating cells in central

canal where 34% of the proliferating cells were confined to dorsal pole compared to 10% proliferating cells at the ventral pole - this showed the proliferation gradient from dorsal to ventral pole. Further characterisation of proliferating cells showed that 95% of proliferating cells were vimentin^{+} ependymal cells (Hamilton *et al.*, 2009).

Taken together, most of the neural stem cell may be confined to the dorsal and ventral pole of the central canal and ependymal cell proliferation is also concentrated at the dorsal pole showing the capability of only those ependymal cells at the dorsal and ventral pole to become neural stem cells.

Table 1.1 Comparison of cell marker expressions between subventricular zone and central canal (Hamilton *et al.*, 2009)

Cell marker	Cell type	Subventricular zone	Central canal
Vimentin	Ependymal cell	Ependymal layer	Ependymal layer
S100β	Astrocytes	Ependymal layer	Ependymal layer
NG2	Immature oligodendrocytes, pericytes	Present in subependymal region	Present in small numbers at the subependymal region
Olig2	Oligodendrocytes progenitor cells (OPC)	Subependymal region	Present in small numbers at the subependymal region
GFAP	Type B astrocytes and astrocytic stem cell	Subependymal	Subependymal, astrocytic fibres extended to the ependymal layer (dorsal region)
Nestin	Neural stem cell	Ependymal and subependymal region	Ependyma in the dorsal region Long nestin filament sextended to the dorsal midline
Sox2	Stem cell	Ependyma and subependymal layer	Ependymal zone and subependymal region
Ki-67	Proliferating cells	Subependymal layer	Ependymal layer

1.2.3.2 Responses of ependymal cells to injury

Neural stem cells (nestin^{+}) usually are in a quiescent stem cell state until injury occurs. In response to an injury condition created by cutting the dorsal funiculus of spinal cord using microsurgical scissors, the rate of proliferation increased by almost 50-fold compared to the normal situation in the intact cord in order to form the glial cell scar and astrocytes (Johansson *et al.*, 1999).Over time, this response declined and the rate of proliferation was close to the intact situation after one month. , By identifying ependymal cells from the central canal using a FoxJ1-CreEr transgenic mouse, it was determined that these cells proliferated and migrated to the injury site and differentiated into astrocytes for scar formation while also some became oligodendrocytes (Barnabé-Heider *et al.*, 2010). In this fate-mapping study, they also showed the capability of ependymal cells to self-renew and that, they had multilineage differentiation capacity. As a result, the ependymal cells successfully respond to the injuries either involving the central canal or outside the central canal (dorsal funiculus of white matter) by proliferating and differentiating.

Several months after the injury, the area of injury still showed the presence of oligodendrocytes and astrocytes which originate from the differentiation of ependymal precursor cells (Meletis *et al.*, 2008, Barnabé-Heider *et al.*, 2010). Therefore the ependymal cells are very important cell types in proliferation and differentiation of cells in neurogenesis as it may act as precursor for different lineages of cells (Meletis *et al.*, 2008, Alfaro-Cervello *et al.*, 2012) in this injury state.

The type of injury is critical in determining the extent of the response of the ependymal cells. Lacroix *et al.* (2014) made comparisons between contusion spinal cord injury, focal demyelination and multifocal demyelination with respect to central canal ependymal cell proliferation. Neither focal demyelination nor multifocal demyelination were able to trigger ependymal stem cells to proliferate. However, in contusion spinal cord injury, large numbers of proliferating cells were observed at seven days post-injury. In these

traumatically injured central canal regions, the proliferating cells also expressed Vimentin and Sox2.

Moreover the newly proliferated cells were seen to migrate away from the central canal to the injury site (Lacroix *et al.*, 2014). Thus, demyelination alone or autoimmune induced demyelination did not stimulate the ependymal cell proliferation while contusion-type of injury triggers proliferation of dormant neural stem cells. Do ependymal cells differ in human and rats/mice?

In animals such as rats and mice, ependymal cells were found to be neural stem cells (Barnabé-Heider *et al.*, 2010). What about the ependymal cells in the central canal of human spinal cord? In spinal cord sections taken from human cadavers, Cawsey *et al.* (2015) observed the changes in numbers of nestin-positive ependymal cells in spinal cord after traumatic injury. They found that in both patients who died from traumatic accidents or other causes not involving trauma, 23 out of 41 patients had nestin-positive ependymal cells surrounding the central canal. There were significant increases in numbers of nestin-positive ependymal cells in patients who survived for some time after trauma compared with those who died immediately following trauma and these also showed greater numbers than control patients. This suggested that many ependymal cells reacted in injury conditions to become activated neural stem cells. However, in this human study, the levels of proliferating cells using Ki-67 were not measured to see the extent of cell proliferation. The nestin-ependymal cells were clustered at the dorsal pole and ventral pole of central canal (Cawsey *et al.*, 2015). It is established from previous studies in mice (Hamilton *et al.*, 2009) that nestin-positive cells are mainly in these poles, so there are similarities between these animals and humans.

In comparison, another study on human spinal cord revealed that the central canal was absent in patients. In the majority of cases, along the cord, about ≥ 70% of cadavers did not exhibit a patent central canal. Furthermore, the comparison of canal patency at every level showed that the cervical spinal cord had a significantly higher patency compared

to central canals at lower levels. In injured patients, there was no significant difference in the patency of spinal cord lumen at every level (Garcia-Ovejero *et al.*, 2015). This study also stated that, in human the cells are morphologically and structurally different compared to primate or rodent, and the cells are more reminiscent of an ependymoma. Moreover, ependymomas do express some genes of stem cells. Therefore these may be differences between mice and humans with respect to the ependymal cell gene expression patterns. Moreover, a recent study from Paniagua-Torija *et al.* (2018) showed that there was no significant difference in the extent of cell proliferation at the ependymal region in SCI patients compared to control group. It suggested that the ependymal region does not proliferate in adult human spinal cord.

In transplant studies, the neural stem/progenitor cells (NSPC) were harvested from human spinal cord, taken from the ependymal, subependymal and gray matter surrounding the central canal. These NSPCs were cultured and transplanted into the spinal cord of rats that were subjected to spinal cord compression injury. The NSPCs were transplanted both rostral and caudal to the lesion site. After one week of NSPC transplantation, they observed the proliferation of cells (Ki-67^{+}) identified as adjacent to the transplanted cells showing that, the cells survived and proliferated. Furthermore, they also observed that the Ki67^{+} cells became astrocytes (GFAP), neurones (βIII tubulin) and oligodendrocytes (CC1) showed the cells proliferated and differentiated (Mothe *et al.*, 2011).

Taken together, there is still some controversy about the neural stem cell capacity of the spinal cord in mice and human regarding their capability to respond to stimuli, especially in injury conditions. It is important to keep this in mind and it is worth still considering investigation in animals especially in mice or rat since modulation of proliferation may be possible in both the mouse models and in humans.

1.2.3.3 The function of ependymal cells that do not show neural stem cell capacity

It is mainly established that at the dorsal and ventral poles of the central canal, ependymal cells are nestin-positive stem cells (Hamilton *et al.*, 2009). So what do the other ependymal cells do? The ependymal cells also line the SVZ of brain; they possess tanycyte-like properties and form a blood-cerebrospinal fluid barrier in the circumventricular organ (CVO) in brain. Using immunohistochemistry staining, Langlet *et al.* (2013) showed that tanycytes have processes that penetrate through the CVO to reach the fenestrated capillary and form the blood-CSF barrier. This barrier allows the diffusion of blood-borne molecules to the parenchyma of the brain while the tight junction allows diffusion to the CSF to maintain brain homeostasis. Even though they did not observe the function at the central canal of spinal cord, there are possibilities that ependymal cells show the similar function as in SVZ.

1.3 Factors affecting neurogenesis in the different brain regions

If neurogenesis occurs in these specific niches of the CNS then modulation of these regions may have profound effects on the numbers of proliferating cells that occur and the fate of these new cells. It is therefore a potential therapeutic avenue that researchers have been exploiting in an effort to produce neurones or oligodendrocytes in conditions where these cells have been lost.

There are a lot of factors that can contribute to neurogenesis, stimulating and modulating the neural stem cells by conditions or manipulations such as using pharmacological treatments, environmental enrichment, stress or life-style (Cameron *et al.*, 1998, Rauscher *et al.*, 1998, van Praag *et al.*, 1999). Therefore these can be extrinsic or

intrinsic factors. Example of extrinsic factors can be environmental, such as an enriched environment. In one study, mice were divided into group-housed mice and social isolation mice. In experimental groups, they experienced enriched environments (larger cage contained toys, ribbons, cardboard rolls and plastic shelter) for 7 days. The result showed increased neurogenesis in the enriched environment group compared to groups that did not experience this environment (Monteiro *et al.*, 2014). An example of an intrinsic factor could be release of neurotransmitters from inputs innervating these stem cells. Corns *et al.* (2015) showed that positive allosteric modulation of cholinergic receptors which are α7-containing nicotinic acetylcholine receptors (α7*nACHRs) via PNU 120596 increased numbers of proliferating cells in cultured spinal cord slices and in *in vivo* experimental groups compared to control group.

One neurotransmitter that has received a lot of interest is 5-HT and so I will next focus on this neurotransmitter, considering the function of 5-HT, the receptors through which it mediates its effects and then its potential in modulating neurogenesis in specific neurogenic niches.

1.4 5-hydroxytryptamine (5-HT) and 5-hydroxytryptamine receptors (5-HTRs)

1.4.1 Properties and function of 5-HT

5-HT is a monoamine neurotransmitter that has functions in neuroendocrine regulation, temperature regulation, regulation of anxiety and modulation of depression (Chase and Murphy, 1973). This neurochemical substance is biochemically derived from tryptophan. Tryptophan is an essential amino acid that our body cannot produce. It can be obtained from foods such as nut, milk, red meat, chicken and oats and nowadays people can take

tryptophan supplements that are available over the counter. 5-HT is not the only by-product of tryptophan. This essential amino acid also produces kynurenine. However, only 5% of tryptophan produces 5-HT, while the other 95 % of tryptophan produces kynurenine, meaning that our body does not easily produce 5-HT. Therefore in conditions that are due to low levels of 5-HT, pharmacological approaches are used as modes of treatment rather than dietary advice due to the minimal amount of 5-HT that can be produced from daily food intake.

There are two main steps in the production of 5-HT, the first step is the formation of 5-Hydroxytryptophan from tryptophan by the action of tryptophan hydroxylase and the second step is a conversion of 5-Hydroxytryptophan to 5-HT by L-aromatic amino acid decarboxylase enzyme (Tyce, 1990). In addition to that, 5-Hydroxytryptophan is an essential precursor for 5-HT present in the cytoplasm of the cell (Squire *et al.*, 2012) Figure 1.4).

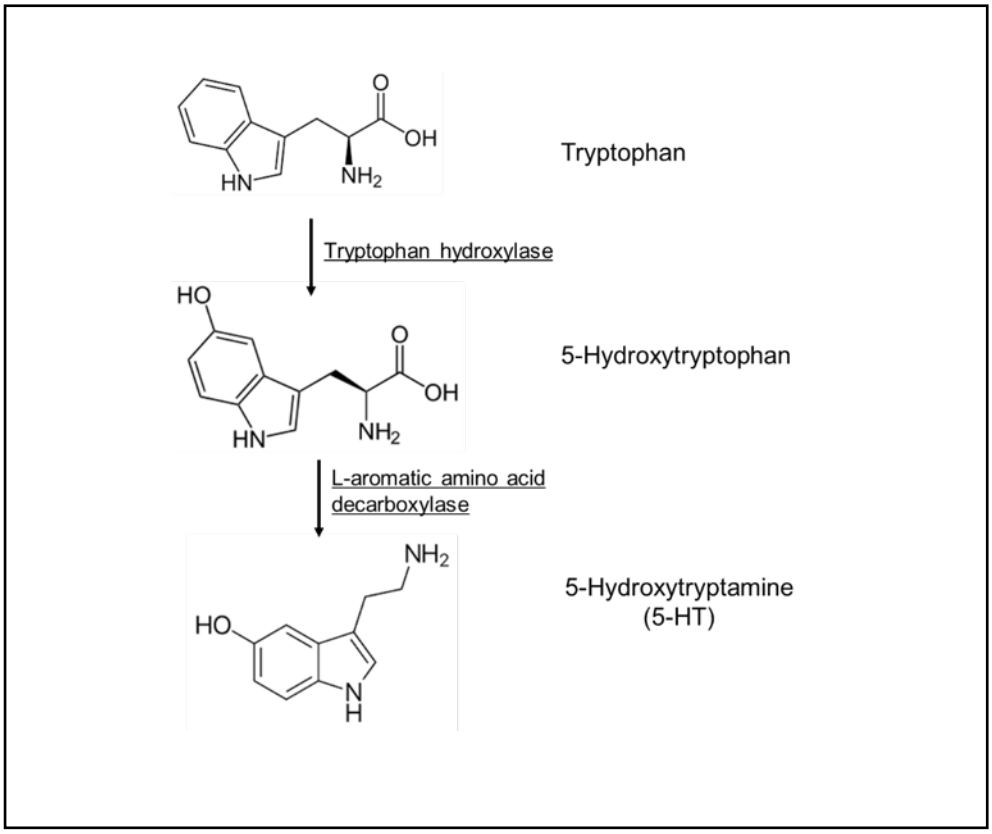

Figure 1.4 Formation of 5-HT. 5-HT is formed from tryptophan than has been converted to 5-hydroxytryptophan by tryptophan hydroxylase enzyme then L-aromatic amino acid decarboxylase enzyme converts 5-hydroxytryptophan to 5-Hydroxytryptamine. The picture is adapted from Tyce (1990).

1.4.2 Distribution of 5-HT in hippocampus, brainstem and spinal cord

The distribution of 5-HT throughout the central nervous is well established. Over 30 years ago, researchers reported the location and distribution of 5-HT throughout the central nervous system, including brainstem, brain and spinal cord region. The 5-HTergic cell bodies are found in the raphe nucleus of the brainstem and they send ascending projections to the brain and descending projections to the spinal cord.

Using immunocytochemical staining, Bowker *et al.* (1981) found a massive distribution of 5-HT-containing neurones especially in the median and ventral area of the medulla of the rat. The cells are specifically located in the median raphe in nucleus raphe obscurus, with a further ventral collection in nucleus raphe pallidus, dorsal and rostral nucleus raphe magnus. Using an autoradiographic techniques and injection of,^{3}H-Paroxetine, which labelled the 5-HT transporter site, researchers showed that the dorsal raphe nuclei have the greatest relative density of radioactivity (150-250 fmol/mg protein) as well as the Islands of Calleja (Souza and Kuyatt, 1987). This indicated, that besides the presence of 5-HT cell bodies, there also terminals of 5-HTergic fibres that innervate the brainstem area. In terms of the level of 5-HT in the brainstem, the highest concentration was found in the raphe nuclei by using an enzymatic isotopic technique (Palkovits *et al.*, 1974). These findings revealed that 5-HT neurones and 5-HTergic fibres are located in the brainstem area and unevenly distributed.

The hippocampal region is one of the regions where 5-HTergic fibres ramified extensively. The hippocampus has a clear laminar pattern of 5-HTergic innervation to dentate gyrus shown by 5-HT-immunoreactive (5-HT-IR) fibres in this region (Zhou and Azmitia, 1986). The laminar pattern defined the different characteristics of 5-HT-IR innervation in the different specific regions. The infragranular layer has tortuous, fine 5-HT-IR fibres with large varicosities that are densely distributed, while moderate innervation was observed in the molecular layer and thin 5-HT fibres were seen in the

granular layer of dentate gyrus (Zhou and Azmitia, 1986). The 5-HTergic fibres that innervate dentate gyrus of the hippocampus originate from the median raphe nucleus of brainstem travelling through the cingulum bundle and fornix-fimbria (Zhou and Azmitia, 1983).

The 5-HTergic fibres travel down from the raphe nucleus to all levels of spinal cord then the tracts that are located within the dorsolateral funiculus ramify into the grey matter and have synaptic contacts with many neurones involved in somatic motor outflow, including interneurones such as commissural interneurones, excitatory interneurones, inhibitory interneuron, Renshaw cell and motor neurons (Perrier and Cotel, 2015). There are also 5-HTergic inputs onto both sensory neurones in the dorsal horn and autonomic preganglionic neurones and interneurons involved in autonomic control (Deuchars and Lall, 2015).

Using immunohistochemical techniques, Steinbusch (1981) located 5-HT-immunoreactivity to describe the distribution and location based on the density of 5-HT-positive terminals. In the white matter of spinal cord, the fibres were observed in funiculus ventralis at all levels of the spinal cord, while in the lateral funiculus, the fibres were observed in cervical, thoracic, lumbar regions and none in sacral and coccyx region. Within the gray matter, they used Rexed laminae as a reference to describe the distribution of 5-HT-immunoreactive fibres. 5-HT innervation of the gray matter of spinal cord is not evenly distributed. High density fibre labelling was visualised at all levels with a different location. At the cervical, lumbar, sacral and coccygeal levels the densest innervation was in the medial part of lamina VIII while at the thoracic level, very high density labelling was found the intermediolateral cell column of lamina VII, the region containing sympathetic preganglionic nucleus. Interestingly, in the peri-ependymal region (central canal), high innervation by 5-HT was observed at every level of the spinal cord (Steinbusch, 1981).

5-HT cell bodies also send the terminals to the brainstem. Here, the 5-HTergic neurones have 5-HTR1A and regulate the release of 5-HT at the synaptic region. Furthermore, the receptors are also located on the non-5-HT neurones in the brainstem and act as heteroreceptors (Riad *et al.*, 2000, Fonseca *et al.*, 2009). Therefore, using fluoxetine (flx) to increase the endogenous 5-HT in synaptic cleft is possible to influence cell proliferation and differentiation since flx is a selective serotonin reuptake inhibitor.

1.4.3 5-HT receptors (5-HTRs)

5-HT has seven major receptors and exerts its action through activation of these receptors. These subclasses of receptor are namely 5-HTR1, 5-HTR2, 5-HTR3, 5-HTR4, 5-HTR5, 5-HTR6 and 5-HTR7 (Pazos and Palacios, 1985, Tecott *et al.*, 1993, Pompeiano *et al.*, 1994, Reynolds *et al.*, 1995, Ward *et al.*, 1995, Gustafson *et al.*, 1996). The effect of 5-HT occurs when the neurotransmitter binds to the 5-HT receptor located at the presynaptic (autoreceptor) or postsynaptic (heteroreceptor) membrane of the target cell and involves activation of cation channels (ionotropic receptor) or G protein-coupled receptors (metabotropic receptor) (Squire *et al.*, 2012). All 5-HTRs are G-coupled protein receptors except 5-HTR3, which is the ionic channel receptor (Thompson and Lummis, 2006). The other receptors are G-coupled proteins namely 5-HTR1, 5-HTR2, 5-HTR4, 5-HTR5, 5-HTR6 and 5-HTR7 (Clawges *et al.*, 1997). The location of 5-HTR expression is critical to investigate the relationship of receptors and the functions itself either in brainstem or spinal cord (Table 1.2 and Table1.3).

Table 1.2 List of 5-HTRs expressed in the brainstem

5-HT receptor (5-HTR)	Where expressed (main location / highest level)	Characters	References/ source of information
5-HTR1A	Dorsal raphe nucleus	Autoreceptor, heteroreceptor	(Riad *et al.*, 2000, Arango *et al.*, 2001, Liu and Wong-Riley, 2010)
5-HTR1B	Substantia nigra	Autoreceptor, heteroreceptors	(Riad *et al.*, 2000, Liu and Wong-Riley, 2010)
5-HTR2A	RM, Rob, RP	Heteroreceptor	(Liu and Wong-Riley, 2010, Borroto-Escuela *et al.*, 2014)
5-HTR3A	NTS, spinal tract of CN V	Presynaptic and postsynaptic	(Miquel *et al.*, 2002)
5-HTR4(a)	Dorsal raphe nucleus, Pre-Boetzinger complex	Postsynaptic receptor	(Waeber *et al.*, 1995, Manzke *et al.*, 2003)
5-HTR5A	unknown	unknown	-
5-HTR5B	Dorsal raphe nucleus, inferior olive	Autoreceptor role detected in some 5-HT transporter	(Kinsey *et al.*, 2001, Serrats *et al.*, 2004)
5-HTR6	unknown	unknown	
5-HTR7	NTS	Post-synaptic receptor	(Matott and Kline, 2016)

Table 1.3 List of 5-HTRs expressed in the spinal cord

5-HT receptor (5-HTR)	Where expressed	Expressed in central canal region?	References/ source of information
5-HTR1A	Dorsal horn	Yes but unknown around in the ependymal cells	Autoradiography (8-OHDPAT), (Croul *et al.*, 1998)
5-HTR2A	Intermediolateral, Ventral horn	Yes	(Doly *et al.*, 2004b)
5-HTR3A	Ventral horn	No	(Fonseca *et al.*, 2001)
5-HTR3B	Ventral horn	No	(Fonseca *et al.*, 2001)
5-HTR4(a)	Ventral horn (cervical spinal cord)	Possible/ Unknown	(Suwa *et al.*, 2014)
5-HTR5A	Dorsal horn (laminae I and II),	Unknown	(Doly *et al.*, 2004a) (Fonseca *et al.*, 2001)
5-HTR6	Laminae I, II, IX and X	Yes Yes Yes (Lumbar)	(Gérard *et al.*, 1997) Allan Brain Atlas Gensat mouse
5-HTR7	Dorsal horn	Unknown	(Doly *et al.*, 2005)

1.5 Can 5-HT influence neurogenesis?

The model of interaction between neurotransmitters and cells that are involved in brain neurogenesis is quite established. However, how neurogenesis in the brainstem and spinal cord is modulated in this way is still unclear. The direct or indirect action of 5-HT on postnatal neurogenesis and the cascade that is used to promote neurogenesis is still debatable. The indirect action of fluoxetine (flx), a selective serotonin reuptake inhibitor (SSRI) promotes the proliferation of cell in the extrahippocampal region of mice (Sachs and Caron, 2015). The SSRI blocks the reuptake of 5-HT from the synapse to the presynaptic terminal. Therefore, there will be an accumulation of 5-HT at the synaptic cleft, which will promote increased levels of this neurotransmitter to activate receptors. However, differing durations of SSRI treatment showed variable impact on neurogenesis in the subventricular zone and dentate gyrus (DG) of hippocampus. The chronic effect of SSRI in adult mice was examined at different time periods after administration of flx. The rates of cell proliferation were examined after three weeks, six weeks and nine weeks of administration of flx. The patterns of neurogenesis were different in the subventricular zone and dentate gyrus of hippocampus. In the DG, cell proliferation increased after three weeks of flx and plateaued after 6 and 9 weeks. At this point after increased cell proliferation, the cells were maintained in the plateau phase whereby the number of new cells and the number of cell deaths were almost equal. This effect of flx may not be entirely dependent on the inhibition of the 5-HT transporter (5-Htt) since similar levels of hippocampal cell proliferation were observed in wildtype and 5-Htt knockout mice (Levy *et al.*, 2019). Since this study also reported flx-mediated increases in brain-derived neurotrophic factor (BDNF)/tropomyosin-related receptor kinase B (TrkB) signalling, these effects may involve direct activation of TrkB.

In the subventricular zone, there is a dense 5-Htergic innervation of this region (Jahanshahi *et al.*, 2011) but here, flx showed the opposite effect. After three weeks of treatment with flx, the SSRI down-regulated cell proliferation and this reduction became significant after six weeks and nine weeks (Ohira and Miyakawa, 2011). The difference in levels of proliferation may be due to the 5-HT receptors expressed in the two regions, since 5-HTR1A receptors are highly expressed in the DG (Tanaka *et al.*, 2012), but in the SVZ, treatment with a 5-HTR1B receptor agonist decreased proliferation (Banasr *et al.*, 2004). Therefore this is important to keep in mind, when using flx as a means to increase 5-HT levels.

1.5.1 Which 5-HTRs are involved in neurogenesis in the central nervous system?

Previous research has highlighted two specific 5-HT receptors in modulating adult neurogenesis in the hippocampus; 5-HTR1A and 5-HTR4. This research was carried out using agonists, antagonists and partial agonists at the 5-HTR1A. Generally, using agonists and partial agonists, there was increased proliferation of new cells at the dentate gyrus, indeed 8-hydroxy-2-dipropylaminotetraline (5-HTR1A agonist) could actually overcome the decreased proliferation of cells caused by a 5-HTR1A antagonist (Radley and Jacobs, 2002, Banasr *et al.*, 2004, Grabiec *et al.*, 2009). Therefore the activation of 5-HTR1A receptors via autoreceptors or heteroreceptors is important in regulating cell proliferation in the subgranular zone of dentate gyrus. 5-HTR4 is the other highlighted receptor that is potentially involved in neurogenesis. There were several studies on the effect of activation of 5-HTR4 on neurogenesis that showed increased cell proliferation in the subgranular hippocampal layer with the treatment of 5-HTR4 agonists. They discovered that the cells started to proliferate as early as three days after treatment with the 5-HTR4 agonist compared to the conventional SSRI that took two weeks to

develop the effect. Therefore, activation of 5-HTR4 produced faster effects than the conventional SSRI (Pascual-Brazo *et al.*, 2012). However, the involvement of activation of 5-HTR4 using SSRI is still unknown. For example, studies using 5-HTR4 antagonists reported only partial block of the neurogenesis from the long term treatment of flx. In another study using knock-out mice, chronic administration of flx significantly increased cell proliferation and numbers of dcx-positive cells in dentate gyrus of wild-type mice compared to the 5-HTR4 knock-out mice (Imoto *et al.*, 2015). From these results, a prediction is made that the activation of 5-HTR1A and 5-HTR4 can potentially modulate neurogenesis in other parts of the central nervous system, especially in the spinal cord. Due to lack of studies regarding the potential of activation of 5-HTR4 to promote cell proliferation in central nervous system, some consideration of activation of 5-HTR4 in other regions also is worthwhile. It was known that 5-HTR4 is abundantly expressed in the gastrointestinal system and has a role in the gastromotility of intestine. In previous experiments, activation of 5-HTR4 receptors using tegaserod maleate (5-HT4 partial agonist) resulted in greater numbers of proliferating cells in the enteric system of mice (Liu *et al.*, 2009). In other conditions where neural stem cells from hippocampus and subventricular zone were transplanted in the anastomosis region of ileum, administration of mosapride citrate (5-HTR4 agonist) facilitated neurogenesis in enteric neurones (Goto *et al.*, 2016). The positive effect of 5-HTR4 agonists in brain and gastrointestinal system proved that activation of 5-HTR4 has potential in promoting proliferation and differentiation in brainstem and spinal cord. However, using 5-HTR4 agonists in *in vivo* studies needs to be carefully considered because of the risk of cardiac arrhythmia due to the presence of 5-HTR4 in cardiac cells (Landrum Michalets and Williams, 2000). Table 1.4 showed activation of 5-HTRs on effect of cell proliferation respectively.

Table 1.4 5-HTRs and neurogenesis

5-HTRs	Proliferative and neurogenesis study	Reference
5-HTR1A	Increase cell proliferation in subgranular and subventricular zone using agonist	(Banasr *et al.*, 2004)
5-HTR1B/1D	Decrease cell proliferation in subventricular zone using agonist	(Banasr *et al.*, 2004)
5-HTR2A	Increase cell proliferation in subventricular zone using agonist	(Banasr *et al.*, 2004)
5-HTR2C	Increase cell proliferation in subventricular zone using agonist	(Banasr *et al.*, 2004)
5-HTR3	5-HTR3-mediated exercise induced cell proliferation in dentate gyrus of hippocampus	(Kondo *et al.*, 2015)
5-HTR4	Promote enteric neurogenesis Reduced effect of flx on hippocampal neurogenesis in 5-HTR4 knock-out mice	(Liu *et al.*, 2009) (Imoto *et al.*, 2015)
5-HTR5	- No data	-
5-HTR6	No effect on cell proliferation using antagonist in dentate gyrus	(Foley *et al.*, 2008)
5-HTR7	No effect on cell proliferation using knockout mice in dentate gyrus	(Sarkisyan and Hedlund, 2009)

1.6 Consequences of High-fat diet (HFD) on neurogenesis

There is an increasing body of evidence that lifestyle can significantly impact on the extent of neurogenesis in the different niches. Exercise may have beneficial effects, first demonstrated by Van Praag et al (1999), who showed that running can stimulate neurogenesis in the dentate gyrus of mice, with BDNF having a pivotal role in this exercise mediated neurogenic response (Liu and Nusslock, 2018). However, many factors are negative regulators of neurogenesis and these are of great concern due to the fact that these lifestyle modifications are becoming more common in the human population. Once such factor is stress since mice injected with corticosterone had lower levels of cells labelled with the marker for immature neurones, doublecortin in the hippocampus (Sawamoto *et al.*, 2016). Furthermore, sleep deprivation, which often accompanies stress or can be due to other causes, is also a negative modulator of neurogenesis. In one study, 56 hours of sleep deprivation significantly reduced basal rate cell proliferation in the dentate gyrus by 36% and interestingly this reduction persisted after an eight hour recovery period (Tung *et al.*, 2005). Since the effects of sleep deprivation on AHN were not normalised after the eight-hour period, it suggests that sleep deprivation may have long term implications on hippocampal neurogenesis. One global issue is that of obesity and worryingly not only might people have an increased risk of developing cardiovascular diseases like hypertension and heart failure, but research indicates that consumption of high-fat diet causes reduced cell proliferation in brain. This is a critical issue since over 4 million people are dying each year as a result of being overweight or obese, while in the last 25 years there has been a fourfold increase in the prevalence of overweight or obese individuals in the population aged 5-19 (Data from WHO). Therefore, the next subtopic will explain the association between high-fat diet and decreased numbers of proliferating cells.

1.6.1 Reduced hippocampal neurogenesis in high-fat diet conditions

A diet rich in fat is believed to impair adult neurogenesis in the hippocampus. A study on neurogenesis in rats that were given 42% fat diet for four weeks showed 50% fewer proliferating cells (BrdU was injected after two weeks of initiation of diet) in high-fat diet group compared to low-fat diet group. (Lindqvist *et al.*, 2006). They also looked at the gender-related effect, showing that males were affected more compared to females. Consumption of high-fat diet for longer durations also caused the same effect. C57Bl/6 mice were given a high-fat diet (45% fat by energy) for seven weeks, and BrdU as proliferation marker was injected twice daily for the last three days. The lower extent of proliferation and hippocampal neurogenesis was observed and at the same time decreases in the levels of brain-derived neurotrophic factor (BDNF) were found in the HFD diet group (Park *et al.*, 2010). BDNF is a growth factor that is considered an important factor in promoting hippocampal neurogenesis (Rossi *et al.*, 2006). In another study using 60% high-fat diet, consumption of high-fat diet for 20 weeks led to decreased cell proliferation (BrdU) in hippocampus, low levels of BDNF and impairment in cognitive function (Kim *et al.*, 2016). Variations in time of consumption of high-fat diet (from a minimum of 4 weeks to 20 weeks), and high-fat diets (ranging from 42% to 60% by energy) still showed the same impact on hippocampal neurogenesis and BDNF growth factors, therefore it indicates that high-fat diet has an influence on the development of central nervous system generally and on postnatal hippocampal neurogenesis specifically (Lindqvist *et al.*, 2006, Park *et al.*, 2010, Kim *et al.*, 2016).

1.6.2 Can decreases in cell proliferation in high fat diet conditions be reversed or ameliorated?

High-fat diet leads to obesity and metabolic syndrome like diabetes, cardiovascular diseases. Therefore, consumption of a high-fat diet over a more extended period of time has a more harmful effect rather than an increase in body fat composition. Moreover, the dietary lifestyle has an implications on neurogenesis especially in the hippocampal regions that may contribute to the impaired cognitive function, learning and memory (Del Rio *et al.*, 2016). There were exciting findings in this area where researchers found the possibility of recovery from lower numbers of proliferating cells caused by consumption of high-fat diet. Indeed 12 weeks treadmill exercise with total times ranging from 30 minutes to 50 minutes can enhance cognitive function through the improvement of neurogenesis in the hippocampal region (Kim *et al.*, 2016). Another study also proved that running exercises can improve hippocampal cell proliferation when high-fat diet and exercise were started at the same time point (Klein *et al.*, 2016). To sum up, exercise is one of the methods that can be used in the recovery of cell proliferation (Kim *et al.*, 2016, Klein *et al.*, 2016).

A pharmacological approach also becomes another option. Administration of 2 mg/kg/day rivastigmine (broad-spectrum cholinesterase inhibitor) subcutaneously for six weeks in type 2 diabetes – Alzheimer model (T2DM-AD mice) successfully ameliorated memory decline and enhanced neurogenesis. In this study, four-month-old mice were fed a high-fat diet for eight weeks to create a type 2 diabetes model (Matsuda and Hisatsune, 2017). Therefore, acetylcholine may play a role in the modification of hippocampal neurogenesis in high-fat diet conditions. A natural product, soy extract, which is isoflavone daidzein, is also known to have a neuroprotective effect. Rats were fed with 60% high-fat diet for 12 weeks and then treated with 50 mg/kg of daidzein for 13

days and they showed an increased extent of cell proliferation in treated compared to high-fat diet group that were given vehicle. The capability of particular factors to rescue the impair hippocampal proliferation and combat the situation by regaining a greater extent of proliferation is important as it helps in getting back to the normal or better condition.

Another potential and pertinent treatment for reversing or slowing the detrimental effects of a high fat diet on neurogenesis is to modulate levels of 5-HT. As discussed in previous sections, flx increases hippocampal neurogenesis in healthy animal models. Furthermore, mice that were fed a high fat diet then given flx at 6 weeks into the diet displayed a reduced weight gain than those in the control group just given a high fat diet (Scabia *et al.*, 2018) indicating that flx may act as an anorexigenic agent, although other factors such as interference with gut metabolism or function.

There have also been previous studies that showed flx successfully reversed reduced neurogenesis in different conditions. In an experimental setting, rats were exposed to inescapable shock in the shuttle box so that the animals learned helplessness, due to failure to acquire the escape response and developed depression. This group of mice had reduced numbers of proliferating cells (BrdU+) in hippocampus compared to control group. This effect was reversed by administration of 10 mg/kg flx (delivery method was not known) twice daily from days 2-8 (Malberg and Duman, 2003). In another study, rats were exposed to psychosocial stress for 5 weeks leading to a reduction of proliferating cells (BrdU+) in dentate gyrus of hippocampus compared to control group. Treatment with oral 10 mg/kg of flx resulted in preservation of numbers of BrdU-positive cells. The flx was administered via a bulb-headed cannula into the buccal cavity, and the animals were allowed to swallow the solution (Czéh *et al.*, 2007).

Overall, this suggests that a viable treatment to ameliorate the reductions in neurogenesis due a high fat diet is treatment with flx.

1.7 Justification of the study

The direct or indirect action of 5-HT on postnatal neurogenesis and the receptors used to promote neurogenesis are still debatable. The indirect effect of flx, the SSRI promotes the proliferation of cells in the extrahippocampal region of mice (Sachs and Caron, 2015). In this condition, SSRI blocked the reuptake of 5-HT from the synapse to the presynaptic terminal. Therefore, there will be an accumulation of 5-HT at the synaptic cleft, which will promote increased levels of 5-HT. However, the proliferation of cells was not examined in other regions, and it may be possible that the proliferation also can occur in other neurogenic niches within the central nervous system generally and at the spinal cord specifically. The SVZ and SGZ of the DG are the two main areas that are more pronounced for neurogenesis (Eriksson, 2003). To date, there is no information regarding potential modulatory roles of 5-HT on neurogenesis in the spinal cord and brainstem. Since nestin-positive neural stem cells are located in the DVC area of brainstem and central canal of the spinal cord and there is dense serotonergic innervation of both brainstem and spinal cord, it is important to understand whether 5-HT can promote neurogenesis and which receptors are involved. There are a number of 5-HT receptors where activation has been reported to modulate neurogenesis in other regions (see above) and single mRNA sequence suggests that ependymal cells express 5-HT1, 5HT2 and 5HT4 receptors (Rosenberg *et al.*, 2018) therefore the role of these receptors in influencing the activity of the ependymal cells merits further investigation, firstly using *in vitro* approaches to enable investigation of all receptors under similar circumstances. It is also clear that many lifestyle factors affect neurogenesis; prominent among them is obesity, which is known to reduce hippocampal neurogenesis, but less is known about whether neurogenesis in other regions is affected. The dorsal vagal complex (DVC), senses insulin levels and subsequently stimulates changes in feeding

behaviour and glucose metabolism, through activation of neuronal circuits. In high fat diet, insulin resistance occurs in the DVC, through increased mitochondrial fission and this leads to changes in the responsiveness of this region (Filippi *et al.*, 2017), however, little is known about whether high fat diet changes the levels of neurogenesis in this region. An understanding of the extent of modulation of HFD on neurogenesis in different regions is therefore important to understand. This includes the spinal cord since other lifestyle factors such as exercise increase spinal cord neurogenesis (van Praag *et al.*, 1999). Once this is established, it is then pertinent to understand if any changes observed in the high fat diet can be modulated by simultaneous or delayed application of flx.

My general hypothesis is that 5-HT influences the extent of cell proliferation and differentiation in neurogenic niches of the central nervous system through activation of specific receptors (Figure 1.5).

My objectives are

1. To determine the relationship between 5-HTergic fibres and neural stem cells using nestin-Green Fluorescent Protein (GFP) mice.
2. To determine whether modulation of 5-HTergic signalling can influence neurogenesis in the spinal cord and brainstem, since these regions receive dense 5-HTergic innervation and prior research indicates that they have neurogenic capacity.
3. To establish which receptors are involved in mediating this effect, focussing on receptors that are known to be present in these regions.
4. To investigate the effects of a high-fat diet on proliferation in these established neurogenic niches of hippocampus, brainstem and spinal cord and determine whether administration of flx can reverse or ameliorate these effects.

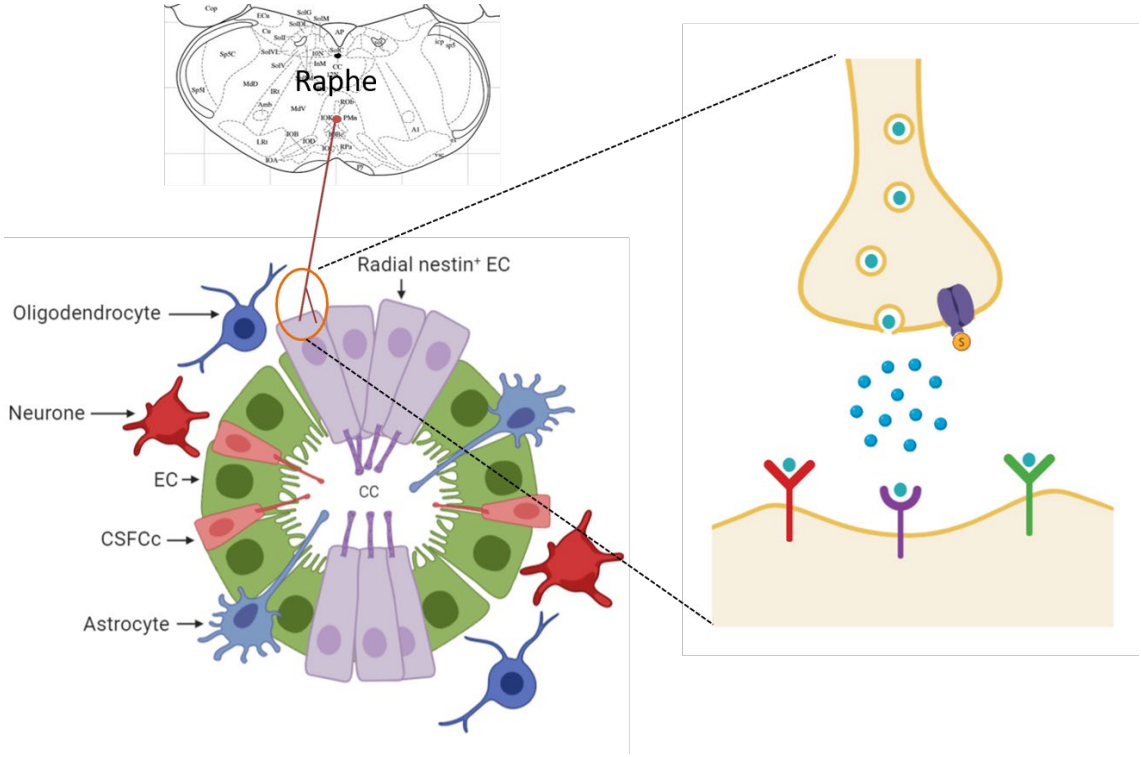

Figure 1.5 Schematic diagram of hypothesised relationship between 5-HTergic terminals with ependymal stem cells in central canal of brainstem and spinal cord
The close relationship of 5-HTergic fibres with ependymal neural stem cells suggests that 5-HT can influence the neural stem cells. Increased ambient 5-HT in the synaptic cleft can be achieved by blocking the 5-HT transporter at the presynaptic terminal so there will be no re-uptake of 5-HT. Thus, increasing the endogenous 5-HT has the potential to affect cell proliferation via a particular receptor.

Chapter 2

GENERAL METHOD AND METHODOLOGY

2.1 Preparation of tissue from animals

2.1.1 Animals

Animals were obtained from the Central Biological Services (CBS) with approval of the animal ethics committee. All the procedures were conducted under regulation of UK Home Office License and UK Animal (Scientific Procedure) Act, 1986. All efforts were made to minimise the number of animals suffering.

2.1.2 Animals and maintenance

C57 / Bl6 mice, male and female, were used for the majority of experiments, except in the determination` of potential serotonergic innervation of the ependymal cell layer of central canal of spinal cord and brainstem, when Nestin-EGFP mice were used. Each chapter provides specific data on the numbers of animals used for each protocol and details on the background of the Nestin-EGFP mouse is given in Chapter 3 introduction. Same sex littermates were kept in individually ventilated cages of four mice per cage. Spruce wood shavings had been provided as bedding. Mice were fed a standardized diet for the mouse and given ad libitum of water. All mice were kept on a regular diurnal light that (12:12, night: dark). All materials, including individual ventilated cages lids, feeders

and water were autoclaved before use. Enriched environmental tools were provided for each cage includes nesting materials, wooden stick and mouse igloo (shelter).

In the *in vivo* studies, mice aged between 6 – 8 weeks were used, while for the *in vitro* studies, a younger age of between 10 – 16 postnatal days was used. Determination of age in a specific area of study is very important in order to obtain the relevant results that can be inferred to the human population later on. The different age groups that were used *in vitro* and *in vivo* were to investigate whether activation of same receptor might have similar actions for different ages.

2.1.3 Preparation of fixed tissue from in vivo experiments and for immunofluorescence studies

2.1.3.1 Perfusion

Animals aged 6-8 weeks of either sex (see numbers for each chapter) were anaesthetised intraperitoneally with sodium pentobarbitone (60 mg/kg, Pentoject, http: // www .animalcare .co.uk / companion-animals). Once the mice were anaesthetised, established using abolition of the pedal reflex to a noxious pinch, they were laid on the dissecting tray with the ventral side facing upwards. The forelimbs and hindlimbs were anchored to the tray using dissecting pins. Blunt forceps were used to lift up the mouse skin at the mid-ventral region and using pointed scissors, the skin was cut. A thoracotomy was carried out from the xiphisternum up to the manubrium until reaching the level of the heart. The right atrium was punctured to reduce the intracardial pressure. First, 20-50 ml of 0.1 M phosphate buffer (PB) was infused to flush out the blood from the animal's system. Then this was followed with 200 ml of 4% paraformaldehyde (PFA) in 0.1M of PB with pH 7.4 at room temperature (20-25°C). It was perfused at a rate of 3-4 ml/min. The rate of perfusate was controlled by peristaltic pump (Warson-Marlow, https://www.watson-marlow.com/gb-en/range/watson-marlow/300-tube-pumps/). After

the perfusion was completed, the spinal cord, brainstem and brain were removed and were kept in 4% PFA 0.1 M PB for 24 hours (post-fixation) at 4°C. After that, the solution was replaced with 0.1 M PB.

2.1.3.2 Extraction of brain, brainstem and spinal cord and preparation for immunofluorescence

After perfusion was complete, the animal was checked to confirm that the PFA had successfully circulated and fixed by checking the tail and the head. The tail and the head become stiffer than usual and blood vessels were white. The skin and limbs were removed, leaving the skull and vertebral column and this was then placed in 35-40 ml of 4% PFA at 4°C overnight for post fixation. Then the PFA was replaced with 0.1M PB. Then the whole brain, brainstem and spinal cord were excised using fine spring scissors. The extraction was started from brain by splitting the skull on the sagittal plane into right and left part. And then a laminectomy was carried out to extract the spinal cord from the vertebral column. The extraction was carried out from the brain to the spinal cord caudally in order to secure the brainstem between the brain and the spinal cord. Lastly, fine forceps were used to extract the pia and dura mater from the brain, brainstem and spinal cord under a dissecting microscope. The tissue was at this point able to be sectioned using a vibrating microtome (Leica VT100S, Microsystems, Milton Keynes, UK) – see section 2.2.2.

2.1.4 Preparation of live tissue for in vitro study (acute slices preparation)

Acute slices of the brain or spinal cord are commonly used for recording techniques in electrophysiology. The acute preparation of slices retains cellular stability and provides a method for evaluating the neurophysiology of specific tissues. Animal preparation for

acute slices ensures that the cells are maintained alive after perfusion for at least 5-6 hours with minimal injury to the tissue. Animals were anaesthetized intraperitoneally with sodium pentobarbitone (60 mg/kg, Pentoject, (http://www.animalcare.co.uk/companion-animals). Both surgery and perfusion procedures were performed as above but the main difference was that perfusion was done using 15-20 ml ice – cold sucrose artificial cerebrospinal fluid containing sodium chloride, sodium bicarbonate, potassium chloride, magnesium sulphate heptahydrate, sodium phosphate monohydrate, glucose and calcium chloride at a pH of 7.4 and 300 osmolarity injected through the left ventricle (aCSF, Table 2.1). The animal was then placed with the dorsal side facing up, after the perfusion had been completed, and the skin over the spinal cord was removed. A dorsal laminectomy was performed using fine spring scissors and fine forceps to expose the whole length of spinal cord from cervical to the sacral region. After that, the spinal nerves were cut to ease the extraction of the spinal cord. The spinal cord was carefully extracted using a small spatula and placed in a 50 mm petri dish containing ice-cold sucrose aCSF. This was followed by meningeal (pia, arachnoid and dura mater) removal under a dissecting microscope using fine forceps. The thoracic and lumbar regions were selected then were cut horizontally into small parts (3-4 mm each). Using a microspatula, the cords were transferred and placed into a weighing boat containing 1.5% agar (Sigma Aldrich, cat # W2751). Stock solution for agar (1.5%) was prepared first by weighing 1.5 g of agar and placing in a glass beaker containing 100 ml of aCSF before dissolving the agar using a microwave for 30 seconds in the same beaker. After the agar dissolved, it was transferred to a small weigh boat (44 mm x 44 mm). Then, it was allowed to cool until it was warm to touch but not yet solidified. Once the agar had solidified, longitudinal agar blocks from the region that contained the segments of the spinal cord were dissected out and glued to the metal base of the vibrating microtome bath using superglue. Transverse thoracolumbar spinal cord slices were cut at 250-500 µm thickness using a vibrating microtome (Campden Instruments, integraslice 7550 PSDS) and collected into a holding chamber containing oxygenated (95% oxygen and 5%

carbon dioxide) aCSF at room temperature. Slices were used in the *in vitro* experiments as described in section 2.4.

Table 2.1 List of components of aCSF and sucrose aCSF. Components in the prepared solutions that were used in the acute slice experiments.

Component	aCSF Concentration (mM)	Sucrose aCSF concentration (mM)
Sucrose	0	217
Sodium chloride	124	0
Sodium bicarbonate	26	26
Potassium chloride	3	3
Magnesium sulphate heptahydrate	2	2
Sodium phosphate monohydrate	2.5	2.5
Glucose	10	10
Calcium chloride	2	1

2.2 Histology procedures

2.2.1 Immunohistochemistry

Immunohistochemistry is a powerful tool in detecting specific proteins and is widely used in many medical research and clinical diagnostic situations especially in neurodegenerative disorders, cancer, brain trauma, and muscle disease (Duraiyan *et al.*, 2012). These methods apply the principle of antibody-antigen interaction when expression of an antigen will be recognised by the specific antibody (Figure 2.1). The site of antibody binding is visualized under a light or fluorescent microscope by a marker such as fluorescent dye, enzyme, radioactive element, or colloidal gold, which is directly

linked to the primary antibody or to an appropriate secondary antibody (Radbruch, 2000). Immunohistochemistry was performed with different types of antibodies (Table 2.2) against specific antigens. An important step in immunohistochemistry methods is to make sure that the antibody is able to penetrate through the tissue matrix and in the case of intracellular antigens, the cell membrane. The permeabilization reagent Triton X-100 (https://www.sigmaaldrich.com) was used, at a concentration of 0.1%, Triton X-100 is a detergent that acts to permeabilise the membrane, basically by making holes in the membrane.

The next important factor in immunohistochemistry is to determine the optimal concentration of antibody, which gives the best staining with minimal background. This concentration was determined by testing multiple series of different dilutions of antibody. Several endogenous substances may interfere with interpretation of binding, such as endogenous biotin, peroxidase, endogenous fluorescent and endogenous antibody binding capability (Fc receptor) (Chen *et al.*, 2010). However, control experiments where all antibodies or only primary antibodies were omitted did not reveal significant issues. Therefore, a conventional step using donkey serum was applied to ensure that any endogenous antibody binding to receptors was masked. Since all the secondary antibodies used in this project were raised from donkey, donkey serum was chosen as blocking agent. The donkey serum blocks the binding of the antibodies to reactive sites (Fc domain) and allows specific antigen/antibody binding. Donkey serum was used since none of the primary antibodies were raised in donkey, so it is in a different species.

The immunofluorescence technique is one example of immunochemistry methods. Immunofluorescence is very useful when 2 or more fluorescent colours are needed to be used as comparison or to look at relationship between proteins (Figure 2.1). Utilising fluorophores with different excitation and emission spectra and appropriate filter sets allows labelling of different tissue constituents with separately identifiable colours and so co-localisation of different markers to be examined. Typical fluorophores were used in this thesis (see also Fig. 2.1) such as DAPI (4′,6-diamidino-2-phenylindole) to label cell

nuclei, which has maximum excitation by light at 350 nm and emits at >470 nm. This is seen as blue labelling. Alexa^{488} typically conjugated to a secondary antibody, with a maximum excitation wavelength of 490 nm and emission > 525 nm. This is visualised as green labelling. Alexa^{555} either conjugated to a secondary antibody or to streptavidin, maximum excitation at 555 nm and emission at > 580nm. This is visualised as red.

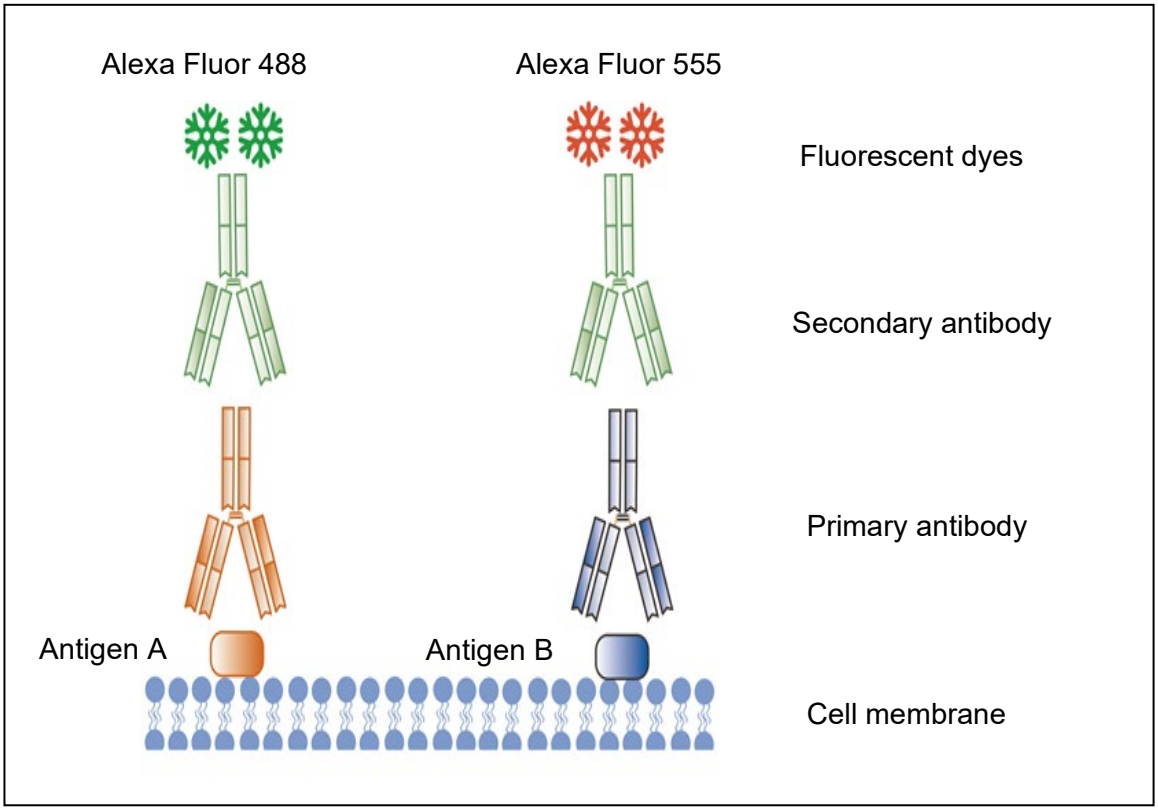

Figure 2.1 Principle for immunofluorescence.. Antigen-antibody interaction using the immunofluorescent technique. Antigen A or B expressed on the surface of a cell is first bound by the primary antibody. Subsequent incubation with the secondary antibody conjugated to fluorescent dyes such as Alexafluor ^{488} (green) or Alexafluor ^{555} (red) results in it binding to the primary antibody.

2.2.2 Protocol for immunolabelling

In order to section the spinal cord transversely, the appropriate region(s) of the spinal cord were first separated from the entire spinal cord. About 1 – 2 mm of spinal cord tissue was then transversely sliced using a scalpel blade and glued to a metal plate with super glue. Once the tissue had fully adhered, the plate was inserted into the bath chamber of the vibrating microtome. The bath contained 0.1M PB in which the tissue was submerged to avoid dryness or dehydration. A sharp razorblade (Campden Instruments) was secured onto the microtome to cut the tissue to the required thickness. The spinal cord tissue was sectioned transversely at a thickness of 50 µm.

For brain tissue, the entire brain was tightly fixed the on metal plate with the coronal plane facing upright then transversely cut to gain 50 µm thick sections containing the dentate gyrus. The same technique was employed for brainstem. All sections were collected and placed into 0.1M phosphate buffered saline (PBS) in designated wells in 24 well plate.

The sections were blocked with 10% donkey serum (100 µl in 900 µl of PBS) for 30 minutes on a shaker to enable thorough mixing and access of the solution to all surfaces of the sections. After that, the sections were washed with phosphate buffered saline (PBS) for 3 times 5 minutes each. Then, the primary antibody was added into experimental wells with the required concentration in PBS with 0.1% Triton (PBST) (Table 2.2). Both experimental and control wells were left in the cold room at 4° C on a shaker overnight. On the next day, the solutions were removed, and sections washed with PBS for 3 times 5 minutes each. Then the sections were incubated in the appropriate Alexa-conjugated secondary antibody (1:1000 PBS) for 2 hours on shaker, see Table 2.3. When secondary fluorescent antibodies were added, all tissue was protected from light to prevent samples being photo-bleached. After 3 washes, the sections were mounted onto glass slides using Vectashield with DAPI (4′,6-diamidino-2-phenylindole)

or without DAPI. Then the sections were covered with a glass coverslip which was secured with nail polish. DAPI emits blue fluorescent colour when bound to DNA and is used to label the nucleus of cells.

Table 2.2 List of primary antibodies

Antibody	Concentration	Raised in	Specificity	Company
5-HT	1:1000	Rabbit	used to identify 5-HTergic projection (García-González *et al.*, 2017)	Neuromics; RA2 0080
S100β	1:750	Rabbit	Used to identify mature astrocytes (Wang and Bordey, 2008)	Abcam; ab52642
PanQKI	1:100	Mouse	Used to identify Oligodendrocytes (Hardy, 1998).	UC Davis/NIH Neuromab Facilities, Lot # 443.2ks.51.
Tuj1	1:500	Rabbit	Used to identify neurons (Akamatsu *et al.*, 2005).	Proteintech
HUC/D	1:1000	Rabbit	Used to identify neurones (Butler-Ryan and Wood, 2021)	Proteintech; Cat No. 13032-1-AP
Iba1	1:1000	Rabbit	Used to identify migroglia (Wendeln *et al.*, 2018)	Wako Wako Chemicals USA; Cat No. 019-19741 A

Permeabilisation agent used was PBST – PBS with 0.1% Triton-X100

Table 2.3 List of secondary antibodies

Antibody	Concentration	Raised in	Specificity	Company
Alexafluor ^{555}	1:1000	Donkey	Rabbit	Invitrogen
Alexafluor ^{488}	1:1000	Donkey	Rabbit	Invitrogen
Alexafluor ^{488}	1:1000	Donkey	Mouse	Invitrogen
Streptavidin ^{555}	1:1000	-	-	Invitrogen

2.2.3 EdU (5-ethynyl-2'-deoxyuridine) detection method

In proliferation and differentiation studies, detection of proliferating cells is a crucial technique in order to quantify the numbers of these cells. The techniques that researchers adopted either use endogenous proliferation markers in the cell itself or use addition of a thymidine analogue such as BrdU or EdU that bind to proliferating cells (Figure 2.2) (Zeng *et al.*, 2010). BrdU and EdU are popular non-radioactive markers but Edu is the marker of choice here. This is because the EdU protocol maintains structural and antigenic integrity of neural tissues to accommodate high resolution, multiple-fluorescence microscopy with antibodies to neuronal and non-neuronal markers. The EdU protocol is also compatible with the deoxyribonucleic acid (DNA) intercalating dye, which is 4′,6-diamidino-2-phenylindole (DAPI). This method covalently binds an azide to an alkyne. It utilizes a copper catalyst and an azide modified fluorescent dye to form a stable triazole ring that can be seen under a fluorescent microscope (Cappella *et al.*, 2008). This method is relatively faster and independent of denaturing steps required to access the DNA when using other thymidine analogues such as 5-bromo-2'deoxyuridine (BrdU) (Buck *et al.*, 2008). This technique using click chemistry approach which is an azide-alkyne cycloaddition. Kolb *et al.* (2001) defined Click chemistry as a reaction that

must be modular, broad in scope, provide very high yields and produce only innocuous by-products that can be eliminated by nonchromatographic techniques, and be stereospecific.

EdU was either added to the aCSF or injected into animals as described below then animals were perfused, tissue removed and sectioned or the slices were fixed. For the EdU detection method, firstly, the sections were incubated in 0.2 % Triton X-100 PBST for 20 minutes to permeabilise the cell membrane. Then, this was followed by 10-minute washes in 0.1 M Tris buffer (Trizma base powder 0.695 gm, Trizma hydrochloride powder 3.03 gm, 500 ml distilled water, pH 7.6). After that, the sections were incubated in 320 µl of distilled water, 25 µl of 2 M Tris Buffer, 50 µl of 10 mM of copper sulphate, 5 µl of biotinylated picolyl azide 1 mM and 100 µl of ascorbic acid for 30 minutes followed by wash with Tris buffer (0.1 M) (Table 2.4). Finally, the sections were incubated in streptavidin ^{555} (1:1000 in PBS) for 2 hours before mounting onto slides with vectashield with 4',6-Diamidino-2-Phenylindole, Dihydrochloride DAPI (Corns *et al.*, 2015). The proliferating cells were labelled using the streptavidin ^{555} and appeared red in colour and scattered throughout the whole area of spinal cord, brainstem and hippocampus area.

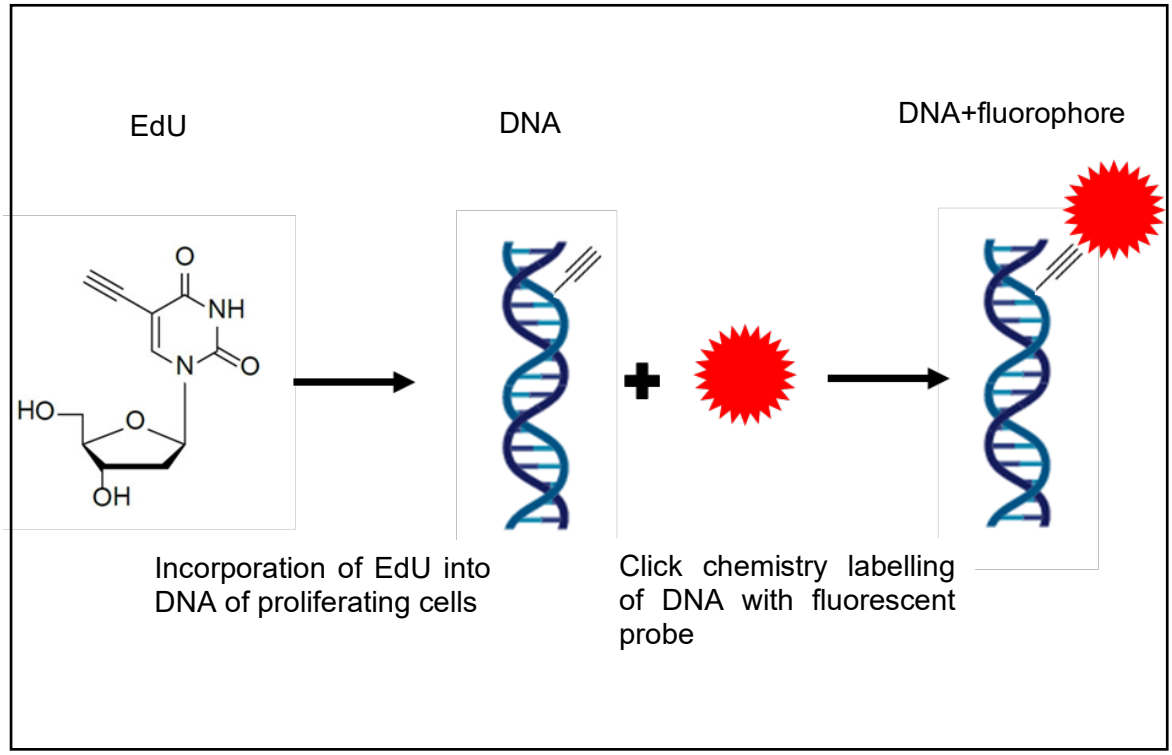

Figure 2.2 Principle of EdU assay. EdU incorporates into the DNA of newly proliferated cells and a fluorescent probe is attached to the EdU using click chemistry as described in the text.

Table 2.4 List of chemicals / solutions that were used in EdU-labelled protocol

Chemicals / Solutions	Properties
0.2 % triton	Permeabilise the cell
0.1 M Tris	Buffer agent
2 M Tris	Buffer agent
Copper Sulphate	Catalyst azide-alkyne click reaction
Biotin Picolyl Azide	linker with an azide group for attachment to alkynes (EdU), a biotin binds to streptavidin
Ascorbic Acid	Activate the reaction

2.3 *In vivo* experiments

In vivo in latin means “in living thing”, when the experiments are conducted in live animals, to recreate a setting as natural as possible that can mimic most closely the human population. Using rodents, especially mice or rats, as experimental models is widely used in the *in vivo* setting. This experimental setting is very important to understand responses in the whole body where there are many conditions that need to be considered such as metabolism, tissue distribution, excretion of chemicals and their metabolites and side effects.

2.3.1 Administration of Fluoxetine Hydrochloride

In order to determine the effects of modulation of serotonin on cell proliferation and differentiation, fluoxetine hydrochloride (flx) was used because it promotes a high extent of cell proliferation in hippocampus when injected intraperitoneally for 10 days (Faillace *et al.*, 2015). Flx is a selective serotonin reuptake inhibitor (SSRI) that blocks reuptake of 5-HT and promotes increases in 5-HT in the synaptic region.

Eight mice weighing 20-25 gwere placed in 2 groups of 4 animals, on 12-hour light/dark cycles and had access to food and water at all times. Flx (10 mg/kg; HelloBio, Bristol,UK; HB1600) and vehicle (saline) were delivered daily for 10 days. On the last 5 days, EdU (10 mg/kg; Carbosynth, Berkshire, UK; NE08701) was co-administered. They were injected intraperitoneally (i.p) (Figure 2.3). The animals were sacrificed on day 11 as described above for immunofluorescence, then the EdU detection method was followed by immunofluorescent methods to detect differentiation markers, carried out as above. Both flx and EdU were dissolved in distilled water/saline.

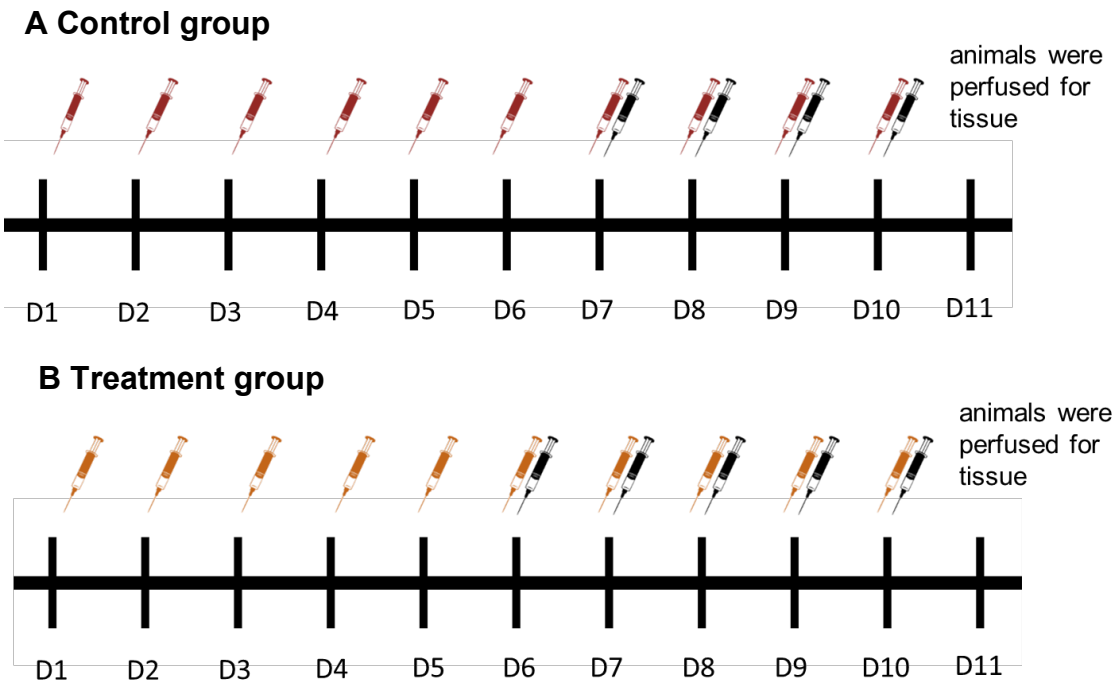

Figure 2.3 Protocol for *in vivo* experiment using fluoxetine. (A) In control group, animals were injected with saline (red syringe). (B) In treatment group, fluoxetine (orange syringe) was injected intraperitoneally for 10 days. EdU (black syringe) was injected for the last 5 days of treatment in both control and treatment groups.

2.3.2 Administration of Tegaserod Maleate

The second set of *in vivo* experiments involved investigation of a specific 5-HT receptor that has the potential to modulate cell proliferation. In previous experiments, activation of 5-HTR4 receptors using tegaserod maleate (a 5-HT4 partial agonist) resulted in greater numbers of proliferating cells in the enteric system of mice (Liu *et al.*, 2009). Tegaserod was used since, although cisapride (a 5-HTR4 full agonist) was found in an *in vitro* experiment to increase cell proliferation in the ependymal cell region around the central canal of spinal cord (this thesis), it is generally avoided for *in vivo* studies because of the risk of cardiac arrhythmia (Landrum Michalets and Williams, 2000).

Eight mice weighing 20-25 gwere housed in 2 groups of 4 animals, experimental group and control group. In the experimental group, tegaserod maleate (1 mg/kg; Tocris

Biotechne, Abingdon UK; 4613) dissolved in saline with 0.5% dimethyl sulfoxide (DMSO) (which was used as vehicle for control group) was injected intraperitoneally on a daily basis for 7 days. EdU injections as above were given daily for 7 days, at the same time (Figure 2.4). Animals were left for 7 days and were sacrificed on day 15 of the experiment then the EdU detection method was followed by immunofluorescent labelling for differentiation markers.

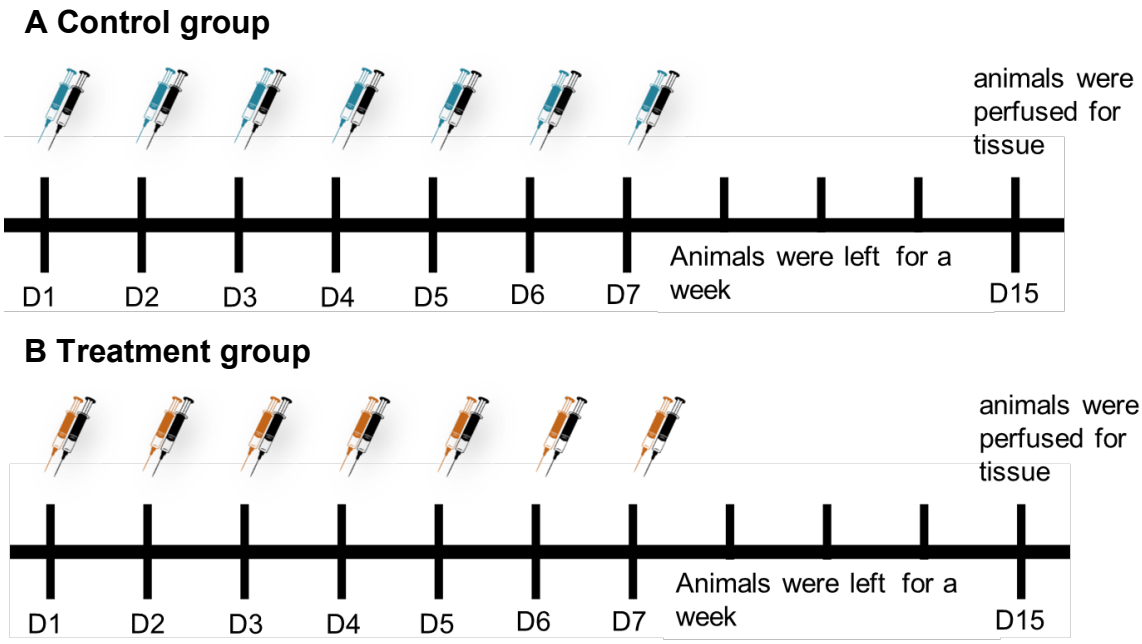

Figure 2.4 Protocol for *in vivo* experiment using tegaserod. (A) In control group, animals were injected with vehicle contained saline and 0.5% DMSO (blue syringe). (B) In treatment group, tegaserod (orange syringe) was injected intraperitoneally for 7 days. Both groups received EdU (black syringe) at the same time for 7 days of treatment.

2.4 *In vitro* experiments

In vitro experiments are very important to understand the fundamental biological effects when the environment of the tissue or cell can be controlled locally. Using this experimental setting, multiple drugs could be tested separately on the same tissue in

one animal, or different concentrations of drugs also could be applied to establish which concentrations were effective in changing the extent of proliferation.

2.4.1 Experimental procedure

The spinal cord slices were prepared as described in section 2.1.4 then divided into groups which were control group and experimental group. The slices were incubated in vials filled with aCSF (4 ml for each vial) for 30 minutes then EdU (4 µl of 1 mM) was added to each vial. Different agonists (Table 2.5) were added to their respective vials. All vials were oxygenated with 95% oxygen and 5% carbon dioxide and placed in a water bath at 37° Celsius (Figure 2.5). The agonists and EdU were changed every hour and the spinal cord slices were fixed in 4% PFA 0.1 M PB overnight after 4 hours' treatment with the drug (Banasr *et al.*, 2004). The 4% PFA was changed to 0.1 M PB solution. After that, the 500 µm spinal cord slices were embedded in 10% gelatin in distilled water (Sigma Aldrich-gelatin from porcine skin) so that transverse sections could be cut on the vibratome and left at 4° C for 1 hour to solidify before fixing the gelatin with fixative (8% PFA in 0.2 M PB) for 4 hours. Upon fixation of the gelatin blocks, the sections were re-sectioned into 50 µm sections, using a vibrating microtome (Leica VT 1000S, Microsystems). The sections were then collected into 24 well-plates containing PBS (1 ml). After that all re-sectioned slices underwent processing for EdU as described above for identification of cell proliferation.

The method that was described above was adopted for two cohorts of *in vitro* experiments which were on Experiment 1 (5-CT vs 8-OHDPAT) and Experiment 2 (cisapride vs α-methyl-5HT-maleate). The process of embedding and re-sectioning had to be carefully done in order to get the complete whole section of the spinal cord. During the embedding step, the section had to be held as flat as possible in the gelatine however, the holding process could damage the sections. Sometimes the fixation

process after the incubation made the spinal cord section become curled or folded, which made the flattening process difficult and the risk of losing the spinal cord sections very high. Since there was an issue with the embedding and re-sectioning of the spinal cord sections, a new method using 250 µm thickness of spinal cord without re-sectioning was adopted for the final cohort (Experiment 3, Tegaserod). Viewing thick sections under fluorescent microscope is difficult, however, this problem was resolved by introducing a clearing step.

Tissue clearing method made the section become transparent. The tissue is composed of lipids and proteins, all of which vary in how they interact with light that propagates through the tissue. Its refractive index (RI), how much slower light propagates through a given substance compared to a vacuum, is among the properties that differ between these components. When a material contains a mix of small - sized components with different RIs, the interactions between light and these heterogeneous components lead to a lack of transparency (Richardson and Lichtman, 2015). Tissue clearing methods enhance transparency by homogenizing a sample's RI through the removal, substitution and alteration of some of its components.

Table 2.5 List of agonists for in vitro experiments

Agonist (*in vitro*)	Agonist at which receptor	Concentration (µM)	Incubation
Cisapride	5-HTR4	1 and 10	4 hours
Alphamethyl-5HT-maleate	5-HTR2	1 and 10	4 hours
8-OH-DPAT	5-HTR1A	30	4 hours
5-CT	5-HTR1A	1	4 hours
Tegaserod maleate	5-HTR4	0.1 and 1	4 hours

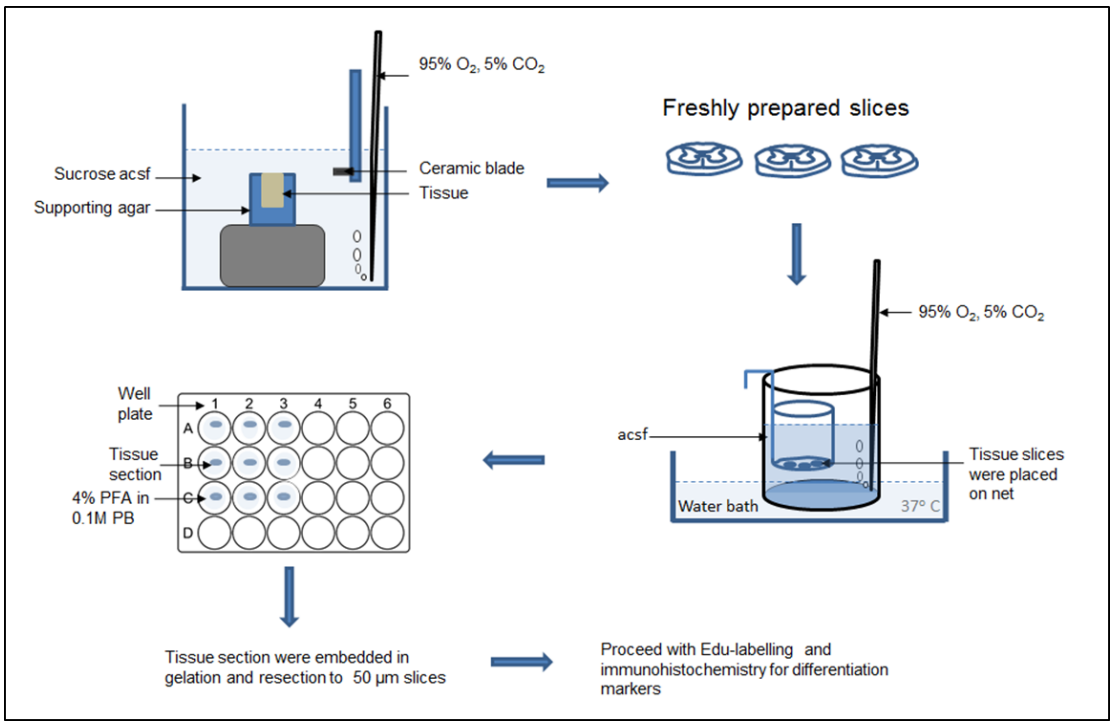

Figure 2.5 Acute slices technique

2.4.2 Clearing method

Adding a tissue clearing step in the EdU or immunostaining protocols provided a better view for analysis of the sections. The clearing methods Sca*l*es was performed. In this method, the main components are urea, sorbitol and glycerol. Urea causes hydration, leading to expansion of the tissue, while sorbitol causes dehydration, leading to tissue shrinking. Therefore, by regulating each component's concentration ratio it was possible to achieve tissue clearing while preserving the original sample volume, even though there was a process of expansion and contraction. Glycerol could further counterbalance the expansion of the urea-induced tissue and encourage more dehydration; sorbitol is hydrophilic but glycerol is amphipathic and is expected to target regions of lipophilic tissue (Hama *et al.*, 2015).

In my study, the clearing method was applied for spinal cord sections of 250 µm thickness. After acute slices were processed for the EdU-labelling protocol, slices were fixed in 4% PFA in 0.1M PB for 1 hour, then placed into 0.1M PB. The clearing solution (isosca*l*e SQ solution, Table 2.6) was warmed in the water bath at 37°C, because at room temperature, the solution crystallizes. After the crystals had dissolved, a suitable amount of the solution was taken out and put in a well plate to ensure that it was enough to just cover the sections. Then, the well plate was left floating in the water bath for 45 min to 1 hour. The timing was very crucial here because**,** longer periods of incubation time might damage the sections. After 1 hour, the clearing solution was replaced with Sca*l*e S4(0) solution (Table 2.7). This is the solution in which they were mounted. The sections were placed onto a glass slide and left to dry at room temperature. Since the solution was quite thick, after a few minutes of drying, there was still some solution left on the sections. However, the solution did not interfere with the mounting process. The sections were mounted with vectashield with or without DAPI, then the cover slip was gently placed onto the sections to make sure the pressure applied did not damage the sections. The coverslip was sealed with nail polish. The section did spread out a little bit when the coverslip was placed during the mounting process but the shape of the section and the fluorescence was still intact.

Table 2.6 Components of Isosca*l*e SQ solution

Component	Molarity / percentage
Urea	9.1 M
Sodium Chloride	200 mM
Triton	2 %
D-sorbitol	22.5 %

Table 2.7 Components of Scale S4(O) solution

Component	Molarity / percentage
D-sorbitol	40 %
Glycerol	10 %
DMSO	15 %
Urea	4 M

2.5 High-Fat diet experiment

2.5.1 Animals

C57/Bl6 male mice, aged 5 weeks, were housed in 4 cages, five animals per cage. The mice were acclimatised for a week and body weight, food intake and water intake were monitored as baseline measurements before starting with different diets. In this set of experiments, acclimatisation is very important to make sure animals were familiar with the surroundings and therefore eat and drink enough throughout the experiment without stressful conditions. They could freely access food and water and were subjected to 12/12 day/night cycle. They were divided into four groups. Three groups were fed with a high fat diet [60% kcals from fat (lard), Table 2.8] and 1 group was fed with a low-fat diet (10%, Table 2.9). Body weight, water and food intake were measured twice in a week during the experimental period. The weighing was not done every day to avoid any stress to mice that can make them eat less. Each mouse has an individual notched system (Figure 2.6) to enable identification. The first mouse (M1) did not have any notch, second mouse (M2) had notch code 1, third mouse had notch code 3, fourth mouse had notch code 8 and fifth mouse had notch code 10. For ear notching, the mouse was picked up from the cage by holding the tail and placed the mouse on the cage lid. After that, the mouse was firmly restrained using the scruff technique by grasping the loose skin behind

the neck. An ear puncher (Roboz Surgical Instruments Co.) was used to make a hole in the ears follow the Ear notching chart provided by Central Biomedical Services, University of Leeds (Figure 2.6).

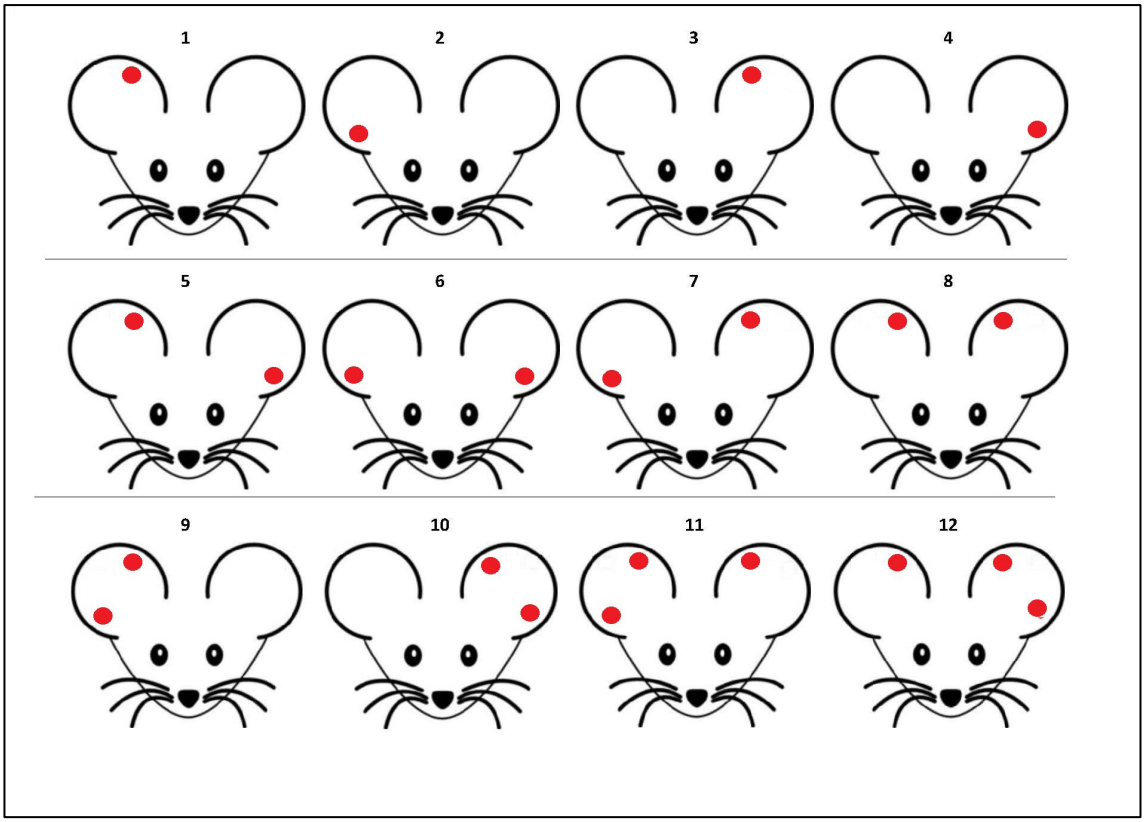

Figure 2.6 Ear notching chart. The ear notching code was used to identify individual mice in shared cage.

2.5.2 Glucose tolerance test (GTT) and Insulin tolerance test (ITT)

In high-fat diet experiments, measurement of glucose tolerance and insulin tolerance before starting the diet, during the diet and after the diet is critical.

2.5.2.1 Preparing animals for fasting

To put mice on a fasting period, food was removed, the mice were transferred to new and clean bedding to avoid mice eating food particles that fall onto the bedding. An empty hopper was placed in the cage with a drinking water bottle. Water was allowed during the fasting period.

2.5.2.2 Method restraining mice

A mouse restrainer was used to hold the mouse during the tail vein blood sampling. The red acrylic cylinder strainer had an adjustable head gate and end plate. The mouse was picked up from the cage by the tail and was allowed to walk in through the tail gate, once the mouse was in the cylinder, the tail gate was closed, with the tail outside the cylinder. Then the head gate was moved to the mouse head and tightly screwed to make sure the mouse was safely secured in the restrainer, before performing the vein blood sampling.

2.5.2.3 Protocol for GTT

Animals were fasted overnight but for not more than 16 hours. 10 % glucose was prepared fresh on the day of the procedure. One gram of glucose was diluted in 10 ml of PBS and was mixed until fully dissolved. The solution was filtered using 0.2 µm syringe filter (Minisart PES, https://www.scientificlabs.co.uk/product/16541K. Fasting blood glucose was recorded using a glucometer (Abbott Freestyle Optium Neo, https://freestylediabetes.co.uk).Tail vein blood samples were collected from the tail through a small incision that was made (about 1 inch from the tail end) using a scalpel blade. The blood was dripped onto a glucometer strip (Freestyle Optium, https://freestylediabetes.co.uk) and the measurement was recorded in mmol/L. After

fasting blood glucose levels were recorded, the mice were intraperitoneally injected with 10 % glucose solution with the appropriate volume of solution according to the individual mouse weight to allow 1mg/g glucose. Then the glucose level was recorded again at 30 minutes, 60 minutes, 120 minutes and 120 minutes after glucose injection (Figure 2.7)

Date of experiment					Concentration of D-Glucose solution 10%							
Start fasting					Injection amount is 1mg/g							
End fasting					Glucose reading in mmol/L							
Total fasting (hours)	00:00											
Mosue ID	**Ear code**	**Genoytpe**	**Diet**	**Age**	**Weight (g)**	**Volume (10% glucose) (ul)**	**Glucose level, mmol/L**	**Injection time**	**30'**	**60'**	**90'**	**120'**
						0			00:30	01:00	01:30	02:00
						0			00:30	01:00	01:30	02:00
						0			00:30	01:00	01:30	02:00
						0			00:30	01:00	01:30	02:00
						0			00:30	01:00	01:30	02:00
						0			00:30	01:00	01:30	02:00
						0			00:30	01:00	01:30	02:00

Figure 2.7 Measurement of GTT. Glucose readings were recorded in an Excel table for every mouse. 10% glucose solution was intraperitoneally injected according to the weight of the individual mouse and glucose readings were recorded for fasting, 30, 60, 90 and 120 minutes (2 hours after injection).

2.5.2.4 Protocol for ITT

The animal was fasted for 2 hours before the procedure. Insulin (0.75 IU/kg) was prepared fresh on the day of the experiment and diluted in PBS. The insulin was prepared in individual insulin syringes according to the weight of every mouse. Fasting blood glucose was recorded after 2 hours of fasting time, then insulin was injected. Glucose levels were measured at 30, 60, 90 and 120 minutes after injection time (Figure 2.8). The function of insulin is to convert glucose to glycogen and some mice might experience hypoglycaemia. Therefore, during the procedure, mice were observed for any hypoglycaemia signs such as weakness, lethargy or reduced activity or if the glucose level dropped below three mmol/L, i.p injections of 10% glucose were administered.

Date of experiment
Start fasting
End fasting
Total fasting (hours) 00:00

Concentration of Insulin in PBS 0.1 IU/ml
Injection dose is 0.75 IU/kg
Glucose reading in mmol/L

If glucose need to be injected, use volume in mkl =10xbody weight (in g)

Colony

Mouse ID	Ear code	Genoytpe	Diet	Age	Weight (g)	Volume (insulin) (ul)	Glucose level, mmol/L	Injection time	30'	60'	90'	120'	Comments
									00:30	01:00	01:30	02:00	
									00:30	01:00	01:30	02:00	
									00:30	01:00	01:30	02:00	
									00:30	01:00	01:30	02:00	
									00:30	01:00	01:30	02:00	

Figure 2.8 Measurement of ITT. ITT measurements were recorded in an Excel table above with all information needed for an individual mouse. Fasting glucose levels were recorded 2 hours after fasting then at 30, 60, 90 and 120 minutes after 0.75 IU/kg i.p injection of insulin.

2.5.3 Diet

High-fat diet (http://datesand.com/; F3282) used in this study was formulated to induce and maintain obesity in mice models. It is successfully used in diabetes and obesity studies. The control diet (http://datesand.com/; F4031) was used, also from the same company, so the food has the same smell and same colour as a HF diet. Table 2.8 and Table 2.9 show the nutritional profile in high-fat diet and low-fat diet.

Table 2.8 Nutritional profile in high-fat diet

Component	Percentage (%)	kcal/gm
Protein	20.5	-
Fat	36.0	-
Fibre	0.0	-
Ash	3.5	-
Moisture	< 10	-
Carbohydrate	36.2	-
Calories	-	5.51

Table 2.9 Nutritional profile in low-fat diet

Component	Percentage (%)	kcal/gm
Protein	20.5	-
Fat	7.2	-
Fibre	0.0	-
Ash	3.5	-
Moisture	< 10	-
Carbohydrate	61.6	-
Calories	-	3.93

2.5.4 Preparation of flx in drinking water

In this experiment, flx was delivered using drinking water to avoid stressful events to the mice during the experiment. Flx hydrochloride (HelloBio, Bristol,UK; HB1600) was dissolved in drinking water at 166 mg/L (Scabia *et al.*, 2018) and prepared fresh every week. The control group received normal drinking water.

2.5.5 Experimental procedures for drug administration

After one week of acclimatisation, GTT and ITT procedures were performed. The point when the animal started the high-fat or low-fat diets was considered as week 1 of the experiment. Two of the four groups were then assigned flx given for different time periods (Figure 2.9). All groups were given EdU for five days at week 6. At the end of the 8 week period, after final weighing and GTT and ITT tests, animals were perfused as described above to test for cell proliferation and differentiation in hippocampus, brainstem and spinal cord regions.

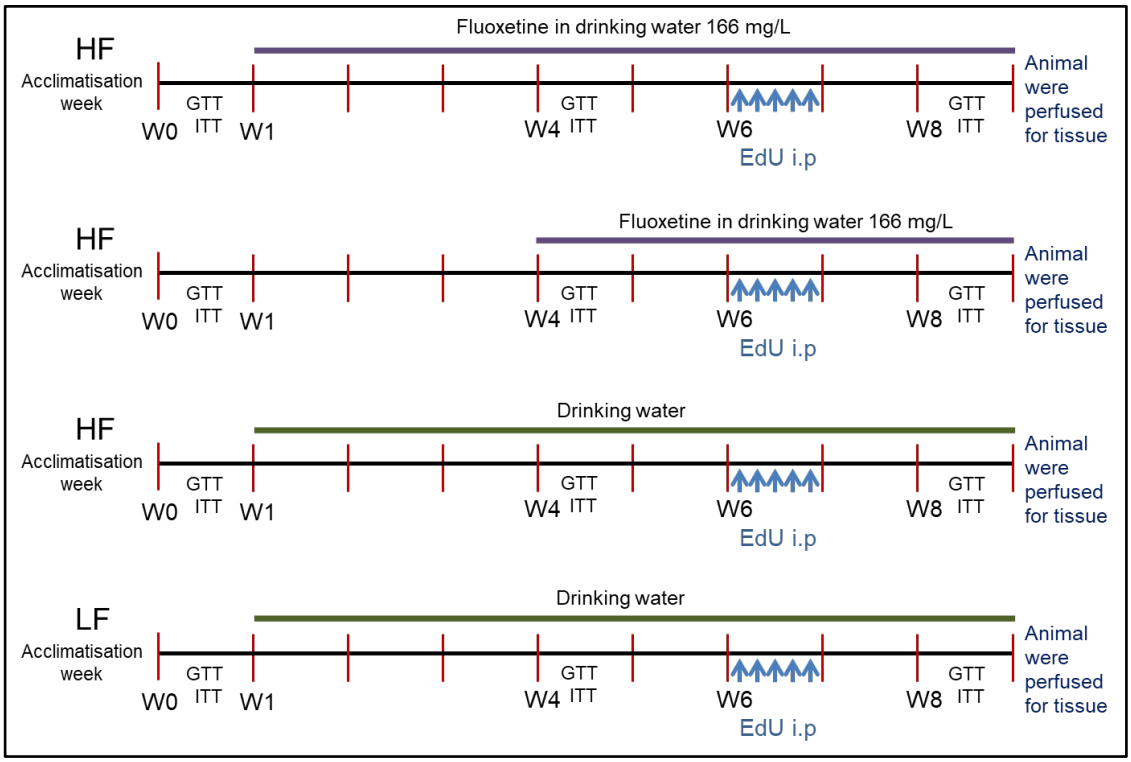

Figure 2.9 Protocol for high-fat diet experiment (n = 5 per group).

2.6 Cell counting

For all experiments, counting of EdU-positive cells and colocalisation with the specific antibody markers was conducted. The counter was not aware (blinded experiment) whether the slices were from the experimental or control groups. The blinding was done before the counting started. The microscope slides that contained the specimen sections were re-labelled by another person using specific codes. However, the identity of the primary antibody was known. The codes were revealed to the counter after counting was completed. Blinded experiments are important to eliminate bias during counting.

I employed manual counting for this experiment since issues were encountered in obtaining images for automated counting such as difficulties to obtain high resolution with multiple tile-region and Z-stack images. This technique also is time-consuming and expensive since each section need to be captured. Manual cell counting is still considered the method of choice in many studies since there were no significant differences between manual and automated cell counting (Cadena-Herrera *et al.*, 2015, Zeidler-Erdely *et al.*, 2016, Kaufhold *et al.*, 2018). González-González *et al.* (2016) suggested that automated cell counting can be applied when appropriate calibrations are obtained. However, in manual counting, human error cannot be eliminated and several precautions were implemented such as one person counting to reduce variability between experimenters and blinded experiments, so that the person did not know the identity of the condition or groups when counting.

In all experiments and regions examined, cells were counted in a number of sections per animal and then the average number of cells per section per animal calculated for further statistical analyses.

2.6.1 Areas for counting

Regions of interest (ROI) for each part of the central nervous system were determined for counting. Averages of 7-12 sections per region were examined for each animal. In hippocampus, the focus was on dorsal dentate gyrus (dDG) while in the brainstem, the specific areas targeted were the dorsal vagal complex (DVC), ependymal cell layer surrounding the central canal, raphe obscurus, inferior olive and pyramid. In spinal cord, all thoracolumbar regions (ependymal cell layer surrounding the central canal, gray matter, white matter) were counted (Figure 1.10).

Figure 2.10 Regions of interest (ROI) in specific areas of the central nervous system. (A-B) Templates were adapted from Gaidica (2015) showing the region of interest in hippocampus and brainstem (red box) and boxed areas are shown immunofluorescent images in Ai-Bi. C. Schematic diagram of thoracic spinal cord adapted from Allen Brain Atlas. (Ci) Immunofluorescent image showing gray matter, white matter and ependymal cell layer.

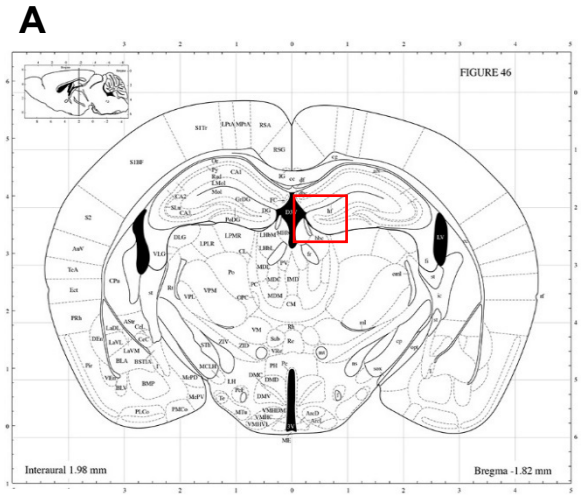
A
FIGURE 46
Interaural 1.98 mm
Bregma -1.82 mm

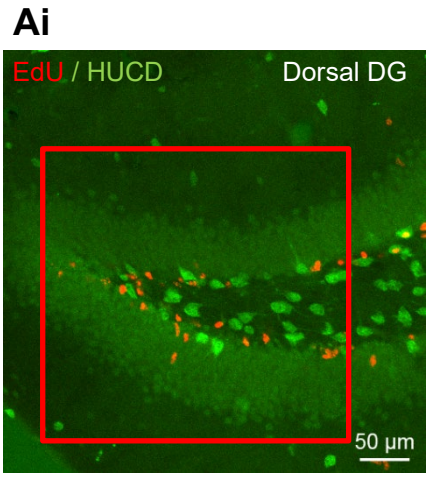
Ai
EdU / HUCD
Dorsal DG
50 µm

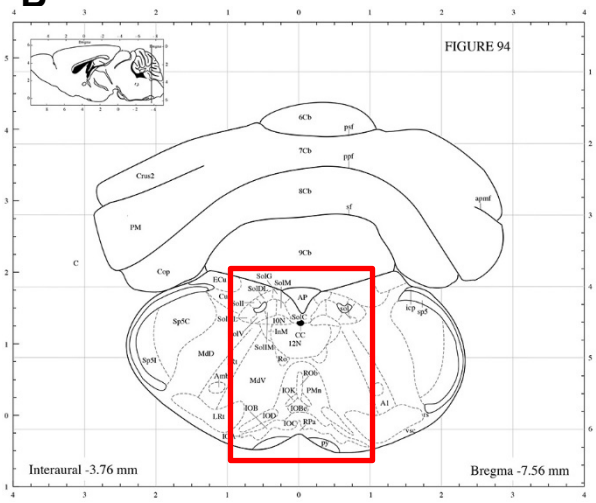
B
FIGURE 94
Interaural -3.76 mm
Bregma -7.56 mm

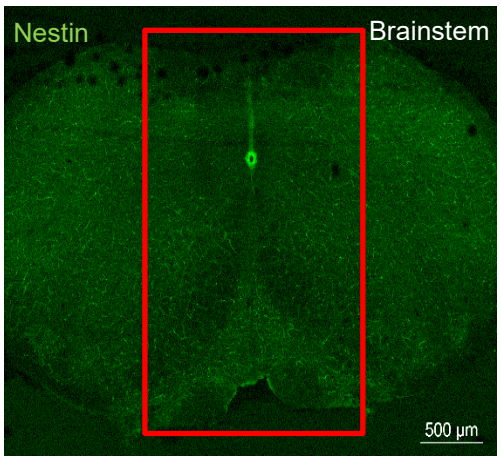
Bi
Nestin
Brainstem
500 µm

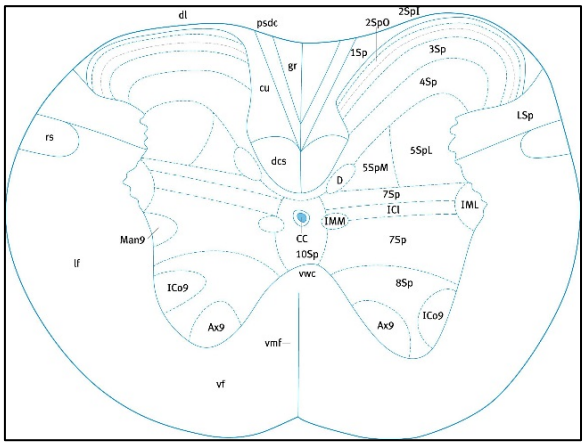
C
dl
psdc
2SpO
2SpI
1Sp
3Sp
4Sp
gr
cu
LSp
rs
dcs
5SpL
5SpM
D
7Sp
ICl
IML
IMM
Man9
CC
10Sp
7Sp
lf
vwc
8Sp
ICo9
Ax9
Ax9
ICo9
vmf
vf

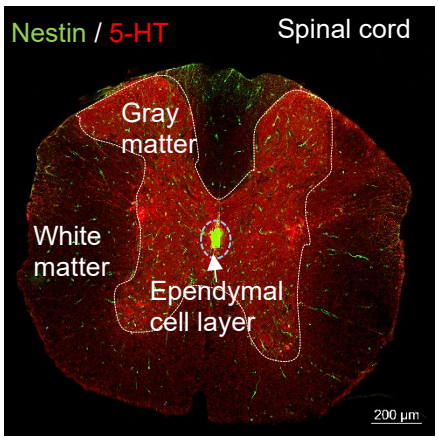
Ci
Nestin / 5-HT
Spinal cord
Gray matter
White matter
Ependymal cell layer
200 µm

2.6.2 Quantification in hippocampus

Sections of bregma level -1.34 mm to -2.92 mm (Gaidica, 2015) were included in the count. The pointed end of the dorsal dentate gyrus (dDG) was positioned at the boundary of the x40 magnification field of view, and only the cells within this field of view were included in the count. Quantification was therefore carried out using NIKON 600 fluorescent microscope. Cells were mapped on a template (Figure 1.11) of the DG adapted from Gaidica (Gaidica, 2015). Counts were given as a total number of EdU positive cells per 50 µm section and the percentage of EdU-positive cells colocalised with the antibody marker was determined.

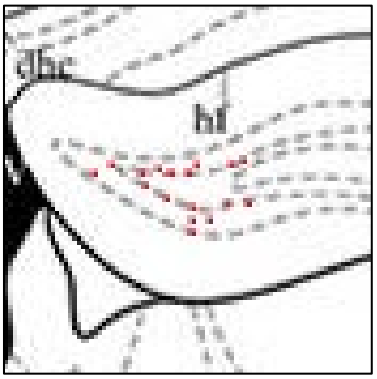

Figure 2.11 Example of EdU-positive cells annotated map in hippocampus Picture of dDG of hippocampus showing the location of proliferating cells.

2.6.3 Quantification in caudal medulla

The counting of EdU-labelled cells and those differentiation markers that colocalised was conducted on blinded sections. The bregma level of each section was determined using an atlas of the mouse brainstem, only sections identified to be of bregma level -6.72 mm to -7.76 mm were included, in accordance with the location of the DVC (Gaidica, 2015). Mapping and quantification were performed at 40x magnification using NIKON 600 fluorescent microscope. Counts were given as a total number of EdU positive cells per 50 µm section and the percentage of EdU-positive cells colocalised with the antibody marker was determined. Fluorescent images for each marker were obtained.

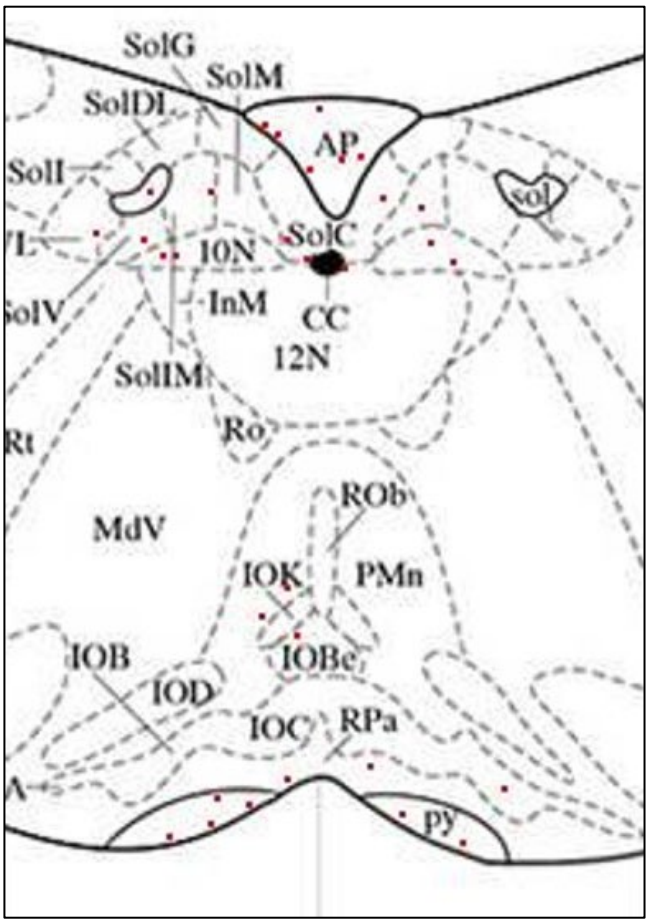

Figure 2.12 Example of EdU-positive cells in an annotated map in selected brainstem areas Picture of brainstem showing the mapped proliferating cells.

2.6.4 Quantification in the spinal cord

EdU-positive cells were counted in whole spinal cord then divided into the central canal region, gray matter and white matter area (see figure 2.10). The ependymal cell layer was identified as the area within 10 µm of the abluminal edge of the ependymal cells and could be visualized directly through the NIKON 600 microscope under 40x magnifications (Corns *et al.*, 2015). Cells were mapped and counted Counts were given as a total number of EdU positive cells per 50 µm section and the percentage of EdU-positive cells colocalised with the antibody marker was determined.

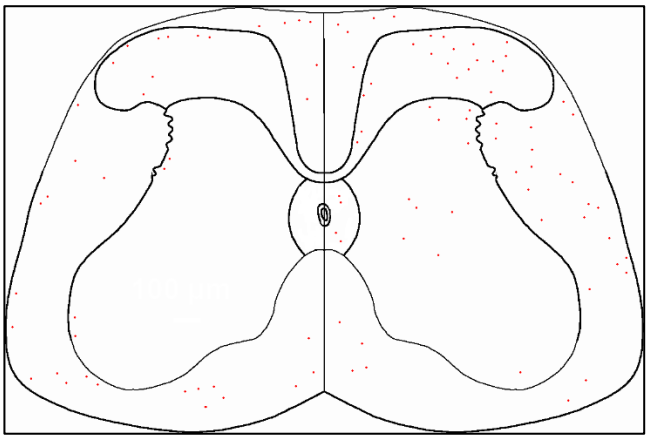

Figure 2.13 Example of annotated map of EdU-positive cells in spinal cord Picture of spinal cord showing the mapped proliferating cells.

2.6.5 Quantification for co-localisation

Co-localisation was counted as percentages of EdU-positive cells that co-localised with the different antibody markers which label s100β for astrocytes, PanQKI for oligodendrocytes and HUC/D for neurones. Example of co-localisation of EdU positive cells with markers for differentiated cell in spinal cord (Figure 2.14) and example of annotated image for co-localisation in brainstem (Figure 2.15).

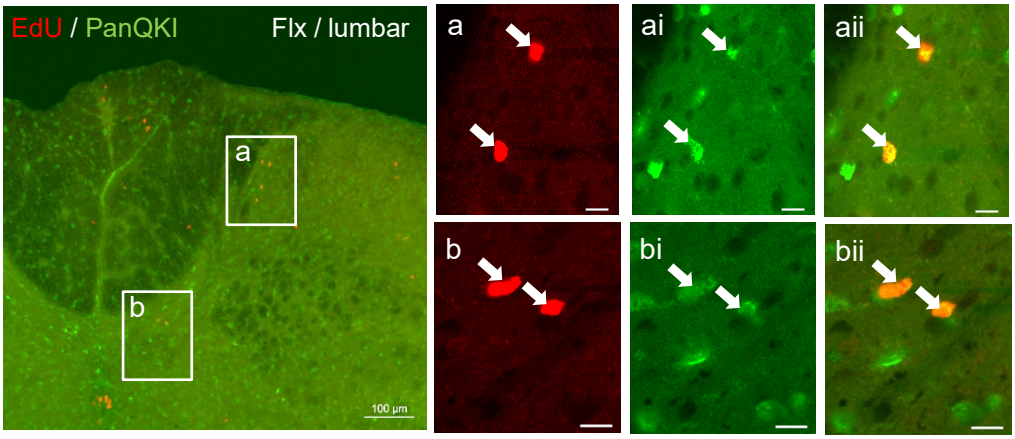

Figure 2.14 Example of co-localisation of EdU+ve cells with markers for differentiated cells Immunofluorescence images of spinal cord showed co-localisation of EdU-labelled cells (red) with anti-PanQKI (green) (aii-bii). Scale bar = 10 µm

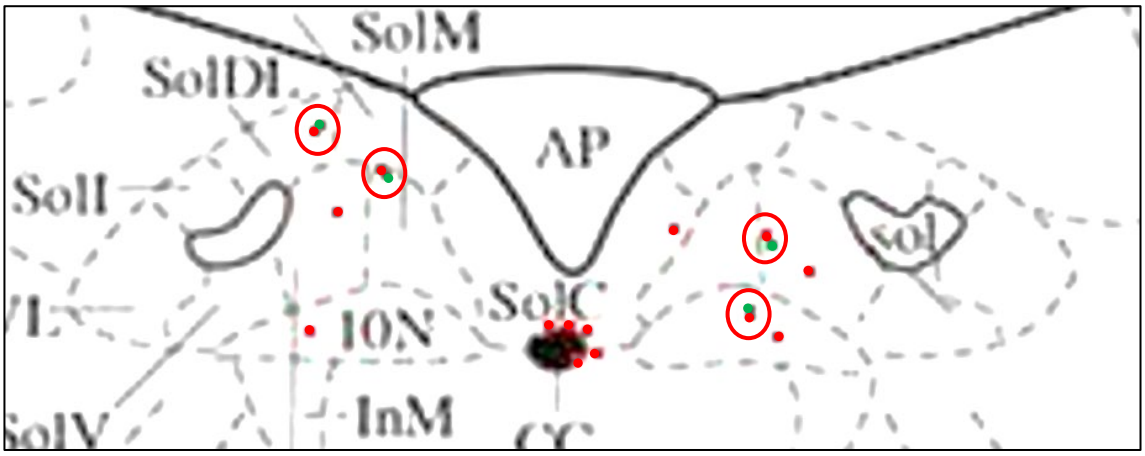

Figure 2.15 Example of annotated image of co-localisation between Edu+ve cell (red) with marker for differentiated cell (red) Picture of brainstem showing the mapped co-localisation (red round shape) of proliferating cell (red) with marker for differentiated cell (green).

2.7 Sample size estimation

Even though power analysis approach is recommended for calculating sample size, in some experiments with no reference to standard deviation and effect size, an alternative to the power analysis approach for determining the sample size in animal study is the 'resource equation' approach (Festing and Altman, 2002) . Therefore, sample size for each experiment was estimated using 'resource equation' approach. Using resource equation approach, the sample size estimation was 6 mice per group for *in vivo* experiments which are fluoxetine and tegaserod experiments. However, previous experiments in our laboratory (Corns *et al.*, 2015) had indicated that significance was reached at 4 mice per group in similar experiments. Therefore, 4 animals per group were used and since significance was reached for proliferation, analysis was carried out on 4 mice per group to due to practise of the 3R. For *in vitro* experiment the sample size estimation was 4 mice per group. In the high-fat diet experiment, the sample size estimation was 5 mice per group.

2.8 Analysis of data

All data were entered and analysed using the GraphPad Prism 8. All the data were checked for normality using Shapiro-Wilk Tests then parametric tests were used for normally distributed data and non-parametric test used for non- normally distributed data. The data were shown as mean ± standard error of mean (SEM). Independent t-test (parametric) or Mann Whitney test (non-parametric) was used to compare means between two groups and one-way ANOVA (parametric) or Kruskal Wallis (non-parametric) was used to compare means between the groups. When ANOVA revealed significant effect ($p<0.05$), Bonferroni post-hoc test was applied. For correlation, Pearson correlation was performed. P-values less than 0.05 ($p<0.05$) were indicated as the significant level. The data are presented in either histogram, line graph or table format.

2.9 Obtaining images

All sections were first visualised under a fluorescent Nikon Eclipse E600 microscope to confirm labelling with appropriate antibodies and EdU and for manual counting. By changing the focus, counts of cells throughout the Z axis were made. Then, to take better images for presentation, sections were also imaged using Zeiss LSM880 upright or inverted Confocal microscope with Airyscan laser scanning microscope equipped with argon and He-Ne lasers using both 20x and 40x objectives to take better images for documentation. The images presented are either single plane or Z-stacks with maximum intensity fluorescence projection.

Chapter 3

DO 5-HTERGIC FIBRES HAVE CLOSE APPOSITIONS TO NESTIN-GREEN FLUORESCENT PROTEIN (GFP) CELLS?

3.1 Introduction

The location of the 5-HTergic fibres and the relationship of these terminals to neural stem cells could complement and inform investigation of the effect of 5-HT on neural stem cells. Nestin is an intermediate filament protein type VI that is expressed in normal cells in different tissues and organs. Nestin positive cells have the characteristics of multilineage and regenerative potential due to the capability of these cells to develop into the neuroectodermal, endodermal and mesodermal lineage. Furthermore, nestin is thought to be expressed exclusively by neural stem and progenitor cells (NPC) in developing and adult animals (Lendahl *et al.*, 1990). It is therefore suggested that nestin could be a marker for neural stem cells in the spinal cord. In a spinal cord injury study, (Namiki and Tator, 1999) showed that after injury there was an increase in proliferating cells and an associated increase in nestin expression, seen in the ependymal cell layer and adjacent region near the central canal, suggesting migration of ependymal-nestin-positive cells in response to clip compression injury.

Nestin-enhanced green fluorescent protein (Nestin-EGFP) mice were created by Mignone *et al.* (2004) using a fragment of the nestin gene. They produced Nestin-EGFP construct in which the enhanced version of GFP (EGFP) expression was under control of the 5.8 kb promoter and the 1.8 kb second intron of the nestin gene. The fragment

was used for pronuclear injection to fertilised oocytes from C57Bl/6 x Balb/cBy hybrid mice. All three lines from these mice produced an identical pattern in EGFP expression (Mignone *et al.*, 2004). Thus, due to the success of nestin-EGFP transgenic mice in generating Nestin-EGFP expression, this type of mouse was mated with C57Bl/6 mice (wild type) to create a further generation of nestin-EGFP mice. In this transgenic line, (nestin) GFP is selectively expressed in progenitor cells and pericytes (Birbrair *et al.*, 2013, Licht *et al.*, 2016), and diminishes in differentiated cells; allowing for the identification and isolation of neural stem cells (NSCs) (Mignone *et al.*, 2004).

Therefore, this study utilised the nestin-EGFP mice to locate nestin-positive (putative neural stem) cells and combined this with immunofluorescence staining to detect the 5-HTergic neurones and fibres.

3.2 Hypothesis

1. There is close proximity of 5-HTergic fibres to nestin-EGFP positive cells in the brainstem and spinal cord.

3.3 Aims

1. To investigate the location of 5-HT neurones and 5-HTergic fibres in the brainstem and spinal cord
2. To investigate the location of nestin-EGFP cells in brainstem and spinal cord.
3. To observe the relationship between 5-HTergic fibres and nestin-EGFP cells in the brainstem and spinal cord.

3.4 Materials and methods

3.4.1 Animals

Male transgenic nestin-EGFP mice were mated with C57BL/6 (wild-type, WT) females. They were bred in-house as heterozygotes, housed in standard conditions with 12-hour light and dark cycle and had access to food and water *ad libitum.* Nestin-EGFP mice of either sex (n = 4), aged 6-8 weeks were used. Every effort was made to minimise the number of animals used and their suffering. All the protocols were performed in line with the UK Animals (Scientific Procedures) Act 1986 and ethical standards set out by the University of Leeds Ethical Review Committee.

3.4.2 Immunofluorescence techniques

Immunofluorescence techniques [Chapter 2 (2.2.2)] were used in detecting 5-HT containing neurones and fibres and determining if they were in close proximity to Nestin EGFP positive cells.

3.5 Results

3.5.1 Distribution of 5-HTergic fibres in the caudal medulla of brainstem

The locations of 5-HTergic fibres may determine if 5-HT could influence the neural stem cells. There are known from previous studies (see introduction) that many 5-HT-containing cell bodies and processes in more rostral regions of the medulla, midbrain, some of which project to the cord. For this study, 5-HT positive cell bodies were identified in the caudal medullary raphe, specifically in the nucleus raphe obscurus. In the caudal medulla area, immunofluorescent fibres were prominent in the ependymal cell layer (ECL), as well as in area postrema (AP), nucleus tractus solitarii (NTS) and dorsal vagal motor nucleus (DMX) (Figure 3.1).

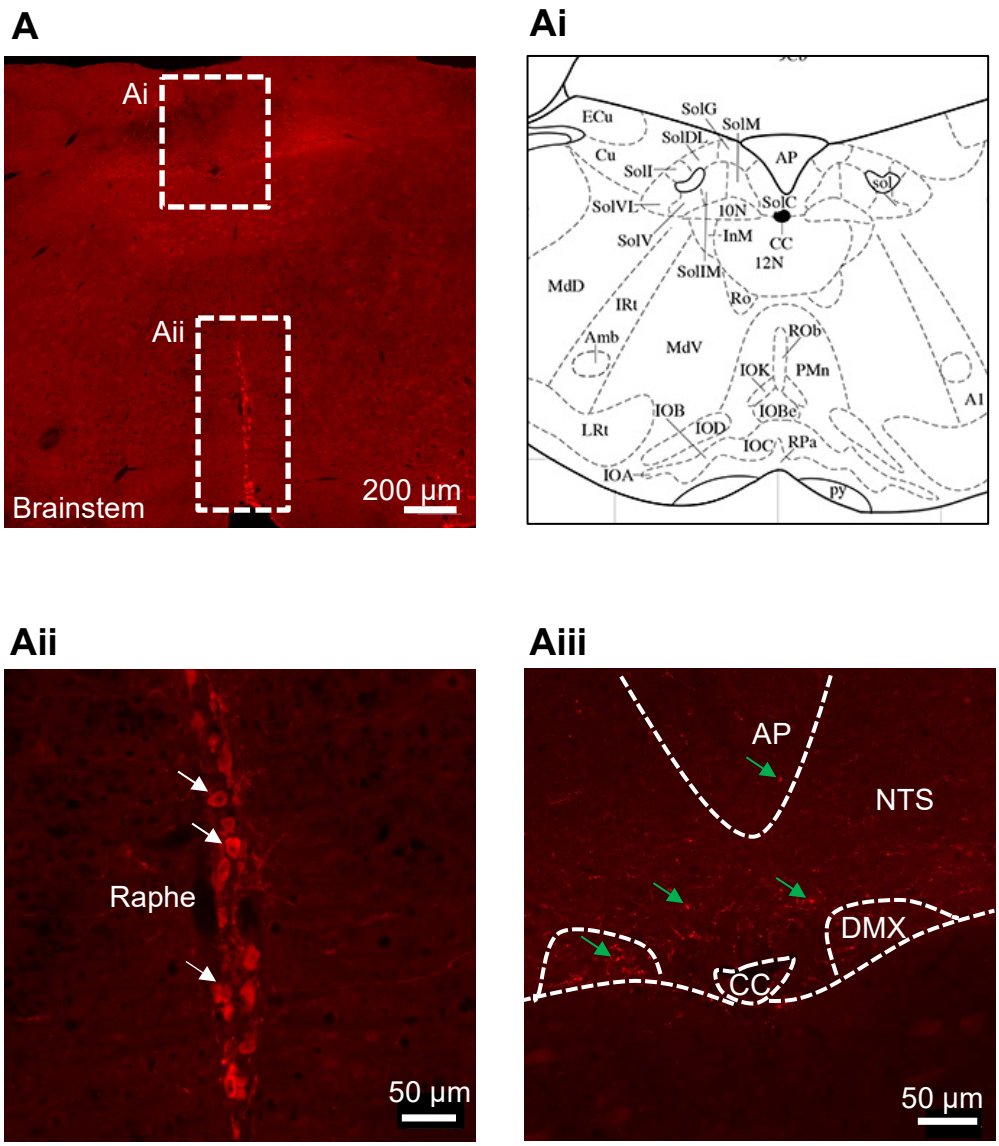

Figure 3.1 5-HT neurones and fibres were prominent in the caudal medulla. (A) 5-HTergic neurones were located in the nucleus raphe obscurus while there were 5-HTergic fibres in the nucleus tractus solitarii (NTS). (Ai) Mouse brain atlas from Gaidica (2015). (Aii) In higher magnification, the 5-HT neurones (white arrows) are arranged along the midline in raphe obscurus. (Aiii) In a closer view, the fibres (green arrows) are profusely distributed in the AP, NTS, DMX and surround the central canal region.

3.5.2 Distribution of 5-HTergic fibres in the spinal cord region

5-HTergic fibres were found throughout the spinal cord from cervical to sacral levels. At the thoracic level, the 5-HTergic fibres were abundant in the intermediolateral cell column (IML) region of gray matter. These fibres travelled medially from IML to the ependymal cell layer and surrounded the ependymal cell layer (ECL) around the central canal (Figure 3.2).

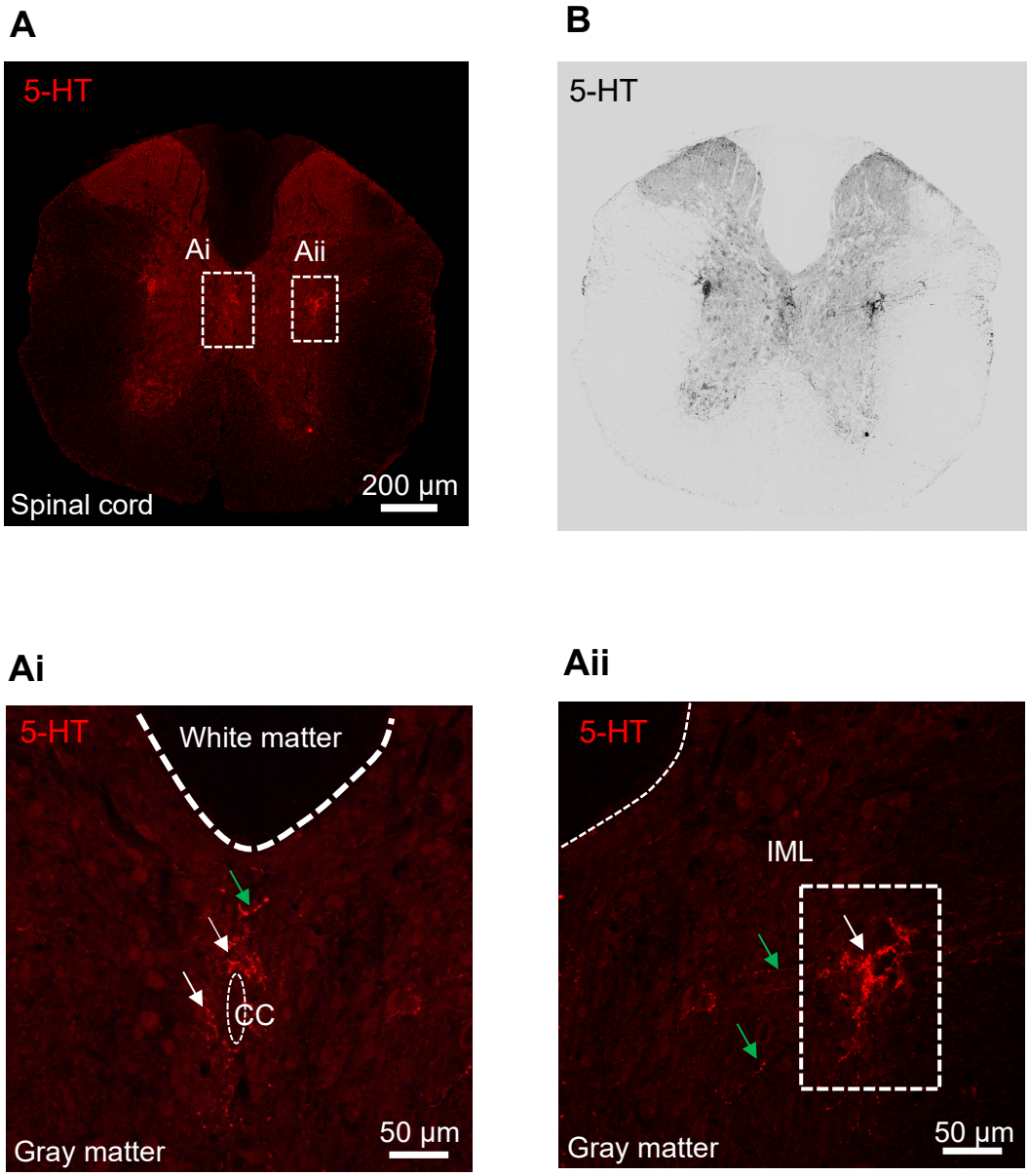

Figure 3.2 5-HTergic fibres were observed throughout the spinal cord region. (A) Immunofluorescent image of the thoracic spinal cord showing the 5-HTergic fibres (red) in the region surrounding the central canal (CC) and the intermediolateral (IML) cell column of gray matter. (B) Transformation of (A) into greyscale image enhanced the appearance of the fibres in the central and IML regions. (Ai) Magnified view of the central canal (CC) region, to show the 5-HTergic fibres (white arrows) near the ependymal cell layer. There are also fibres extending away from the CC (green arrow). (Aii) Magnified view of the IML region, where the fibres are very dense (white arrows), and there are also thin fibres (green arrows) that travelled away from the IML region.

3.5.3 Distribution of Nestin-EGFP cells in the ECL, NTS and AP region of the brainstem

Nestin-EGFP cells were identified surrounding the central canal, within the AP area and also at the border of NTS and AP. There were different levels of immunofluorescence intensity of EGFP in the ECL and the AP region (Figure 3.3).

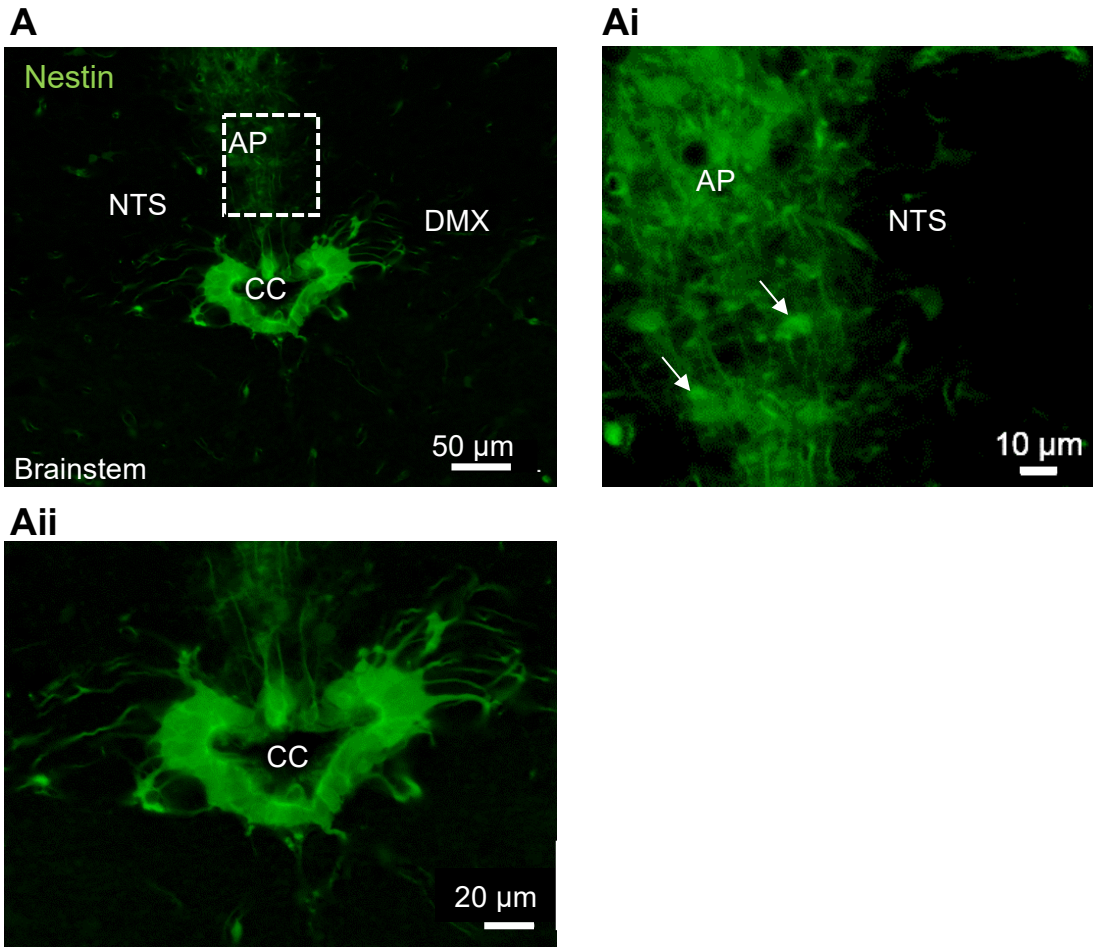

Figure 3.3 Nestin-EGFP cells were prominent at the ependymal cell layer (ECL) and area of postrema (AP) region of the brainstem. (A) Cross-section of the brainstem of the Nestin-EGFP mouse showing the intensely stained Nestin-EGFP cells located in the ependymal layer at the central canal (ECL). In the area postrema (AP), there are also Nestin-EGFP cells that have less intense fluorescence compared to the ependymal cell layer. (Ai) High magnification of AP showing Nestin-EGFP cells (white arrows). (Aii) High magnification of central canal (CC) region showing Nestin-EGFP cells surrounding the CC.

3.5.4 Distribution of Nestin-EGFP cells in spinal cord

Nestin-EGFP cells were also found surrounding the CC of spinal cord (Figure 3.4). There were small Nestin-EGFP cells located in the gray matter (GM) and white matter (WM) that labelled type-1 pericytes of blood vessels (Birbrair *et al.*, 2014). However, since the focus is on potential neural stem cells, therefore the ECL is the main area of focus.

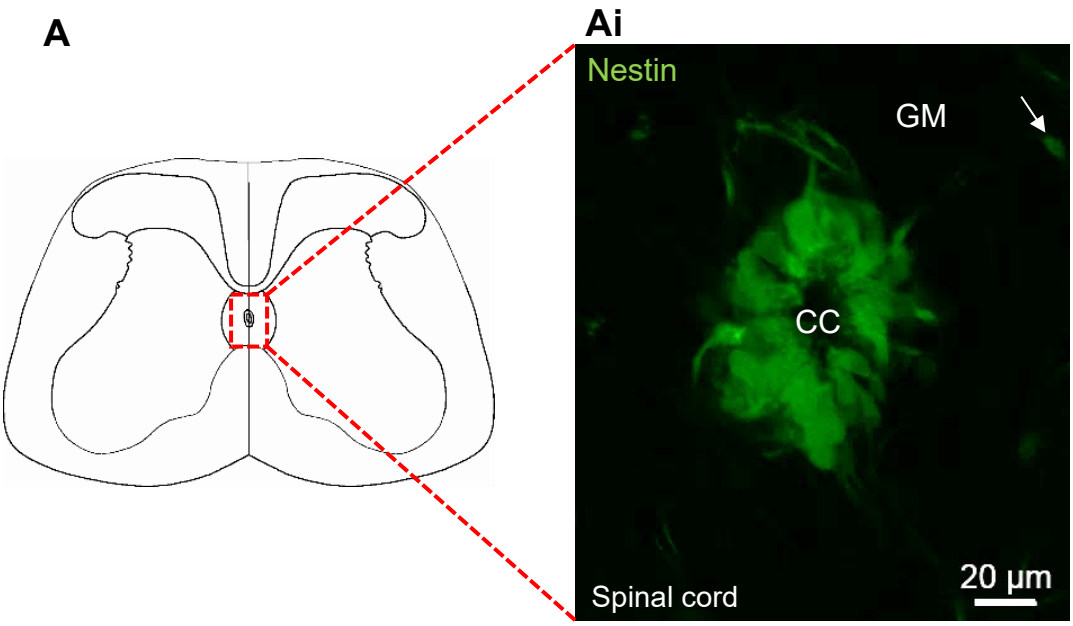

Figure 3.4 Nestin-EGFP cells at the ECL of the spinal cord. (A) The diagrammatic picture of spinal cord, in red-dotted box shows CC area. (Ai) In a closer view, there are also paler nestin-EGFP cells that are located away from the central canal (white arrow) in gray matter (GM) - these are pericytes that lie close to blood vessels.

3.5.5 Close proximity of 5-HTergic fibres to Nestin-EGFP cells in the brainstem and spinal cord

The relationship between neurogenic niches and 5-HTergic fibres is one of the factors that determine the likelihood of 5-HT modulating cell proliferation. In order to investigate these two critical factors, 5-HT immunofluorescent staining was conducted on sections taken from Nestin-EGFP mice, and the areas of close proximity noted (Figure 3.5, Figure 3.6). There are 5-HT immunoreactive cell bodies in the medullary raphe, 5-HT immunoreactive profiles in the DVC and CC region and that some of these profiles appear to be associated with nestin. As known in previous studies, nestin was used as a potential neural stem cell marker (Bauer *et al.*, 2005, Charrier *et al.*, 2006).

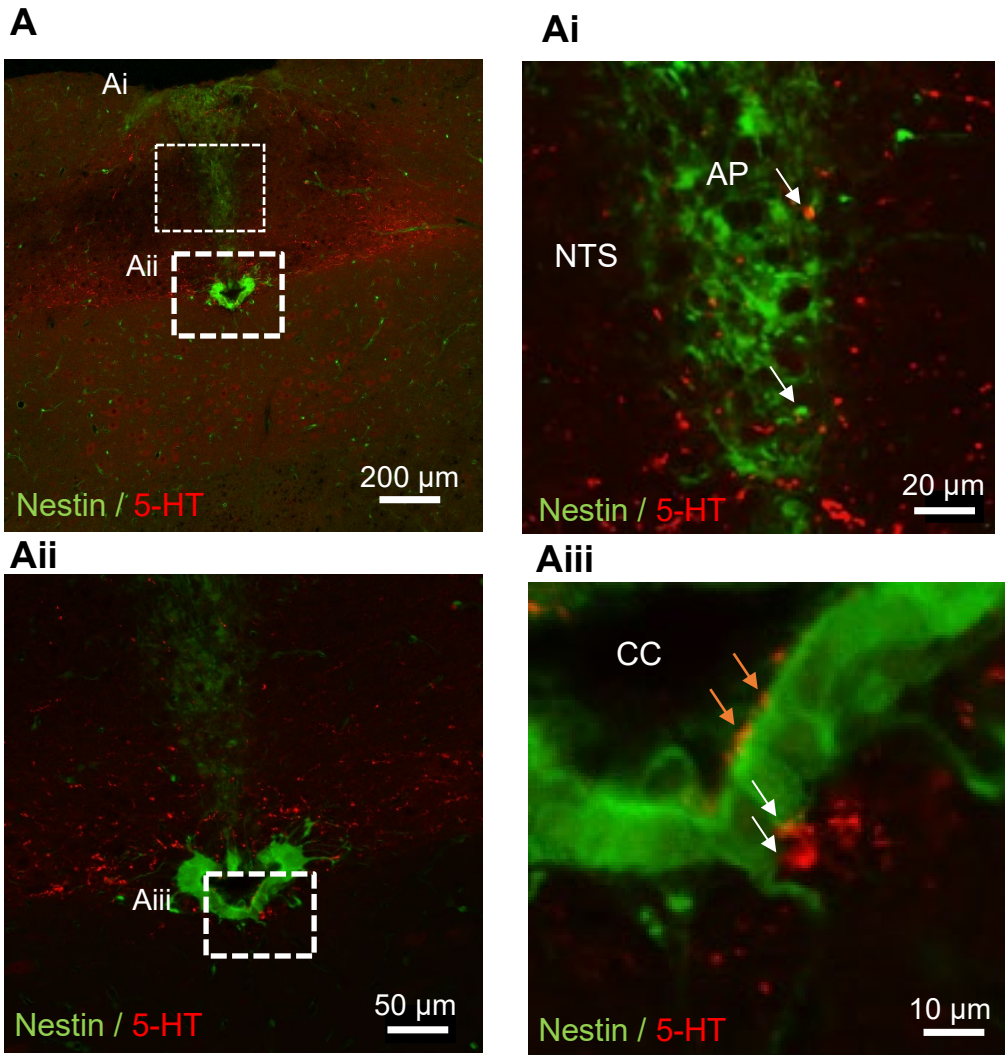

Figure 3.5 Close proximity of 5-HTergic fibres to the Nestin-EGFP cells in the caudal medulla. (A) Two significant areas where close proximity can be observed. (Ai) At a higher magnification, 5-HTergic fibres (red) are close to the Nestin-EGFP cells (white arrows) within AP and at the border of AP and NTS. (Aii) The representative images showed the relationship at the ECL. (Aiii) At higher magnification, the close proximity of 5-HTergic fibres (red) with Nestin-EGFP cells (white arrows) is observed while there are 5-HTergic fibres (orange arrows) running along the membrane of the cells inside the central canal.

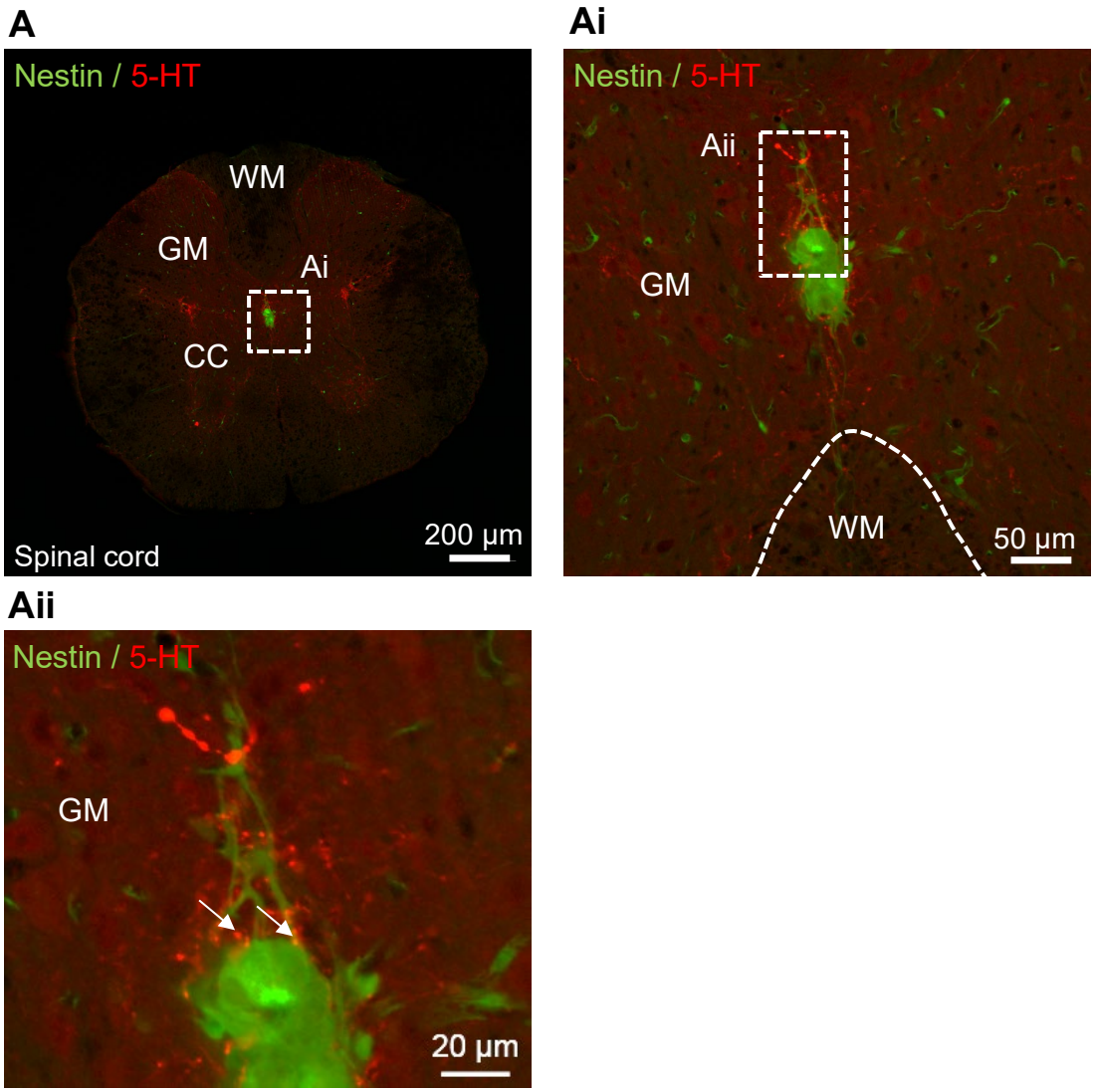

Figure 3.6 Close proximity of 5-HTergic fibres with Nestin-EGFP cells in the ECL of the spinal cord. (A) Nestin-EGFP cells (green) with 5-HTergic fibres (red) in the spinal cord (Ai) At higher magnification, 5-HTergic fibres are in close proximity to Nestin-EGFP cells at the central canal (CC) (Aii) In a closer view, it is clearly seen that 5-HTergic fibres (red) are very close (white arrows) to the Nestin-EGFP cells (green). Gray matter (GM), White Matter (WM), Central Canal (CC).

3.6 Discussion

5-HT cell bodies are known from previous studies (see introduction) to be located within the raphe nuclei and send projections to the brainstem itself, as well as projecting rostrally to ramify extensively in the brain and projecting 5-HTergic fibres caudally to every level of spinal cord, with extensive distribution of 5-HTergic terminals in the brainstem and spinal cord. In this study, close proximity of 5-HTergic fibres with Nestin-EGFP neural stem cells were observed, indicating that 5-HT may influence Nestin-EGFP neural stem cells.

3.6.1 Extensive distribution of 5-HT in the brainstem and spinal cord

In this chapter, immunofluorescent techniques, with a specific antibody against 5-HT, revealed the 5-HTergic cell bodies located within the caudal medullary raphe, mainly the nucleus obscurus and possibly including nucleus raphe pallidus while fibres were also densely located in the brainstem area. My finding has agreement with Alonso *et al.* (2013) who reported the organisation of the 5-HT neurones in nucleus obscurus in Swiss Albino mice (postnatal day 1-10) using in-situ hybridisation technique. Another study using ePet-Cre mice injected with adeno-associated viral vector double-floxed inverse open reading frame of *ChR2-mCherry* reported expression of 5-HTergic neurones (ChR2 – expressing neurones) in raphe obscurus, raphe pallidus and raphe magnus. Raphe obscurus contained the most ChR2 – expressing neurones (DePuy *et al.*, 2011). This pattern is similar to that reported in rat, with high numbers of 5-HTergic neurones in raphe obscurus (Steinbusch, 1981). Taken together the location of 5-HTergic neurone in raphe nuclei in mice appears similar to that in rat.

At the spinal cord level, the 5-HTergic immunofluorescent fibres are observed in profiles present in the thoracic spinal cord. These 5-HTergic fibres were especially numerous in the region surrounding the central canal and the ventral and dorsal horns. Additionally, for the thoracic spinal cord, fibres were dense in intermediolateral cell column, in the vicinity of SPNs and these fibres also extended medially to the central canal and central autonomic area. Another study by Au - Liang *et al.* (2016), showed the extensive distribution of 5-HTergic fibres in the spinal cord, mainly in the ventral horn compared to the dorsal horn region. In the ventral horn, the fibres were highest at the ventromedial portion while some fibres ramified out towards the lateral part. Furthermore, the fibres also extended towards the dorsal horn and ependymal cell layer.

Therefore, my findings concerning the distribution of 5-HTergic fibres in the brainstem and spinal cord are consistent with reported patterns of labelling. Furthermore, in addition to the known roles of 5-HT (Charnay and Léger, 2010), these findings suggest that 5-HT may also play a role in controlling the activity of cells in the ependymal cell layer identified by nestin-EGFP expression

3.6.2 Nestin-EGFP cells are located in the brainstem and spinal cord

Nestin is an intermediate filament type IV that is known to be present in progenitor cells and may be a potential marker for neural stem cells. In my study, the Nestin-EGFP mouse was used and showed the location of the cells that expressed nestin through expression of EGFP. Nestin-EGFP cells (and thus potential neural stem cells) were found in the ECL of the caudal medulla as well as within the AP and at the border between NTS and AP regions in the brainstem. Furthermore, the ependymal cell layer in the spinal cord also had many Nestin-EGFP cells within it, similar to the ependymal cell layer in the brainstem. In a human study, the spinal cords from patients who died from

non-traumatic causes were examined as control group, which considered the spinal cord still intact (Cawsey *et al.*, 2015). Using immunofluorescent techniques, nestin staining was observed in ependymal cells surrounding the central canal area, suggesting that humans also have potential neural stem cells in this region.

Using nestin as a neural stem cell marker has previously been reported in the brainstem in previous studies (Bauer *et al.*, 2005, Charrier *et al.*, 2006), so my use of Nestin-EGFP mouse seems feasible to identify the location of potential neural stem cells in brainstem areas. We observed that the Nestin-EGFP cells with high fluorescent intensity were confined to the ECL area. This may suggest that the ECL is a neurogenic niche for brain stem and that ependymal cells are potential neural stem cells. Since the brainstem also has a central canal up to bregma level -7.48 (Gaidica, 2015), the ECL of the brainstem might share the same properties with the ECL in the spinal cord area.

However, in my Nestin-EGFP mouse, at the ECL region showed Nestin-EGFP cells were found in the whole ependymal layer which contradicts with findings by Hamilton *et al.* (2009) and Alfaro-Cervello *et al.* (2012). They found the nestin-positive cells predominantly at the dorsal and ventral poles of ECL in spinal cord. This difference can be due to the different techniques for detecting nestin-immunoreactivity. In my study, green fluorescent protein (GFP) is selectively expressed in nestin expressing cells in the Nestin-EGFP mouse, while in Alfaro-Cervello *et al.* (2012) and Hamilton *et al.* (2009) they used antibodies to detect nestin positive neural stem cells. It is possible that the expression of EGFP results in visualisation of cells with low nestin protein levels that would not be detected with immunofluorescence. This would be consistent with single cell mRNA sequence studies that revealed nestin expression in ependymal cells in the spinal cord central canal (Rosenberg *et al.*, 2018).

In brainstem, due to the complex organisation at every level, the Nestin-EGFP cells were observed rostro-caudally in serial sections of the brainstem area. Other than central canal, Nestin-EGFP staining was also seen at the AP area. This finding is slightly

different from Bauer *et al.* (2005), where nestin-immunoreactivity was found only in between AP and NTS, not within the AP region. Charrier *et al.* (2006), found the same location of nestin-immunoreactivity at the AP level in mice and this was increased by vagotomy. This different finding might be due to the different techniques to detect the nestin expression as noted above as we used Nestin-EGFP mouse while these other studies used antibodies to detect nestin protein.

3.6.3 5-HTergic fibres are in close proximity to Nestin-EGFP cells showing the potential influence of 5-HT on Nestin-EGFP cells

Our data showing the pattern of 5-HT immunofluorescent fibres in the brainstem and spinal cord is similar to that reported previously. Curtis *et al.* (2013) proved that there is immunolabelling of 5-HT that shows varicosities of fibres in NTS region, while in spinal cord, serotonergic fibres travel down to all levels of spinal cord, the tracts are located at the dorsolateral funiculus then ramify into the grey matter and establish the synaptic contacts with neurons that are involved in somatic outflow (Perrier and Cotel, 2015). Besides that, there also serotonergic inputs onto sensory neurons, autonomic preganglionic neurones and interneurons (Deuchars and Lall, 2015). The serotonergic fibres are concentrated in the intermediolateral part of the thoracic spinal cord and then course medially to surround the central canal area. It is also located in the dorsal horn of the spinal cord (Thor *et al.*, 1993, Croul *et al.*, 1998).

Although there are 5-HT cell bodies in the caudal medulla and immunoreactive profiles in the cord, some of which run close to nestin-positive cells, in this study there is no evidence for functional connectivity. However, Tong *et al.* (2014) found 5-HTergic supraependymal axons that make close contact to ependymal surfaces of ventricular-subventricular zone using electron microscopy, which is more definitive evidence that these may form functional connections. Another study using anti-psychotic drugs

(clozapine and olanzapine) showed increases in c-Fos active cells in ependymal cells, an effect mediated via 5-HTR2A (Joshi and Panicker, 2018), therefore this evidence suggested that functional connectivity between 5-HTergic fibres and ependymal cells was potentially present.

Detection of 5-HTergic distribution in Nestin-EGFP mice showed close proximity of 5-HTergic fibres with nestin-positive neural stem cell around the central canal of both spinal cord and brainstem. These findings suggest that 5-HT may influence the activity of nestin-positive neural stem cell as the position is very close and by modulating 5-HT level, we may be able to modify the degree of cell proliferation and cell differentiation at that area.

3.7 Conclusion

The current investigation showed that, there are 5-HT immunoreactive cell bodies in the medullary raphe, 5-HT immunoreactive profiles in the DVC and ECL and that some of these profiles appear to be associated with nestin-EGFP expressing cells.

Chapter 4

DOES MODULATION OF 5-HT USING FLUOXETINE AFFECT POSTNATAL NEUROGENESIS?

4.1 Introduction

The effects of modulation of 5-HT on cell proliferation and differentiation cells that are involved in brain neurogenesis are quite established in higher brain regions. For example, increasing ambient levels of 5HT by chronic administration of the selective serotonin re-uptake inhibitor (SSRI) fluoxetine (flx) *in vivo*, promoted cell proliferation in the hippocampal subgranular zone of mice (Sachs and Caron, 2015). Proliferation was also increased in the medial habenula and hypothalamus. In all areas, the highest percentage of newborn cells expressed the neuronal marker NeuN, with others identified as GFAP positive (Sachs and Caron, 2015). However, proliferation of cells was not examined throughout the CNS and it may therefore be possible that the proliferation also can occur in other neurogenic niches, more specifically at the brainstem and spinal cord area.

4.2 Hypotheses

1. There will be a greater extent of cell proliferation in flx group compared to control groups in hippocampus, brainstem and thoracolumbar spinal cord region
2. Flx treated mice will exhibit significantly greater colocalisation of EdU-labelled cells with differentiation markers for astrocytes, oligodendrocytes and neurones than control groups.

4.3 Aims

1. To determine the level of cell proliferation in hippocampus, brainstem and thoracolumbar spinal cord in response to flx administration *in vivo*.
2. To determine the percentages of colocalisation of EdU-labelled cells with s100β (marker for astrocytes), PanQKI (oligodendrocytic marker), HUC/D (neuronal marker) for hippocampus and brainstem and Tuj1 (neuronal marker) in the spinal cord.

4.4 Materials and methods

4.4.1 Animals

Eight adolescent (6-8 weeks old) male and female C57/B16 mice (Central Biological Services), each weighing 20-25 g at the beginning of the experiment, were housed in a 12-hour light/dark cycle with ad libitum access to food and water. All procedures involving animal care were conducted in compliance with the UK Home Office License, the UK

Animals (Scientific Procedures) Act 1986 and ethical guidelines asserted by the University of Leeds Ethical Review Committee. The number of animals used and their suffering was minimized in accordance with the 3Rs – replacement, reduction and refinement.

4.4.2 Experimental Procedure

C57/Bl6 mice (n = 4 for each group) were intraperitoneally injected with 0.1 ml of solution contain 10 mg/kg flx hydrochloride or an equivalent volume of normal saline (NaCl) for 10 days. EdU was dissolved in saline at 10 mM concentration and 0.1 ml of which was i.p injected daily for the last 5 days of the 10-day treatment process (Table 4.1). This method of drug administration was used due to previous success in increasing neurogenesis in adolescent rats by giving 10 mg/kg ip injection of flx for 10 days (Faillace *et al.*, 2015).

Table 4.1 Concentration of flx and EdU

Drug	Molecular weight	Concentration (mg/kg)	Concentration	Reference
Fluoxetine hydrochloride	345.78	10 mg/kg	6 mM in 0.1 ml of solution (dissolved in saline)	(Faillace *et al.*, 2015)
5-ethynyl-2'-deoxyuridine	252.22	10 mg/kg	10 mM in 0.1 ml of solution (in saline)	(Zeng *et al.*, 2010)

4.5 Results

4.5.1 High levels of proliferating cells in the dorsal dentate gyrus of hippocampus in fluoxetine-treated group compared to control

Consistent with previous studies, there was a greater degree of proliferation, indicated by higher numbers of EdU-positive cells, in the dorsal dentate gyrus of flx-treated mice compared to control mice (64.92 ± 10.2 vs 37.73 ± 3.8 EdU positive cells per section, $p = 0.05$; $n = 4$; Figure 4.1).

4.5.2 Fluoxetine treated animals did not display higher extents of differentiation of EdU-labelled cells in the hippocampus compared to controls.

The fate of EdU-labelled cells within the hippocampus was investigated using antibodies against astrocytes, oligodendrocytes and neurones (Figure 4.2). The numbers of EdU-labelled cells and green immunofluorescent cells were counted, and the percentages of EdU-labelled cells that were also immunopositive for the different markers are presented. None of the differentiation markers showed significant differences in flx-treated animals from control animals. Percentages of EdU-labelled cells which were considered astrocytes (2.45 ± 1.4 vs 2.93 ± 2.1), oligodendrocytes (3.45 ± 2.4 vs 2.08 ± 1.2) or neurones (4.21 ± 2.5 vs 4.03 ± 2.4) in flx and control groups respectively were not significantly different (Figure 4.1).

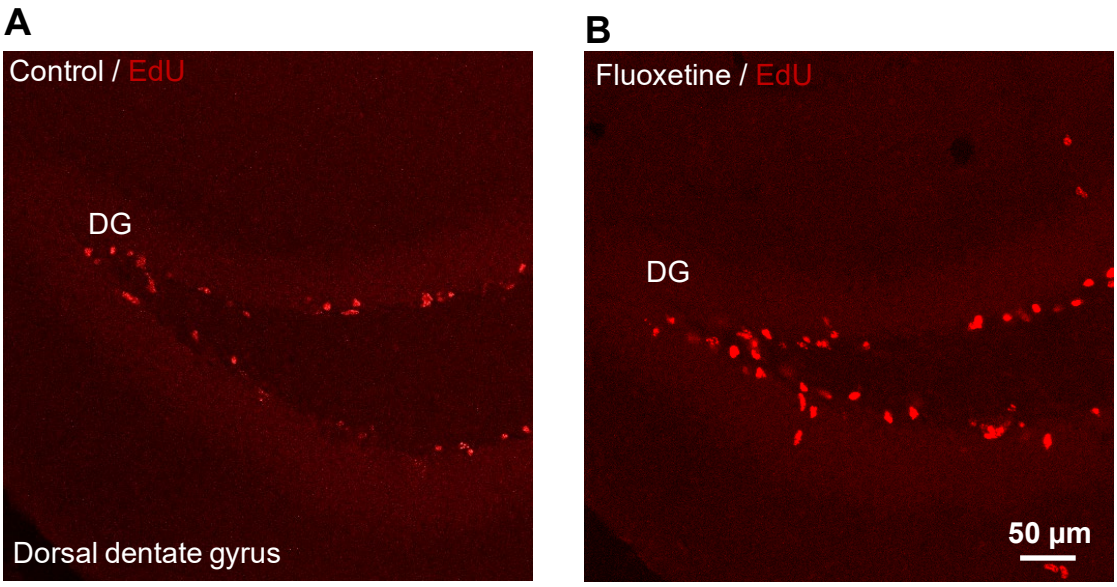

Figure 4.1 Representative images of EdU-labelled cells in hippocampus Example of images of EdU-labelled cells (red) in the dorsal dentate gyrus of hippocampus in control (A) and flx treated (B) mice are shown in objective 20x magnification.

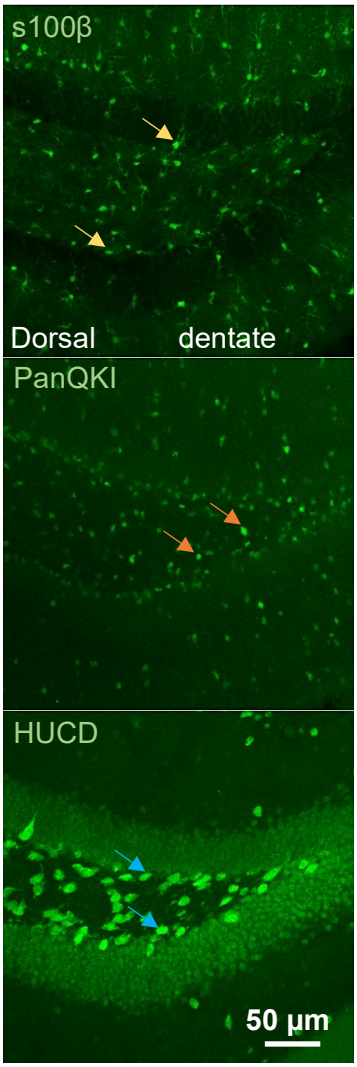

Figure 4.2 Representative images of illustration of immunoreactivity for astrocytes (s100β), oligodendrocytes (PanQKI) and neurones (HUCD) Example of images of differentiation markers (green) in the dorsal dentate gyrus of hippocampus. These images show immunoreactivity profile of astrocytes (yellow arrow), oligodendrocytes (orange arrow) and neurones (blue arrow) are shown in objective 20x magnification.

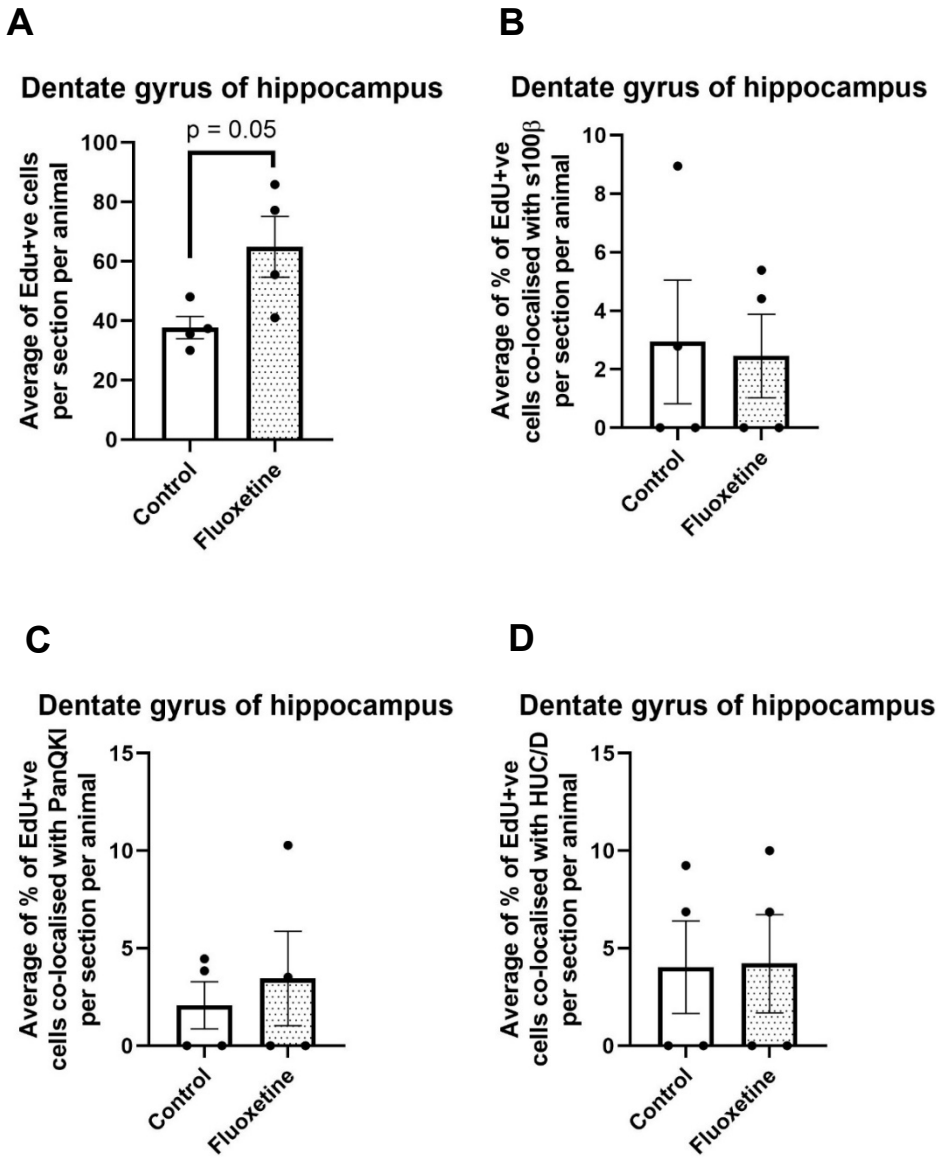

Figure 4.3 Fluoxetine-treated animals exhibited significantly higher numbers of proliferating cells compared to control but did not induce differentiation of proliferating cells in the dorsal dentate gyrus of hippocampus. (A) There were significantly higher levels of EdU-labelled cells in the dentate gyrus (DG) of hippocampus in the flx group compared with control. (B-D) Histograms showing the extent of co-labelling in control versus flx-treated animal was not significantly different. Black rounded dots on the bar graph refers to the mean value of each animal in each group. n = 4 for each group. Statistical analysis, independent t-test was applied with significant value, $p \leq 0.05$)

4.5.3 Fluoxetine promotes cell proliferation in selected area of the brainstem

Treatment with flx promotes a greater extent of cell proliferation in the whole region of the brainstem compared to control (70.71 ± 6.4 vs 37.61 ± 3.9, p = 0.004). The dorsal vagal complex (DVC) is comprised of area postrema (AP), nucleus tractus solitarii (NTS) and dorsal motor nucleus of vagus nerve (DMX). In the entire DVC area, there were significantly more EdU positive cells in flx-treated animals compared to control (37.96 ± 4.6 vs 19.00 ± 3.2, p = 0.015), while further examination of the NTS (26.33 ± 3.4 vs 13.18 ± 2.3, p = 0.018) and AP (9.8 ± 0.7 vs 5.89 ± 0.5, p = 0.003) regions also showed higher levels of proliferating cells in the flx treated animals compared to control. However, in the DMX area there were no significant differences between groups (4.50 ± 1.1 vs 3.04 ± 0.5). There were also other regions showing a higher degree of cell proliferation in flx-treated animals compared to control; these were the inferior olive (18.08 ± 1.5 vs 9.46 ± 0.9, p = 0.003) and raphe (18.08 ± 1.5 vs 9.46 ± 0.9, p = 0.003). The ependymal cell layer (5.00 ± 1.3 vs 4.88 ± 0.5), pyramidal region (9.46 ± 1.0 vs 7.71 ± 0.9) did not exhibit differences in numbers of EdU-positive cells between the 2 groups (Figures 4.4 and 4.5).

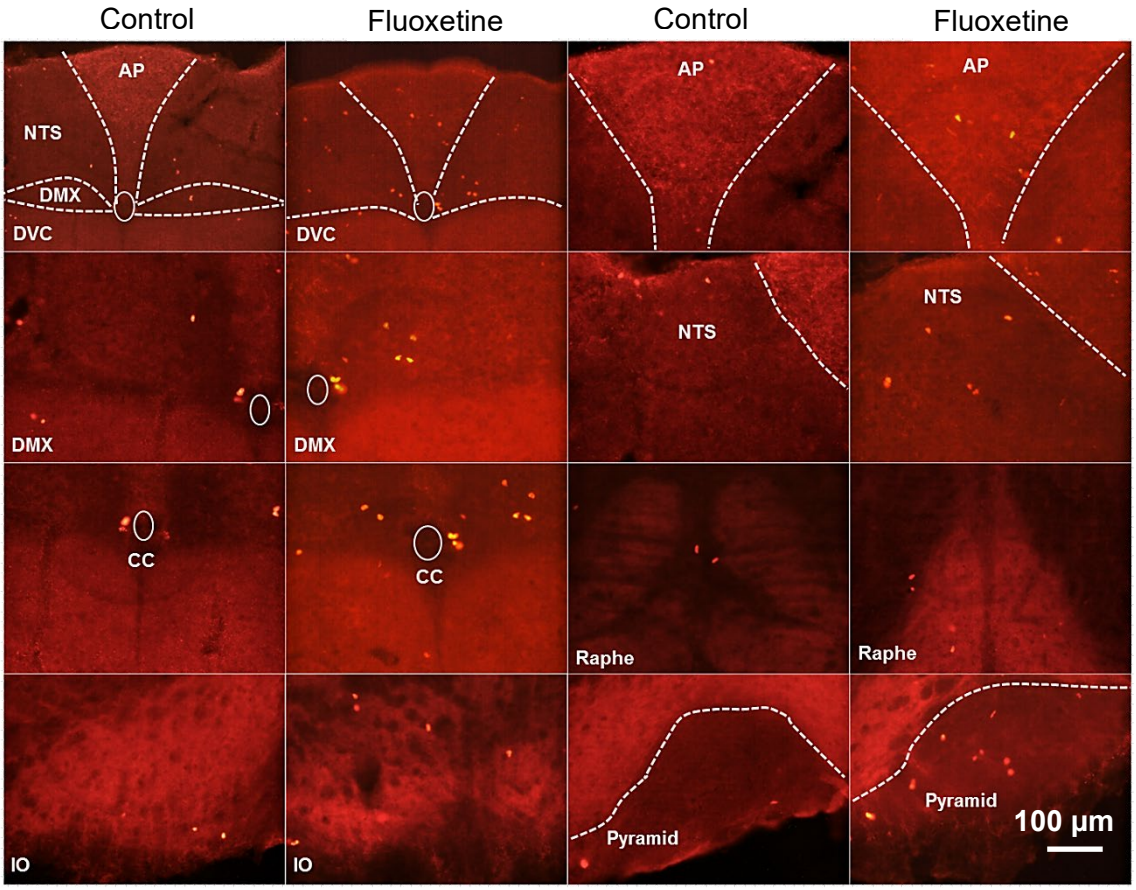

Figure 4.4 Representative fluorescent images of the EdU labelling (red nuclear labelling) in brainstem Examples of EdU-labelled cells are shown and representative images of both the flx-treated and control groups are shown. Objective 20x magnification.

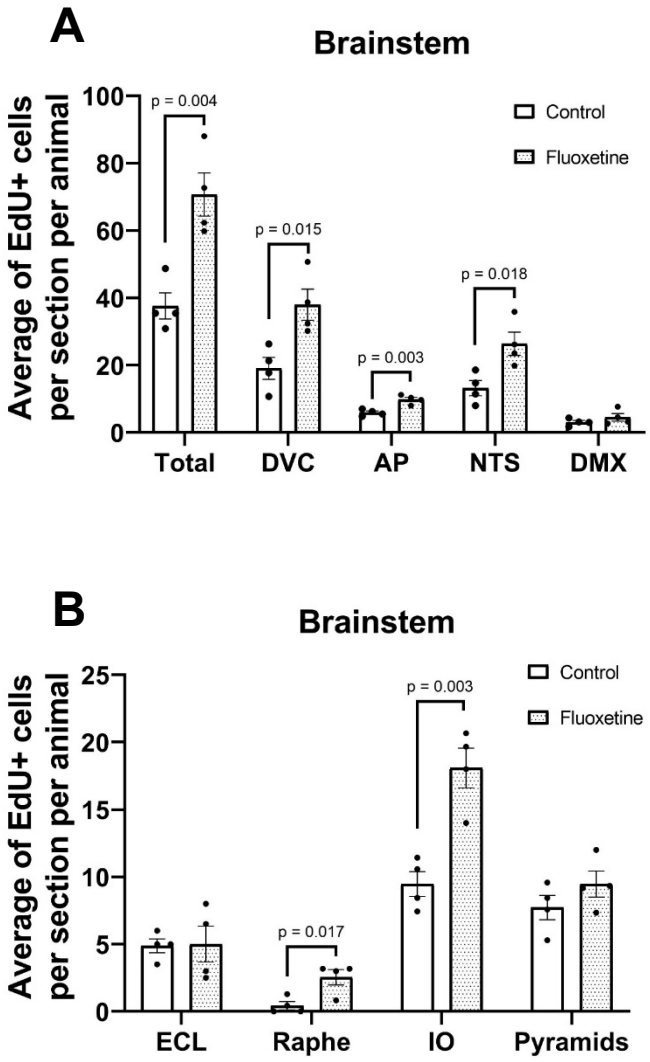

IO = Inferior Olives
DVC = Dorsal Vagal Complex,
AP = Area of Postrema,
NTS = Nucleus Tractus Solitarii,
DMX = Dorsal Vagal Motor Nucleus
ECL = Ependymal Cell Layer

Figure 4.5 Fluoxetine treated animals had higher numbers of EdU-labelled cells in selected regions of brainstem. (A) The average numbers of EdU-labelled cells in the total brainstem and dorsal vagal complex (DVC) which comprises area postrema (AP), nucleus tractus solitarii (NTS) and dorsal vagal motor nucleus (DMX) are significantly higher in flx treated animals compared to control animals. When looking into specific areas of the DVC, AP and NTS but not the DMX had higher numbers of cells in flx-treated animals compared to control. (B) In other brainstem regions, there were increased numbers of proliferating cells in raphe and inferior olive (IO) area but not in the ependymal cell layer (ECL), nor pyramidal tract areas. Black rounded dots on the bar graph refers to the mean value of each animal in each group. n = 4 for each group. Statistical analysis, independent t-test was applied with significant value, $p \leq 0.05$)

4.5.4 The proportion of EdU-positive cells that differentiate into astrocytes, oligodendrocytes and neurones is not significantly different in brainstem between groups

Determination of cell fate is very important in order to investigate the capability of 5-HT to promote neurogenesis. Antibodies against astrocytes, oligodendrocytes and neurones were selected and percentages of EdU-positive cells that were also labelled with differentiation markers were counted. Colocalisation of EdU positive cells with differentiation markers was found in these regions but flx did not significantly affect numbers of proliferating cells that differentiated into astrocytes (3 ± 2.1 % vs 3.7 ± 3.0 %) , oligodendrocytes (11.9 ± 7 % vs 7.5 ± 4.4 %) or neurones (9.19 ± 5.3 % vs 9.51 ± 5.5 %) (Figure 4.6).

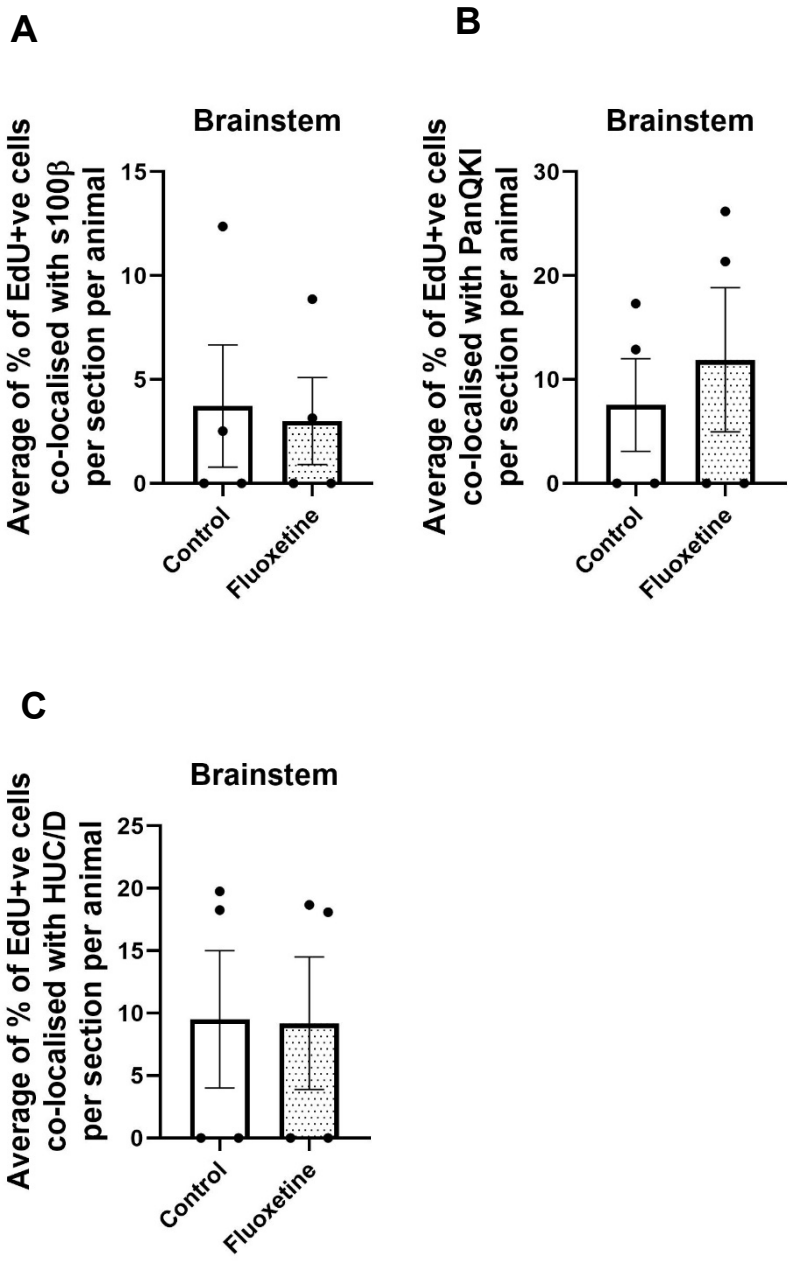

Figure 4.6 No difference in numbers of EdU-positive cells that differentiated into astrocytes, oligodendrocytes and neurones in the brainstem with fluoxetine treatment. (A-C) Histogram of percentages of EdU-labelled cells that were colocalised with cell markers for the whole area and specific area of the brainstem. The graphs show there are no significant differences between control and flx-treated group in percentages of (A) astrocytes, (B) oligodendrocytes and (C) neurones. Black rounded dots on the bar graph refers to the mean percentages value of each animal in each group. n = 4 for each group. Statistical analysis, independent t-test was applied with significant value, $p \leq 0.05$)

4.5.5 Fluoxetine treated animals showed higher levels of cell proliferation in the gray matter in the thoracolumbar spinal cord.

In the thoracolumbar gray matter, there were significantly more proliferating cells per 50 µm section in mice treated with flx compared with control (28.56 ± 1.0 vs 24.16 ± 1.3, p = 0.04) (Figure 4.6A, Figures 4.7 and 4.8). However, there were no significant differences in the numbers of EdU-positive cells between flx treated and control mice in the whole thoracolumbar spinal cord (77.35 ± 2.6 vs 73.11 ± 3.8), ependymal cell layer (3.28 ± 0.7 vs 3.34 ± 0.3) and white matter (45.51 ± 2.3 vs 44.99 ± 2.5) (Figure 4.8A).

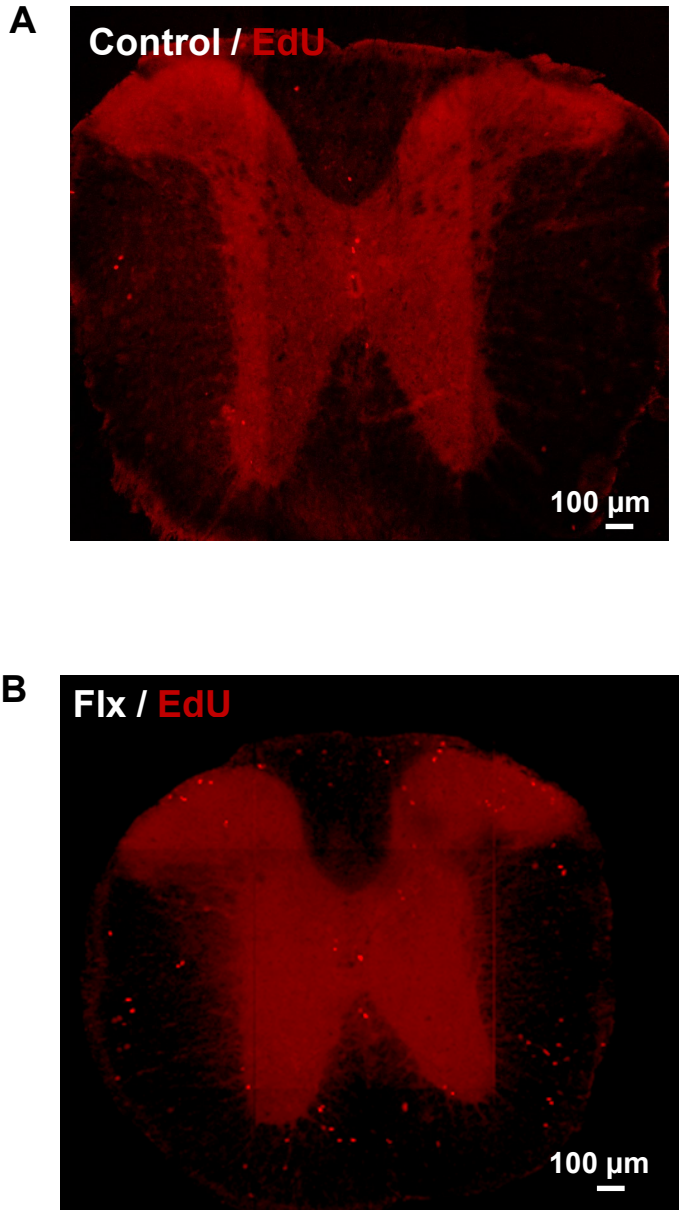

Figure 4.7 Representative images of EdU-labelled cells in thoracic spinal cord. (A) Fluorescent image of EdU-positive cells (red nuclear staining) in control group. (B) Fluorescent image of EdU-labelled cells in flx-treated group. Scale bar :100 µm. Objective 20x magnification

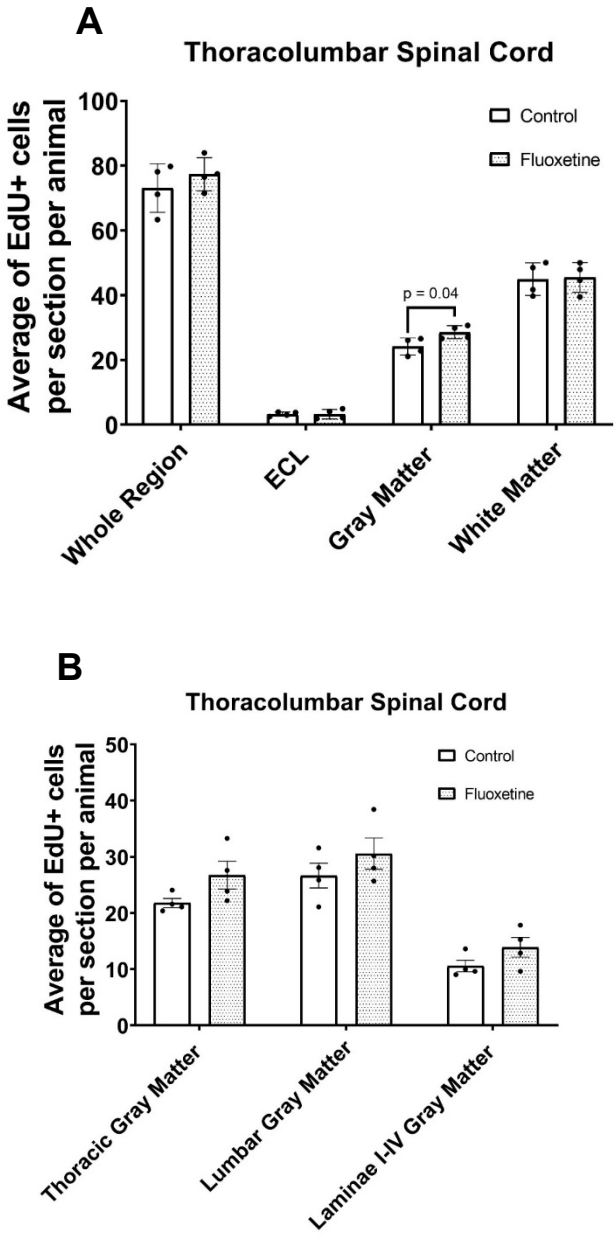

Figure 4.8 Numbers of EdU-positive cells were significantly higher in gray matter of thoracolumbar spinal cord in flx-treated group compared to control. (A)The thoracolumbar region showed significantly higher numbers of proliferating cells in the gray matter area of flx-treated animals compared to control. Further examination of other areas such as the ependymal cell layer (ECL), white matter and whole thoracolumbar spinal cord showed no significant difference in cell proliferation between groups. (B) Looking at the specific areas in the gray matter, none of the thoracic gray matter, lumbar gray matter and laminae I-IV of thoracolumbar gray matter showed significant differences between both groups. Black rounded dots on the bar graph refers to the mean value of each animal in each group. n = 4 for each group. Statistical analysis, independent t-test was applied with significant value, $p \leq 0.05$)

4.5.6 Fate of EdU-positive cells is not influenced by flx in spinal cord

Like brainstem regions, in flx-treated animals, the proportions of EdU-positive cells that differentiated into astrocytes (3.0 ± 2.1 % vs 3.72 ± 2.9 %), oligodendrocytes (11.89 ± 6.9 % vs 7.55 ± 4.5 %) and neurones (9.2 ± 5.3 % vs 9.51 ± 5.5 %) were not significantly different between groups (Figure 4.9).

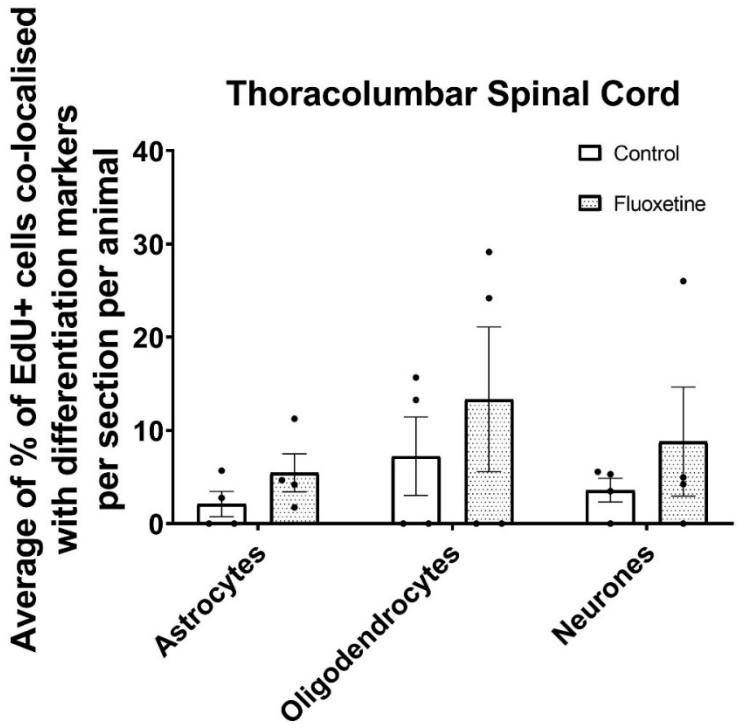

Figure 4.9 Fluoxetine did not induce differentiation of proliferating cells in the thoracolumbar spinal cord. The bar graph of percentages of proliferating cells that were immunopositive for markers of astrocytes, oligodendrocytes and neurones revealed no significant differences between groups. Black rounded dots on the bar graph refers to the mean value of each animal in each group. n = 4 for each group. Statistical analysis, independent t-test was applied with significant value, $p \leq 0.05$)

4.6 Discussion

Using pharmacological modulation, animals treated with flx for 10 days had higher numbers of proliferating cells compared to control in the dentate gyrus of hippocampus, and the NTS and AP regions of the DVC . Other areas that also showed the same pattern were raphe nuclei and inferior olives. Furthermore, in the gray matter of thoracolumbar spinal cord, flx-treated animals showed a greater extent of cell proliferation compared to control. However, the proportion of proliferating cells that had differentiated into specific cell types was not different between the flx-treated and control groups.

4.6.1 Does modulation of 5-HT affect cell proliferation in the dentate gyrus?

4.6.1.1 Consistent results in the hippocampus with different delivery methods of flx

Flx is a commonly prescribed antidepressant drug and widely used. The mode of action as a SSRI, to enhance the increased level of 5-HT in the synaptic cleft. 5-HT is also known as the 'happy hormone' and SSRIs are considered successful drugs to treat depression (Rossi *et al.*, 2004). Besides treating depression, flx showed other positive effects by improving cognitive functions and boosting the number of proliferating cells in dorsal dentate gyrus (Marwari and Dawe, 2018). In this study, the finding of increased numbers of proliferating cells in the dentate gyrus of hippocampus showed agreement with other papers that found similar results even though the methods of administration is different. Previously, researchers found that, mice administered flx (10 mg/kg) in drinking water for 15 days showed improved cognitive function and at the same time showed

higher numbers of BrdU-labelled proliferating cells in dentate gyrus in hippocampus (Marwari and Dawe, 2018). Faillace *et al.* (2015), by giving 10 mg/kg flx i.p injection for 10 days, showed similar results and they were able to rescue the low proliferative activity caused by nicotine. Administration of 5 mg/kg flx daily via oral gavage for 3 weeks promoted higher numbers of $Ki67^{+}$-labelled proliferating cells in dorsal dentate gyrus of hippocampus (Klomp *et al.*, 2015). Differences in dosage, duration and methods of drug delivery did not change the consistent results observed in dentate gyrus of hippocampus with chronic administration of 5 mg/kg flx for 3 weeks or 10 mg/kg for 10 – 15 days exerting similar effects (Faillace *et al.*, 2015, Klomp *et al.*, 2015, Marwari and Dawe, 2018). All these findings showed that flx successfully increased cell proliferation in hippocampus.

4.6.1.2 Functional significance of flx effects in the dorsal dentate gyrus (dDG) and ventral dentate gyrus (vDG)

The hippocampus is a part of the limbic system and has a central role in processing long-term memory and learning process. The hippocampus has further anatomical divisions including CA1, CA2, CA3 and dentate gyrus. My ROI is the subgranular part of dentate gyrus which is the potential area of neural stem cells showing the capability to divide and differentiate to other cells (Cameron and Gould, 1994, Gould *et al.*, 1999, Kornack and Rakic, 1999). Emotion and stress are controlled by the vDG while the dDG has a role in the memory and learning process. In treating depressed patients, the target organ is the vDG where emotion and anxiety are being controlled (Weeden *et al.*, 2015, Anacker *et al.*, 2018). Treatment with 5-Methoxy-N,N-dimethyltryptamine (5-MeO-DMT), a dimethyltryptamine analogue (a hallucinogenic drug that may increase 5-HT levels) increased cell proliferation ($BrdU^{+}$) in vDG compared to the control group. This research focused on the vDG since they surmised that this was the region important in emotional

control. In my study, in flx-treated animals there was an increase in proliferating cells in dDG but the vDG was not examined. However, another study by Klomp *et al.* (2015) had analysed Ki-67^{+} cells as the proliferating marker in subregions of dentate gyrus in both ventral and dorsal parts. Administration through oral gavage of flx (5 mg/kg) daily for 21 days enhanced proliferation mainly in dDG compared to vDG in adolescent rat. Furthermore the R-flx stereoisomer also increased cell proliferation in the dorsal region of the dentate gyrus (Marwari and Dawe, 2018). Thus, administration of antidepressant effect can have effects on both dDG and vDG of hippocampus.

Taken together, in my study, the increased proliferative activity was seen in dDG however, the vDG was not examined.

4.6.1.3 Association of flx and Brain-derived neurotrophic factor (BDNF) in the hippocampus

An important relationship between flx and expression of BDNF factor in hippocampus is very well-known due to the involvement of BDNF in promoting proliferative activity via the tropomyosin receptor kinase (TrkB) (Tauber *et al.*, 2005). The involvement of flx in promoting high levels of proliferating cells might be associated with BDNF although BDNF levels were not measured in this experiment. Many studies proved that administration of flx or 5-HT precursors promotes higher expression of BDNF in hippocampus. In ageing rats, a high tryptophan diet for a month was able to rescue an age-related decline in BDNF expression in hippocampus and prefrontal cortex (Musumeci *et al.*, 2015). Tryptophan is a dietary source of 5-HT, where it has to be converted to 5-hydroxytryptophan by tryptophan hydroxylase enzyme then the carboxyl group is removed by decarboxylation to form 5-HT (Tyce, 1990). Using high tryptophan diet promotes increased 5-HT levels and thus BDNF levels. In another study, administration of 18 mg/kg flx (in drinking water) in early life (postnatal day 21 of mice)

for three weeks increased BDNF levels that were measured using the ELISA method in samples collected from the hippocampal area (Dincheva *et al.*, 2017). Therefore, flx increased the BDNF levels in hippocampus region in mouse. Interestingly in rat, similar treatment did not result in increased BDNF levels in hippocampus, although increases were seen in frontal cortex (Balu *et al.*, 2008). This may suggest some degree of species difference.

Even though in my study, BDNF levels were not measured, previous studies have shown the important relationship between administrations of flx with the level of BDNF. Therefore, the measurement of BDNF might be crucial in determining the possible mechanism underlying the increase in proliferating cells.

4.6.2 Influence of 5-HT on proliferative activity in the DVC area of brainstem.

4.6.2.1 Dense complexes of 5-Htergic fibres in DVC may be the source of increased 5-HT.

The DVC is capable of proliferative activity since there are low basal levels of BrdU and Ki-67 positive proliferating cells but deafferentation through vagotomy in mice triggered increases in BrdU and Ki-67 positive proliferating cells (Bauer *et al.*, 2005, Charrier *et al.*, 2006). Looking at the extensive distribution of the 5-HTergic fibres in brainstem, especially at the DVC area, there are potentially high levels of 5-HT in that area compared to other regions of brainstem. The cell bodies of the 5-HT neurones are located in the raphe nucleus and the fibres project to the dorsal region and surround the central canal, the projections also ramify in the DMX, AP and NTS area (Chapter 3). This extensive source of 5-HT has the potential to influence neural stem cells to actively proliferate and differentiate. Even though the ependymal cell layer surrounding the

central canal did not show significant changes in numbers of proliferating cells in flx-treated mice, the NTS and AP have shown a significantly higher level compared to control animals. The raphe nuclei and inferior olives also exhibited a higher extent of proliferative activity in response to increasing 5-HT levels with flx. Since flx requires an endogenous supply of 5-HT to exert its effects, through inhibition of 5-HT uptake, my findings indicate that this is likely to be due to release of 5-HT from these 5-HTergic fibres. However, it cannot be ruled out completely that some of these effects are due to volume transmission of 5-HT as seen in many CNS regions (Taber and Hurley, 2014). Volume transmission is considered to be the release of a neurotransmitter from an extrasynaptic site rather than from vesicles in the conventional presynaptic terminal and therefore the 5-HT diffuses further to receptors away from the terminals (Fuxe *et al.*, 2013). This signal, which is slow and diffuses in a space larger than the synaptic cleft, involves a low concentration of neurotransmitters. Since 5-HT may be taken up into these extrasynaptic sites using 5-HT transporters, flx may also exert an effect here to increase 5-HT away from the terminal itself.

4.6.2.2 BDNF influence on proliferative activity in the brainstem

Considering the mechanism of action of 5-HT in the caudal medulla in relation to the current results 5-HT and BDNF are two factors that are closely related to each other in term of neural plasticity and proliferation where 5-HT stimulates the expression of BDNF and BDNF helps in maintaining the growth and survival of 5-HT neurones (Lyons *et al.*, 1999). In relation to administration of flx for 10 days, it might promote the increased level of BDNF in brainstem. A previous study measured central BDNF using enzyme-linked immunosorbent assay (ELISA) methods in adult rats after administration of 10 mg/kg of flx for 1 day as acute treatment and 21 days for chronic treatment. Neither treatment regime elicited significant changes in BDNF in brainstem, suggesting a different

underlying mechanism for 5-HT induced changes in proliferation (Balu *et al.*, 2008). It must be noted that these experiments were conducted in rats, which may imply species differences (see section on hippocampus) but again, which may be that at the present time we cannot be sure whether BDNF is involved but further experiments would be needed. It is worthwhile testing whether in brainstem of mice, BDNF levels are affected by flx.

4.6.3 Modulation of proliferating cells in the spinal cord by 5-HT.

Detection of 5-HTergic distribution in nestin-GFP mice showed close proximity of 5-HTergic fibres with nestin-positive cells in the central canal regions of both spinal cord and brainstem. These findings suggest that 5-HT can influence the activity of nestin-positive cells and modulating 5-HT levels may be able to modify the degree of cell proliferation and cell differentiation in that area. In this study, flx-treated animals did not show any increases in EdU-positive cells within the region of the central canal of spinal cord. It is possible that the proliferating cells in central canal might migrate to the gray matter of thoracolumbar of spinal cord since the numbers of proliferating cells were higher in that area. Altman (1969) suggested that cells proliferate and migrate from subependymal layer of lateral ventricle to olfactory bulb in normal conditions. This same process that occurs in brain areas might also apply to the spinal cord area. To explore this further, the use of mice where ependymal cells are labelled with fluorescent markers for fate mapping (using a FoxJ1 promotor) would enable cells originating from the central canal to be visualised as they proliferate and migrate (Barnabé-Heider *et al.*, 2010). This suggestion is further supported by a study on proliferative responses to injury, Rusanescu and Mao (2015) suggested the migration of proliferating cells happened from lamina X (which contains the ependymal cells) to the dorsal horn region of the gray

matter of spinal cord after constriction injury of sciatic nerve in rats since neuropathic pain can stimulate an increase in the level of 5-HT (Sommer, 2004). Another source of potential stem cells adjacent to spinal cord is in the meningeal layer. Bifari *et al.* (2015) successfully characterized the host cells in meningeal layer of brain that showed common properties of other stem cells by expressing neuronal precursor markers such as nestin, vimentin, sox2 and doublecortin. Since the meningeal layer that encapsulates brain has continuation with spinal cord meningeal layer, we postulate that they share similar properties. Furthermore, due to the close adherence of DH of spinal cord to the meningeal layer, 5-HT has the potential to influence meningeal stem cells in order to stimulate higher number of proliferating cells in dorsal horn. Since meninges are removed from our spinal cords of nestin-GFP mice when carrying out the immunohistochemical location of 5-HT fibres, we cannot test whether there is close proximity of these to the meninges.

4.7 Conclusion

In conclusion, application of flx increases the numbers of proliferating cells in the DG, NTS, AP and the gray matter of the thoracolumbar spinal cord, suggesting that higher levels of 5-HT can indeed increase the proliferative response in specific brain regions. Pharmacological application is one approach that has been used in order to investigate how neurotransmitters may modulate neurogenesis by increasing or reducing levels of a particular neurotransmitter. Flx is a selective serotonin reuptake inhibitor (SSRI) used in this study as it increases levels of 5-HT in synaptic cleft by blocking the reuptake of 5-HT to the presynaptic terminals. This high level of 5-HT will give continuous stimulation to 5-HT receptors either via G-couple protein or ion-gated channel receptors. The potential influence of endogenous 5-HT in promoting high levels of proliferating cells in dentate gyrus of hippocampus, NTS, AP, raphe and inferior olive regions of brainstem

and gray matter of thoracolumbar spinal cord without knowing which receptors that may be involved in promoting the response has triggered a further investigation. Potential receptors have been identified and suggested that these may include involvement of a number of different receptors namely 5-HTR1A, 5-HTR2 and 5-HTR4 (Radley and Jacobs, 2002, Banasr *et al.*, 2004, Grabiec *et al.*, 2009, Pascual-Brazo *et al.*, 2012). Thus, the next experiment involves *in-vitro* investigation of which receptors may underlie this positive effect.

Chapter 5

IDENTIFICATION OF 5-HT RECEPTORS INVOLVED IN POSTNATAL NEUROGENESIS

5.1 Introduction

5-HT receptors can be classified into seven major receptors that are further divided into subclasses of the receptor. The major receptors known for their function are 5-HT1, 5-HT2, 5-HT3, 5-HT4, 5-HT6 and 5-HT7 (Berg *et al.*, 2013). 5-HT action is activated when the neurotransmitter binds to the 5-HT receptor located at the presynaptic or postsynaptic membrane of the target cell involving activation of cation channels (ionotropic receptor) or G protein-coupled receptors (metabotropic receptor) (Tyce, 1990). 5-HT_3 receptors are ionotropic (linked to ion channels), and the only receptor that activates cation channels and depolarizes the cell membrane. All other 5-HT receptors are metabotropic (G-protein coupled). 5-HTR1 and 5-HTR5 linked with Gi/Go and decrease cyclic adenosine monophosphate (cAMP) intracellular concentration (inhibitory). However, 5-HTR4, 5-HTR6 and 5-HTR7 linked with Gs-protein coupled will increase intracellular cAMP (excitatory). On the other hand, 5-HTR2 linked with Gq-protein coupled will increase intracellular inositol triphosphate (IP_3) and diacylglycerol (DAG) (excitatory) (Figure 5.1).

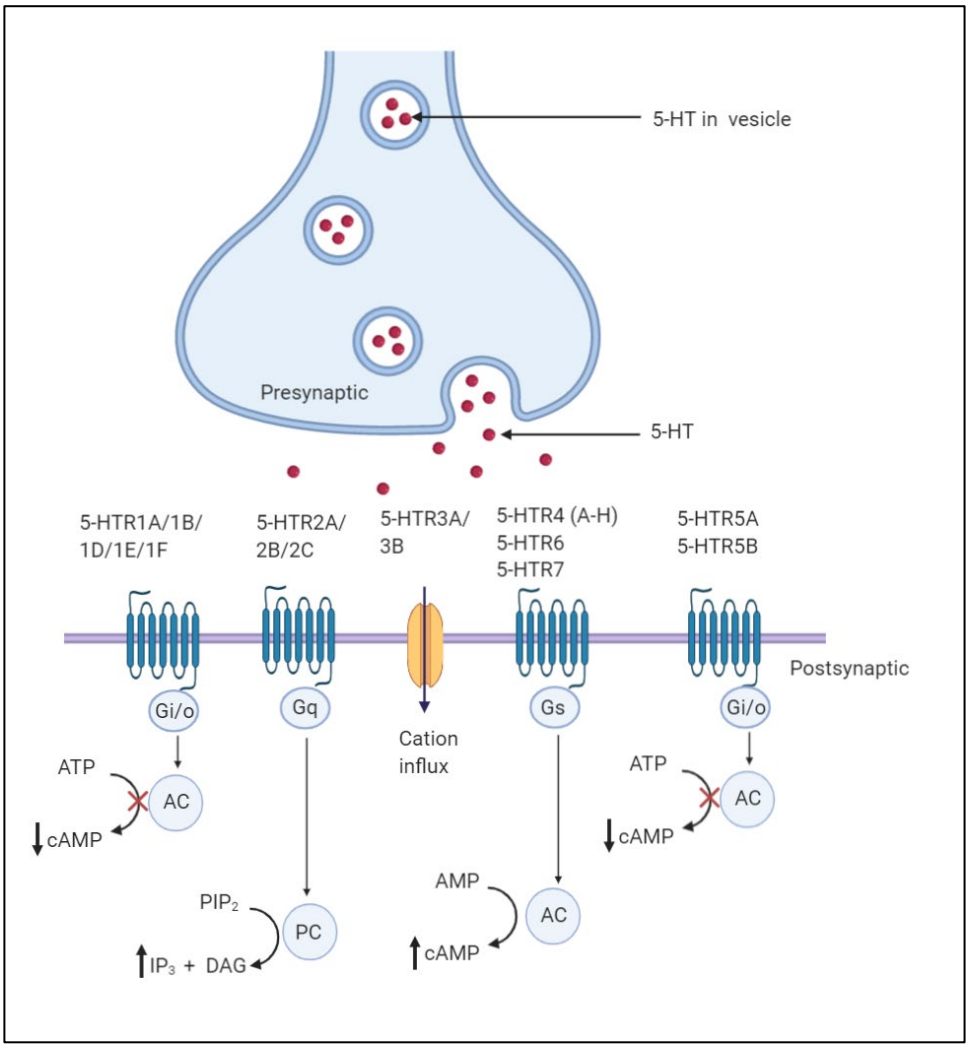

Figure 5.1 Diagram of 5-HT receptors and their downstream signalling pathways. 5-HTR1 and 5-HTR5 coupled to Gi/Go protein will decrease the intracellular concentration of cAMP. 5-HTR2 coupled to Gq protein will increase intracellular concentration of IP_3 and DAG. 5-HTR4, 5-HTR6 and 5-HTR7 coupled to Gs increases intracellular cAMP. 5-HTR3 are involved in direct activation of cation channels and depolarisation of cell membrane (Pytliak *et al.*, 2011). Diagram is created using Biorender.com. Abbreviations: IP_3: inositol triphosphate; DAG: diacylglycerol; cAMP: cyclic adenosine monophosphate; AC: adenylate cyclase; PC: phospholipase C; ATP: adenosine triphosphate

Previous research has highlighted specific 5-HT receptors in modulating adult neurogenesis in the hippocampus; these are 5-HTR1A, 5-HTR2 and 5-HTR4 (Banasr *et al.*, 2004, Liu *et al.*, 2009, Klempin *et al.*, 2010, Mori *et al.*, 2014, Takaki *et al.*, 2014, Barreiro-Iglesias *et al.*, 2015).

In experiments using acute treatment of 8-OH-DPAT (5-HTR1A agonist, given at 1 mg/kg intraperitoneally), comparisons were made in the. cell proliferation rate in the subventricular zone and subgranular zone with the duration of activation of the receptor. Activation of 5-HTR1A for 4 hours significantly increased cell proliferation (BrdU+ve cells) by 57% compared to control. On the other experiment, no changes in cell proliferation occurred when activating the receptor for 2 hours and 30 minutes. (Banasr *et al.*, 2004). This is therefore important to take into account when considering the role of 5-HTR1A activation in cell proliferation in other regions of the CNS.

The contribution of 5-HTR2 on cell proliferation in brain is still debatable and the previous results are inconsistent. Administration of a 5-HTR2C agonist (RO 600175, 2.5 mg/kg, i.p) increased cell proliferation in the subventricular zone while the 5-HTR2 antagonist (Ketanserin, 1 mg/kg, i.p) decreased cell proliferation in the subgranular zone with 4 hours treatment (Banasr *et al.*, 2004). However, in another experiment examining cell proliferation in the subgranular zone of hippocampus, acute administration of a different 5-HTR2 antagonist, cinanserin given at 2 mg/kg increased cell proliferation *in vivo*.

The 5-HTR4 has positive effects on cell proliferation in the gastrointestinal tract. Under culture conditions, many neurons normally undergo apoptosis. The 5-HT4 (tegaserod) agonists considerably increased neuronal survival and decreased apoptosis. Tegaserod also promoted extension of neurites *in vitro* (Liu *et al.*, 2009).

Since it is clear that activation of these specific receptors influences cell proliferation in other regions, this formed the focus of *in vitro* studies to determine if similar modulatory effects could be seen in spinal cord.

Using specific agonists that selectively activate these receptors is an approach taken by many researchers however, it is hard to get agonists that can work selectively on the target receptors. In this study, I used 8-OHDPAT, 5-CT as 5-HTR1A agonists, α-methyl-5-HT-maleate as a 5-HT2 agonist, cisapride and tegaserod as 5-HTR4 agonists since these agonists have potential to increase cell proliferation. However, these agonists also have binding affinity to other 5-HT receptors that may also slightly contribute to the cell proliferation and differentiation (Table 5.1). To enable rapid assessment of the role of specific receptors in mediating proliferative responses, these experiments were carried out in vitro using spinal cord slices. Since the time course of these experiments was much shorter, it is likely that proliferating cells have not had time to migrate or differentiate. Therefore, proliferating cells will be retained in the ECL region of the spinal cord at this time point

Table 5.1 List of drugs and receptors they bind to with agonist or * antagonist functions

Drug	Receptors
8-OH DPAT	5-HTR1A, 5-HTR7 (Hedlund *et al.*, 2004)
5-CT	5-HTR1A, 5-HTR1B, 5-HTR1E, 5-HTR5, 5-HTR7 (Nelson, 2004, Papageorgiou and Denef, 2007, Pithadia and Jain, 2009)
α-methyl-5HT-maleate	5-HTR2B, 5-HTR2A, 5-HTR2C (Sasaki *et al.*, 2003, Abzalov *et al.*, 2015)
Cisapride	5-HTR4, *5-HTR2 (antagonist), *5-HTR3 (antagonist) (De Maeyer *et al.*, 2008, Keller *et al.*, 2018)
Tegaserod	5-HTR4, 5-HTR1, *5-HTR2B (antagonist) (Beattie *et al.*, 2004, De Maeyer *et al.*, 2008)

5.2 Hypothesis

1. 5-HT promotes higher numbers of proliferating cells in ECL of spinal cord through activation of 5-HTR1A, 5-HTR2 and 5-HTR4.

5.3 Aims

1. To determine the extent of cell proliferation after activation of selected 5-HTRs *in vitro* using the acute spinal cord slice technique.

5.4 Methods

5.4.1 Animals

Animals were obtained from the CBS. All the procedures were conducted under regulation of UK Home Office License and UK Animal (Scientific Procedure) Act, 1986. Postnatal mice age 10 – 16 days were used of either sex. All ethical aspects were considered in order to reduce the suffering of animals during the experiment and to minimize the number of animals used.

5.4.2 Experimental procedure for 5-HTR1A agonists (5-CT, 8-OHDPAT), 5-HTR4 agonist (Cisapride) and 5-HTR2 agonist (Alphamethyl-5HT-maleate)

The animals were prepared according to the protocol described in Chapter 2, spinal cord slices obtained and divided into groups. The slices were incubated in vials filled with

aCSF (4 ml for each vial) for 30 minutes then EdU (4 µl of 1 mM) was added to each vial. The drugs were added to their respective vials (Table 5.2) but for each drug, there was a vial of just EdU to act as a control. All vials were oxygenated with 95% oxygen and 5% carbon dioxide and placed in a water bath at 37° Celsius. The drugs and EdU were changed every hour and after 4 hours treatment, the spinal cord slices were fixed in 4% PFA 0.1 M PB overnight (Banasr *et al.*, 2004). The 4% PFA was changed to 0.1 M PB solution. Then the 500 µm slices were embedded in gelatin and were resectioned at 50 µm before proceeding with EdU localisation.

Two different concentrations were used for cisapride and α-methyl-5HT-maleate in order to find the suitable concentration that was able to enhance cell proliferation in *in vitro.*

Table 5.2 List of ligands being used in *in vitro* experiments.

Drug	Receptor	Dissolved in	Stock concentration	Volume	Final concentration
8-OH DPAT	5-HTR1A	water	20 mM	6 µl	30 µM
5-CT	5-HTR1A	water	10 mM	4 µl	1 µM
Cisapride	5-HTR4	DMSO	10 mM	4 µl	1 µM
Cisapride	5-HTR4	DMSO	10 mM	40 µl	10 µM
α-methyl-5HT-maleate	5-HTR2	water	10 mM	4 µl	1 µM
α-methyl-5HT-maleate	5-HTR2	water	10 mM	40 µl	10 µM

5.4.3 Experimental procedure for 5-HTR4 partial agonist (tegaserod)

The protocol for preparing acute slices was slightly different in this tegaserod experiment. The spinal cords were sliced at 250 µm. The final concentrations used were 0.1 µM and 1 µM (Liu *et al.*, 2009) (Table 5.3). After the 4-hour incubation period, the sections were fixed in 4% PFA in 0.1 M PB followed by EdU-labelled protocol and clearing methods. This method was applied as a modification from the previous procedure in order to preserve as many sections as possible. In the previous technique the spinal cords were cut in 500 µm for incubation then were embedded in gelatin for resectioning to 50 µm. During the embedding process, the spinal cord needed to be placed as flat as possible and sometimes the spinal cord slices become a little bit curved after fixation. During resectioning, the curved slice did not cut properly, damaging the precious sections and fewer intact sections were left for counting, meaning more experiments needed to be undertaken to get enough sections. This new method did not require embedding and resectioning and the 250 µm sections are thicker compared to 50 µm sections, so after staining, a clearing method was introduced to maximise the visibility of the sections.

Table 5.3 Concentrations of tegaserod used in *in vitro* experiments.

Drug	Receptor	Dissolved in	Stock concentration	Final concentration
Tegaserod maleate	5-HTR4	DMSO	10 mM	0.1 µM
Tegaserod maleate	5-HTR4	DMSO	10 mM	1 µM

5.5 Results

5.5.1 Proliferation in the ependymal cell layer was not affected by addition of two different 5-HT1AR agonists (5-CT and 8-OH DPAT)

Proliferating cells were mapped and counted in the control, 5-CT and 8-OH DPAT groups. The experimental (5-CT and 8-OH DPAT) groups had similar numbers of EdU labelled cells compared to the control group. The mean numbers ± SEM of EdU-positive cells for each group were control group (7.23 ± 0.7), 5-CT (7.20 ± 0.6), and 8-OH-DPAT (5.93 ± 0.6). The difference between the three groups did not reach significance (Figure 5.2).

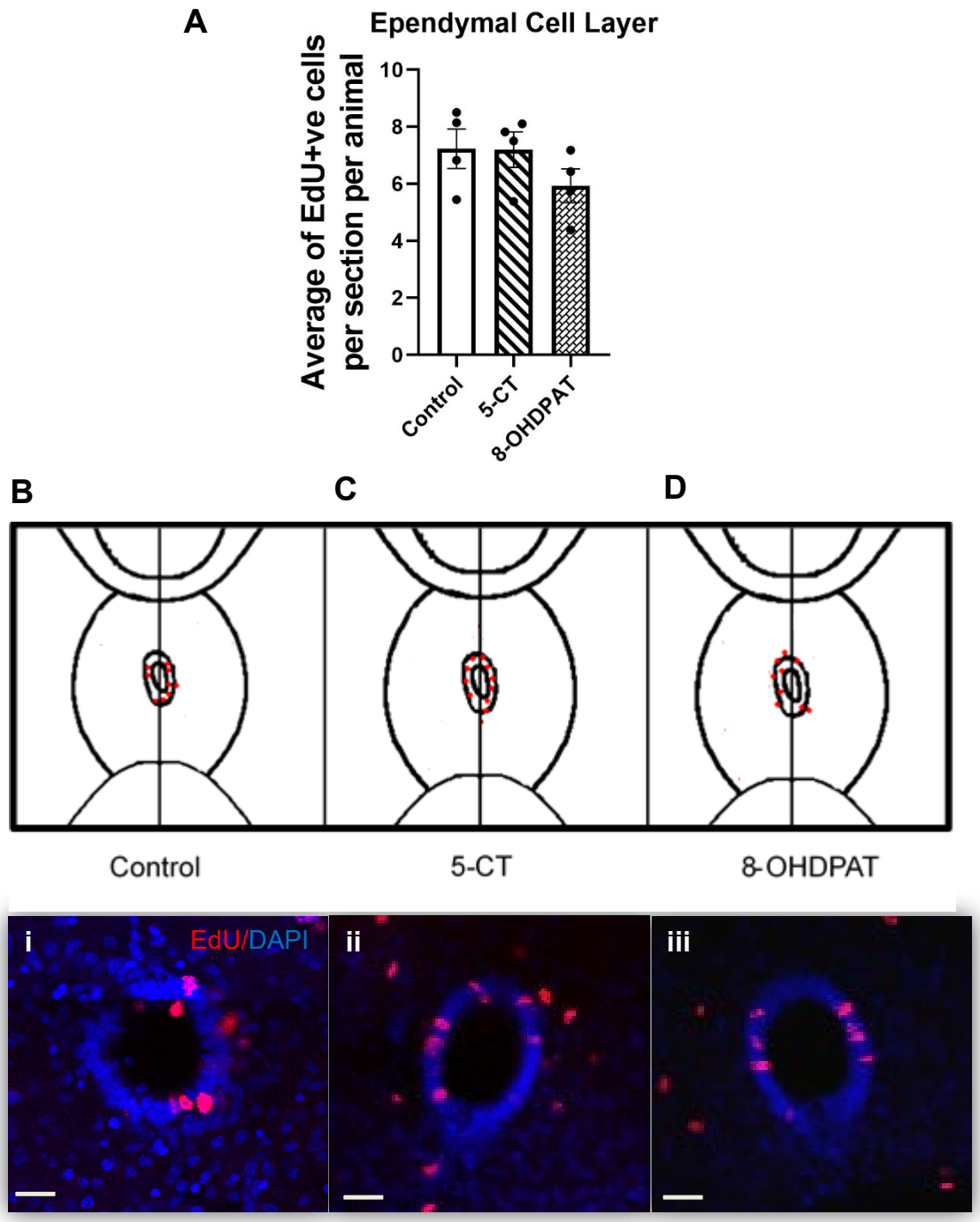

Figure 5.2 No difference in the number of EdU labelled cells in the presence of 5-HTR1A agonists. (A) Bar chart showing the average numbers of EdU labelled cells in central canal region of spinal cord following incubation with 5-CT and 8-OH-DPAT. There are no significant differences. (B-D) Schematic diagram of location of EdU-positive cells (red) in ependymal cell layer (ECL) that was plotted for counting for each group. (i-iii) Examples of immunofluorescence images showing EdU-positive cells (red) for each group. Blue refers to DAPI that stained cell nuclei. Scale bar: 30 µm. Black rounded dots on the bar graph refers to the mean value of each animal in each group. n = 4 for each group. Statistical analysis, one-way ANOVA was applied with significant value, $p \leq 0.05$)

5.5.2 Selective activation of different 5-HT receptors has different effects on proliferation

The effects of 2 different concentrations of cisapride and α-methyl-5HT-maleate were tested on spinal cord slices. In slices treated with 10 μM of cisapride (5-HTR4 agonist) there were significantly more EdU-positive cells in central canal area compared to control (4.0 ± 0.4 vs 2.22 ± 0.4; $p = 0.019$). However, there was no significant difference in numbers of proliferating cells treated with cisapride at 1 μM concentration compared to control slices. Furthermore, there were also no significant differences between control and treated-group for both concentrations (1 μM and 10 μM) of α-methyl-5HT-maleate (Figure 5.3 & Figure 5.4).

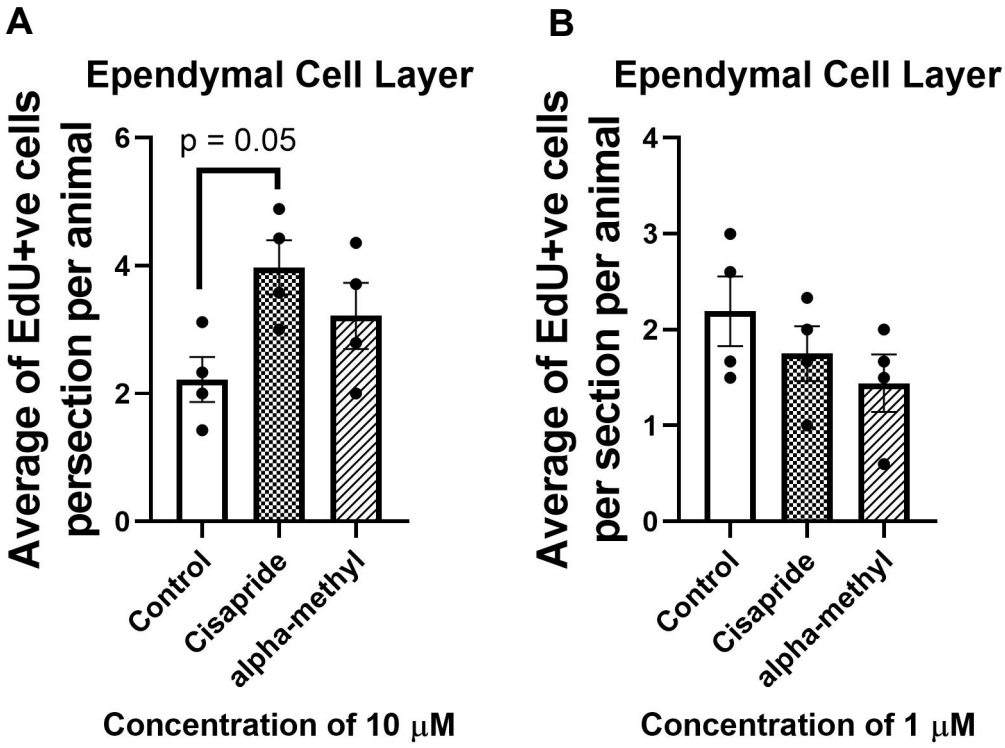

Figure 5.3 10 μM Cisapride increased the number of EdU labelled cells in ECL of spinal cord in acute slices.. (A) Numbers of EdU-positive cells after treatment with different 5-HTR agonists showing sections of spinal cord treated with 10 μM cisapride (5-HTR4 agonist) had higher numbers of EdU-labelled cells in ependymal cell layer of spinal cord compared to 10 μM alpha-methyl-5-HT-maleate. (B) 1 μM cisapride did not affect cell proliferation. Both concentrations of α-methyl-5HT-maleate also did not alter the extent of cell proliferation. Black rounded dots on the bar graph refers to the mean value of each animal in each group. n = 4 for each group. Statistical analysis, one-way ANOVA was applied with significant value, $p \leq 0.05$)

Figure 5.4 Representative images of EdU labelled cells for each agonist in acute slices experiment. (A) Schematic diagram of spinal cord showing the selected region (red-dotted box) in spinal cord. (B-D) Immunofluorescence images showing EdU-positive cells (red) in spinal cord sections in control slices or in the presence of the 5-HTR4 agonist (cisapride; C) or the 5HTR2 agonist (α-methyl-5HT-maleate; D) at concentrations of 10 μM. White-dotted line represents the region around the central canal that was selected for cell counting. (Bi-Di) Schematic diagram of spinal cord showing the EdU-positive cells in ECL plotted (red) for each group. Images at 40x objective. Scale bar 20 μm.

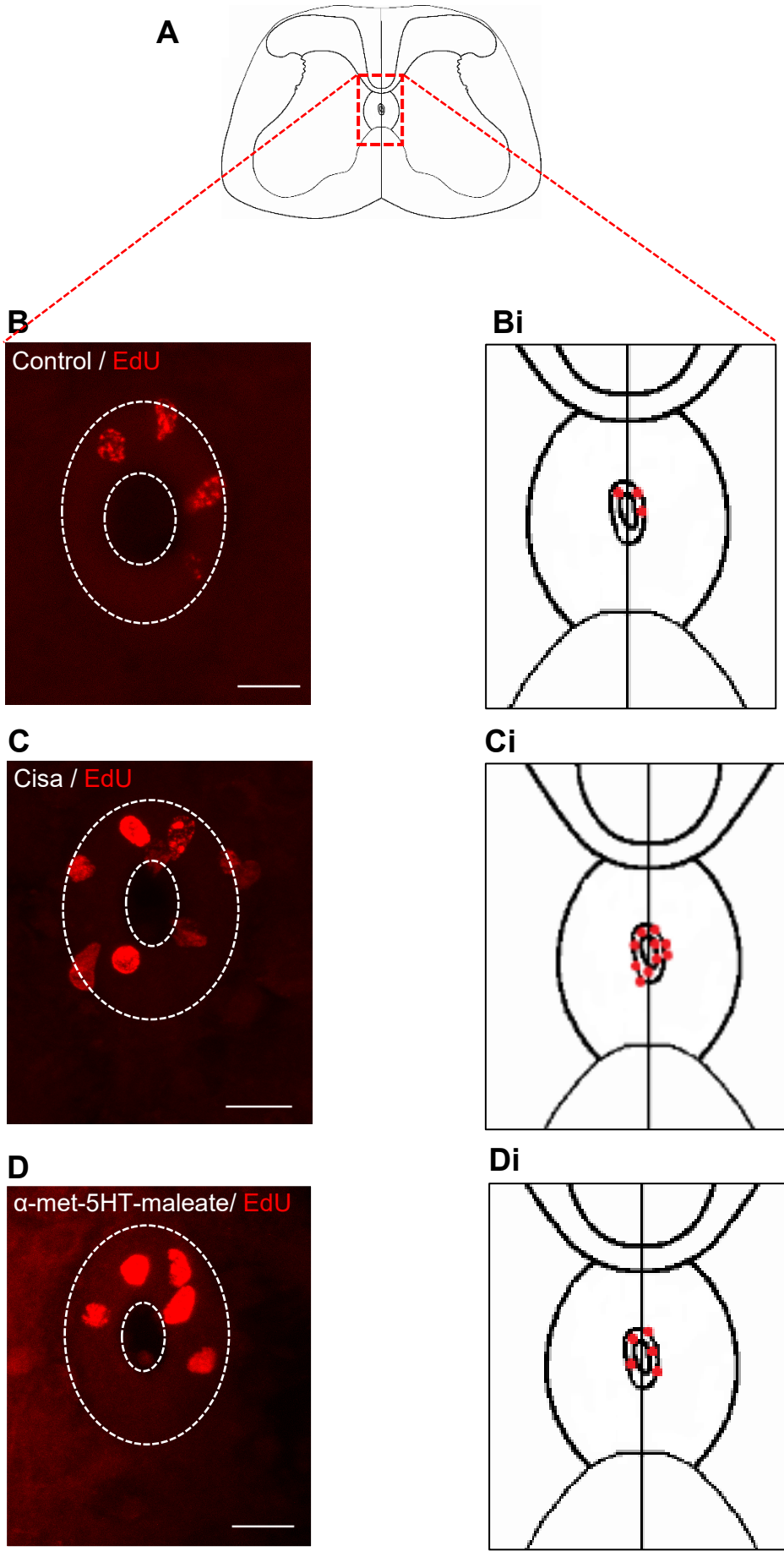
A
B
Control / EdU
Bi
C
Cisa / EdU
Ci
D
α-met-5HT-maleate/ EdU
Di

5.5.3 Activation of 5-HTR4 using tegaserod reduced the numbers of proliferating cells in ECL of spinal cord

In acute slices, spinal cord slices were treated with 2 different concentrations of tegaserod maleate (5-HTR4 agonist) in a 4-hour incubation period. At a concentration of 1 μM tegaserod, there were significantly fewer EdU positive cells in ECL of spinal cord compared to control group (7.02 ± 0.6 vs 13.31 ± 2.2, $p = 0.04$) while at 0.1 μM tegaserod there was no significant difference in the numbers of proliferating cells (12.95 ± 1.5) compared to control (13.31 ± 2.2; Figure 5.5).

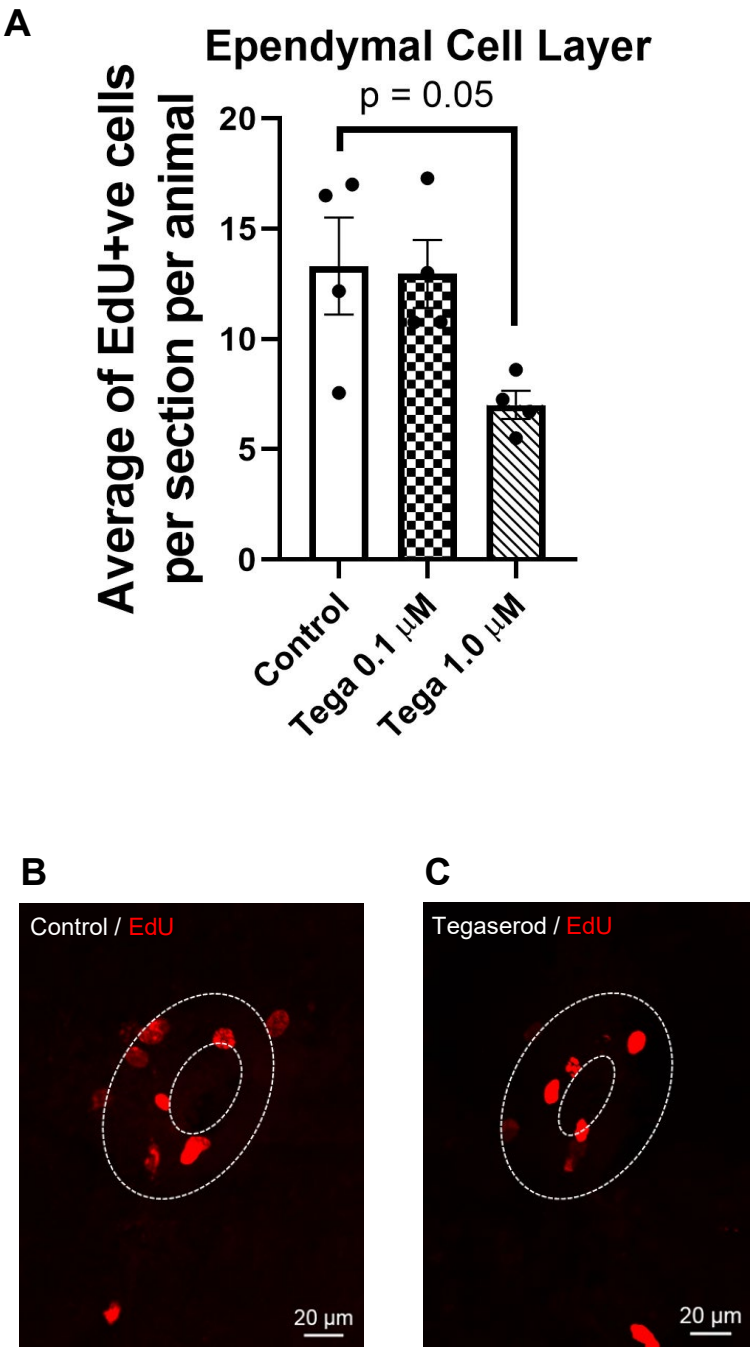

Figure 5.5 Slices treated with tegaserod at 1 μM had significantly fewer EdU-positive cells than control. (A) Bar chart of the numbers of proliferating cells in spinal cord sections treated with 0.1 μM and 1 μM tegaserod maleate shows the higher concentration of 1 μM reduced numbers of proliferating cells in ECL compared to control group. (B-C) Immunofluorescence images showing EdU-labelled cells in ECL (dotted line) in control and high tegaserod treated sections. Images at 40x objective. Black rounded dots on the bar graph refers to the mean value of each animal in each group. n = 4 for each group. Statistical analysis, one-way ANOVA was applied with significant value, $p \leq 0.05$)

5.6 Discussion

In these in *vitro* experiments using acute spinal cord slices, application of the 5-HTR4 via cisapride promoted higher numbers of proliferating cells in the ependymal cell layer but application of another 5HTR4 agonist, tegaserod, resulted in lower numbers of EdU positive cells. Activation of 5-HTR1A and 5-HTR2 did not cause significant changes in extent of cell proliferation.

5.6.1 Opposing effects of two 5-HTR4 agonists on proliferation

In this acute spinal cord experiment, activation of 5-HTR4 using cisapride significantly increased the numbers of proliferating cells in the ECL of spinal cord. In a 4-hour incubation of viable spinal cord slices using different concentrations of 1 μM and 10 μM, only the higher concentration of cisapride significantly enhanced cell proliferation. However, when a higher dose of tegaserod (1.0 μM) was given, there was a significant decrease in the numbers of proliferating cells. I will discuss these results, first considering the presence and role of the 5-HTR4 and then examining the possible reasons of the opposing effects.

An important factor that contributes to this effect is whether the 5-HTR4 itself is present in the spinal cord. Several studies had examined topographical distribution of 5-HTR4 in the spinal cord using immunohistochemical methods. It revealed that at the cervical level, 5-HTR4 are located at the ventral horn, which may include the region of the ependymal cell layer but this was not reported extensively and they only looked at cervical level (Suwa *et al.*, 2014). A study from Pineda-Farias *et al.* (2017) showed the location of 5-HTR4 in dorsal horn of lumbar spinal cord and a recent findings from Zhu *et al.* (2020) found 5-HTR4 are located at the dorsal horn of lumbar spinal cord. So far, they reported the location of 5-HTR4 are located at ventral horn of cervical, dorsal horn of lumbar and

dorsal horn of sacral of rat spinal cord (Suwa *et al.*, 2014, Pineda-Farias *et al.*, 2017, Zhu *et al.*, 2020)

There are still lacking of studies on this area, that reported the location of 5-HTR4 in spinal cord to confirm the specific location of the receptor especially in mice. Since my observation suggests the possibility of a role for 5-HTR4 around the central canal of spinal cord, future experiments confirming the location of 5-HTR4 in this central canal area of spinal cord would be worthwhile since this is where the potential neural stem cells are located.

5-HTR4 are abundant in the gastrointestinal system where the function is to control gastromotility and drugs that activate these receptors are used to treat constipation and reduce symptoms of irritable bowel syndrome (Evans *et al.*, 2004). However, there are fewer studies that examined the role of 5-HTR4 in the central nervous system especially related to the spinal cord. For instance, there is a study that observed increased numbers of proliferating cells ($BrdU^+$) in SGZ of hippocampus with 3 days administration of 1.5 mg/kg/day RS 67333, a partial 5-HTR4 agonist compared to control group. The drug was administered through osmotic minipumps (Lucas *et al.*, 2007). There are several studies on cell proliferation related to the enteric nervous system showing that activation of 5-HTR4 mediates neuroprotection and promotes neurogenesis. For example, incorporation of BrdU into cells was enhanced in the enteric nervous system and these cells became neurones that were eventually incorporated into the myenteric ganglia (Liu *et al.*, 2009). However, in this study, they did not examine whether this also occurred *in vitro* and they did not use cisapride so it is not possible to compare our two opposing effects with their results.

5.6.1.1 Tegaserod vs cisapride

Administration of cisapride and tegaserod in spinal cord acute slices for 4 hours produced very different results with respect to cell proliferation. Even though both agonists are thought to activate 5-HTR4, there might be other contributing factors that lead to different results. Both drugs are non-selective receptor agonists and have the potential to interact with multiple receptors which may provide an explanation for the difference observed. Tegaserod is also known to act as a polysialic acid mimicking agent, both in vitro and in vivo (Bushman *et al.*, 2014) and it can act in this way to promote 5-HT axon growth in a model of SCI (Pan *et al.*, 2014). Furthermore, it is well known that newly formed neurones in both the DG and SVZ express PSA-NCAM (Bonfanti and Seki, 2021), which may be involved in neuronal migration. In the ECL region of spinal cord however, it is expressed in the CSFcNs, not the ependymal cells (Marichal *et al.*, 2009) and tegaserod in these experiments decreased rather than increased cell proliferation. Therefore, although it cannot be entirely ruled out, it is unlikely that tegaserod is acting here as a PSA-mimetic. Binding affinity is one of the explanations that might contribute to the result.

Binding affinity (pK_i) is the strength of binding interaction between the agonist and the receptors. In an *in vitro* study using transfected cells, tegaserod has high-affinity binding to 5-HTR4 (pK_i = 8.4) but at the same time has affinity binding to 5-HTR2A (pK_i = 7.5), 5-HTR2B (pK_i = 8.4) and 5-HTR2C (pK_i = 7.0) (Beattie *et al.*, 2004). This finding also shows the potential non-selective effect of tegaserod. Another interesting finding in this affinity study showed that when delivering the same concentration of tegaserod, it had an agonist effect on 5-HTR4 and an antagonist effect on 5-HTR2B (Beattie *et al.*, 2004). Therefore, tegaserod has the potential to affect 2 receptors at the same time and the combination of agonist and antagonist activation may lead to lower numbers of proliferating cells in central canal of spinal cord. However, in my study, α-methyl-5HT-maleate, the 5-HTR2 agonist had little effect on cell proliferation so it is unlikely that the

different effects are due to activation or antagonism of a 5-HTR2. Cisapride also has a different affinity towards different 5-HTRs. Cisapride has an agonist effect on 5-HTR4 and weak antagonist effect on 5-HTR3 (De Maeyer *et al.*, 2008). Therefore, it is possible that cisapride is exerting some of its effects through 5-HT3 receptor antagonism. However, in hippocampus, the presence of the 5-HT3 receptor is essential for exercise induced neurogenesis so blockade of this receptor would be expected to decrease cell proliferation (Kondo *et al.*, 2015). This therefore does not explain the opposing effects of tegaserod and cisapride.

The most likely explanation may come from the fact that tegaserod can also act as a 5-HT1A, 1B and 1D receptor agonist (De Maeyer *et al.*, 2008) since although 8-OHDPAT, a 5-HTR1A agonist, had no effect on cell proliferation, other effects may be exerted through the other 5-HTR1. Indeed, Banasr and colleagues (2004) showed that the 5-HT1B/D agonist sumatriptan, decreased cell proliferation in SVZ so tegaserod may also be exerting the decrease in proliferation through activation of these receptor subtypes. In future, testing of tegaserod in the presence of a 5-HT1B or 1D receptor antagonist may enable more selective activation of the 5-HTR4 and thus a similar effect of tegaserod to cisapride.

According to Katayama *et al.* (1995), cisapride is the most potent agonist when compared to other agonists which are 5-HT (1.9-fold), 5-methoxytryptamine (5-MeOT) (7.3-fold), mosapride (4.3-fold), zacopride (11-fold), metoclopramide (26-fold). Cisapride may be the best and most selective 5-HTR4 agonist however, due to proarrthymic effects of cisapride, the drug is not suitable to use in *in vivo* experiments (Rampe *et al.*, 1997). Therefore, due to the selectivity of the 5-HTR4 agonist (tegaserod and cisapride), a new potential selective 5-HTR4 agonist needs to be used to establish the full extent of 5-HTR4 potential to increase cell proliferation (Figure 5.6).

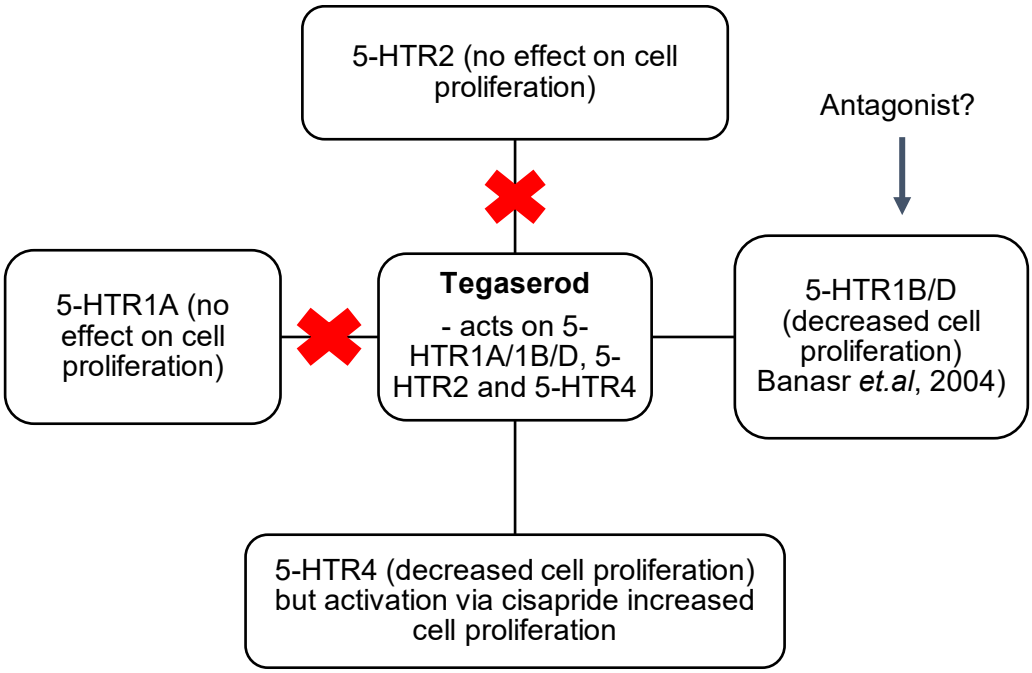

Figure 5.6 Proposed mode of action of tegaserod and suggested use of 5-HTR1B/D antagonist to see effect solely due to action via 5-HT4R.

5.6.2 Penetration of drug in 500 µm vs 250 µm of spinal cord slices

Two different thickness of spinal cord slices were used in this experiment, 500 µm and 250 µm. The technical issue of using 500 µm slices was addressed in Chapter 2 and thus 250 µm spinal cord slices were used in the *in vitro* experiments for the tegaserod group. Therefore, the potential that the different thickness of the spinal cord slices affects drug penetration must be considered. The need to ensure an adequate drug delivery deep into the healthy layers of the tissue makes pharmacological spinal cord acute slice experiments complicated, because there is no blood supply in tissue and thus delivery relies solely on passive drug diffusion. The 500 µm spinal cord slice is thicker than 250 µm spinal cord slices and we expect the penetration of drug, oxygen and nutrient into deep tissue in thicker slices may be different compared to thinner slices however, the different thickness (500 vs 250 µm) of slices were not tested for the same drug therefore we can't make a conclusion on that.

To date, there are no studies considering how the thickness of spinal cord acute slices may affect results obtained. However, in general, acute slice studies using other organs such as liver, lung, kidney and small intestine have used slices of 100 and 250, 600, 250 and 300 µm thickness respectively (L. Fisher *et al.*, 2001, de Graaf *et al.*, 2006). These different thickness slices still maintain the viability of the slices (Graaf *et al.*, 2007). For whole cell patch clamp recording technique on spinal cord slices, researchers recommended the thickness for acute spinal cord slices should be no more than 600 µm to satisfy cell visibility (Au - Zhu *et al.*, 2019). Therefore, the penetration of nutrient, oxygen and drug is unlikely to significantly differ if the different thickness of the spinal cord slices is less than 600 µm. However, it seems worth investigating this in future in *in vitro* experiments using spinal cord slices of different thickness to investigate if there any difference in cell proliferation with specific compounds.

5.6.3 Is there a role for 5-HT1A receptors in modulating cell proliferation in the spinal cord?

Acute activation of 5-HT1ARs using agonists that are reasonably selective for this receptor (5-CT and 8-OHDPAT) showed no significant increase in cell proliferation the the ECL region. In the acute phase, where the exposure of the drug is just 4 hours, this may not be enough to promote a significant change in cell proliferation due to the timing used here. There are mixed results observed from *in vivo* treatment with 8-OH DPAT with different timings of treatment. When the agonist was given for 14 days, it had no effect on cell proliferation in dentate gyrus compared to the group that received 1 month of treatment. BrdU and Ki67 were used as cell proliferation markers in order to see the cell proliferation and survival of cell proliferation (Huang and Herbert, 2005). It indicates that 8-OH DPAT did not enhance cell proliferation with drug exposure of less than 14

days. The time of drug exposure is very crucial in the treatment because the effectiveness of certain treatments depends on the time and amount of drug that is needed.

Other researchers also proved that exposure to 5-HT1A agonist for 2 hours 30 minutes did not affect cell proliferation at the subgranular layer but when the 8-OH-DPAT was given for 4 hours via intraperitoneal injection, it produced significantly increases in cell proliferation (Banasr *et al.*, 2004). In another *in-vivo* experiment, the use of 5-HT1AR antagonists to investigate cell proliferation was able to prove that 3 different antagonists which are NAN-190, p-MPPI (4-Iodo-N-[2-[4-(methoxyphenyl)-1-piperazinyl]ethyl]-N-(2-pyridinyl)benzamide monohydrochloride) and WAY 100635 significantly decreased cell proliferation after 2 hours drug exposure by about 30% compared to the control group (Radley and Jacobs, 2002). Among those 3 antagonists, WAY 100635 showed the lowest number of BrdU-labelled cells. Exposure to buspirone, a 5-HT1AR partial agonist for 3-4 weeks also showed increased cell proliferation in the subventricular area, olfactory bulb and dentate gyrus. Partial agonists have partial efficacy at the receptor, and it was suggested that buspirone needs a longer time to fully activate the 5-HT1AR. Therefore, the studies suggested that cell proliferation depends on the activation of 5-HT1AR and the proliferation can be seen as fast as 4 hours after exposure to 8-OH-DPAT (Banasr *et al.*, 2004). In a different study, animals that were injected with 8-OH-DPAT for a day showed significant increases in cell proliferation in dentate gyrus but no effect after 7 days of exposure to the agonist. In the same paper but using different animals, WAY 100125 (5-HT1AR antagonist) significantly reduced the degree of cell proliferation after 7 days exposure to the drug. All the experiments were focussed in the brain especially at the subgranular zone and the ventricular area which are the established stem cell niches.

The inconsistent results in cell proliferation that are obtained from the previous and current research on activation of 5-HT1AR need to be clarified by further experiments that are conducted for longer periods of time and at the same time other methods, such

as *in vivo* administration of drugs need to be utilised. There is also a possibility that the 5-HT1ARs were not actually present in the central canal area of the spinal cord since the Allen Mouse Brain and spinal cord Atlas shows negligible expression, although it was detected by autoradiography (Thor *et al.*, 1993). Therefore, further investigation needs to be carried out in order to confirm the findings.

5.7 Conclusion

Using 2 different agonists of 5-HTR4 led to interesting findings on the level of cell proliferation on ECL of spinal cord using acute *in vitro* experiments. Cisapride and tegaserod had significant effects, even though the effects were opposing each other. Cisapride enhanced the numbers of proliferating cells while tegaserod reduced the extent of cell proliferation (Figure 5.7). These findings are believed to be due to the non-selectivity of these agonists. It would be good to know the rate of cell proliferation after activation of 5-HTR4 via cisapride in *in vivo* however, due to the risk of cisapride causing cardiac arrhythmias, it is not appropriate to carry out this. Therefore in *in vivo* experiments will focus on tegaserod to determine the extent of proliferation when 5-HTR4 are activated via tegaserod.

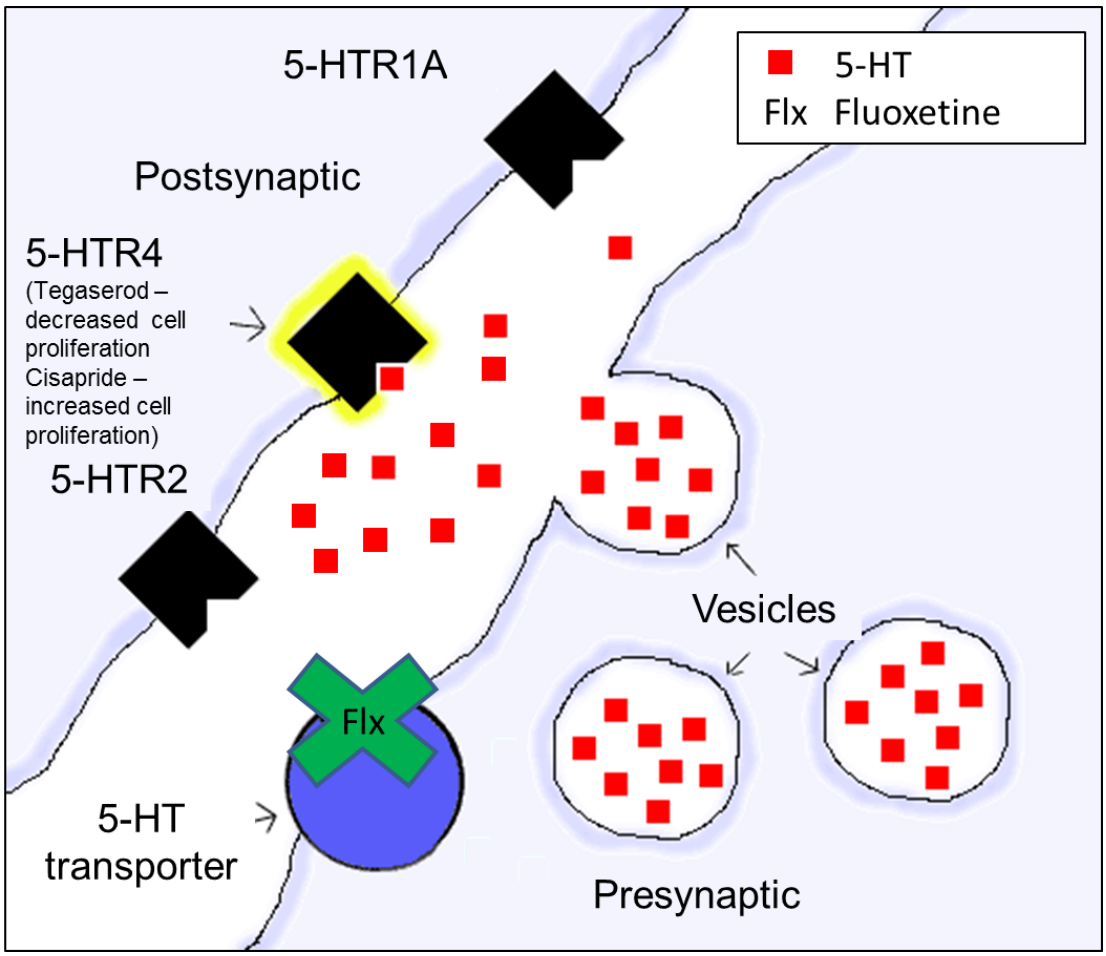

Figure 5.7 Action of SSRI and involvement of 5-HTR4 on cell proliferation Fluoxetine increases the endogenous 5-HT by blocking the 5-HT transporter. Activated 5-HTR4 via tegaserod reduced the number of cell proliferation while activated 5-HTR4 via cisapride increased numbers of proliferating cells.

Chapter 6

EFFECTS OF ACTIVATION OF 5-HTR4 via TEGASEROD ON NEUROGENESIS *IN VIVO*

6.1 Introduction

In the previous 2 chapters, increasing the level of endogenous 5-HT through flx successfully increased numbers of proliferating cells in selected areas of the central nervous system and *in vitro* experiments revealed that application of the 5-HTR4 agonist cisapride increased numbers of proliferating cells, whilst the other 5-HTR4 agonist tested, tegaserod, reduced cell proliferation in the ECL of the spinal cord. 5-HTR4 are found abundantly in the enteric nervous system and are physiologically important in gastric emptying and intestinal motility. Application of 5-HTR4 agonists increased cell proliferation and differentiation in the enteric nervous system and these receptors are also important for maintenance and neuronal growth (Liu *et al.*, 2009). In a transplant study, neural stem cells from embryos were transplanted into the tail vein of mice. Administration of a 5-HTR4 agonist (mosapride citrate) facilitated the formation of new-born enteric neurones from transplanted neural stem cells transplanted to the ileum which had been transected and anastomosed in mice (Goto *et al.*, 2016). The transplanted neural stem cells were mobilised to the anastomosed area, proliferated and differentiated into neurones. Since 5-HTR4 activation successfully promoted neurogenesis in the enteric nervous system and has significant yet apparently opposing effects in the ECL of spinal cord through in *vitro* experiments, it is worthwhile to investigate if 5-HTR4 agonists have significant effects in central nervous system through

in *vivo* experiments. Since cisapride might induce cardiac arrhythmias in *vivo* (Wysowski *et al.*, 2001), I investigated how tegaserod modulates cell proliferation in hippocampus, brainstem and spinal cord region.

6.2 Hypotheses

1. Decreased cell proliferation in the tegaserod-treated group in hippocampus, brainstem and spinal cord compared to control.
2. Changes in the percentages of colocalisation of EdU-labelled cells with differentiation markers for astrocytes, oligodendrocytes and neurones.

6.3 Aims

1. To determine the levels of cell proliferation in hippocampus, brainstem and spinal cord in control and tegaserod-treated groups of mice.
2. To determine the percentages of colocalisation of EdU-labelled cells with PanQKI (differentiation marker for oligodendrocytes), s100β (differentiation marker for astrocytes) or HUC/D (differentiation marker for neurones) in control and treatment group.

6.4 Methods

6.4.1 Animals

Refer to Chapter 2 (2.1)

6.4.2 Preparation of tegaserod maleate and EdU

Tegaserod maleate was prepared to give a final dose of 1 mg/kg and EdU was administered at 10 mg/kg. Tegaserod is soluble in DMSO at 0.5% final concentration and so this percentage in saline was used as the control treatment. EdU was dissolved in saline at 10 mM (Table 6.1).

Table 6.1 Concentration of 5-HTR4 agonist and EdU

Drug	Molecular weight	Concentration (mg/kg)	Concentration	DMSO
Tegaserod maleate	417.46 gm	1 mg/kg	500 µM in 0.1 ml of solution	0.5%
5-ethynyl-2'-deoxyuridine	252.22 gm	10 mg/kg	10 mM in 0.1 ml of solution	-

6.4.3 Protocol for in *vivo* experiment

Refer to Chapter 2 (2.3.2)

6.4.4 Area for counting

Quantification areas were identified and followed the same regions of interest described in chapter 2 (Figure 2.10). Since the 5-HTR4 were located at cervical, lumbar and sacral, the cell counting was extended to these regions (Suwa *et al.*, 2014, Pineda-Farias *et al.*, 2017, Zhu *et al.*, 2020).

6.5 Results

6.5.1 Tegaserod-treated mice had fewer cell proliferation compared to control experiments

The dorsal dentate gyrus was examined, (Figure 6.1) and in tegaserod treated animals there were significantly fewer proliferating cells compared to control group (32.56 ± 0.9 vs 40.46 ± 1.7; $p = 0.05$).

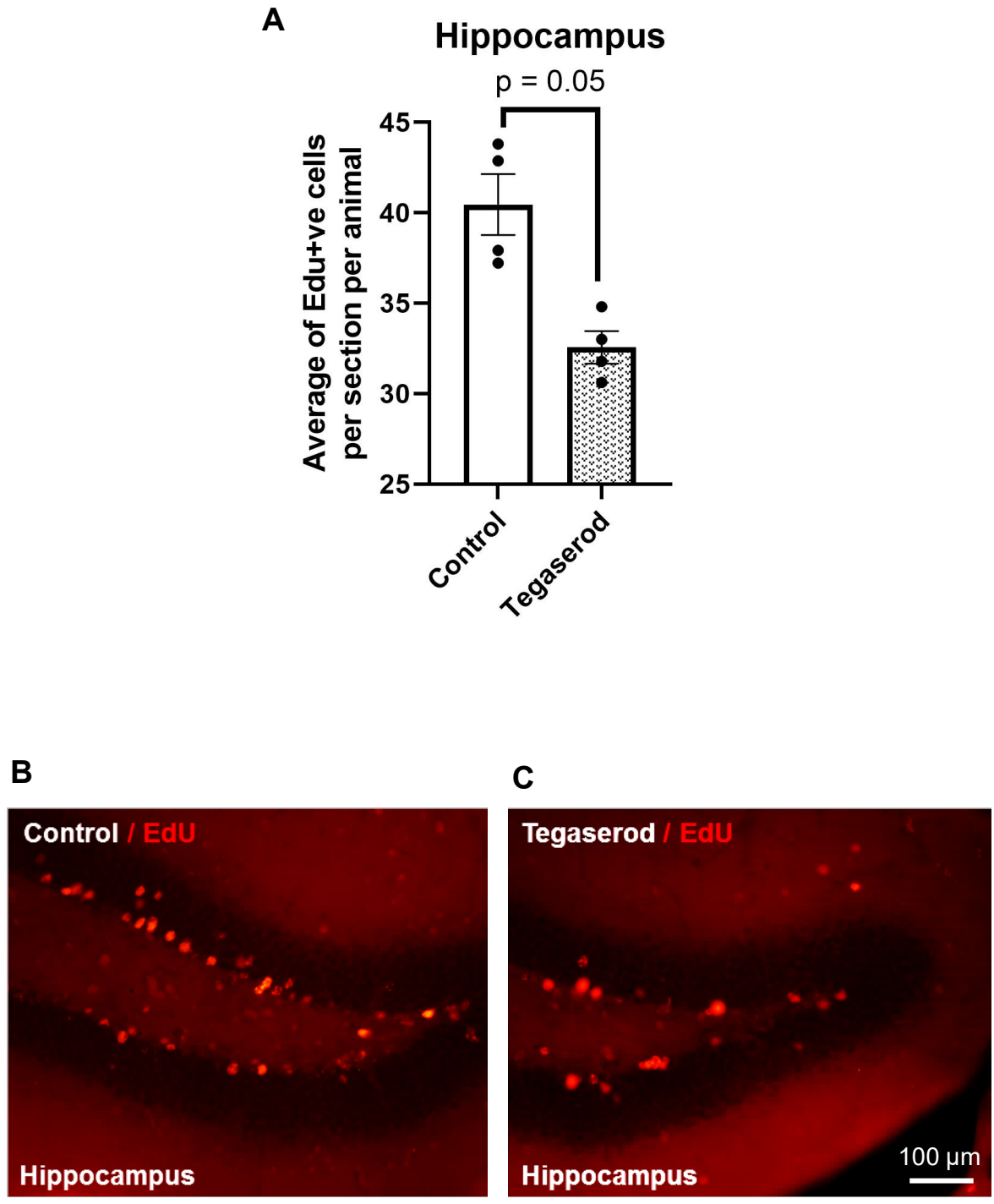

Figure 6.1 Cell proliferation was lower in dDG of tegaserod-treated animals. (A) Bar chart showing the numbers of proliferating cells were lower in tegaserod-treated compared to control mice. (B-C) Representative fluorescent images of EdU-labelled cells (red) in control and tegaserod groups. 40x objectives. Black rounded dots on the bar graph refers to the mean value of each animal in each group. n = 4 for each group. Statistical analysis, independent t-test was applied with significant value $p \leq 0.05$).

6.5.2 The proportion of EdU-positive cells that differentiated into astrocytes, oligodendrocytes and neurones were not significantly different in dDG of tegaserod treated animals

Percentages of EdU-positive cells that colocalised with differentiation markers for astrocytes (s100β), oligodendrocytes (PanQKI) and neurones (HUC/D) were calculated. In mice treated with tegaserod, there were no significant differences in the proportion of EdU positive cells that expressed these differentiation markers. Percentages of EdU-positive cells that differentiated into astrocytes (3.81 ± 1.3 vs 5.10 ± 2.2), oligodendrocytes (3.00 ± 1.2 vs 3.27 ± 2.4) and neurones (6.22 ± 3.0 vs 8.91 ± 3.0) (Figure 6.2).

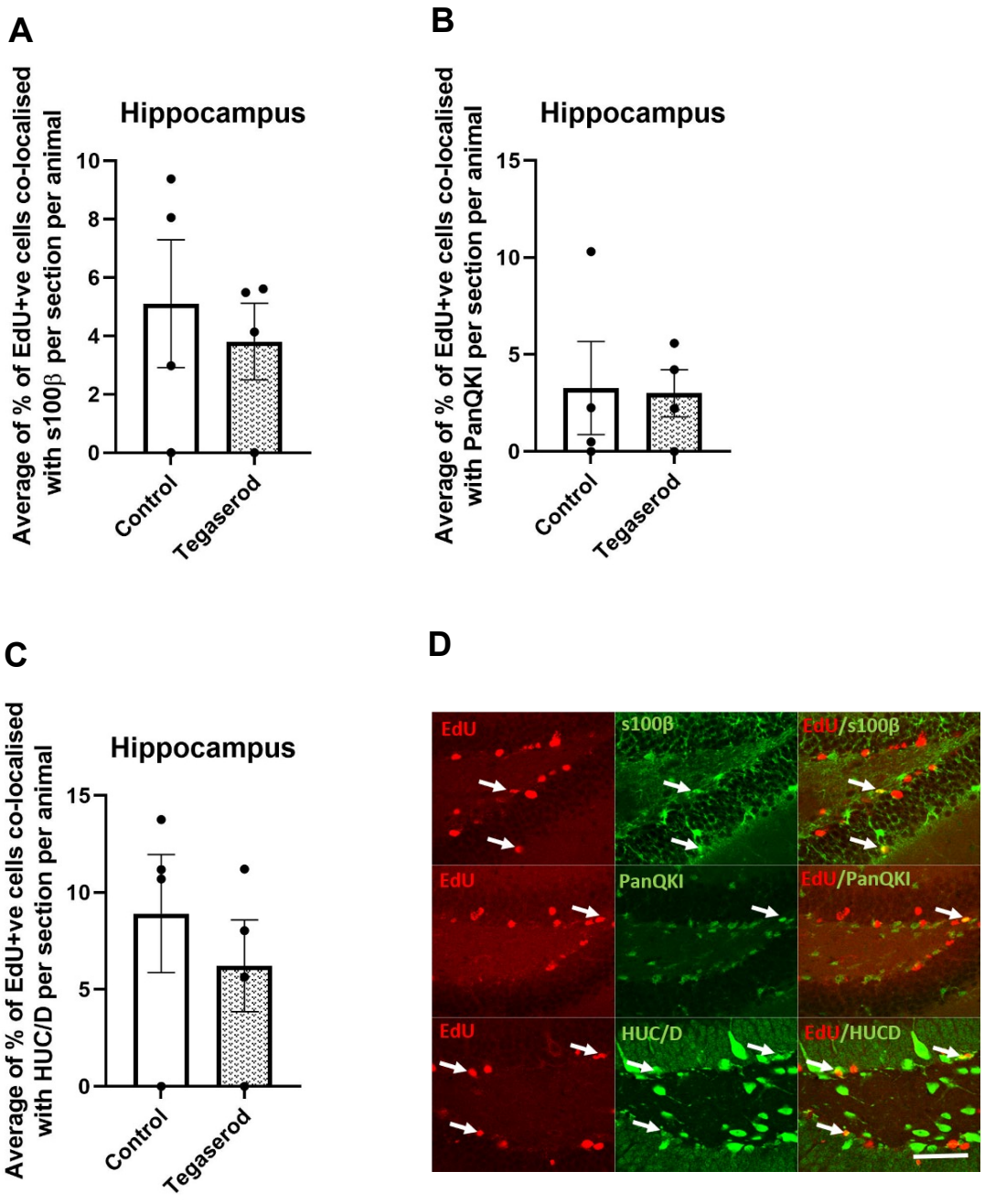

Figure 6.2 Tegaserod had no effect on cell differentiation on dDG of hippocampus (A-C) Bar chart showing percentages of EdU+ve cells that co-localised with differentiation markers in tegaserod and control groups. The differentiation markers are s100β (astrocytes), PanQKI (oligodendrocytes) and HUC/D (neurones). Black rounded dots on the bar graph refers to the mean value of each animal in each group. n = 4 for each group. Statistical analysis, independent t-test was applied with significant value, $p \leq 0.05$). (D) Representative images for each differentiation marker in dorsal dentate gyrus of hippocampus in tegaserod treated animals. EdU+ve (red), differentiation marker (green). 40x objective.

6.5.3 Tegaserod treated animals had lower numbers of proliferating cells in brainstem compared to control

There were significantly lower numbers of EdU-positive cells in the whole brainstem of tegaserod-treated compared to control mice (15.81 ± 5.0 vs 29.98 ± 2.9, p = 0.018). Upon closer examination of specific regions, there were also lower numbers of EdU positive cells in DVC (7.96 ± 3.0 vs 15.16 ± 1.1, p = 0.05), NTS (3.82 ± 1.4 vs 9.32 ± 0.9, p = 0.006) and ECL (2.28 ± 0.3 vs 4.65 ± 0.4, p = 0.003) (Figure 6.3). There were no significant differences between treated and control groups in AP (2.86 ± 1.0 vs 3.70 ± 0.4), DMX (1.21 ± 0.7 vs 2.13 ± 0.3), raphe (0.0 ± 0 vs 0.03 ± 0.03), IO (2.04 ± 1.0 vs 4.23 ± 0.9) and pyramidal region (3.53 ± 0.9 vs 5.91 ± 0.7) (Figure 6.3).

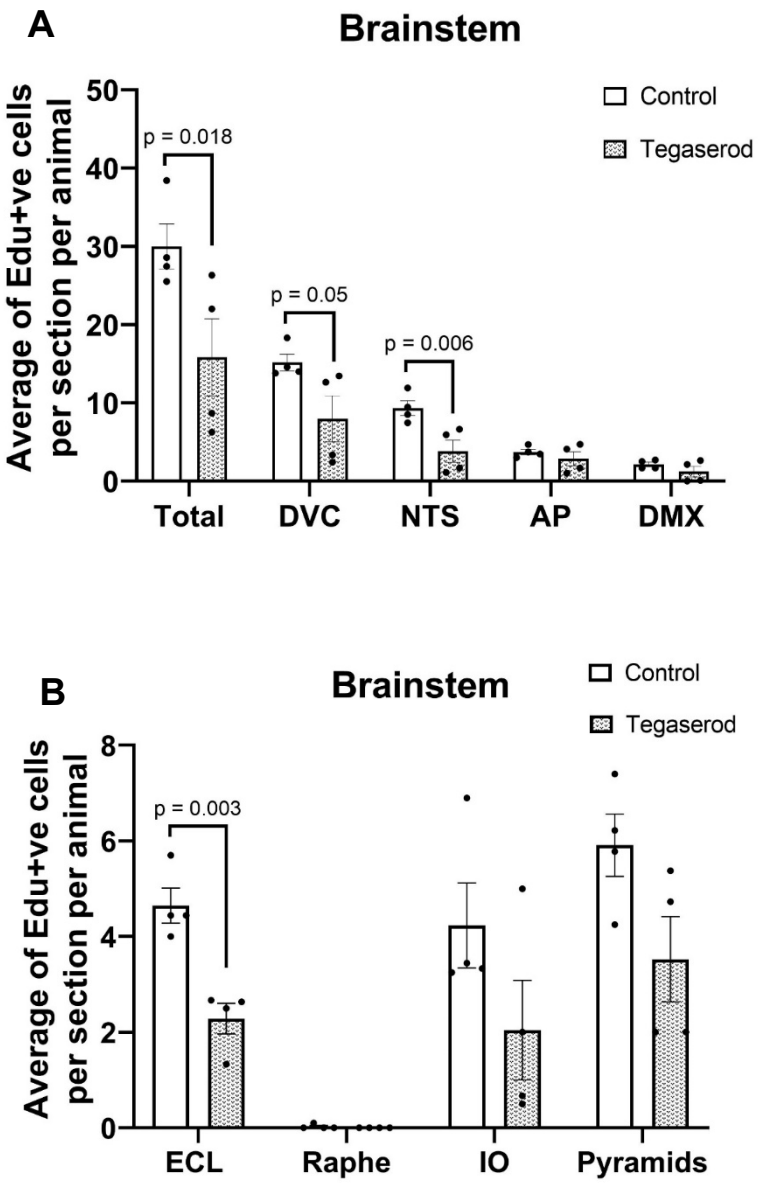

Figure 6.3 There were significantly fewer proliferating cells in some brainstem regions of tegaserod treated mice. (A) Bar chart showing that cell proliferation was significantly lower in the tegaserod-treated group compared to control group in total area of brainstem and selective regions of interest which are dorsal vagal complex (DVC) and nucleus tractus solitarii (NTS). (B) Bar graph of the quantification of other brainstem regions reveals that the ependymal cell layer (ECL) had significantly fewer proliferating cells in tegaserod group than control group. Raphe, inferior olive (OI) and pyramidal area do not show any significant difference. Black rounded dots on the bar graph refers to the mean value of each animal in each group. n = 4 for each group. Statistical analysis, independent t-test was applied with significant value, $p \leq 0.05$)

6.5.4 In brainstem of tegaserod-treated animals, the proportion of EdU-positive cells differentiating into astrocytes, oligodendrocytes and neurones was not significantly different compared to control.

Administration of tegaserod for seven days did not influence the proportion of proliferating cells that differentiated into astrocytes, oligodendrocytes and neurones. The percentages of co-localisation of EdU-positive cells with differentiation markers for tegaserod vs control animals for s100β was 9.77 ± 3.5 vs 13.57 ± 4.29, for PanQKI was 5.54 ± 1.9 vs 3.79 ± 2.8 and for HUC/D was 21.09 ± 7.3 vs 20.64 ± 7.6 (Figure 6.4).

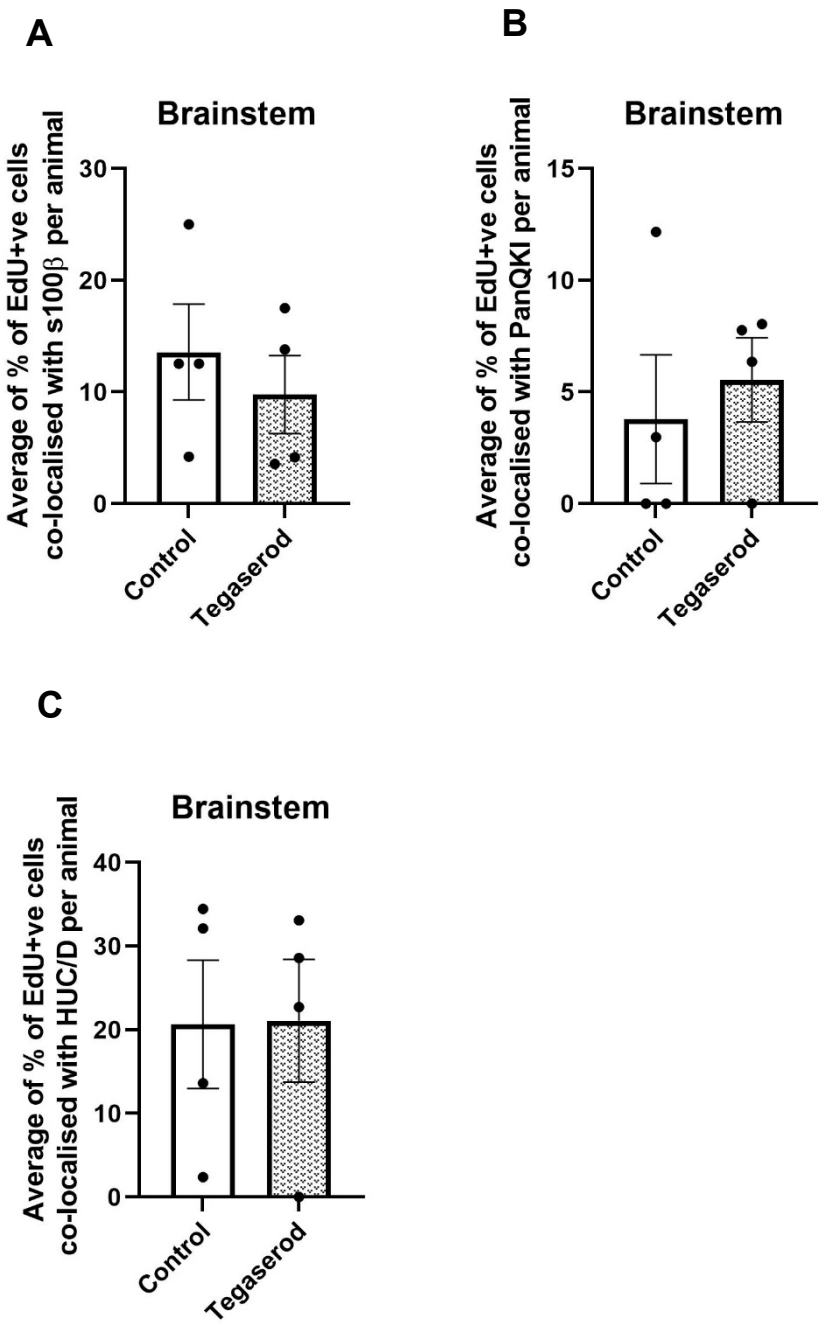

Figure 6.4 Percentages of co-localisation were not significantly different between groups in the brainstem. Bar chart showing that the percentages of co-localisation of proliferating cells with markers for (A) astrocytes, (B) oligodendrocytes and (C) neurones were not significantly different between groups in all regions of interest in brainstem. Black rounded dots on the bar graph refers to the mean value of each animal in each group. n = 4 for each group. Statistical analysis, independent t-test was applied with significant value, $p \leq 0.05$)

6.5.5 A lower number of proliferating cells in the tegaserod-treated group in spinal cord

Like brainstem, the spinal cord also has 5-HTergic fibres that are located in close proximity to nestin-GFP cells located in the cell layer surrounding the central canal of spinal cord at every level. Quantification of EdU-positive cells was carried out in cervical, thoracic, lumbar and sacral sections of spinal cord, looking specifically in the ECL, white matter and gray matter and total for the whole region. In spinal cord, regardless of the level examined, there were significantly fewer EdU-positive cells in the whole sections of tegaserod-treated animals compared to control, which was 55.66 ± 4.7 vs 76.87 ± 2.6; p = 0.008. On closer inspection of different regions, ECL (3.49 ± 0.6 vs 5.88 ± 0.7; p = 0.05), gray matter area (21.69 ± 1.7 vs 33.67 ± 1.6; p = 0.002) and white matter (28.54 ± 2.1 vs 37.60 ± 2.0; p = 0.02) all showed lower numbers of EdU labelled cells in the tegaserod treated animals compared with controls (Figure 6.5). When looking into different levels of spinal cord, the lumbar area (37.66 ± 7.3 vs 54.68 ± 9.4; p = 0.02) and sacral area (53.4 ± 4.4 vs 86.05 ± 10.4; p = 0.04) showed significant fewer numbers of proliferating cells in tegaserod-treated group compared to control group. However, there were no significant differences in cervical area (79 ± 19.1 vs 102.8 ± 12.6) and thoracic area (51.74 ± 6.4 vs 69.32 ± 10.8) (Figure 6.5). Looking more closely at the lumbar and sacral region, there were changes observed in specific regions. At sacral level, the white matter of treated animals had significantly fewer cells, (28.3± 2.9 vs 47.4 ± 5.6; p = 0.02), while at lumbar level, none of the specific regions had significant differences (Figure 6.7).

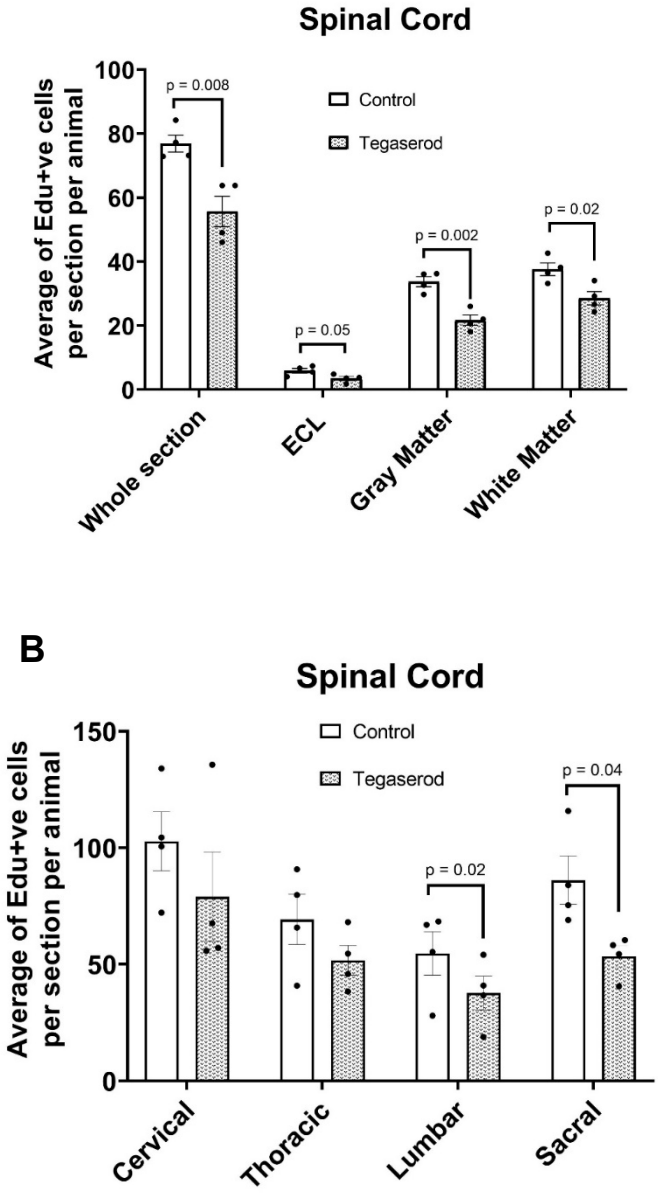

Figure 6.5 Animals treated with tegaserod had lower extent of cell proliferation in selected regions of spinal cord. (A) Bar chart representing proliferating cells in the cervical to sacral region, showing decreased numbers of proliferating cells in whole section of spinal cord, ependymal cell layer (ECL), gray matter and white matter in tegaserod treated compared to control mice. (B) The lumbar and sacral regions showed reduced cell numbers in the whole section of treated animals. Black rounded dots on the bar graph refers to the mean value of each animal in each group. n = 4 for each group. Statistical analysis, independent t-test was applied with significant value, $p \leq 0.05$)

Figure 6.6 Example images of EdU-positive cells in the tegaserod-treated and control groups. (A) Control group has more EdU-labelled cells (red) when compared to tegaserod-treated group in (B) in spinal cord region. (Ai-Aii) Control group showing higher EdU-labelled in ECL, white matter and gray matter compared to tegaserod-treated group in (Bi-Bii). (Aii and Bii) close up view at the dorsal horn area of gray matter of spinal cord.

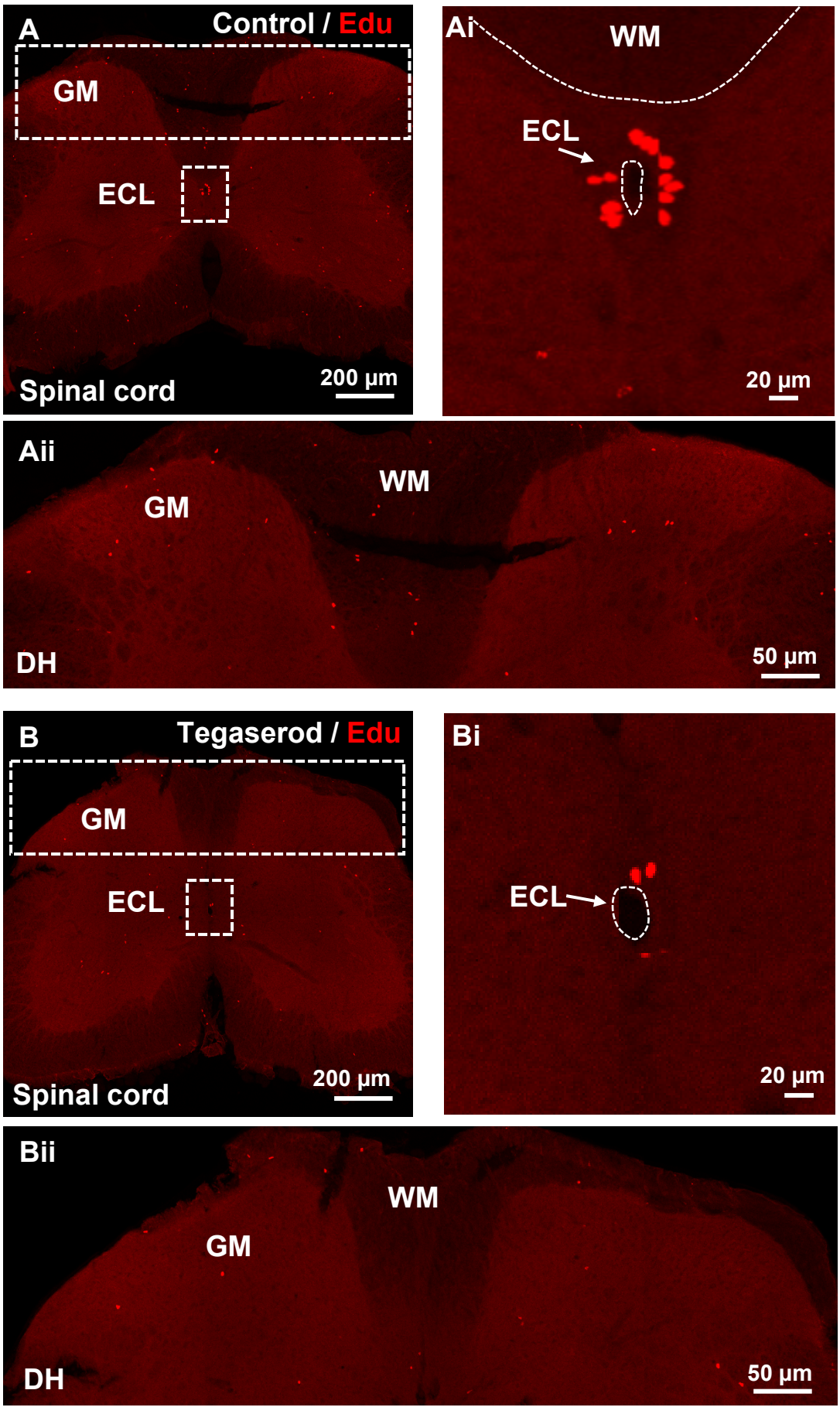
A
Control / Edu
GM
ECL
Spinal cord
200 µm
Ai
WM
ECL
20 µm
Aii
WM
GM
DH
50 µm
B
Tegaserod / Edu
GM
ECL
Spinal cord
200 µm
Bi
ECL
20 µm
Bii
WM
GM
DH
50 µm

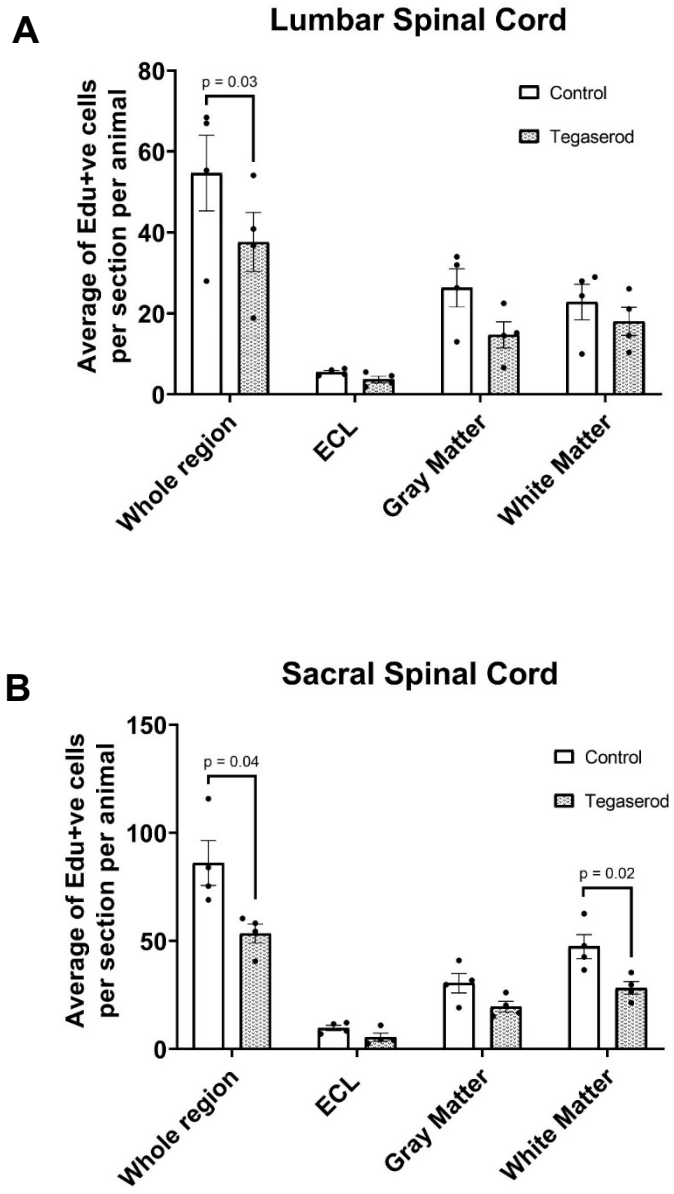

Figure 6.7 Lower numbers of proliferating cells in lumbar and sacral spinal cord in tegaserod-treated group. (A) Lumbar spinal cord has lower numbers of EdU-labelled cells in tegaserod-treated group for whole section however, not specifically in ECL, gray matter and white matter regions. (B) Sacral region has the same pattern of decreased cell proliferation in treated group, but only white matter area showed a significant decrease. Black rounded dots on the bar graph refers to the mean value of each animal in each group. n = 4 for each group. Statistical analysis, independent t-test was applied with significant value, $p \leq 0.05$)

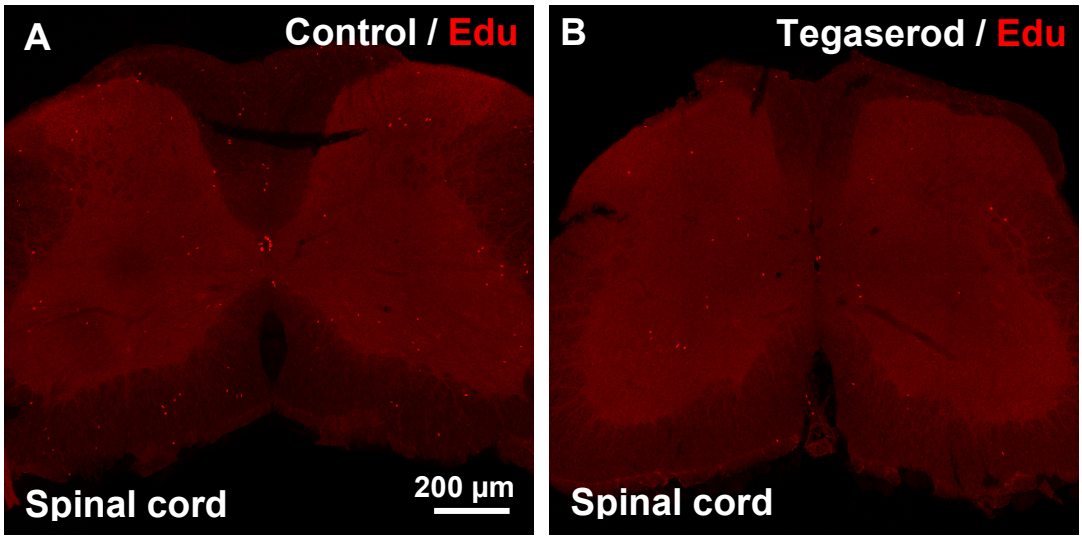

Figure 6.8 Example images of EdU-positive cells in the tegaserod-treated and control groups. (A) Control group has more EdU-labelled cells (red) when compared to tegaserod-treated group in (B) in spinal cord region. Scale bar 200 µm

6.5.6 Tegaserod did not influence differentiation in spinal cord

Administration of tegaserod daily for 7 days does not modulate the differentiation of proliferating cells into neurones or supporting glial cells. In the spinal cord, the percentages of co-localisation of markers for astrocytes (5.33 ± 0.2 vs 3.82 ± 0.8), oligodendrocytes (7.27 ± 2.2 vs 7.02 ± 3.4) and neurones (7.12 ± 1.8 vs 11.38 ± 2.0) in EdU-labelled cells in tegaserod-treated group did not differ from control group (Figure 6.8).

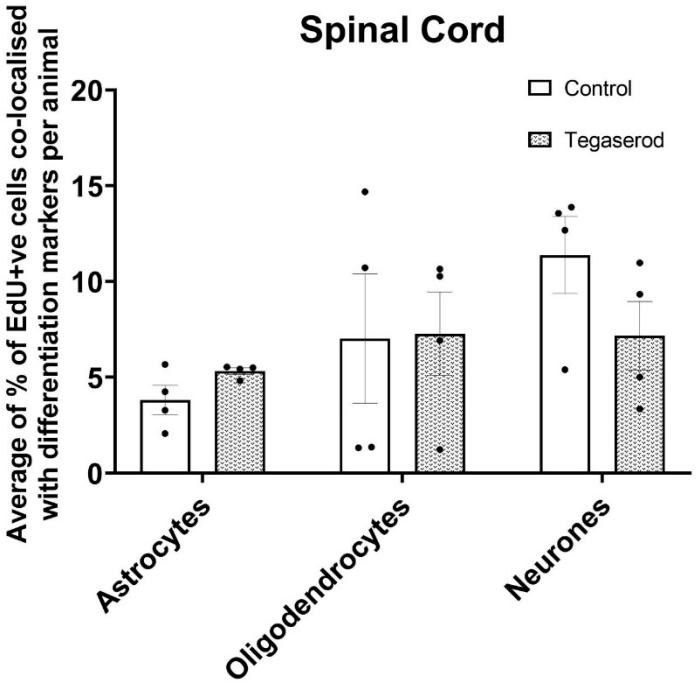

Figure 6.9 Tegaserod did not significantly affect proliferating cell differentiation to astrocytes, oligodendrocytes or neurones. Bar chart showing percentages of co-localisation of EdU+ cells with markers of astrocytes, oligodendrocytes and neurones in brainstem area. There were no significant differences between control and treated groups. Black rounded dots on the bar graph refers to the mean value of each animal in each group. n = 4 for each group. Statistical analysis, independent t-test was applied with significant value, $p \leq 0.05$)

6.6 Discussion

Administration of the 5-HTR4 agonist tegaserod significantly decreased the numbers of proliferating cells in dentate gyrus of hippocampus, and selective regions in brainstem and spinal cord. However, the proportions of EdU-positive cell becoming astrocytes, oligodendrocytes and neurones were not significantly different in hippocampus, brainstem and spinal cord region of control vs tegaserod treated animals. This suggests that activation of 5-HTR4 via tegaserod has a dampening effect on cell proliferation in hippocampus, brainstem and spinal cord. However, these results contrast with previous gastrointestinal work on 5-HTR4, which merits further consideration.

6.6.1 High-affinity binding, high efficacy and desensitisation of 5-HTR4 to tegaserod

Tegaserod has high-affinity binding to 5-HTR4 and is used in treating irritable bowel syndrome with constipation in women although this is not yet established in men (Wagstaff *et al.*, 2003, Cole and Rabasseda, 2004). Some agonists (even partial agonists) have the potential to develop desensitisation when the receptors are continuously activated (Charlton, 2009). Desensitisation is a process that diminishes the positive effect and can occur through repeated treatment or very high concentrations of drug. The possible mechanisms may involve receptor phosphorylation by G-couple protein receptor kinases (GRK) and G-protein uncoupling. In the gastrointestinal system (GIT), tegaserod desensitisation has been associated with G-protein coupled receptor kinase. Tegaserod mediated desensitisation has been proved by Nedi *et al.* (2011) using the desensitisation protocol (*in vitro*) from Rondé *et al.* (1995) and applying it to oesophagus (tunica muscularis mucosae) and distal colon. They showed that when 10

μM (no data in mg/kg provided) of tegaserod was added, after 20 minutes the effect on muscle contraction was reduced. In the same study, to confirm which GRK receptors were involved in desensitisation, a desensitisation protocol followed by co-immunoprecipitation in western blot was carried out. It revealed that desensitisation of 5-HTR4 by tegaserod is regulated by GRK2 and GRK6 in rat oesophagus and distal colon respectively (Nedi *et al.*, 2011). In a different study, acute administration of 5 mg/kg intraperitoneal injection of tegaserod did not affect the expression of GRK2 and GRK6 in the same regions (Nedi *et al.*, 2018). These studies suggested tegaserod did not change the expression of GRK2 and GRK6 and they concluded that the basal level of GRK2 and 6 was sufficient to cause desensitisation to tegaserod. These studies provide a possibility that in my study, administration of tegaserod desensitised the 5-HTR4 through activation of GRK2 and GRK6.

In *in vitro* studies using distal colon, tegaserod showed a desensitisation effect at concentrations as low as 5 nM and the effect increased with higher concentrations up to 5 μM (Grider, 2006). In control they use mucosal brush stroke to provoke the contraction (Figure 6.10). Even in the recovery phase, when the tegaserod is being washed out, the contraction appeared again revealed that the desensitisation was solely caused by tegaserod.

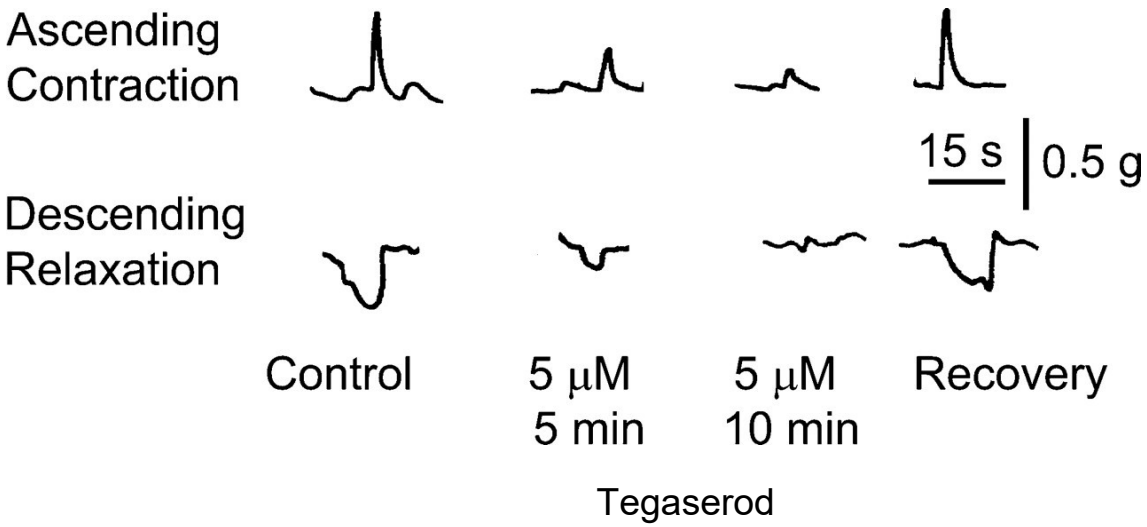

Figure 6.10 In vivo experiment of dose-dependent desensitisation(Grider, 2006).Recordings were from rat colon, with ascending colon contraction and descending colon relaxation stimulated by mucosal brush strokes. The responses were reduced in the presence of tegaserod.

In my study, the concentration of tegaserod is higher (1 mg/kg (500 μM), so the occurrence of desensitisation is highly plausible. The experiment by Grider (2006) was an *in vitro* study where even a small amount of tegaserod was able to trigger desensitisation while in this *in vivo* experiment, the concentration might be different because the agonist needs to go through the whole pharmacokinetic process in order reach the target cells. Another point to consider is that most of the desensitisation studies to date used gastrointestinal organs while in central nervous system, the concentration of tegaserod that can trigger desensitisation is still unknown, therefore, 1mg/kg of tegaserod might be able to trigger desensitisation in brain and spinal cord. The desensitisation of tegaserod on 5-HTR4 is regulated by GRK2 and GRK6 and depends on dosage that has influence on the degree of desensitisation. Thus, the desensitisation may reduce the ability of receptors to stimulate the downstream mechanism leading to lower levels of stimulation and potentially reducing the rate of proliferative activity in hippocampus and spinal cord region. However, due to lack of research in desensitisation of tegaserod in central nervous system especially in brain and spinal cord, it is important

to establish in future studies whether the desensitisation shares the same mechanism as in gastrointestinal system with central nervous system. One proposed method to test this would be a desensitisation protocol applied to acute brain slices or acute spinal cord slices. Since 5-HT 4 receptors are abundantly expressed in the dorsal raphe nucleus, (Waeber *et al.*, 1995), patch clamp recordings could be made from these neurones and the effects of increasing doses of tegaserod on spontaneous action potential firing frequencies investigated

6.6.2 Tegaserod also activates 5-HTR1 (agonist) and acts at 5-HTR2 (antagonist)

Tegaserod is a partial agonist for 5-HTR4. As discussed in Chapter 5, tegaserod also activates 5-HTR1A/1B/1D and 5-HTR2. The same explanation may therefore be applied to my *in vivo* experiments. Findings from my *in vitro* experiments revealed that activation of 5-HTR1A did not produce any effect on cell proliferation. Furthermore, activation of 5-HTR2 also has no significant effect on cell proliferation. However, activation of 5-HT1B/1D in acute slice experiments was not carried out. Even though the experiment was not performed, previous studies using sumatriptan as an agonist for 5-HTR1B/1D showed decreased cell proliferation in subventricular zone and GR127935, an antagonist for 5-HTR1B/1D, increased cell proliferation at the same region. However, both drugs did not have an effect on numbers of proliferating cells in subgranular zone (Banasr *et al.*, 2004). Activation of 5-HTR1B/1D via tegaserod in my experiment may mimic the activation of the same receptor using sumatriptan which significantly reduced the number of proliferating cells. In order to get the full effect of tegaserod on 5-HTR4, using GR127935 as an antagonist of 5-HTR1B/1D could be useful in future proliferation studies.

6.6.3 Minimal penetration across the blood-brain barrier

Methods of drug delivery determine the level of effectiveness of the drug. Oral administration of drug has lower absorption due to the first-pass effect in the liver before the drug enters the systemic circulation. Tegaserod has better absorption when taken without food compared to with food (Appel-Dingemanse *et al.*, 2000). Therefore, to achieve the effectiveness of the drug to the maximum level, tegaserod was delivered using intraperitoneal injection to reach the systemic circulation through the peritoneal membrane and then cross the blood-brain barrier. A further issue may be penetration of tegaserod through the blood-brain barrier, due to the size and polarity of tegaserod, however, in a randomised control study, people prescribed tegaserod suffered from side effects like headache and migraine along with diarrhoea (Tack *et al.*, 2005, Quigley *et al.*, 2006). Therefore, it seems that tegaserod does indeed cross the blood-brain barrier. However, to date, there are not many studies that investigate the extent of penetration of tegaserod across the blood brain barrier, so the statements are inconclusive. Since in this study, tegaserod has an effect on cell proliferation in hippocampus and spinal cord, this indicates the potential of tegaserod to cross the blood brain barrier. It is worth knowing the rate of tegaserod penetration across the blood-brain barrier in order to determine the exact dose that can act effectively on the receptor.

6.7 Conclusion

In general, activation of 5-HTR4 via tegaserod *in vivo* reduced the numbers of proliferating cells in the dentate gyrus of hippocampus and selective regions of spinal cord. Interestingly, there was no effect on any brainstem region. However, the extent of differentiation into neurones, astrocytes and oligodendrocytes was not significantly different between groups. Lower expression of 5-HTR4 in central nervous system compared to the gastrointestinal system, desensitisation and minimal penetration through blood-brain-barrier are potential reasons for a smaller effect of tegaserod on numbers of proliferating cells in different regions of the central nervous system. For example, if there are no receptors in the brainstem region then no effect would be expected.

Chapter 7

DOES FLUOXETINE REVERSE THE REDUCTION OF CELL PROLIFERATION IN MICE ON A HIGH-FAT DIET?

7.1 Introduction

Reductions in cell proliferation in the hippocampus happen in certain conditions such as prenatal stress, alcohol consumption, nicotine and high-fat diet (Jang *et al.*, 2002, Kawamura *et al.*, 2006, Lindqvist *et al.*, 2006). Several studies have attempted to reverse the reduction of cell proliferation, for example by using physical activities like exercise, or pharmacological treatment. Obesity is one of the factors that can reduce the numbers of proliferating cells in the hippocampus (Jackson-Guilford *et al.*, 2000, Lindqvist *et al.*, 2006). In my study, I used C57Bl/6 mice that were given a high-fat diet for eight weeks to promote obesity or glucose intolerance. At the same time, flx was given to help in modulating changes in cell proliferation. In previous studies using mice on normal diets, flx successfully increased cell proliferation in hippocampus, brainstem and spinal cord (see intro relevant section). Therefore, administration of flx in high fat-diet mice may help reverse the reduction of cell proliferation observed in high-fat diet.

7.2 Hypothesis

1. Administration of flx in drinking water can reverse or ameliorate the reduced numbers of proliferating cells in high-fat diet condition.

7.3 Aims

1. To determine the metabolic changes such as glucose levels after glucose tolerance test (GTT) and insulin tolerance test (ITT), weight gain, food intake, water intake in the low-fat diet group, high-fat diet group, high-fat diet with the administration of flx for four weeks and high-fat diet with administration of flx for eight weeks.
2. To determine the extent of cell proliferation in all groups.
3. To determine the percentages of colocalisation of s100β (astrocytes), PanQKI (oligodendrocytes), HUC/D (neurones) and Iba1 (microglia) with Edu-labelled cells (proliferating cells) in all groups.

7.4 Methods

C57/Bl6 male mice, aged 5 weeks, were housed in 4 cages, five animals per cage. Other methods were described in Chapter 2 (2.5)

Table 7.1 List of experimental group and number of animal in each group

Groups	Number of animals
Low-fat diet	5
High-fat diet	5
High-fat diet with 4-weeks of fluoxetine	5
High-fat diet with 8-weeks of fluoxetine	5

7.5 Results

7.5.1 Administration of fluoxetine did not improve glucose levels after Glucose Tolerance Test (GTT)

Glucose measurements were taken before the start of the experiment (Week 0), in the middle of the experiment (week 4) and the final week of the experiment (week 8). The result showed glucose levels during GTT were higher in all three groups that had a high-fat diet compared to the low-fat diet group. This was observed at all times tested. Normal glucose levels should be below 7.8 mmol/L after 120 minutes of GTT. If the glucose level is between 7.9 – 11 mmol/L, the condition is considered as impaired glucose tolerance, and if it is more than 11 mmol/L, this is a diabetic state. The results showed that after eight weeks' consumption of high-fat diet only and high-fat diet with four weeks administration flx, the mice were in an impaired glucose tolerance state, while in high-fat diet mice with eight weeks administration of flx, they were in a diabetic state (Figure 7.1). The glucose levels at 120 minutes, are shown in Table 7.2.

Table 7.2 Glucose levels at 120 minutes after glucose tolerance test (GTT)

	Glucose level (mmol/L) at 120 minutes of GTT		
Group	Week 0 (±SEM)	Week 4 (±SEM)	Week 8 (±SEM)
Low-fat diet	7.6 ± 0.83	5.5 ± 0.18	6.38 ± 0.37
High-fat diet	7.70 ± 0.71	7.32 ± 0.59	10.58 ± 0.84
High-fat diet + 4 weeks of flx	8.08 ± 0.51	8.92 ± 0.71	11.0 ± 0.86
High-fat diet + 8 weeks of flx	6.56 ± 0.35	10.22 ± 0.41	11.5 ± 0.74

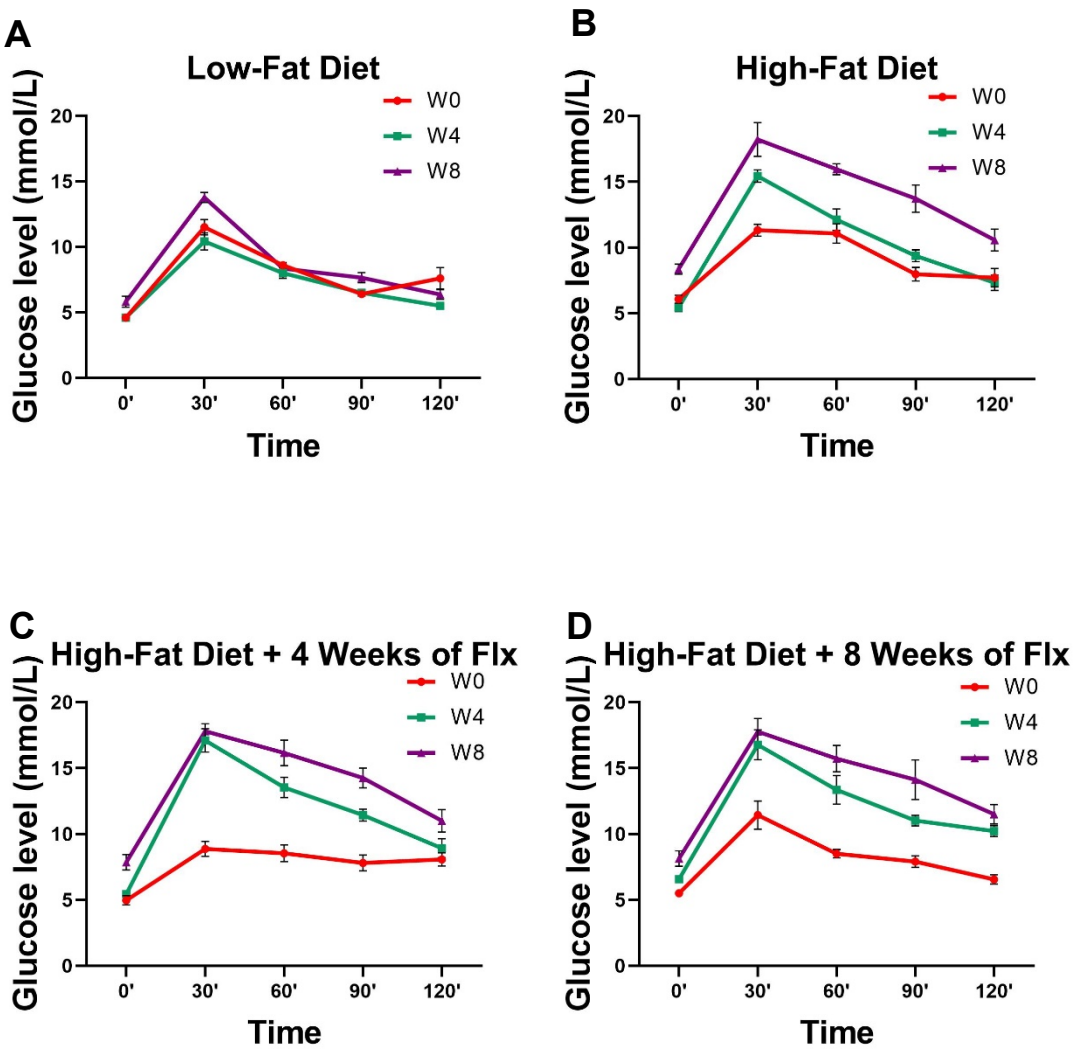

Figure 7.1 Fluoxetine did not improve glucose levels in the high-fat diet group. (A) Glucose levels in low-fat diet groups. (B) Glucose levels in the high-fat diet group. (C) In the high-fat diet group with administration of four weeks of flx, at week 8, the mice were in impaired glucose tolerance state. (D) High-fat diet with eight weeks of treatment were treated with flx, where the mice reached a diabetic state in week 8.

7.5.2 Glucose levels did not improve with flx treatment during Insulin Tolerance Test (ITT)

Animals fasted for 2 hours before the procedure. Fasting blood glucose was considered as time 0 (basal measurement); after the injection of insulin, the measurement was taken every 30 minutes until 120 minutes. The glucose levels (mmol/L) varied across the groups (Figure 7.2) but flx did not improve the levels in the high fat diet group.

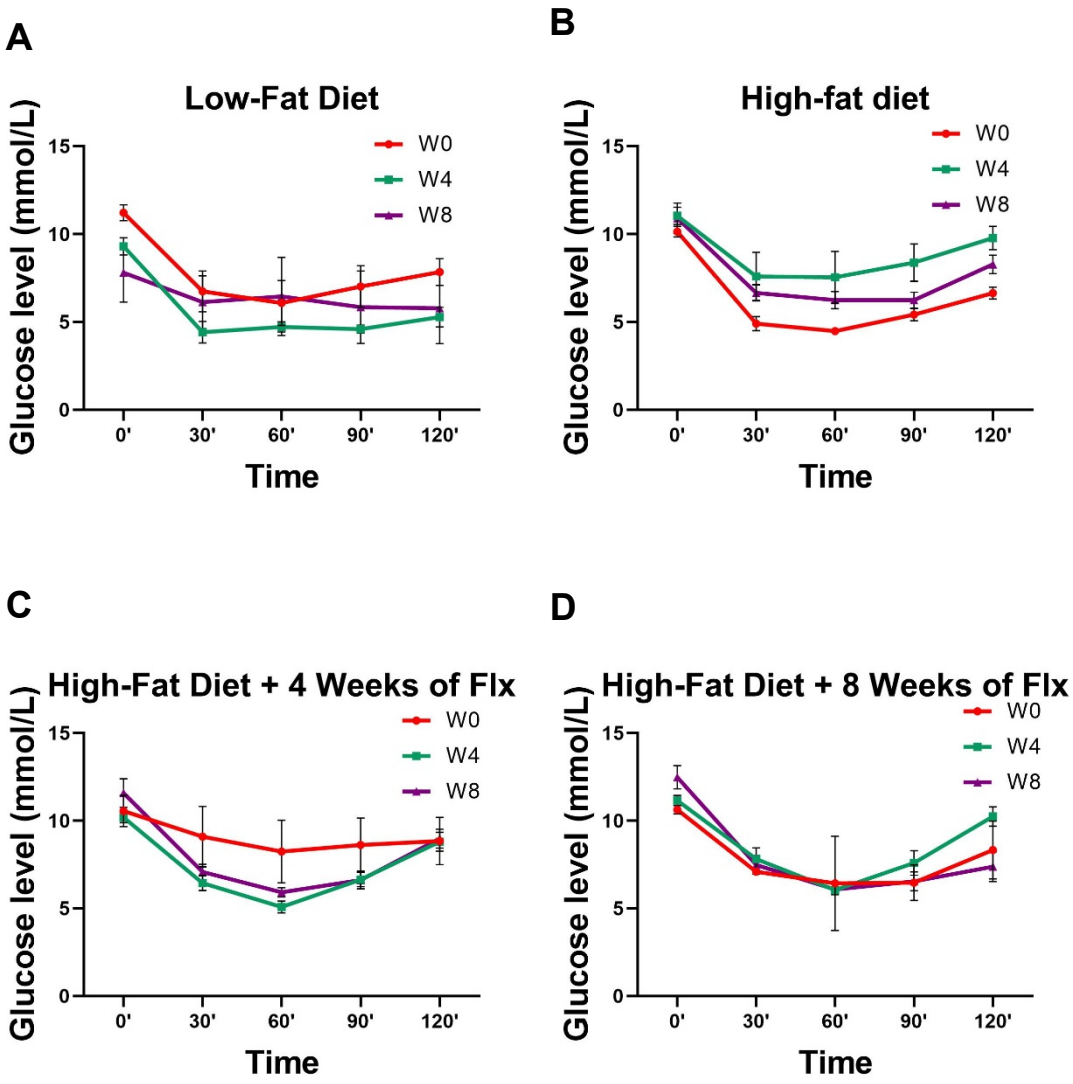

Figure 7.2 The glucose levels did not improve in the ITT with the administration of flx for eight weeks. (A) Glucose levels in low-fat diet group. (B) In the high-fat diet group, the insulin response was less sensitive at weeks 4 and 8 compared to week 0. (C) In the high-fat diet group with administration of flx for four weeks, the insulin sensitivity at t120 remains the same over the weeks. (D) In the high-fat diet group that received 8 weeks of flx, there was little variation in insulin sensitivity from week 0 to week 8.

7.5.3 Increased weight gain in the high-fat diet groups, regardless of flx.

The high-fat diet groups significantly increased weight over the weeks when compared to the low-fat diet group. Indeed at the end of 8 weeks, all the high-fat diet groups had significantly increased weight gain compared to the low-fat group (Table 7.3). However, there was no significant change in weight between all three high-fat diet groups, regardless of whether they had been administered flx (Figure 7.3).

Table 7.3 Mean (± SEM) for weight variant at week eight.

Group	Mean ± SEM	p-value	Significant
HF vs LF	14.00 ± 1.8 vs 5.68 ± 0.5	0.001	**Yes
HF + 4 wks flx vs LF	14.68 ± 1.0 vs 5.68 ± 0.5	0.002	**Yes
HF + 8 wks flx vs LF	16.22 ± 2.1 vs 5.68 ± 0.5	0.002	**Yes

** significant $p \leq 0.001$, one-way ANOVA statistical test

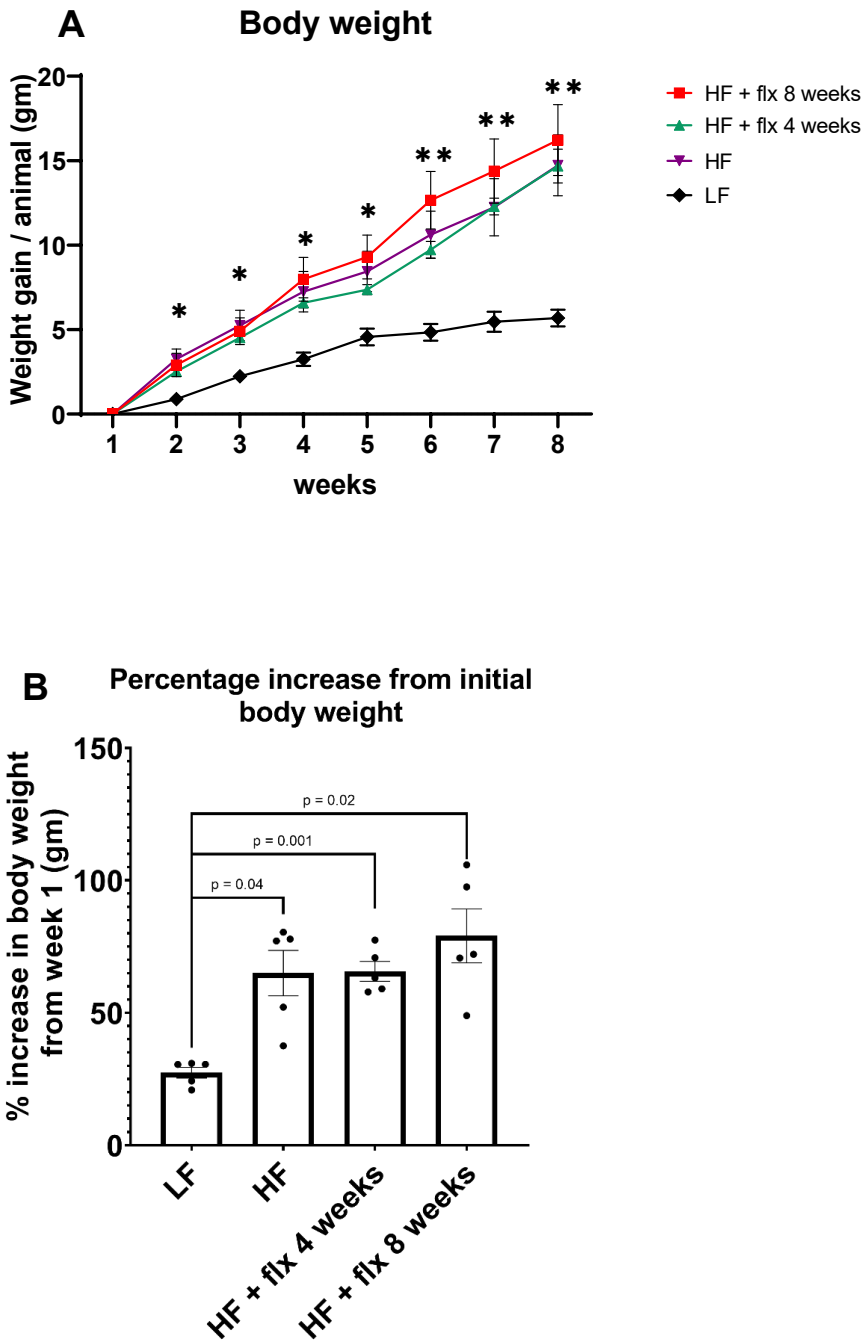

Figure 7.3 Increased weight gain over the weeks. (A) Increases in weight gain for all groups on high-fat diet regardless of flx administration compared to the low-fat group. (B) Percentages of body weight increased from week 1 to end of study plotted as % increase from initial weight. The weight gain was significantly greater in high-fat diet groups compared to low-fat diet group regardless of additional treatment. Two-way ANOVA statistical test was applied.

7.5.4 Increased weight in all groups over the eight weeks

The weight gain for individual mice for every week was plotted to observe the increased weight gain pattern in all groups. In low-fat diet group, the increases for each mouse were quite flat and did not exceed 10 g at the end of the experiment. However, in the high-fat diet group, all the groups showed a rapid increase in weight gain including flx-treated group especially after week 4 and week 5. Therefore, flx did not change the rapidly increased weight gain caused by the high-fat diet (Figure 7.4). It was clear that, there was a high degree of variability in weight gain in each individual mouse for high-fat diet and high-fat diet with 8 weeks flx compared to other groups.

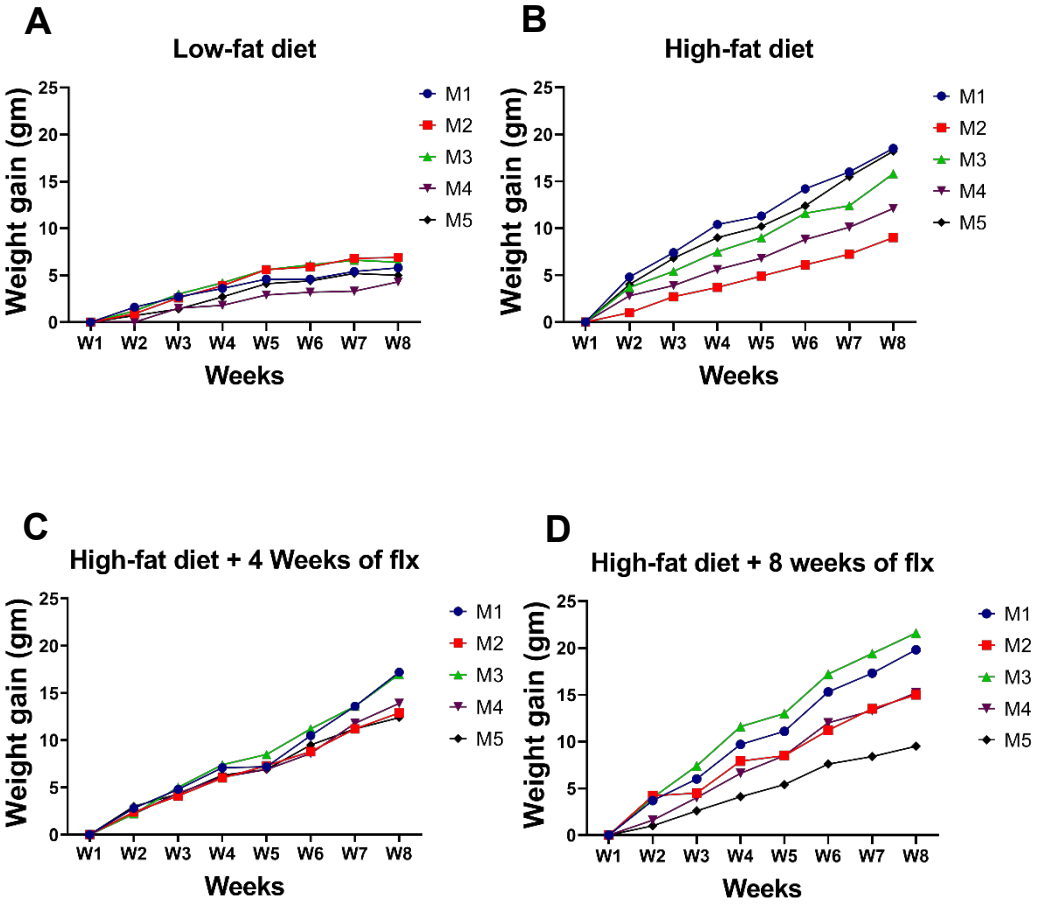

Figure 7.4 Fluoxetine did not show an anorexigenic effect. (A) Low-fat diet group showed expected weight gain over the eight weeks, while (B) high-fat diet showed rapid increases. (C-D) High-fat diet groups given flx for four weeks and eight weeks also had the same trends in weight gain as (B) but there was a high degree of variability between mice.

7.5.5 Variations in food intake for each group

The amount of food intake was measured to know how much the consumption of food varied per group per day. Food intake did in fact vary amongst groups, although due to the group housing conditions to reduce stress in mice, it was not possible to obtain data on this for individual mice. Mice on the high-fat diet with eight weeks treatment of flx consumed significantly lower amounts of food compared to mice on high-fat diet with four weeks flx (87.81 ± 2.0 gm/group/week vs 275.8 ± 32.2 gm/group/week, p-value = 0.0001). Similarly, those on high-fat diet with eight weeks flx treatment had significantly lower food consumption compared to high-fat diet only (87.81 ± 2.0 gm/group/week vs 280.3 ± 16.5, p-value = 0.0001). Those on high-fat diets had significantly higher food intake compared to low-fat diet group (280.3 ± 16.5 gm/group/week vs 87.81 ± 2.0 gm/group/week, p-value = 0.0001) while those on high-fat diet with 4 weeks flx also had significantly higher food intakes compared to low-fat diet group (275.8 ± 32.2 gm/group/week vs 89.77 ± 2.0, p-value ≤ 0.0001) (Figure 7.5).

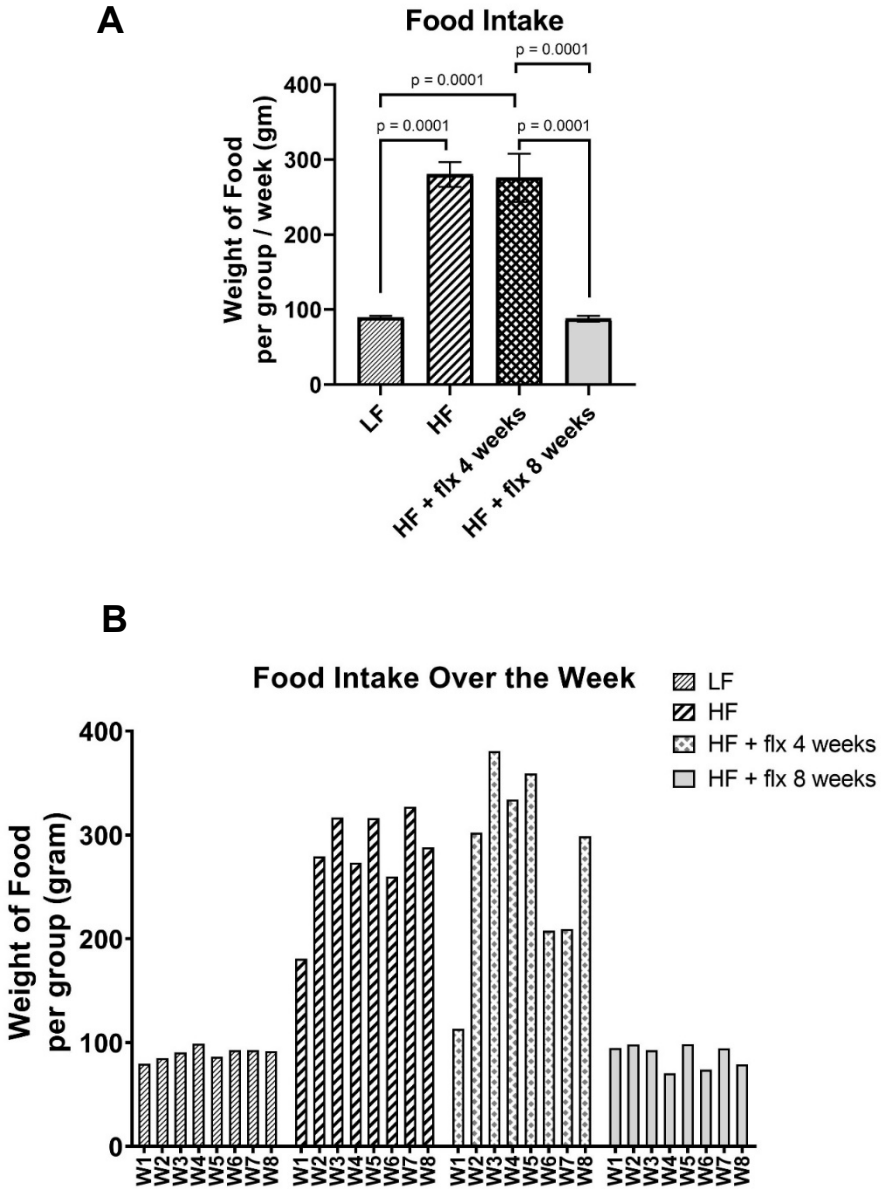

Figure 7.5 Variation in food intake amongst groups. (A) The bar graph shows the control low-fat diet group consumed significantly less food compared to groups on high-fat diet and high-fat diet with 4 weeks of flx (p-value = 0.0001). The high fat diet with 8 weeks of flx group overall consumed lower amounts of food intake compared to high-fat diet and high-fat diet with treatment of 4 weeks of flx. However, intake between low-fat and high-fat diet with 8 weeks of flx is not significantly different. (B) The bar graph showed the pattern of food intake between groups from week 1 until week 8. The control group and high-fat diet group showed quite similar patterns with food intake approximately 100 gm per week. However, the high-fat diet group and high-fat diet with 4 weeks of flx showed fluctuations in the pattern of food intake starting from week 1 until week 8. Overall, the pattern in the high-fat diet and high-fat diet with 4 weeks of flx indicated more food consumption compared to control group and high-fat diet with 8 weeks of flx. The statistical analysis, one-way ANOVA with significant p-value < 0.05.

7.5.6 No difference in the amount of water intake amongst high-fat diet groups

Flx was administered via drinking water using the water bottle. Using this method can reduce stress to mice in terms of handling and injection. A non-significant difference in the amount of water intake amongst the high-fat diet groups showed the mice on flx consumed the same amount as control high-fat diet group. However, in the control low-fat diet group, mice consumed significantly more water compared to high-fat diet groups. The mean ± SEM of each group is given (as ml/group/week) : LF vs HF (167.5 ± 7.3 ml vs 130.6 ± 3.2 ml, $p \leq 0.0016$), LF vs HF + 4 weeks of flx (167.5 ± 7.3 ml vs 126.3 ± 6.9, $p = 0.0004$), LF vs HF + 8 weeks of flx (167.5 ± 7.3 ml vs 106.9 ± 7.0, $p = 0.0001$) (Figure 7.6).

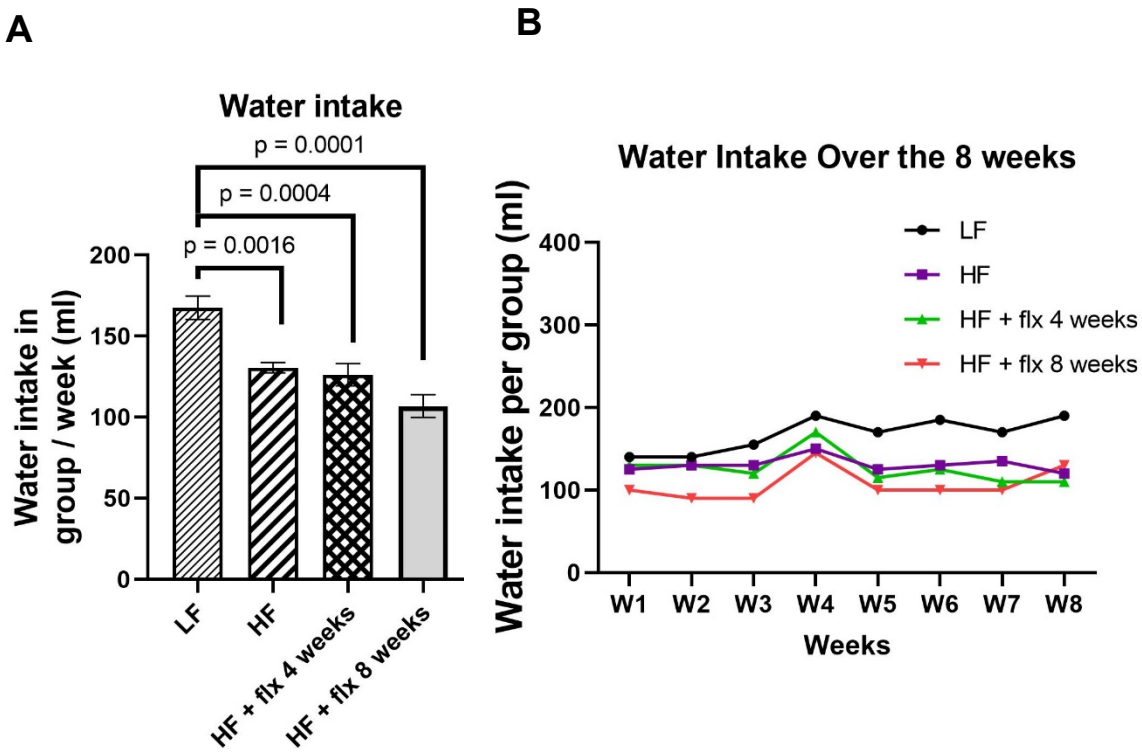

Figure 7.6 Administration of flx in drinking water did not change the amount of water consumption in the high-fat diet groups. (A) The amount of water consumption per group per week showed a significantly higher water intake in a low-fat diet compared to high-fat diet groups. However, amongst three groups of high-fat groups, the water intake was not changed. (B) the amount of water intake over eight weeks showed that water intake did not significantly change among the high-fat diet groups. Significant p-value ≤ 0.05, statistical analysis one-way ANOVA. n = 5 animals in each group.

7.5.7 Fluoxetine did not affect cell proliferation in the dorsal dentate gyrus of the hippocampus

Firstly, there was no significant difference in the numbers of proliferating cells in the hippocampus between low-fat diet group and any of the high-fat diet groups. Administration of flx via drinking water for eight weeks or four weeks in the high-fat diet group did not significantly affect the numbers of proliferating cells. Mean and SEM values for each group; low-fat group as control (26.22 ± 7.6), high-fat diet group (18.79 ± 7.4), high-fat with four weeks of flx (19.84 ± 7.3) and high-fat with eight weeks of flx (19.64 ± 8.0) (Figure 7.7A). Since the weight of individual mice in each group was highly variable, the correlation between weight gain and numbers of proliferating cells for each animal in each group was determined. However, there was no significant correlation between individual weight gain and individual extent of proliferation for animals in each group (Figure 7.7B – 7.7F).

Figure 7.7 No effect on numbers of proliferating cells in flx-treated high fat diet groups. (A) Extent of cell proliferation in each group of the experiment showed there is no significant difference amongst groups. Black rounded dots on the bar graph refers to the mean value of each animal in each group. n = 5 for each group. Statistical analysis, one-way ANOVA was applied with significant value, $p \leq 0.05$). (B-F) Correlation between cell proliferation and weight gain were plotted and analysed. (B) showed the correlations were not significant in all experimental groups. (C-F) showed no correlation for each group. Statistical analysis Pearson correlation was performed with significant value, $p \leq 0.05$.

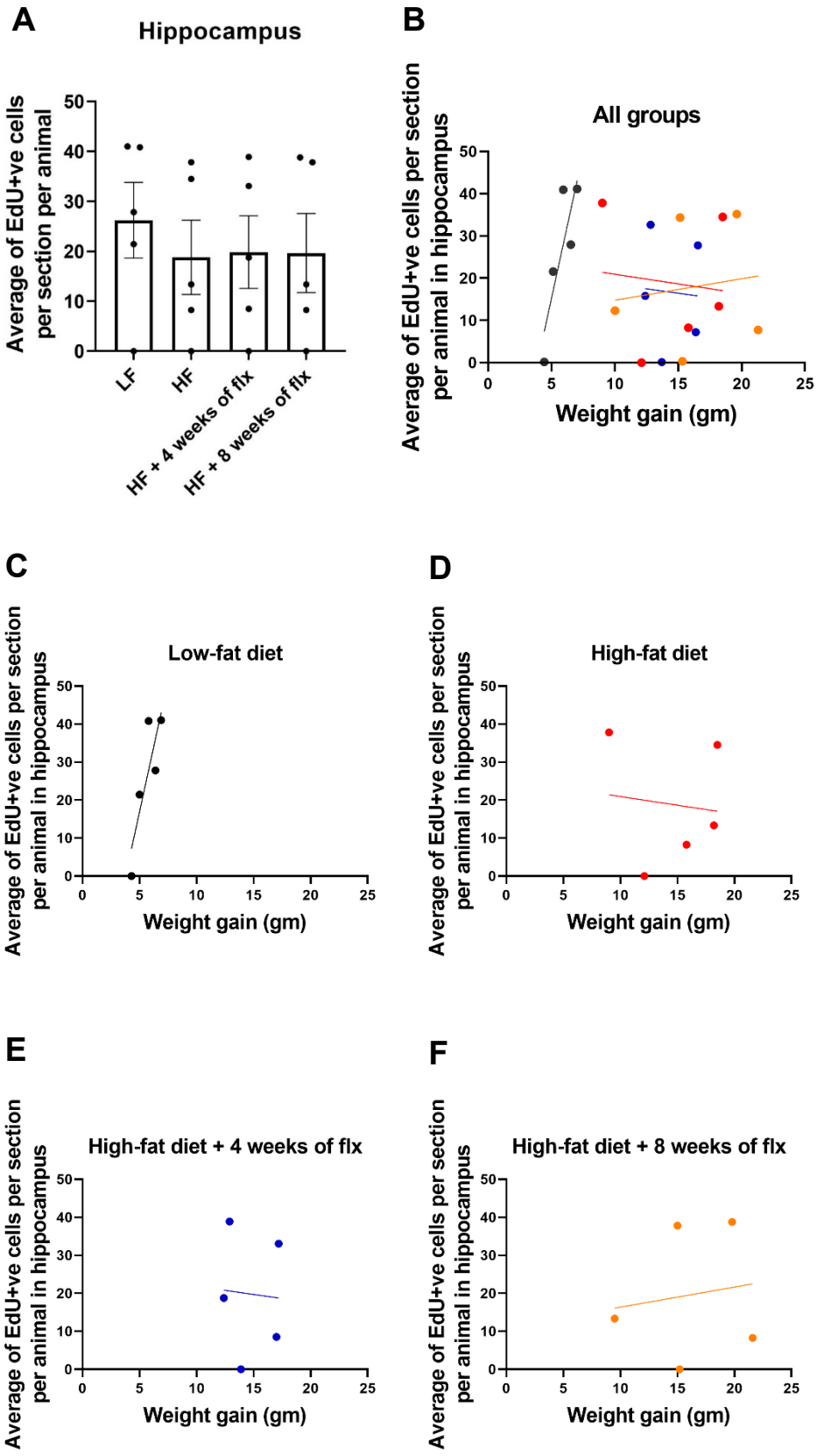
A
Hippocampus
Average of EdU+ve cells per section per animal
LF
HF
HF + 4 weeks of flx
HF + 8 weeks of flx
B
All groups
Average of EdU+ve cells per section per animal in hippocampus
Weight gain (gm)
C
Low-fat diet
Average of EdU+ve cells per section per animal in hippocampus
Weight gain (gm)
D
High-fat diet
Average of EdU+ve cells per section per animal in hippocampus
Weight gain (gm)
E
High-fat diet + 4 weeks of flx
Average of EdU+ve cells per section per animal in hippocampus
Weight gain (gm)
F
High-fat diet + 8 weeks of flx
Average of EdU+ve cells per section per animal in hippocampus
Weight gain (gm)

7.5.8 Administration of flx did not affect cell differentiation in the dorsal dentate gyrus of the hippocampus in all groups

Neither high-fat diet nor additional flx in high-fat diet affected cell differentiation. The percentages of mean and SEM for each type of cells were shown (Table 7.4). The proportions of proliferating cells that differentiated into astrocytes, oligodendrocytes, neurones or microglia were not significantly different in each group of the experiment (Figure 7.8).

Table 7.4 Mean (± SEM) percentages of EdU-positive cells that were colocalised with differentiation markers in the dDG

Types of cells identified (with associated antibodies)	LF (n) (% of EdU +ve cells that were double labelled for each marker)	HF (n)	HF + 4 week of flx (n)	HF + 8 weeks of flx (n)
Astrocytes	2.04 ± 1.6 (5)	5.10 ± 2.6 (5)	2.29 ± 1.0 (5)	1.00 ± 1.0 (5)
Oligodendrocytes	2.89 ± 2.9 (5)	1.24 ± 1.2 (5)	6.25 ± 2.1 (5)	5.33 ± 3.4 (5)
Neurones	2.46 ± 1.5 (5)	1.89 ± 0.9 (5)	3.09 ± 1.5 (5)	1.68 ± 1.2 (5)
Microglia	0.00 ± 0.0 (5)	7.54 ± 4.6 (5)	1.82 ± 1.8 (5)	2.17 ± 1.4 (5)

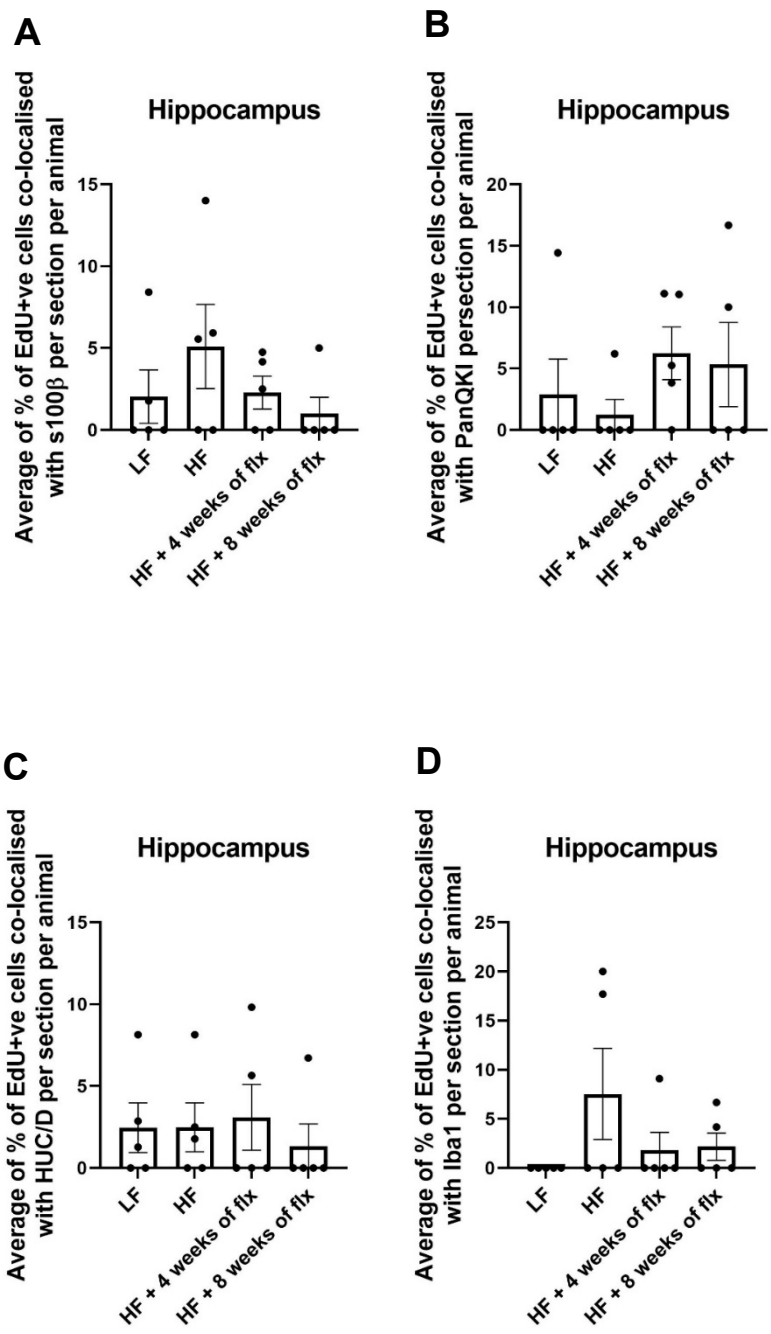

Figure 7.8 Flx did not cause significant changes in extent of cell differentiation in the high fat diet groups in hippocampus. (A-D) Scatter plot graphs showing, no significant changes in cell differentiation in all groups. Many sections showed no cells differentiating into the different cell types, thus many points for each graph are at 0%. Black rounded dots on the bar graph refers to the mean value of each animal in each group. n = 5 for each group. Please note differing y-axis scales. Statistical analysis, one-way ANOVA was applied with significant value, $p \leq 0.05$)

7.5.9 Fluoxetine did not cause any effect on cell proliferation and differentiation in the brainstem region of high fat diet groups

In the brainstem, administration of flx did not affect cell proliferation in the whole brainstem (Figure 7.9A) nor indeed in any specific region of the brainstem, such as ependymal layer region, area of postrema, nucleus tractus solitarii, dorsal motor of vagus nerve, raphe, inferior olive and pyramid area. Furthermore, there is no correlation between there was no significant correlation between individual weight gain and individual extent of proliferation for animals in each group (Figure 7.9B – 7.9F).

Moreover, in the differentiation quantification, none of the differentiation markers showed any significant changes in proportion of double-labelled cells in the group (Table 7.5, Figure 7.10)

Figure 7.9 Flx did not affect cell proliferation in brainstem. (A) The scatter plot graphs show non-significant changes in numbers of proliferating cells in brainstem. Black rounded dots on the bar graph refers to the mean value of each animal in each group. n = 5 for each group. Statistical analysis, one-way ANOVA was applied with significant value, $p \leq 0.05$). (B-F) Line graph of correlation between weight gain for each animal and numbers of proliferating cells. (B) showed no significant correlation between cell proliferation and weight gain in all groups, while (B-F) showed no correlation in each group. Statistical analysis pearson correlation was performed with significant value, $p \leq 0.05$.

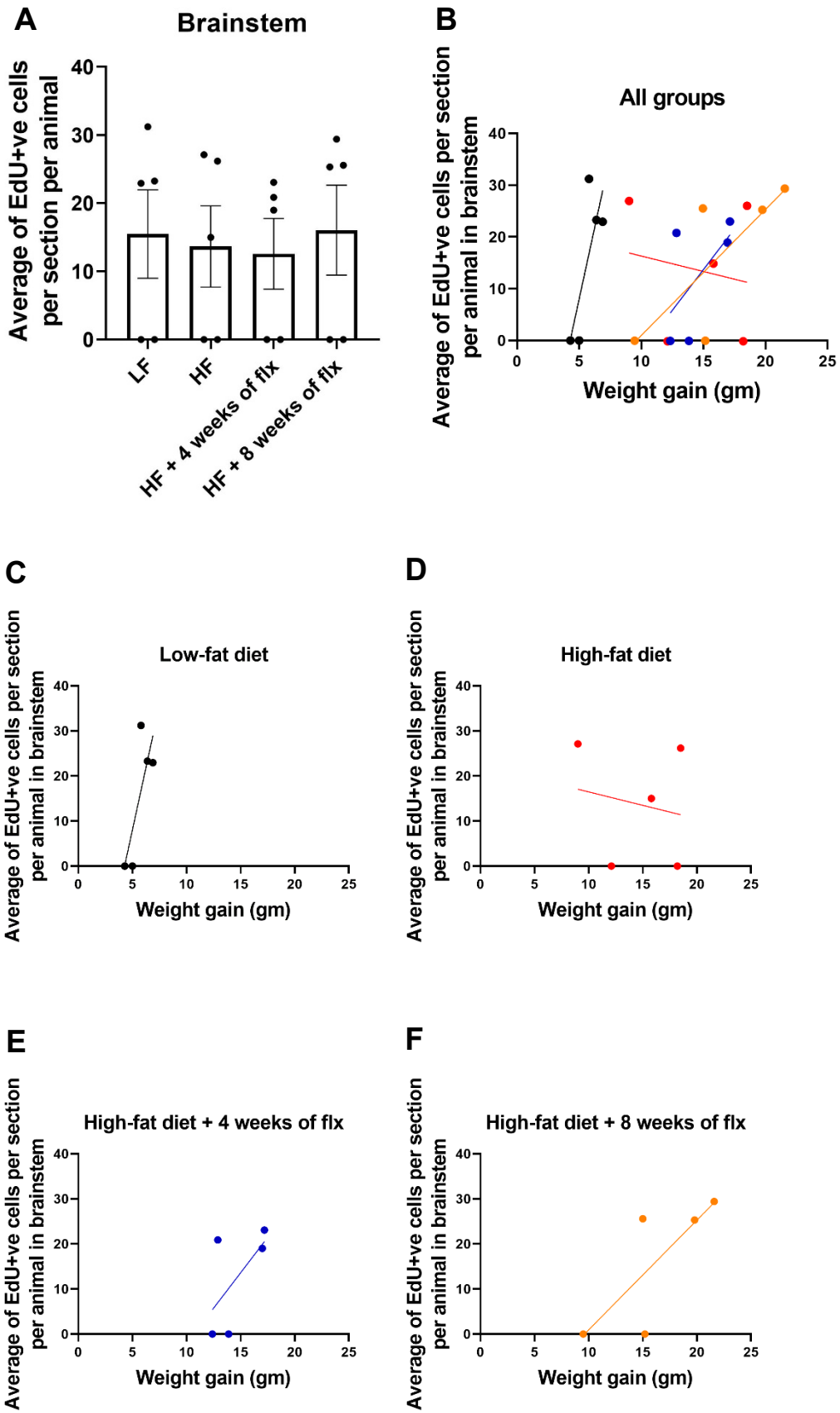
A
Brainstem
Average of EdU+ve cells per section per animal
40
30
20
10
0
LF
HF
HF + 4 weeks of flx
HF + 8 weeks of flx
B
All groups
Average of EdU+ve cells per section per animal in brainstem
Weight gain (gm)
C
Low-fat diet
D
High-fat diet
E
High-fat diet + 4 weeks of flx
F
High-fat diet + 8 weeks of flx

Table 7.5 Mean (± SEM) value of percentages of EdU-positive cells that were colocalised with differentiation markers in the brainstem region.

Type of cells examined with antibodies	LF (n) (% of EdU +ve cells that were double labelled for each marker)	HF (n)	HF + 4 week of flx (n)	HF + 8 weeks of flx (n)
Astrocytes (s100β)	3.46 ± 1.8 (5)	3.12 ± 1.3 (5)	4.46 ± 2.7 (5)	5.71 ± 3.1 (5)
Oligodendrocytes (PanQKI)	6.52 ± 4.4 (5)	7.52 ± 4.0 (5)	9.23 ± 4.2 (5)	14.47 ± 7.1 (5)
Neurones (HUCD)	0.84 ± 0.7 (5)	0.83 ± 0.8 (5)	0.15 ± 0.1 (5)	1.14 ± 0.5 (5)
Microglia (Iba1)	4.66 ± 2.4 (5)	5.91 ± 2.7 (5)	4.92 ± 2.3 (5)	6.22 ± 3.2 (5)

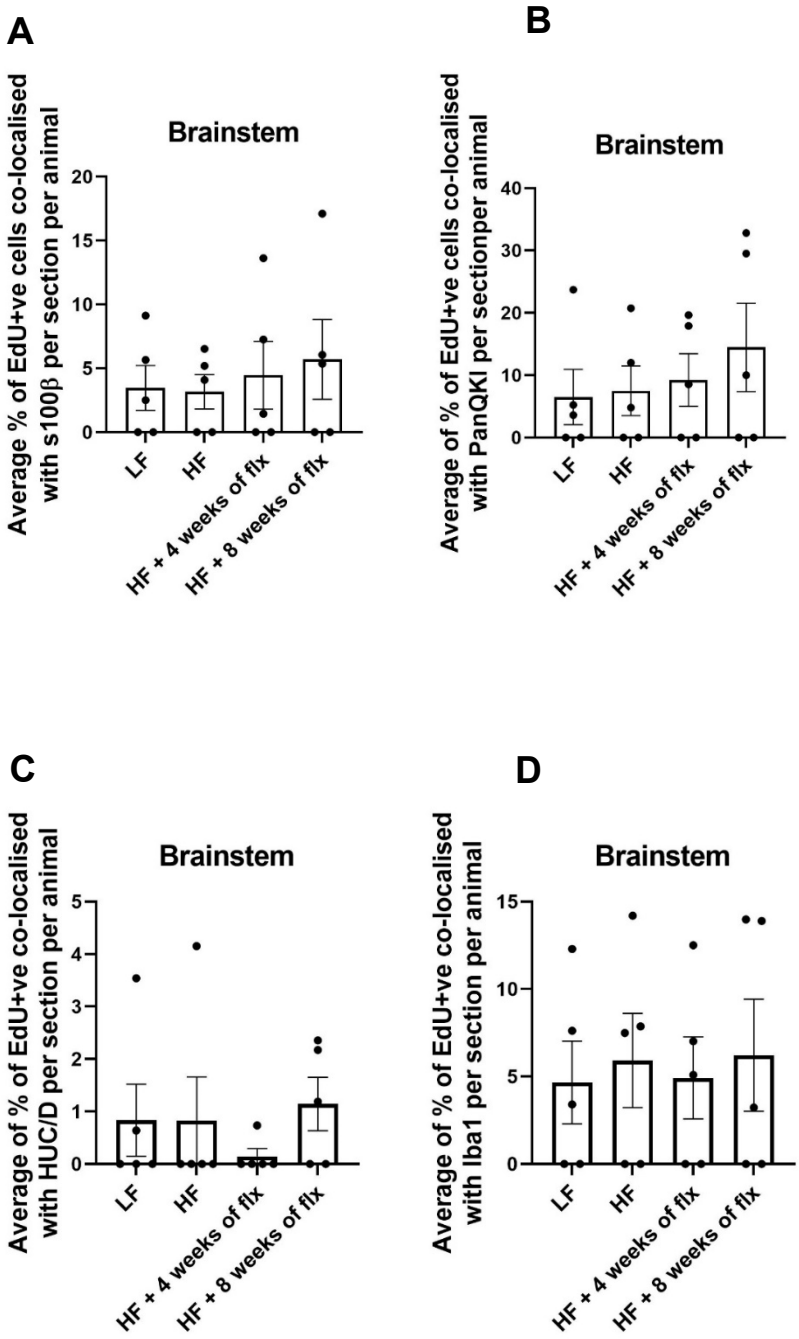

Figure 7.10 The extent of cell differentiation was not affected by the administration of flx in mice on high-fat diet in brainstem. (A-D) Percentages of co-localisation of Edu-positive cells with differentiation markers were not significantly different in all groups. Black rounded dots on the bar graph refers to the mean value of each animal in each group. n = 5 for each group. Statistical analysis, one-way ANOVA was applied with significant value, $p \leq 0.05$).

7.5.10 Administration of fluoxetine has no effect on cell proliferation in the thoracic spinal cord of high fat diet fed animals.

Administration of flx has no effect on the numbers of proliferating cells in the groups fed a high fat diet. The numbers of proliferating cells in control group, high-fat diet group, high-fat diet with 4 weeks of flx and high-fat diet with 8 weeks of flx are 32.32 ± 1.0, 31.33 ± 2.8, 35.79 ± 2.6, 36.28 ± 1.8 respectively (Figure 7.11A). Furthermore, there is no correlation between cell proliferation and weight gain in all groups (Figure 7.11B – 7.11F).

Figure 7.11 Administration of flx did not significantly change the number of proliferating cells in spinal cord in high fat diet fed groups. (A) The bar chart shows similar extents of cell proliferation in every group. Black rounded dots on the bar graph refers to the mean value of each animal in each group. n = 5 for each group. (B) Line graph of correlation between weight gain for each animal and numbers of proliferating cells. Statistical analysis, one-way ANOVA was applied with significant value, $p \leq 0.05$). (B-F) Line graph of correlation between weight gain for each animal and numbers of proliferating cells. (B) showed no significant correlation between cell proliferation and weight gain in all groups, while (B-F) showed no correlation in each group. Statistical analysis pearson correlation was performed with significant value, $p \leq 0.05$.

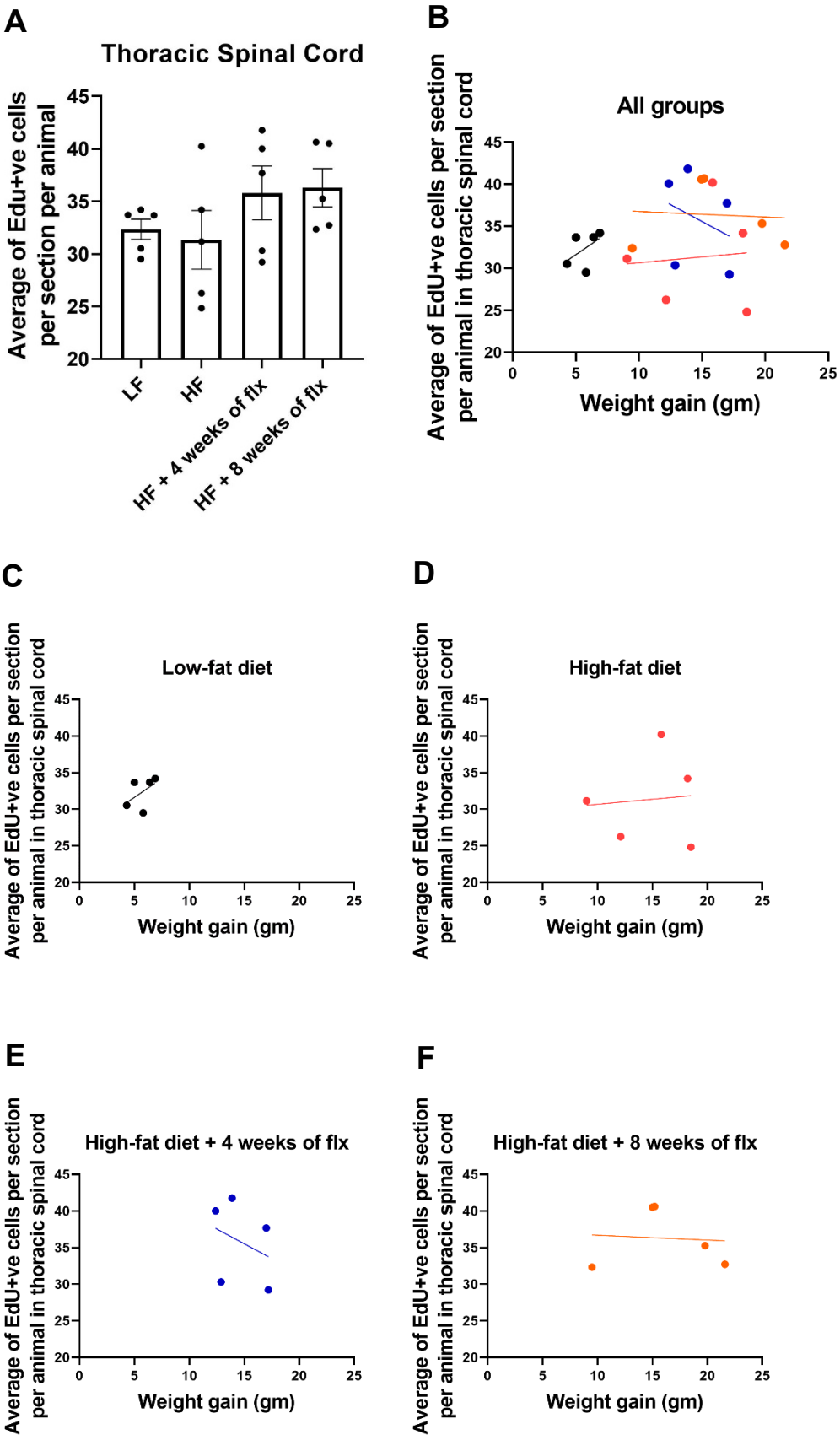
A
Thoracic Spinal Cord
Average of Edu+ve cells per section per animal
45
40
35
30
25
20
LF
HF
HF + 4 weeks of flx
HF + 8 weeks of flx
B
All groups
Average of EdU+ve cells per section per animal in thoracic spinal cord
Weight gain (gm)
C
Low-fat diet
D
High-fat diet
E
High-fat diet + 4 weeks of flx
F
High-fat diet + 8 weeks of flx

7.5.11 Fluoxetine did not influence the differentiation of cells in the thoracic spinal cord

Administration of flx did not significantly promote proliferating cells to become astrocytes, oligodendrocytes, neurones or microglia (Table 7.6, Figure 7.12).

Table 7.6 Mean (± SEM) percentages of EdU-positive cells that were colocalised with differentiation markers in the spinal cord

Type of cells identified (with associated antibodies	LF (n) (% of EdU +ve cells that were double labelled for each marker)	HF (n)	HF + 4 weeks of flx (n)	HF + 8 weeks of flx (n)
Astrocytes (s100β)	0.80 ± 0.4 (5)	0.95 ± 0.4 (5)	0.51 ± 0.3 (5)	0.77 ± 0.5 (5)
Oligodendrocytes (PanQKI)	9.12 ± 4.5 (5)	10.46 ± 4.9 (5)	13.32 ± 7.1 (5)	14.73 ± 8.0 (5)
Neurones (HUCD)	2.82 ± 1.2 (5)	6.01 ± 3.6 (5)	6.01 ±3.2 (5)	4.40 ± 2.1 (5)
Microglia (Iba1)	7.20 ± 3.6 (5)	9.77 ± 2.1 (5)	9.06 ± 0.6 (5)	12.55 ± 3.5 (5)

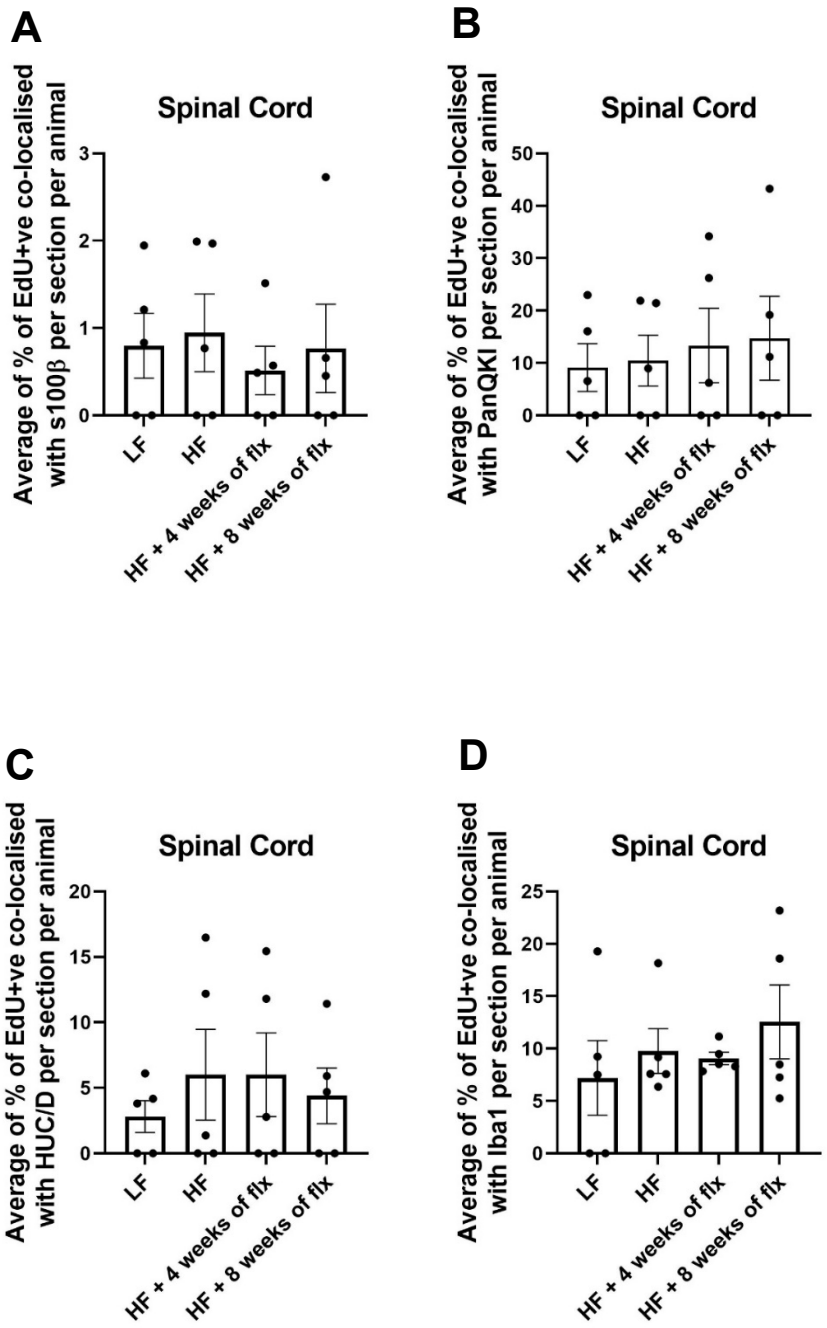

Figure 7.12 Fluoxetine did not affect cell differentiation in spinal cord of high fat diet animals. (A-D) Percentages of proliferating cells differentiating into astrocytes, oligodendrocytes, neurones and microglia were counted and none of them were significantly different amongst groups. Black rounded dots on the bar graph refers to the mean value of each animal in each group. n = 5 for each group. Statistical analysis, one-way ANOVA was applied with significant value, $p \leq 0.05$)

7.6 Discussion

The current investigation showed that administration of flx for 4 weeks or 8 weeks, did not improve the glucose tolerance level in the high-fat diet groups. Weight increases reached significance in all high-fat diet groups compared to the low-fat diet group. Even though the weight increased, the food intake was different in each group; for example in high fat diet + 8 weeks of fluoxetine group, they ate less but gained some weight. Water intake was slightly less in the high-fat diet groups compared to low-fat diet group. However, amongst all three high-fat diet groups, water consumed was not different, which indicated that the amount of flx consumed is similar between groups.

When considering the extent of cell proliferation, consumption of high-fat diet and administration of flx did not show any significant different in the hippocampus, brainstem and thoracic spinal cord. Furthermore, this amount of flx concentration did not affect the cell differentiation in any of those areas.

7.6.1 Fluoxetine did not improve glucose levels during GTT

Obesity is one of the most important risk factors that can lead to type-2 diabetes. This condition is characterised by abnormal elevation of blood glucose levels. It is due to resistance of insulin-stimulated glucose uptake and gross decompensation of systemic glucose metabolism (Adeghate, 2001). In normal conditions, glucose from dietary intake stimulates the secretion of insulin from the pancreas to help cells to take in the glucose to be used as energy. Then insulin will signal the liver to store glucose in the form of glucagon (Aronoff *et al.*, 2004). In a chronic over-feeding example, consumption of high-fat diet triggers an inflammatory response that leads to alteration in the signalling of peripheral insulin-receptors thus affecting the sensitivity of insulin. These events result

in increased glucose levels in the blood and impaired glucose tolerance (Moreno-Fernández *et al.*, 2018).

In my study, in the high-fat diet group, 8 weeks of high-fat diet consumption showed the expected result when the glucose levels increased over the weeks. Moreover, in the other high-fat diet groups that received flx for 4 weeks and 8 weeks the same patterns of elevated glucose level were observed. Thus, administration of flx did not help in improving the glucose levels. This is similar to one study that investigated the effect of different SSRIs (Imipramine, moclobemide, clonazepam, flx and sertraline) given acutely (30 minutes before the GTT) on fasting blood glucose levels. They showed that non-diabetic rats given 20 mg/kg of flx had higher fasting blood glucose levels than the control group that received vehicle (Gomez *et al.*, 2001b).

Furthermore, in the same study but another experiment, they also checked on the fasting glucose level in streptozocin-induced diabetic mice after receiving flx. The flx was administered 30 minutes before the GTT procedure. The glucose level was higher compared to the non-diabetic group. Therefore, flx did not improve the glucose level in GTT in the non-diabetic and diabetic group, but sertraline did reduce the glucose level in both non-diabetic and diabetic mice by increasing the plasma insulin level (Gomez *et al.*, 2001a) However, they didn't mention how they administered the flx (Gomez *et al.*, 2001b).

In a human study, flx was given 60 mg once daily (oral) to obese patients with non-insulin-dependent diabetic mellitus (NIDDM) for a month. In the control group, patients were given a placebo. Fasting blood glucose testing revealed that, there were non-significant differences between control obese and treatment group on flx, suggesting that flx did not have a role in reduced or increased fasting blood glucose in human. (Maheux *et al.*, 1997). However, they did not perform GTT on the patients.

However, another study investigated the effect on blood glucose levels of administration of flx in normoglycemic mice and alloxan-induced hyperglycaemic mice. After 21 days

administration of flx (30 mg/kg i.p injection), the plasma glucose levels were reduced in the flx-treated group compared to the control group. Furthermore, in a clinical case report, patients with type-1 diabetes mellitus presented with hypoglycaemia after the introduction of flx (20 mg once daily) to treat the depressive symptoms. After several episodes of hypoglycaemia, the flx was stopped, and the insulin requirements of the patient returned to normal. This study therefore showed an association of flx with hypoglycaemic conditions (Biagetti and Corcoy, 2013).

To sum up, there are inconsistent results in the effect of flx to help control the fasting blood glucose levels. It is worth looking at other SSRIs, for example sertraline, since this had an effect on improved glucose levels after acute administration.

7.6.2 Fluoxetine did not show an anorexigenic effect

Flx is often associated with reductions in weight (Gomez and Garcia-Garcia, 2017, Scabia *et al.*, 2018). However, in my study, all high-fat diet groups regardless of treatment, showed increased weight gain over the 8 weeks compared to the low-fat diet group. When examining the data more carefully, considering each animal in turn, it was clear that there was considerable variability in the weight gain of individual mice particularly within the high fat diet and high fat diet + flx for 8 weeks group. This may have some bearing on the overall effects on cell proliferation since there were similar variations in extent of cell proliferation between mice in each group. However, in the analysis of correlation between weight gain and cell proliferation, there was no significant correlation observed in any region for any group and this will discuss in more detail later.

In a cohort study, the data based on UK Clinical Practice Research Datalink (CPRD) were used to investigate the utilisation and incidence of weight gain during 10 years' follow up. People that were prescribed antidepressants showed ≥ 5% increased weight gain regardless of the type of antidepressant. The incidence of new episodes of ≥ 5 %

weight gain in participants prescribed antidepressants was 11.2 per 100 people compared to participants NOT prescribed antidepressants (8.1 per 100 people) so, in general, antidepressants caused weight gain (Gafoor *et al.*, 2018).

Interestingly, another clinical study showed the changes of weight gain in acute treatment versus chronic treatment of flx. The subjects were patients that had remitted after 12 weeks of 20 mg/kg flx treatment and they were randomly assigned to continue receiving flx or placebo. The treatment was divided into 14-week trial, 26-week trial, 38-week trial and 50-week trial. The result showed that, during the initial period of flx therapy (4 weeks), weight decreases were observed in patients but the weight increased with the continuation of the treatment until 50 weeks (Figure 7.13) (Michelson *et al.*, 1999).

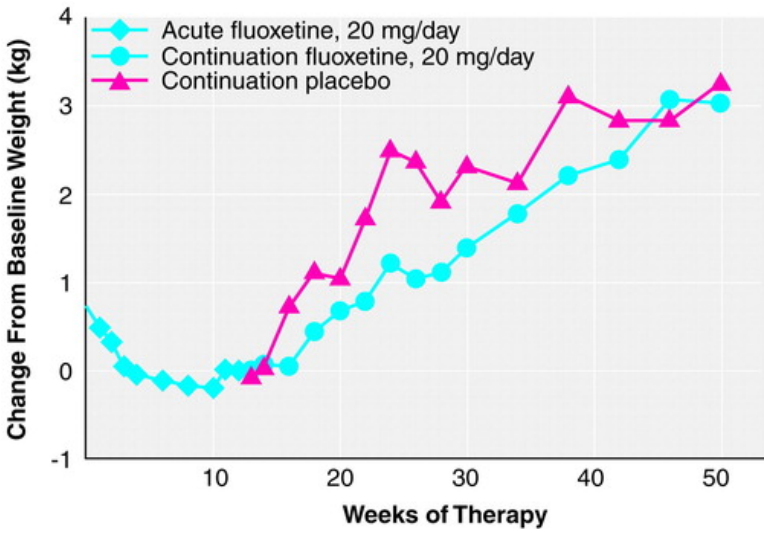

Figure 7.13 Decreased weight after the initial treatment of flx, followed by increased weight Graph adapted from (Michelson *et al.*, 1999) showed that after 12 weeks, the weight gain increased with the prolong treatment of flx.

However, in this study, the group that received placebo also had the same pattern of increased weight as the group that received flx, thus it is more likely due to the placebo effect. The placebo effects need to be considered in studies involved in depression, sleep disorders, pain and many more. However, most of the studies solely investigated the flx

and weight gain, so whether or not there will be the same pattern of weight increases in subjects that are already obese is still inconclusive.

There was a different story in the animal studies, administration of 14.2 mg/kg/day flx in drinking water for 3 weeks was able to reduce weight in flx-treated mice compared to the control group. In another experimental setting, the mice were fed with a high-fat diet for 8 weeks and received flx (10.8 mg/kg/day in drinking water) at week 6 after the high-fat diet was started. It showed the weight gain reduced in flx-treated group compared to the control group. This suggested that flx has an anorexigenic effect in both groups consuming a normal diet and high-fat diet and the effect required BDNF receptors which are neurotrophic tyrosine kinase receptor, type 2 (TrkB) (Scabia *et al.*, 2018). Moreover, in another study, rats were examined for cumulative body weight gain after acute administration of flx (10 mg/kg, i.p) for 3 days. In flx-treated animals, the bodyweight changes were lower than the control group (Gomez and Garcia-Garcia, 2017). In conclusion, using animal studies, acute or chronic treatment of flx showed reduced weight gain, and flx has the potential to have anorexigenic effects in the animal. However, in my study, the results contradicted this and fit here with human data.

Taken together, the discussion suggested that the data from human and animal studies were not consistent. Therefore, the anorexigenic effect of flx is still inconclusive. It is worthwhile to continue the research in this area by using a different amount of flx and different method of administration to establish the association between flx and bodyweight.

7.6.3 High-fat diet and administration of fluoxetine in high-fat diet condition did not affect cell proliferation

These findings address the impact of high-fat diet consumption on the neurogenic effects of the antidepressant fluoxetine. Mice from high fat diet group received flx daily in a

dosage for 4 weeks and 8 weeks leading to relevant plasma concentrations that has potential to increase cell proliferation. In flx study (Chapter 4), we could confirm that fluoxetine promotes cell proliferation in normal conditions. When comparing numbers of proliferating cells between the 2 studies, there were clearly fewer EdU +ve cells here than in Chapter 4. This is most likely due to the fact that the animals survived for 2 weeks after the final EdU injection, compared to the original experiments when brains were fixed one day following the final injection. It is likely that newly proliferated cells will only survive if there is a function for them and many are lost through natural apoptosis, which may be the case here (Taylor *et al.*, 2008). In this study the fluoxetine also did not affect cell proliferation in high-fat diet condition. Once more, this might be due to the balance between the cell proliferation and apoptotic activity. There is also no correlation between cell proliferation and weight gain in all groups, therefore it seems that the variability in weight gain does not influence cell proliferation significantly in this study. This is obviously an issue with such variability in weight gain over the groups, therefore perhaps a further study with a larger cohort of animals may be worthwhile to see if this correlation exists. It is also worthwhile considering whether a further experiment should individually house mice to be able to monitor exact fluid and food intake but this is turn raises concerns about stressing animals with single cage housing.

Even though 10 mg/kg flx successfully enhances cell proliferation in hippocampus, selected areas of brainstem and spinal cord regions in normal conditions, the dosage did not affect cell proliferation in the high-fat diet group. The proliferative activity might be present due the neurogenic effect of the flx, however, the cell proliferation was compensated by increasing of apoptotic activity due to the high-fat diet consumption since high-fat diet could induce apoptosis of neurons and a reduction in arcuate and lateral hypothalamic synaptic inputs (Moraes *et al.*, 2009).

Another possible explanation is the effect of high-fat consumption on the levels of 5-HT in the body. In the recent study by Labban *et al.* (2020), they measured the brain 5-HT of rats after four weeks on high-fat diet and reported remarkably lower 5-HT levels

compared to control group. In another study using C57BL/6 mice, bioanalysis of serotonin showed significantly decreased serotonin levels in high-fat diet group when compared to normal diet. The mice were fed for 8 weeks (Kim *et al.*, 2013). These indicate that the high-fat diet group mice are in state of lower 5-HT in the body, so even with the administration of 10 mg/kg flx, the concentration of 5-HT may not reach high enough levels to promote cell proliferation as they did in the normal mice.

Various factors can be proposed for the lack of effects of fluoxetine on neurogenesis in high-fat diet study. For example, the fluoxetine treatment paradigm used may not be enough to make up for the high fat dietary reduction of the levels of 5-HT. Since the high-fat can reduce the concentration of brain 5-HT, it may be worthwhile modifying the amount of flx given or the other alternative is to give supplementation of 5-hydroxytryptophan (5-HTP) as a precursor for 5-HT synthesis.

7.7 Conclusion

In conclusion, the administration of flx in drinking water was not able to affect cell proliferation in high-fat diet condition in the hippocampus, selected brainstem regions and thoracic spinal cord. Furthermore, it also did not influence cell differentiation. Regarding metabolic changes, the flx did not improve the fasting blood glucose levels and did not reverse the increased bodyweight.

Chapter 8

GENERAL DISCUSSION

8.1 Summary

Research on stem cells continues to address knowledge of how an organism develops from a single cell and how healthy new cells may replace damaged or degenerated cells in the adult organism. This fascinating area of research raises scientific questions regarding how proliferation and differentiation of new cells on the postnatal central nervous system may be modulated through endogenous and exogenous influences, which in turn generates discoveries and potential new therapeutic avenues. My study investigated the influence of the neurotransmitter 5-HT on cell proliferation and differentiation in the brainstem and spinal cord of adult and obese mice. In the brainstem, cells located at the border of between NTS and AP or around the central canal are proposed as neural stem cells (Bauer *et al.*, 2005). The same neural stem cell properties may apply to the ependymal cells surrounding the central canal of the spinal cord following the first identification of these as potential endogenous neural stem cells (Hamilton *et al.*, 2009).

Therefore, this thesis focused on investigating the influence of increased levels of 5-HT in the synaptic cleft or on activation of specific 5-HT receptors on cell proliferation and differentiation in the brainstem and spinal cord in normal adult and obese mice. My studies provided evidence that cell proliferation in the adult spinal cord and brainstem is significantly enhanced *in vivo* by increased 5-HT levels through activation of non-specified 5-HT receptors. I also showed for the first time, that ependymal cells showed

different behaviours through activation of selected 5-HTRs in an *in vitro* experimental set-up. There is a lesser extent of proliferation with activation of 5-HTR4 via tegaserod, although there were increased numbers of proliferating cells with activation of 5-HTR4 via cisapride. Furthermore, in *in vivo* experiments, fewer cells proliferated following activation of 5-HTR4 through tegaserod. Therefore, by activation of 5-HTR4 through tegaserod, very few cells proliferated in both *in vivo* and *in vitro* experiments.

The lineage of these newly proliferated cells was also investigated. Under normal conditions, following the exposure to flx, there was no change in the proportion of cells expressing astrocytic, oligodendrocytic or neuronal markers.

I also investigated, using a high-fat diet study, whether increasing 5-HT levels could modulate the extent of cell proliferation and differentiation in the brainstem, hippocampus and spinal cord. However, in flx-treated obese animals, there was no change in the proliferative activity compared to both control low-fat diet and high-fat diet groups. Furthermore, there was no change in the proportion of newly proliferating cells that expressed markers for astrocytes, oligodendrocytes, and neurones.

Overall, my data indicate a role for specific 5-HT receptors in modulating levels of cell proliferation in the intact spinal cord but these have limited effects in a model of obesity.

8.2 Applicability of these findings to neurogenesis

8.2.1 Ependymal cells proliferate in normal conditions, a process that can be enhanced by endogenous 5-HT modulation

It is clear from research conducted by various research groups (Johansson *et al.*, 1999, Meletis *et al.*, 2008, Barnabé-Heider *et al.*, 2010) that the ependymal cells in the spinal cord exhibit plasticity after injury. In the normal adult mice, the ependymal cells are in a

dormant state, but can be activated when there is an injury, therefore the aim of this study was to determine if it was possible to transform the dormant cells to the proliferative state by increasing ambient 5-HT levels or by activating specific 5-HT receptors. This will provide a better understanding of adult neurogenesis and propose methods that can modulate cell proliferation by a pharmacological approach.

In my study, the identification of newly proliferating cells was using EdU, the thymidine analogue, in the adult mice *in vivo*. My experiment revealed significantly higher numbers of proliferating cells in the DVC region, inferior olives and raphe nuclei of the brainstem and the gray matter of the thoracolumbar spinal cord in the flx-treated group compared to the control, however, there were no differences in the extent of proliferation in the ECL itself. There may be a number of reasons for this, as discussed in chapter 4. Increased 5-HT and activation of non-specified 5-HTRs may have transformed the quiescent cells to proliferate and which could in turn trigger the migration of these cells to the DVC area in the brainstem and gray matter of the thoracic spinal cord. This suggestion is consistent with Meletis *et al.* (2008) who showed the capability of ependymal cells to proliferate and migrate to the site of spinal cord injury and Rusanescu and Mao (2015), who suggested that sciatic nerve constriction injury may trigger proliferation and migration of new cells from the ECL region to the grey matter of dorsal spinal cord. Even though I am not using the injury mouse model, the principle of proliferating and migrating of ependymal cells is still relevant here and could be further tested using fate mapping of FoxJ1 positive ECL stem cells as carried out by Barnabé-Heider *et al.* (2010). However, it is important to bear in mind that, in the brainstem area, another source of potential neural stem cell are nestin-GFP cells located in the border between AP and NTS region. These nestin-GFP cells in the AP, NTS regions also receive extensive innervation of 5-HTergic fibres and thus may proliferate and migrate to other DVC regions in the presence of flx. Further experiments using the fate mapping procedures in both regions would be an important step to discover the origin of these newly proliferated cells in both brainstem and spinal cord.

However, the proportion of proliferating cells that had differentiated into specific cell types was not different between the flx-treated and control groups. Indeed the proportion of EdU cells that had differentiated into the specific cell types investigated in this study was low in both groups (around 10-25% in different brain regions). This may be due to them becoming different cell types such as pericytes (Barnabé-Heider *et al.*, 2010) or that they had not differentiated sufficiently.

8.2.2 Activation of specific 5-HTRs resulted in differing levels of proliferating cells

Direct targeting of specific receptors for selective activation would be the best therapeutic approach and thus can reduce any undesirable side effects and enable a better control of the direction of modulation. This could enable specific drugs to induce an increase in proliferation (which could replace lost cells such as oligodendrocytes in multiple sclerosis Gao et al 2015) or a decrease in proliferation (which could reduce recurrence of spinal ependymomas post-surgery in children, for example, Lundar *et al.* (2021). Therefore, further investigation of selected receptors was carried out. Globally increasing 5-HT by flx significantly increased the numbers of proliferating cells compared to the control group without knowing which receptors were activated. Several receptors that have the potential to increase cell proliferation were identified and tested. The receptors are 5-HTR4, 5-HTR1A and 5-HTR2 (Banasr *et al.*, 2004, Liu *et al.*, 2009).

Interestingly, ependymal cells acted differently towards different agonists. I investigated 2 types of 5-HTR4 agonist which were cisapride and tegaserod, and these triggered opposing proliferative activities. Activation of 5-HTR4 via cisapride increased the numbers of proliferating cells, however, activation of 5-HTR4 via tegaserod led to a lower extent of cell proliferation in central canal of spinal cord. Moreover, the numbers of

proliferating cells did not change after activation of 5-HTR1A and 5-HTR2, which indicated that these receptors did not contribute to the changes in the proliferative activity, at least in this *in vitro* setting.

The possible explanation on how the activation of 2 different 5-HTR4 agonists acted differently was already discussed in Chapter 5. As mentioned before, even though cisapride successfully increased the proliferative activity, this agonist was not suitable to use for *in vivo* since it develops cardiac arrhythmias (Wysowski *et al.*, 2001). Desensitisation of ependymal cell responses to tegaserod is relevant here. Direct activation by tegaserod of the ependymal cells may develop desensitisation, so that the cells were no longer responding to the tegaserod (Grider, 2006). The same effect may have happened in the *in vivo* experiments, since the tegaserod-treated group had fewer numbers of proliferating cells in hippocampus, DVC and spinal cord, compared to the control group.

Administration of tegaserod, through intraperitoneal injection or direct to the cells, showed a lower extent of cell proliferation when 5-HTR4 was activated. However, activation of 5-HTR4 still has potential to promote cell proliferation, as observed with cisapride *in vitro,* and another 5-HTR4 agonist should be investigated.

8.3 Can our findings be employed as therapeutic strategies?

8.3.1 Therapeutic strategies in the overall healing process

In reference to my study, the success of flx in promoting proliferation of cells demonstrates potential benefits in treating injury, for example spinal cord injury. Since flx has been shown to exhibit anti-inflammatory effects and has the ability to reduce the release of pro-inflammatory factors, it also may help boost the healing process. In one interesting study on the wound healing of skin, endogenous 5-HT has been shown to

enhance keratinocyte and fibroblast proliferation and migration for adequate wound (Sadiq *et al.*, 2018). Therefore treatment with flx may have multiple sites of action to enhance recovery after injury. Furthermore in conditions such as multiple sclerosis (MS) which also have a strong inflammatory response, leading to loss of oligodendrocytes (Thompson *et al.*, 2018), there could be a two-fold effect of enhancing 5-HT levels, as an anti-inflammatory mediator and potentially to boost production of new cells that may become oligodendrocytes in a model of MS.

It is important however, to consider that in my studies, flx did not change the extent of differentiation of the newly proliferated cells into oligodendrocytes and this is something that needs addressing in the future. There are a number of potential ways reported previously to drive maturation of oligodendrocyte precursor cells to fully functioning oligodendrocytes and thus enable remyelination (reviewed in Lubetzki *et al.* (2020). These include compounds such as the selective estrogen receptor (ER) modulator bazedoxifene, which is already approved for clinical use and the muscarinic antagonist clemastine, which has been proven clinically to enhance myelin repair in people with MS, even following prolonged damage (Green *et al.*, 2017). Furthermore, recent studies in aged stem cells has indicated that metformin, the clinically approved diabetic drug, can restore the regenerative capacity of these cells, which is important in those older people with MS (Neumann *et al.*, 2019). Therefore, it would be of clinical relevance to test if combinations of flx, which is also clinically approved for use in many conditions, with other pro-myelinating compounds could further increase remyelination and functional recovery in models of MS.

8.3.2 Therapeutic strategies in cancerous conditions

In my reference to my *in vivo* and *in vitro* study of tegaserod, the capability of tegaserod to inhibit cell proliferation, demonstrates the potential benefit in cancerous conditions.

Tegaserod inhibits cell proliferation and could potentially inhibit the rapid growth of cancerous lesions. In a study on melanoma, Liu *et al.* (2020) reported tegaserod functions effectively as an anti-cancer drug that induces apoptosis in human malignant cell lines. Besides that, tegaserod also exhibits anti-metastatic effects through inhibition of the phosphatidylinositol 3-kinase / serine/threonine protein kinase B / mechanistic Target of Rapamycin (PI3K/Akt/mTOR) pathway. Perhaps most relevant to this project is consideration of paediatric spinal ependymomas, which involve ependymal cells of the spinal cord, since there is a high propensity for these ependymomas to further disseminate along the neural axis, even after the original ependymoma has been removed (Abdallah *et al.*, 2020). Indeed in a study that involved extended follow-up of cases where children and young adults were diagnosed with paediatric ependymomas, unexpected and late recurrences were reported. Therefore, it may be possible to combine resection surgery with a drug such as tegaserod to inhibit proliferation post-surgery and thus reduce chances of a recurrence of the tumour. To date, my research was confined to the intact spinal cord conditions, so it is worth understanding the mechanism underlying the reduction in cell proliferation and then carry out further study using cancer cell lines which involve brain, brainstem, and spinal cord areas. These could include ependymoma or glioma cell lines to test the efficacy of tegaserod in reducing proliferation. Recent advances in characterisation of these cell lines indicate that they are suitable for testing of novel therapeutics to reduce relapse rates of ependymomas that can be as high as 50% (Amani *et al.*, 2017).

8.4 Technical considerations and implications

All experiments conducted in this project were carefully designed and carried out under the best technical conditions possible. However, the limitations of the study need to be considered.

8.4.1 *In-vitro* experiments

The acute slice technique is an experimental model that allows us to test a variety of drug responses on tissue from the same animal thus reducing the number of animals required and minimising the variability in the study. This method is less expensive and time-consuming than *in vivo* experiments. However, due to the loss of tissue viability over time periods longer than one day, this method only allows a short incubation period which might be an issue for drugs that require a longer time to produce significant effects. Cultured spinal cord slices would be a useful way to determine longer term effects of drugs whilst still reducing numbers of animals required. Both these methods involve preparation of slices that would be considered an excessive type of spinal cord injury so to test these drugs in an intact situation, *in vivo* experiments are still the best option.

8.4.2 Cell Counts

Manual counting was used in this thesis for several reasons such as issues in obtaining images for automated counting due to difficulties in obtaining images of high enough resolution with multiple tile-region and Z-stack images. This technique also is time-consuming and expensive since each section needs to be captured. Manual cell counting is still considered a method of choice in many studies since there were no significant differences between manual and automated cell counting (Cadena-Herrera *et al.*, 2015, Zeidler-Erdely *et al.*, 2016, Kaufhold *et al.*, 2018). González-González *et al.* (2016) suggested that automated cell counting can be applied when appropriate calibrations are obtained but many studies have reported lower standard deviations between manually counted groups carried out by different scientists compared to those using image analysis software. However, in manual counting, human error cannot be eliminated, and several precautions were implemented such as one person counting to reduce variability

between experimenters and blinded experiment, so that the person did not know the identity of the condition or groups when counting and this was not revealed until after statistical analysis.

8.4.3 Timing of drug and EdU administration

In all my *in vivo* experiments, the timing of drug delivery and EdU administration has a different time frame. Since different drugs have different pharmacodynamic and pharmacokinetic properties, the individual experiment was designed and adapted from previous studies that proved to be successful in increasing neurogenesis and each of these is discussed and justified in the relevant chapters. The reasons are to obtain the exact timing of each individual drug to get the positive effect.

8.5 Future work

The aim of this project is to provide an alternative and efficient treatment for patients suffering from spinal cord injuries and/or multiple sclerosis. Since my study describes the potential of flx in promoting increased cell proliferation, it is important to further explore this area to gain a deeper understanding of its full effects as a potential therapeutic treatment.

Since my study suggested but did not emphatically prove that ependymal cells are the cells proliferating and migrating in response to flx in the spinal cord, it is important to

employ the use of transgenic fate mapping in normal intact spinal cords to trace the individual cell lineage together with EdU to label proliferating cells in future experiments. This method will allow us to trace the source of proliferating cells, for example, using transgenic mice FoxJ1-CreER, Cx30-CreER and Olig2-CreER lines that provide recombination in ependymal cells, astrocytes and oligodendrocytes respectively (Barnabé-Heider *et al.*, 2010).

Another interesting aspect to look at is the apoptosis events in experiments where there is reduced cell proliferation. Whether or not apoptosis is the possible underlying mechanism is worth exploring. As cell death occurs in several pathways, multiple apoptosis markers need to be examined to confirm the mechanism of cell death in future experiments (Smyth and Berman, 2002, Karmakar and Lal, 2021).

8.6 Conclusion

Overall, this study provided evidence that cells surrounding the central canal respond to increases in endogenous 5-HT and activation of 5-HTR4. Furthermore, cells in the brainstem respond to increases in endogenous 5-HT and respond to the activation of 5-HTR4. The proliferative responses were confined to selective areas in brainstem and spinal cord. Since, in the high-fat diet experiment, we do not get any significant difference in the proliferative activity of ependymal cells, therefore some modification on the amount of flx given, may produce positive effect. We postulate that, these results provide another therapeutic avenue for future investigations in treating spinal cord injury or conditions where there are changes in number of cell proliferation.

REFERENCES

Abdallah, A., Emel, E., Gündüz, H. B., Sofuoğlu Ö, E., Asiltürk, M. & Abdallah, B. G. 2020. Long-Term Surgical Resection Outcomes of Pediatric Myxopapillary Ependymoma: Experience of Two Centers and Brief Literature Review. *World Neurosurg,* **136,** e245-e261.

Abzalov, R. A., Abzalov, R. R., Valeev, A. M., Abzalov, N. I. & Gulyakov, A. A. 2015. Role of 5-Ht(2b) Serotonin Receptor Agonist in the Regulation of Pumping Function of the Heart. *Bull Exp Biol Med,* **159,** 302-4.

Adeghate, E. 2001. Diabetes Mellitus–Multifactorial in Aetiology and Global in Prevalence. *J Archives of physiology biochemistry,* **109,** 197-199.

Akamatsu, W., Fujihara, H., Mitsuhashi, T., Yano, M., Shibata, S., Hayakawa, Y., Okano, H. J., Sakakibara, S., Takano, H., Takano, T., Takahashi, T., Noda, T. & Okano, H. 2005. The Rna-Binding Protein Hud Regulates Neuronal Cell Identity and Maturation. *Proc Natl Acad Sci U S A,* **102,** 4625-30.

Alfaro-Cervello, C., Soriano-Navarro, M., Mirzadeh, Z., Alvarez-Buylla, A. & Garcia-Verdugo, J. M. 2012. Biciliated Ependymal Cell Proliferation Contributes to Spinal Cord Growth. *The Journal of Comparative Neurology,* **520,** 3528-3552.

Alonso, A., Merchán, P., Sandoval, J. E., Sánchez-Arrones, L., Garcia-Cazorla, A., Artuch, R., Ferrán, J. L., Martínez-de-la-Torre, M., Puelles, L. J. B. s. & function 2013. Development of the Serotonergic Cells in Murine Raphe Nuclei and Their Relations with Rhombomeric Domains. **218,** 1229-1277.

Altman, J. 1969. Autoradiographic and Histological Studies of Postnatal Neurogenesis. Iv. Cell Proliferation and Migration in the Anterior Forebrain, with Special Reference to Persisting Neurogenesis in the Olfactory Bulb. *Journal of Comparative Neurology,* **137,** 433-457.

Altman, J. & Das, G. D. 1965. Autoradiographic and Histological Evidence of Postnatal Hippocampal Neurogenesis in Rats. *J Comp Neurol,* **124,** 319-35.

Amani, V., Donson, A. M., Lummus, S. C., Prince, E. W., Griesinger, A. M., Witt, D. A., Hankinson, T. C., Handler, M. H., Dorris, K., Vibhakar, R., Foreman, N. K. & Hoffman, L. M. 2017. Characterization of 2 Novel Ependymoma Cell Lines with Chromosome 1q Gain Derived from Posterior Fossa Tumors of Childhood. *Journal of neuropathology and experimental neurology,* **76,** 595-604.

Anacker, C., Luna, V. M., Stevens, G. S., Millette, A., Shores, R., Jimenez, J. C., Chen, B. & Hen, R. 2018. Hippocampal Neurogenesis Confers Stress Resilience by Inhibiting the Ventral Dentate Gyrus. *Nature,* **559,** 98-102.

Appel-Dingemanse, S., Rawls, J., Heggland, J., Campestrini, J. & Séchaud, R. 2000. Similar Pharmacokinetics of Tegaserod (Htf 919) in Patients with Constipation- and Diarrhea-Predominant Irritable Bowel Syndrome. *Gastroenterology,* **118,** A1160.

Arango, V., Underwood, M. D., Boldrini, M., Tamir, H., Kassir, S. A., Hsiung, S.-c., Chen, J. J. X. & Mann, J. J. 2001. Serotonin 1a Receptors, Serotonin Transporter Binding and Serotonin Transporter Mrna Expression in the Brainstem of Depressed Suicide Victims. *Neuropsychopharmacology,* **25,** 892-903.

Aronoff, S. L., Berkowitz, K., Shreiner, B. & Want, L. 2004. Glucose Metabolism and Regulation: Beyond Insulin and Glucagon. *Diabetes Spectrum,* **17,** 183.

Au - Liang, H., Au - Schofield, E. & Au - Paxinos, G. 2016. Imaging Serotonergic Fibers in the Mouse Spinal Cord Using the Clarity/Cubic Technique. *JoVE***,** e53673.

Au - Zhu, M., Au - Zhang, D., Au - Peng, S., Au - Liu, N., Au - Wu, J., Au - Kuang, H. & Au - Liu, T. 2019. Preparation of Acute Spinal Cord Slices for Whole-Cell Patch-Clamp Recording in Substantia Gelatinosa Neurons. *JoVE***,** e58479.

Balu, D. T., Hoshaw, B. A., Malberg, J. E., Rosenzweig-Lipson, S., Schechter, L. E. & Lucki, I. 2008. Differential Regulation of Central Bdnf Protein Levels by Antidepressant and Non-Antidepressant Drug Treatments. *Brain Research,* **1211,** 37-43.

Banasr, M., Hery, M., Printemps, R. & Daszuta, A. 2004. Serotonin-Induced Increases in Adult Cell Proliferation and Neurogenesis Are Mediated through Different and Common 5-Ht Receptor Subtypes in the Dentate Gyrus and the Subventricular Zone. *Neuropsychopharmacology,* **29,** 450-460.

Barnabé-Heider, F., Göritz, C., Sabelström, H., Takebayashi, H., Pfrieger, F. W., Meletis, K. & Frisén, J. 2010. Origin of New Glial Cells in Intact and Injured Adult Spinal Cord. *Cell Stem Cell,* **7,** 470-482.

Barreiro-Iglesias, A., Mysiak, Karolina S., Scott, Angela L., Reimer, Michell M., Yang, Y., Becker, Catherina G. & Becker, T. 2015. Serotonin Promotes Development and Regeneration of Spinal Motor Neurons in Zebrafish. *Cell reports,* **13,** 924-932.

Bauer, S., Hay, M., Amilhon, B., Jean, A. & Moyse, E. 2005. In Vivo Neurogenesis in the Dorsal Vagal Complex of the Adult Rat Brainstem. *Neuroscience,* **130,** 75-90.

Beattie, D. T., Smith, J. A. M., Marquess, D., Vickery, R. G., Armstrong, S. R., Pulido-Rios, T., McCullough, J. L., Sandlund, C., Richardson, C., Mai, N. & Humphrey, P. P. A.

2004. The 5-Ht4 Receptor Agonist, Tegaserod, Is a Potent 5-Ht2b Receptor Antagonist in Vitro and in Vivo. *British journal of pharmacology,* **143,** 549-560.

Berg, D. A., Belnoue, L., Song, H. & Simon, A. 2013. Neurotransmitter-Mediated Control of Neurogenesis in the Adult Vertebrate Brain. *Development,* **140,** 2548-2561.

Bernier, P. J., Bedard, A., Vinet, J., Levesque, M. & Parent, A. 2002. Newly Generated Neurons in the Amygdala and Adjoining Cortex of Adult Primates. *Proc Natl Acad Sci U S A,* **99,** 11464-9.

Biagetti, B. & Corcoy, R. 2013. Hypoglycemia Associated with Fluoxetine Treatment in a Patient with Type 1 Diabetes. *World journal of clinical cases,* **1,** 169-171.

Bifari, F., Berton, V., Pino, A., Kusalo, M., Malpeli, G., Di Chio, M., Bersan, E., Amato, E., Scarpa, A., Krampera, M., Fumagalli, G. & Decimo, I. 2015. Meninges Harbor Cells Expressing Neural Precursor Markers During Development and Adulthood. *Frontiers in Cellular Neuroscience* [Online], **9**. Available: http://europepmc.org/abstract/MED/26483637 [Accessed 2015].

Binder, M. D., Hirokawa, N. & Windhorst, U. 2009. Dorsal Vagal Complex (Dvc). *In:* Binder, M. D., Hirokawa, N. & Windhorst, U. (eds.) *Encyclopedia of Neuroscience.* Berlin, Heidelberg: Springer Berlin Heidelberg.

Birbrair, A., Zhang, T., Files, D. C., Mannava, S., Smith, T., Wang, Z.-M., Messi, M. L., Mintz, A. & Delbono, O. 2014. Type-1 Pericytes Accumulate after Tissue Injury and Produce Collagen in an Organ-Dependent Manner. *Stem cell research & therapy,* **5,** 122-122.

Birbrair, A., Zhang, T., Wang, Z.-M., Messi, M. L., Mintz, A. & Delbono, O. 2013. Type-1 Pericytes Participate in Fibrous Tissue Deposition in Aged Skeletal Muscle. *American Journal of Physiology-Cell Physiology,* **305,** C1098-C1113.

Bonfanti, L. & Seki, T. 2021. The Psa-Ncam-Positive "Immature" Neurons: An Old Discovery Providing New Vistas on Brain Structural Plasticity. *Cells,* **10,** 2542.

Borroto-Escuela, D. O., Romero-Fernandez, W., Narvaez, M., Oflijan, J., Agnati, L. F. & Fuxe, K. 2014. Hallucinogenic 5-Ht2ar Agonists Lsd and Doi Enhance Dopamine D2r Protomer Recognition and Signaling of D2-5-Ht2a Heteroreceptor Complexes. *Biochem Biophys Res Commun,* **443,** 278-84.

Bowker, R. M., Westlund, K. N. & Coulter, J. D. 1981. Origins of Serotonergic Projections to the Spinal Cord in Rat: An Immunocytochemical-Retrograde Transport Study. *Brain Research,* **226,** 187-199.

Brandt, M. D., Jessberger, S., Steiner, B., Kronenberg, G., Reuter, K., Bick-Sander, A., Behrens, W. v. d. & Kempermann, G. 2003. Transient Calretinin Expression Defines

Early Postmitotic Step of Neuronal Differentiation in Adult Hippocampal Neurogenesis of Mice. *Molecular and Cellular Neuroscience,* **24,** 603-613.

Buck, S. B., Bradford, J., Gee, K. R., Agnew, B. J., Clarke, S. T. & Salic, A. 2008. Detection of S-Phase Cell Cycle Progression Using 5-Ethynyl-2'-Deoxyuridine Incorporation with Click Chemistry, an Alternative to Using 5-Bromo-2'-Deoxyuridine Antibodies. *Biotechniques,* **44,** 927-9.

Bushman, J., Mishra, B., Ezra, M., Gul, S., Schulze, C., Chaudhury, S., Ripoll, D., Wallqvist, A., Kohn, J., Schachner, M. & Loers, G. 2014. Tegaserod Mimics the Neurostimulatory Glycan Polysialic Acid and Promotes Nervous System Repair. *Neuropharmacology,* **79,** 456-466.

Butler-Ryan, R. & Wood, I. C. 2021. Efficient Infection of Organotypic Hippocampal Slice Cultures with Adenovirus Carrying the Transgene Rest/Nrsf. *Journal of Neuroscience Methods,* **356,** 109147.

Cadena-Herrera, D., Esparza-De Lara, J. E., Ramírez-Ibañez, N. D., López-Morales, C. A., Pérez, N. O., Flores-Ortiz, L. F. & Medina-Rivero, E. 2015. Validation of Three Viable-Cell Counting Methods: Manual, Semi-Automated, and Automated. *Biotechnology Reports,* **7,** 9-16.

Cameron, H. A. & Gould, E. 1994. Adult Neurogenesis Is Regulated by Adrenal Steroids in the Dentate Gyrus. *Neuroscience,* **61,** 203-9.

Cameron, H. A., Hazel, T. G. & McKay, R. D. 1998. Regulation of Neurogenesis by Growth Factors and Neurotransmitters. *Journal of neurobiology,* **36,** 287-306.

Cappella, P., Gasparri, F., Pulici, M. & Moll, J. 2008. Cell Proliferation Method: Click Chemistry Based on Brdu Coupling for Multiplex Antibody Staining. *Curr Protoc Cytom,* **Chapter 7,** Unit7.34.

Cawsey, T., Duflou, J., Weickert, C. S. & Gorrie, C. A. 2015. Nestin-Positive Ependymal Cells Are Increased in the Human Spinal Cord after Traumatic Central Nervous System Injury. *J Neurotrauma,* **32,** 1393-402.

Charlton, S. J. 2009. Agonist Efficacy and Receptor Desensitization: From Partial Truths to a Fuller Picture. *British journal of pharmacology,* **158,** 165-168.

Charnay, Y. & Léger, L. 2010. Brain Serotonergic Circuitries. *Dialogues in clinical neuroscience,* **12,** 471-487.

Charrier, C., Coronas, V., Fombonne, J., Roger, M., Jean, A., Krantic, S. & Moyse, E. 2006. Characterization of Neural Stem Cells in the Dorsal Vagal Complex of Adult Rat by in Vivo Proliferation Labeling and in Vitro Neurosphere Assay. *Neuroscience,* **138,** 5-16.

Chase, T. N. & Murphy, D. L. 1973. Serotonin and Central Nervous System Function. *Annu Rev Pharmacol,* **13,** 181-97.

Chen, X., Cho, D.-B. & Yang, P.-C. 2010. Double Staining Immunohistochemistry. *North American journal of medical sciences,* **2,** 241.

Clawges, H. M., Depree, K. M., Parker, E. M. & Graber, S. G. 1997. Human 5-Ht1 Receptor Subtypes Exhibit Distinct G Protein Coupling Behaviors in Membranes from Sf9 Cells. *Biochemistry,* **36,** 12930-12938.

Cole, P. & Rabasseda, X. 2004. Tegaserod: A Serotonin 5-Ht4 Receptor Agonist for Treatment of Constipation-Predominant Irritable Bowel Syndrome. *Drugs of today (Barcelona, Spain : 1998),* **40,** 1013-1030.

Corns, L. F., Atkinson, L., Daniel, J., Edwards, I. J., New, L., Deuchars, J. & Deuchars, S. A. 2015. Cholinergic Enhancement of Cell Proliferation in the Postnatal Neurogenic Niche of the Mammalian Spinal Cord. *STEM CELLS,* **33,** 2864-2876.

Croul, S., Radzievsky, A., Sverstiuk, A. & Murray, M. 1998. Nk1, Nmda, 5ht1a, and 5ht2 Receptor Binding Sites in the Rat Lumbar Spinal Cord: Modulation Following Sciatic Nerve Crush. *Experimental Neurology,* **154,** 66-79.

Curtis, J. T., Anderson, M. B. & Curtis, K. S. 2013. Regional Differences in Serotonin Content in the Nucleus of the Solitary Tract of Male Rats after Hypovolemia Produced by Polyethylene Glycol. *The Journal of Physiological Sciences,* **63,** 39-46.

Czéh, B., Müller-Keuker, J. I. H., Rygula, R., Abumaria, N., Hiemke, C., Domenici, E. & Fuchs, E. 2007. Chronic Social Stress Inhibits Cell Proliferation in the Adult Medial Prefrontal Cortex: Hemispheric Asymmetry and Reversal by Fluoxetine Treatment. *Neuropsychopharmacology,* **32,** 1490-1503.

D.Binder, M. 2009. Area Postrema (Ap). *In:* Binder, M. D., Hirokawa, N. & Windhorst, U. (eds.) *Encyclopedia of Neuroscience.* Berlin, Heidelberg: Springer Berlin Heidelberg.

de Graaf, I. A., de Kanter, R., de Jager, M. H., Camacho, R., Langenkamp, E., van de Kerkhof, E. G. & Groothuis, G. M. 2006. Empirical Validation of a Rat in Vitro Organ Slice Model as a Tool for in Vivo Clearance Prediction. *Drug Metab Dispos,* **34,** 591-9.

De Maeyer, J. H., Lefebvre, R. A. & Schuurkes, J. A. 2008. 5-Ht4 Receptor Agonists: Similar but Not the Same. *Neurogastroenterol Motil,* **20,** 99-112.

Del Rio, D., Morales, L., Ruiz-Gayo, M. & Del Olmo, N. 2016. Effect of High-Fat Diets on Mood and Learning Performance in Adolescent Mice. *Behavioural Brain Research,* **311,** 167-172.

DePuy, S. D., Kanbar, R., Coates, M. B., Stornetta, R. L. & Guyenet, P. G. J. J. o. N. 2011. Control of Breathing by Raphe Obscurus Serotonergic Neurons in Mice. **31,** 1981-1990.

Deuchars, S. A. & Lall, V. K. 2015. Sympathetic Preganglionic Neurons: Properties and Inputs. *Comprehensive Physiology.* John Wiley & Sons, Inc.

Dincheva, I., Yang, J., Li, A., Marinic, T., Freilingsdorf, H., Huang, C., Casey, B. J., Hempstead, B., Glatt, C. E., Lee, F. S., Bath, K. G. & Jing, D. 2017. Effect of Early-Life Fluoxetine on Anxiety-Like Behaviors in Bdnf Val66met Mice. *The American journal of psychiatry,* **174,** 1203-1213.

Doly, S., Fischer, J., Brisorgueil, M.-J., Vergé, D. & Conrath, M. 2005. Pre- and Postsynaptic Localization of the 5-Ht7 Receptor in Rat Dorsal Spinal Cord: Immunocytochemical Evidence. *The Journal of Comparative Neurology,* **490,** 256-269.

Doly, S., Fischer, J., Brisorgueil, M. J., Vergé, D. & Conrath, M. 2004a. 5-Ht5a Receptor Localization in the Rat Spinal Cord Suggests a Role in Nociception and Control of Pelvic Floor Musculature. *Journal of Comparative Neurology,* **476,** 316-329.

Doly, S., Madeira, A., Fischer, J., Brisorgueil, M.-J., Daval, G., Bernard, R., Vergé, D. & Conrath, M. 2004b. The 5-Ht2a Receptor Is Widely Distributed in the Rat Spinal Cord and Mainly Localized at the Plasma Membrane of Postsynaptic Neurons. *The Journal of Comparative Neurology,* **472,** 496-511.

Duraiyan, J., Govindarajan, R., Kaliyappan, K. & Palanisamy, M. 2012. Applications of Immunohistochemistry. *Journal of pharmacy & bioallied sciences,* **4,** S307.

Eriksson, P. 2003. Neurogenesis and Its Implications for Regeneration in the Adult Brain. *Journal of rehabilitation medicine,* **35,** 17-19.

Eriksson, P. S., Perfilieva, E., Bjork-Eriksson, T., Alborn, A.-M., Nordborg, C., Peterson, D. A. & Gage, F. H. 1998. Neurogenesis in the Adult Human Hippocampus. *Nat Med,* **4,** 1313-1317.

Evans, B. W., Clark, W. K., Moore, D. J. & Whorwell, P. J. 2004. Tegaserod for the Treatment of Irritable Bowel Syndrome. *Cochrane Database of Systematic Reviews*.

Faillace, M. P., Zwiller, J. & Bernabeu, R. O. 2015. Effects of Combined Nicotine and Fluoxetine Treatment on Adult Hippocampal Neurogenesis and Conditioned Place Preference. *Neuroscience,* **300,** 104-115.

Festing, M. F. & Altman, D. G. 2002. Guidelines for the Design and Statistical Analysis of Experiments Using Laboratory Animals. *Ilar j,* **43,** 244-58.

Filippi, B. M., Abraham, M. A., Silva, P. N., Rasti, M., LaPierre, M. P., Bauer, P. V., Rocheleau, J. V. & Lam, T. K. T. 2017. Dynamin-Related Protein 1-Dependent Mitochondrial Fission Changes in the Dorsal Vagal Complex Regulate Insulin Action. *Cell Rep,* **18,** 2301-2309.

Foley, A. G., Hirst, W. D., Gallagher, H. C., Barry, C., Hagan, J. J., Upton, N., Walsh, F. S., Hunter, A. J. & Regan, C. M. 2008. The Selective 5-Ht6 Receptor Antagonists Sb-271046 and Sb-399885 Potentiate Ncam Psa Immunolabeling of Dentate Granule Cells, but Not Neurogenesis, in the Hippocampal Formation of Mature Wistar Rats. *Neuropharmacology,* **54,** 1166-1174.

Fonseca, F. V., Mecawi, A. S., Araujo, I. G., Almeida-Pereira, G., Magalhaes-Nunes, A. P., Badaue-Passos, D., Jr. & Reis, L. C. 2009. Role of the 5-Ht(1a) Somatodendritic Autoreceptor in the Dorsal Raphe Nucleus on Salt Satiety Signaling in Rats. *Exp Neurol,* **217,** 353-60.

Fonseca, M. I., Ni, Y. G., Dunning, D. D. & Miledi, R. 2001. Distribution of Serotonin 2a, 2c and 3 Receptor Mrna in Spinal Cord and Medulla Oblongata. *Molecular Brain Research,* **89,** 11-19.

Fuxe, K., Borroto-Escuela, D. O., Romero-Fernandez, W., Zhang, W. B. & Agnati, L. F. 2013. Volume Transmission and Its Different Forms in the Central Nervous System. *Chin J Integr Med,* **19,** 323-9.

Gafoor, R., Booth, H. P. & Gulliford, M. C. 2018. Antidepressant Utilisation and Incidence of Weight Gain During 10 Years' Follow-Up: Population Based Cohort Study. **361,** k1951.

Gage, F. H., Coates, P. W., Palmer, T. D., Kuhn, H. G., Fisher, L. J., Suhonen, J. O., Peterson, D. A., Suhr, S. T. & Ray, J. 1995. Survival and Differentiation of Adult Neuronal Progenitor Cells Transplanted to the Adult Brain. *Proceedings of the National Academy of Sciences,* **92,** 11879-11883.

Gaidica, M. 2015. *Mouse and Rat Brain Atlas: An Interactive Online Tool* [Online]. Available: http://gaidi.ca/weblog/mouse-and-rat-brain-atlas-an-interactive-online-tool [Accessed 2017].

García-González, D., Khodosevich, K., Watanabe, Y., Rollenhagen, A., Lübke, J. H. R. & Monyer, H. 2017. Serotonergic Projections Govern Postnatal Neuroblast Migration. *Neuron,* **94,** 534-549.e9.

Garcia-Ovejero, D., Arevalo-Martin, A., Paniagua-Torija, B., Florensa-Vila, J., Ferrer, I., Grassner, L. & Molina-Holgado, E. 2015. The Ependymal Region of the Adult Human Spinal Cord Differs from Other Species and Shows Ependymoma-Like Features. *Brain*.

Geis, G. S. & Wurster, R. D. J. C. r. 1980. Cardiac Responses During Stimulation of the Dorsal Motor Nucleus and Nucleus Ambiguus in the Cat. **46,** 606-611.

Gérard, C., Martres, M.-P., Lefèvre, K., Miquel, M.-C., Vergé, D., Lanfumey, L., Doucet, E., Hamon, M. & El Mestikawy, S. 1997. Immuno-Localization of Serotonin 5-Ht6 Receptor-Like Material in the Rat Central Nervous System. *Brain Research,* **746,** 207-219.

Gomez, F. & Garcia-Garcia, L. 2017. Anxiogenic-Like Effects of Fluoxetine Render Adult Male Rats Vulnerable to the Effects of a Novel Stress. *Pharmacol Biochem Behav,* **153,** 32-44.

Gomez, R., Huber, J., Lhullier, F. & Barros, H. M. T. 2001a. Plasma Insulin Levels Are Increased by Sertraline in Rats under Oral Glucose Overload %J Brazilian Journal of Medical and Biological Research. **34,** 1569-1572.

Gomez, R., Huber, J., Tombini, G. & Barros, H. M. 2001b. Acute Effect of Different Antidepressants on Glycemia in Diabetic and Non-Diabetic Rats. *Braz J Med Biol Res,* **34,** 57-64.

González-González, R., Molina-Frechero, N., Carreón-Burciaga, R. G., López-Verdín, S., Robles-Bonilla, C., Pereira-Prado, V. & Bologna-Molina, R. J. A. C. P. 2016. Comparison between Manual and Automated Methods for Ki-67 Immunoexpression Quantification in Ameloblastomas. **2016**.

Goto, K., Kawahara, I., Inada, H., Misawa, H., Kuniyasu, H., Nabekura, J. & Takaki, M. 2016. Activation of 5-Ht4 Receptors Facilitates Neurogenesis from Transplanted Neural Stem Cells in the Anastomotic Ileum. *The Journal of Physiological Sciences,* **66,** 67-76.

Gould, E., Reeves, A. J., Fallah, M., Tanapat, P., Gross, C. G. & Fuchs, E. 1999. Hippocampal Neurogenesis in Adult Old World Primates. *Proceedings of the National Academy of Sciences,* **96,** 5263-5267.

Gould, E., Vail, N., Wagers, M. & Gross, C. G. 2001. Adult-Generated Hippocampal and Neocortical Neurons in Macaques Have a Transient Existence. *Proceedings of the National Academy of Sciences,* **98,** 10910-10917.

Graaf, I. A. M. d., Groothuis, G. M. M. & Olinga, P. 2007. Precision-Cut Tissue Slices as a Tool to Predict Metabolism of Novel Drugs. *Expert Opinion on Drug Metabolism & Toxicology,* **3,** 879-898.

Grabiec, M., Turlejski, K. & Djavadian, R. L. 2009. The Partial 5-Ht1a Receptor Agonist Buspirone Enhances Neurogenesis in the Opossum (Monodelphis Domestica). *European Neuropsychopharmacology,* **19,** 431-439.

Green, A. J., Gelfand, J. M., Cree, B. A., Bevan, C., Boscardin, W. J., Mei, F., Inman, J., Arnow, S., Devereux, M., Abounasr, A., Nobuta, H., Zhu, A., Friessen, M., Gerona, R., von Büdingen, H. C., Henry, R. G., Hauser, S. L. & Chan, J. R. 2017. Clemastine Fumarate as a Remyelinating Therapy for Multiple Sclerosis (Rebuild): A Randomised, Controlled, Double-Blind, Crossover Trial. *The Lancet,* **390,** 2481-2489.

Grider, J. R. 2006. Desensitization of the Peristaltic Reflex Induced by Mucosal Stimulation with the Selective 5-Ht4 Agonist Tegaserod. *Am J Physiol Gastrointest Liver Physiol,* **290,** G319-27.

Gustafson, E. L., Durkin, M. M., Bard, J. A., Zgombick, J. & Branchek, T. A. 1996. A Receptor Autoradiographic and in Situ Hybridization Analysis of the Distribution of the 5-Ht7 Receptor in Rat Brain. *British Journal of Pharmacology,* **117,** 657-666.

Hama, H., Hioki, H., Namiki, K., Hoshida, T., Kurokawa, H., Ishidate, F., Kaneko, T., Akagi, T., Saito, T., Saido, T. & Miyawaki, A. 2015. Scales: An Optical Clearing Palette for Biological Imaging. *Nat Neurosci,* **18,** 1518-29.

Hamilton, L. K., Truong, M. K. V., Bednarczyk, M. R., Aumont, A. & Fernandes, K. J. L. 2009. Cellular Organization of the Central Canal Ependymal Zone, a Niche of Latent Neural Stem Cells in the Adult Mammalian Spinal Cord. *Neuroscience,* **164,** 1044-1056.

Hardy, R. J. 1998. Qki Expression Is Regulated During Neuron-Glial Cell Fate Decisions. *Journal of Neuroscience Research,* **54,** 46-57.

Hedlund, P. B., Kelly, L., Mazur, C., Lovenberg, T., Sutcliffe, J. G. & Bonaventure, P. 2004. 8-Oh-Dpat Acts on Both 5-Ht1a and 5-Ht7 Receptors to Induce Hypothermia in Rodents. *Eur J Pharmacol,* **487,** 125-32.

Huang, G. J. & Herbert, J. 2005. The Role of 5-Ht1a Receptors in the Proliferation and Survival of Progenitor Cells in the Dentate Gyrus of the Adult Hippocampus and Their Regulation by Corticoids. *Neuroscience,* **135**.

Imoto, Y., Kira, T., Sukeno, M., Nishitani, N., Nagayasu, K., Nakagawa, T., Kaneko, S., Kobayashi, K. & Segi-Nishida, E. 2015. Role of the 5-Ht4 Receptor in Chronic Fluoxetine Treatment-Induced Neurogenic Activity and Granule Cell Dematuration in the Dentate Gyrus. *Molecular Brain,* **8,** 1-12.

Jackson-Guilford, J., Leander, J. D. & Nisenbaum, L. K. 2000. The Effect of Streptozotocin-Induced Diabetes on Cell Proliferation in the Rat Dentate Gyrus. *Neuroscience Letters,* **293,** 91-94.

Jahanshahi, A., Temel, Y., Lim, L. W., Hoogland, G. & Steinbusch, H. W. 2011. Close Communication between the Subependymal Serotonergic Plexus and the Neurogenic Subventricular Zone. *J Chem Neuroanat,* **42,** 297-303.

Jang, M.-H., Shin, M.-C., Jung, S.-B., Lee, T.-H., Bahn, G.-H., Kwon, Y. K., Kim, E.-H. & Kim, C.-J. 2002. Alcohol and Nicotine Reduce Cell Proliferation and Enhance Apoptosis in Dentate Gyrus. **13,** 1509-1513.

Johansson, C. B., Momma, S., Clarke, D. L., Risling, M., Lendahl, U. & Frisén, J. 1999. Identification of a Neural Stem Cell in the Adult Mammalian Central Nervous System. *Cell,* **96,** 25-34.

Joshi, R. S. & Panicker, M. M. 2018. Identifying the in Vivo Cellular Correlates of Antipsychotic Drugs. *eNeuro,* **5**.

Joynt, R. 2015. *Brainstem* [Online]. Encyclopaedia Britannica, inc. Available: https://www.britannica.com/science/brainstem [Accessed August 4 2019].

Karmakar, S. & Lal, G. 2021. Role of Serotonin Receptor Signaling in Cancer Cells and Anti-Tumor Immunity. *Theranostics,* **11,** 5296-5312.

Katayama, K., Morio, Y., Haga, K. & Fukuda, T. 1995. Cisapride, a Gastroprokinetic Agent, Binds to 5-Ht4 Receptors. *Nihon yakurigaku zasshi. Folia pharmacologica Japonica,* **105,** 461-468.

Kaufhold, A. E., Hirschberger, J., Reese, S., Foerster, G. & Hein, J. 2018. A Comparison of Manual Counting of Rabbit Reticulocytes with Advia 2120i Analyzer Counting. *J Vet Diagn Invest,* **30,** 337-341.

Kawamura, T., Chen, J., Takahashi, T., Ichitani, Y. & Nakahara, D. 2006. Prenatal Stress Suppresses Cell Proliferation in the Early Developing Brain. *Neuroreport,* **17,** 1515-8.

Keller, N., Dhein, S., Neumann, J. & Gergs, U. 2018. Cardiovascular Effects of Cisapride and Prucalopride on Human 5-Ht(4) Receptors in Transgenic Mice. *Naunyn Schmiedebergs Arch Pharmacol,* **391,** 975-985.

Kempermann, G., Song, H. & Gage, F. H. 2015. Neurogenesis in the Adult Hippocampus. *Cold Spring Harbor perspectives in biology,* **7,** a018812.

Kim, M., Bae, S. & Lim, K.-M. 2013. Impact of High Fat Diet-Induced Obesity on the Plasma Levels of Monoamine Neurotransmitters in C57bl/6 Mice. *Biomolecules & therapeutics,* **21,** 476-480.

Kim, T.-W., Choi, H.-H. & Chung, Y.-R. 2016. Treadmill Exercise Alleviates Impairment of Cognitive Function by Enhancing Hippocampal Neuroplasticity in the High-Fat Diet-Induced Obese Mice. *Journal of exercise rehabilitation,* **12,** 156-162.

Kinsey, A. M., Wainwright, A., Heavens, R., Sirinathsinghji, D. J. S. & Oliver, K. R. 2001. Distribution of 5-Ht5a, 5-Ht5b, 5-Ht6 and 5-Ht7 Receptor Mrnas in the Rat Brain. *Molecular Brain Research,* **88,** 194-198.

Klein, C., Jonas, W., Iggena, D., Empl, L., Rivalan, M., Wiedmer, P., Spranger, J., Hellweg, R., Winter, Y. & Steiner, B. 2016. Exercise Prevents High-Fat Diet-Induced

Impairment of Flexible Memory Expression in the Water Maze and Modulates Adult Hippocampal Neurogenesis in Mice. *Neurobiology of Learning and Memory,* **131,** 26-35.

Klempin, F., Babu, H., De Pietri Tonel, D., Alarcon, E., Fabel, K. & Kempermann, G. 2010. Oppositional Effects of Serotonin Receptors 5-Ht1a, 2, and 2c in the Regulation of Adult Hippocampal Neurogenesis. *Frontiers in molecular neuroscience,* **3,** 14.

Klomp, A., Václavů, L., Meerhoff, G. F., Reneman, L. & Lucassen, P. J. 2015. Correction: Effects of Chronic Fluoxetine Treatment on Neurogenesis and Tryptophan Hydroxylase Expression in Adolescent and Adult Rats. *PLoS One,* **10,** e0135876.

Kolb, H. C., Finn, M. G. & Sharpless, K. B. 2001. Click Chemistry: Diverse Chemical Function from a Few Good Reactions. *Angew Chem Int Ed Engl,* **40,** 2004-2021.

Kondo, M., Nakamura, Y., Ishida, Y. & Shimada, S. 2015. The 5-Ht3 Receptor Is Essential for Exercise-Induced Hippocampal Neurogenesis and Antidepressant Effects. *Mol Psychiatry,* **20,** 1428-37.

Kornack, D. R. & Rakic, P. 1999. Continuation of Neurogenesis in the Hippocampus of the Adult Macaque Monkey. *Proc Natl Acad Sci U S A,* **96,** 5768-73.

L. Fisher, R., Judith, U., Paul, N. & Klaus, B. 2001. Histological and Biochemical Evaluation of Precision-Cut Liver Slices. *Toxicology Methods,* **11,** 59-79.

Labban, R. S. M., Alfawaz, H., Almnaizel, A. T., Hassan, W. M., Bhat, R. S., Moubayed, N. M. S., Bjørklund, G. & El-Ansary, A. 2020. High-Fat Diet-Induced Obesity and Impairment of Brain Neurotransmitter Pool. *Translational Neuroscience,* **11,** 147-160.

Lacroix, S., Hamilton, L. K., Vaugeois, A., Beaudoin, S., Breault-Dugas, C., Pineau, I., Levesque, S. A., Gregoire, C.-A. & Fernandes, K. J. J. P. o. 2014. Central Canal Ependymal Cells Proliferate Extensively in Response to Traumatic Spinal Cord Injury but Not Demyelinating Lesions. *PLOS ONE,* **9,** e85916.

Landrum Michalets, E. & Williams, C. R. 2000. Drug Interactions with Cisapride. *Clinical Pharmacokinetics,* **39,** 49-75.

Langlet, F., Mullier, A., Bouret, S. G., Prevot, V. & Dehouck, B. 2013. Tanycyte-Like Cells Form a Blood–Cerebrospinal Fluid Barrier in the Circumventricular Organs of the Mouse Brain. **521,** 3389-3405.

Lendahl, U., Zimmerman, L. B. & McKay, R. D. 1990. Cns Stem Cells Express a New Class of Intermediate Filament Protein. *Cell,* **60,** 585-95.

Levy, M. J. F., Boulle, F., Emerit, M. B., Poilbout, C., Steinbusch, H. W. M., Van den Hove, D. L. A., Kenis, G. & Lanfumey, L. 2019. 5-Htt Independent Effects of Fluoxetine on Neuroplasticity. *Sci Rep,* **9,** 6311.

Licht, T., Rothe, G., Kreisel, T., Wolf, B., Benny, O., Rooney, A. G., ffrench-Constant, C., Enikolopov, G. & Keshet, E. 2016. Vegf Preconditioning Leads to Stem Cell Remodeling and Attenuates Age-Related Decay of Adult Hippocampal Neurogenesis. *Proceedings of the National Academy of Sciences,* **113,** E7828-E7836.

Lindqvist, A., Mohapel, P., Bouter, B., Frielingsdorf, H., Pizzo, D., Brundin, P. & Erlanson-Albertsson, C. 2006. High-Fat Diet Impairs Hippocampal Neurogenesis in Male Rats. *European Journal of Neurology,* **13,** 1385-1388.

Liu, M.-T., Kuan, Y.-H., Wang, J., Hen, R. & Gershon, M. D. 2009. 5-Ht4 Receptor-Mediated Neuroprotection and Neurogenesis in the Enteric Nervous System of Adult Mice. *The Journal of Neuroscience,* **29,** 9683-9699.

Liu, P. Z. & Nusslock, R. 2018. Exercise-Mediated Neurogenesis in the Hippocampus Via Bdnf. *Front Neurosci,* **12,** 52.

Liu, Q. & Wong-Riley, M. T. T. 2010. Postnatal Changes in the Expressions of Serotonin 1a, 1b, and 2a Receptors in Ten Brain Stem Nuclei of the Rat: Implication for a Sensitive Period. *Neuroscience,* **165,** 61-78.

Liu, W., Stachura, P., Xu, H. C., Umesh Ganesh, N., Cox, F., Wang, R., Lang, K. S., Gopalakrishnan, J., Häussinger, D., Homey, B., Lang, P. A. & Pandyra, A. A. 2020. Repurposing the Serotonin Agonist Tegaserod as an Anticancer Agent in Melanoma: Molecular Mechanisms and Clinical Implications. *Journal of Experimental & Clinical Cancer Research,* **39,** 38.

Lledo, P. M., Alonso, M. & Grubb, M. S. 2006. Adult Neurogenesis and Functional Plasticity in Neuronal Circuits. *Nat Rev Neurosci,* **7,** 179-93.

Llorens-Martín, M. 2018. Exercising New Neurons to Vanquish Alzheimer Disease. *Brain Plast,* **4,** 111-126.

Lubetzki, C., Zalc, B., Williams, A., Stadelmann, C. & Stankoff, B. 2020. Remyelination in Multiple Sclerosis: From Basic Science to Clinical Translation. *Lancet Neurol,* **19,** 678-688.

Lucas, G., Rymar, V. V., Du, J., Mnie-Filali, O., Bisgaard, C. & Manta, S. 2007. Serotonin(4) (5-Ht(4)) Receptor Agonists Are Putative Antidepressants with a Rapid Onset of Action. *Neuron,* **55**.

Lundar, T., Due-Tønnessen, B. J., Frič, R., Sundseth, J., Brandal, P. & Due-Tønnessen, P. 2021. Outcome after Treatment of Spinal Ependymoma in Children and Adolescents:

Long-Term Follow-up of a Single Consecutive Institutional Series of 33 Patients Treated over Eight Decades. *World Neurosurg,* **150,** e228-e235.

Lyons, W. E., Mamounas, L. A., Ricaurte, G. A., Coppola, V., Reid, S. W., Bora, S. H., Wihler, C., Koliatsos, V. E. & Tessarollo, L. 1999. Brain-Derived Neurotrophic Factor-Deficient Mice Develop Aggressiveness and Hyperphagia in Conjunction with Brain Serotonergic Abnormalities. *Proceedings of the National Academy of Sciences,* **96,** 15239-15244.

Maheux, P., Ducros, F., Bourque, J., Garon, J. & Chiasson, J. L. 1997. Fluoxetine Improves Insulin Sensitivity in Obese Patients with Non-Insulin-Dependent Diabetes Mellitus Independently of Weight Loss. *Int J Obes Relat Metab Disord,* **21,** 97-102.

Malberg, J. E. & Duman, R. S. 2003. Cell Proliferation in Adult Hippocampus Is Decreased by Inescapable Stress: Reversal by Fluoxetine Treatment. *Neuropsychopharmacology,* **28,** 1562-1571.

Manzke, T., Guenther, U., Ponimaskin, E. G., Haller, M., Dutschmann, M., Schwarzacher, S. & Richter, D. W. 2003. 5-Ht4(a) Receptors Avert Opioid-Induced Breathing Depression without Loss of Analgesia. **301,** 226-229.

Marichal, N., García, G., Radmilovich, M., Trujillo-Cenóz, O. & Russo, R. E. 2009. Enigmatic Central Canal Contacting Cells: Immature Neurons in “Standby Mode”? *The Journal of Neuroscience,* **29,** 10010-10024.

Marwari, S. & Dawe, G. S. 2018. (R)-Fluoxetine Enhances Cognitive Flexibility and Hippocampal Cell Proliferation in Mice. *Journal of Psychopharmacology,* **32,** 441-457.

Matott, M. P. & Kline, D. D. 2016. Activation of 5-Hyrdoxytryptamine 7 Receptors within the Rat Nucleus Tractus Solitarii Modulates Synaptic Properties. *Brain Research,* **1635,** 12-26.

Matsuda, T. & Hisatsune, T. J. J. o. A. s. d. J. 2017. Cholinergic Modification of Neurogenesis and Gliosis Improves the Memory of Aβppswe/Psen1de9 Alzheimer's Disease Model Mice Fed a High-Fat Diet. **56,** 1.

Meletis, K., Barnabé-Heider, F., Carlén, M., Evergren, E., Tomilin, N., Shupliakov, O. & Frisén, J. 2008. Spinal Cord Injury Reveals Multilineage Differentiation of Ependymal Cells. *PLoS Biology,* **6,** e182.

Michelson, D., Amsterdam, J. D., Quitkin, F. M., Reimherr, F. W., Rosenbaum, J. F., Zajecka, J., Sundell, K. L., Kim, Y. & Beasley, C. M. 1999. Changes in Weight During a 1-Year Trial of Fluoxetine. *American Journal of Psychiatry,* **156,** 1170-1176.

Mignone, J. L., Kukekov, V., Chiang, A. S., Steindler, D. & Enikolopov, G. 2004. Neural Stem and Progenitor Cells in Nestin-Gfp Transgenic Mice. *J Comp Neurol,* **469,** 311-24.

Miquel, M.-C., Emerit, M. B., Nosjean, A., Simon, A., Rumajogee, P., Brisorgueil, M.-J., Doucet, E., Hamon, M. & Vergé, D. 2002. Differential Subcellular Localization of the 5-Ht3-as Receptor Subunit in the Rat Central Nervous System. **15,** 449-457.

Miyata, T., Maeda, T. & Lee, J. E. 1999. Neurod Is Required for Differentiation of the Granule Cells in the Cerebellum and Hippocampus. *Genes & development,* **13,** 1647-1652.

Monteiro, B. M., Moreira, F. A., Massensini, A. R., Moraes, M. F. & Pereira, G. S. 2014. Enriched Environment Increases Neurogenesis and Improves Social Memory Persistence in Socially Isolated Adult Mice. *Hippocampus,* **24,** 239-48.

Moraes, J. C., Coope, A., Morari, J., Cintra, D. E., Roman, E. A., Pauli, J. R., Romanatto, T., Carvalheira, J. B., Oliveira, A. L. R., Saad, M. J. & Velloso, L. A. 2009. High-Fat Diet Induces Apoptosis of Hypothalamic Neurons. *PLOS ONE,* **4,** e5045.

Moreno-Fernández, S., Garcés-Rimón, M., Vera, G., Astier, J., Landrier, J. F. & Miguel, M. 2018. High Fat/High Glucose Diet Induces Metabolic Syndrome in an Experimental Rat Model. *Nutrients,* **10,** 1502.

Mori, M., Murata, Y., Matsuo, A., Takemoto, T. & Mine, K. 2014. Chronic Treatment with the 5-Ht1a Receptor Partial Agonist Tandospirone Increases Hippocampal Neurogenesis. *Neurology and Therapy,* **3,** 67-77.

Mothe, A. J., Zahir, T., Santaguida, C., Cook, D. & Tator, C. H. 2011. Neural Stem/Progenitor Cells from the Adult Human Spinal Cord Are Multipotent and Self-Renewing and Differentiate after Transplantation. *PLoS One,* **6,** e27079.

Musumeci, G., Castrogiovanni, P., Castorina, S., Imbesi, R., Szychlinska, M. A., Scuderi, S., Loreto, C. & Giunta, S. 2015. Changes in Serotonin (5-Ht) and Brain-Derived Neurotrophic Factor (Bdfn) Expression in Frontal Cortex and Hippocampus of Aged Rat Treated with High Tryptophan Diet. *Brain Research Bulletin,* **119,** 12-18.

Namiki, J. & Tator, C. H. 1999. Cell Proliferation and Nestin Expression in the Ependyma of the Adult Rat Spinal Cord after Injury. *J Neuropathol Exp Neurol,* **58,** 489-98.

Nedi, T., White, P. J., Coupar, I. M. & Irving, H. R. 2011. Tissue Dependent Differences in G-Protein Coupled Receptor Kinases Associated with 5-Ht4 Receptor Desensitization in the Rat Gastro-Intestinal Tract. *Biochemical Pharmacology,* **81,** 123-133.

Nedi, T., White, P. J., Coupar, I. M. & Irving, H. R. 2018. Effect of the 5-Ht4 Receptor Agonist Tegaserod on the Expression of Grk2 and Grk6 in the Rat Gastrointestinal Tract. *BMC Research Notes,* **11,** 362.

Nelson, D. L. 2004. 5-Ht5 Receptors. *Curr Drug Targets CNS Neurol Disord,* **3,** 53-8.

Neumann, B., Baror, R., Zhao, C., Segel, M., Dietmann, S., Rawji, K. S., Foerster, S., McClain, C. R., Chalut, K., van Wijngaarden, P. & Franklin, R. J. M. 2019. Metformin Restores Cns Remyelination Capacity by Rejuvenating Aged Stem Cells. *Cell Stem Cell,* **25,** 473-485.e8.

Nornes, H. O. & Carry, M. 1978. Neurogenesis in Spinal Cord of Mouse: An Autoradiographic Analysis. *Brain Research,* **159,** 1-16.

Ohira, K. & Miyakawa, T. 2011. Chronic Treatment with Fluoxetine for More Than 6 Weeks Decreases Neurogenesis in the Subventricular Zone of Adult Mice. *Mol Brain,* **4,** 1-12.

Palkovits, M., Brownstein, M. & Saavedra, J. M. 1974. Serotonin Content of the Brain Stem Nuclei in the Rat. *Brain Research,* **80,** 237-249.

Pan, H. C., Shen, Y. Q., Loers, G., Jakovcevski, I. & Schachner, M. 2014. Tegaserod, a Small Compound Mimetic of Polysialic Acid, Promotes Functional Recovery after Spinal Cord Injury in Mice. *Neuroscience,* **277,** 356-366.

Paniagua-Torija, B., Norenberg, M., Arevalo-Martin, A., Carballosa-Gautam, M. M., Campos-Martin, Y., Molina-Holgado, E. & Garcia-Ovejero, D. 2018. Cells in the Adult Human Spinal Cord Ependymal Region Do Not Proliferate after Injury. *The Journal of Pathology,* **246,** 415-421.

Papageorgiou, A. & Denef, C. 2007. Stimulation of Growth Hormone Release by 5-Hydroxytryptamine (5-Ht) in Cultured Rat Anterior Pituitary Cell Aggregates: Evidence for Mediation by 5-Ht2b, 5-Ht7, 5-Ht1b, and Ketanserin-Sensitive Receptors. *Endocrinology,* **148,** 4509-22.

Park, H. R., Park, M., Choi, J., Park, K.-Y., Chung, H. Y. & Lee, J. 2010. A High-Fat Diet Impairs Neurogenesis: Involvement of Lipid Peroxidation and Brain-Derived Neurotrophic Factor. *Neuroscience Letters,* **482,** 235-239.

Pascual-Brazo, J., Castro, E., Díaz, Á., Valdizán, E. M., Pilar-Cuéllar, F., Vidal, R., Treceño, B. & Pazos, Á. 2012. Modulation of Neuroplasticity Pathways and Antidepressant-Like Behavioural Responses Following the Short-Term (3 and 7 Days) Administration of the 5-Ht4 Receptor Agonist Rs67333. *International Journal of Neuropsychopharmacology,* **15,** 631-643.

Pazos, A. & Palacios, J. M. 1985. Quantitative Autoradiographic Mapping of Serotonin Receptors in the Rat Brain. I. Serotonin-1 Receptors. *Brain Research,* **346,** 205-230.

Perrier, J.-F. & Cotel, F. 2015. Serotonergic Modulation of Spinal Motor Control. *Current Opinion in Neurobiology,* **33,** 1-7.

Pineda-Farias, J. B., Barragán-Iglesias, P., Valdivieso-Sánchez, A., Rodríguez-Silverio, J., Flores-Murrieta, F. J., Granados-Soto, V. & Rocha-González, H. I. 2017. Spinal 5-Ht4 and 5-Ht6 Receptors Contribute to the Maintenance of Neuropathic Pain in Rats. *Pharmacological Reports,* **69,** 916-923.

Pithadia, A. B. & Jain, S. M. 2009. 5-Hydroxytryptamine Receptor Subtypes and Their Modulators with Therapeutic Potentials. *Journal of clinical medicine research,* **1,** 72-80.

Pompeiano, M., Palacios, J. M. & Mengod, G. 1994. Distribution of the Serotonin 5-Ht2 Receptor Family Mrnas: Comparison between 5-Ht2a and 5-Ht2c Receptors. *Molecular Brain Research,* **23,** 163-178.

Pontious, A., Kowalczyk, T., Englund, C. & Hevner, R. F. 2008. Role of Intermediate Progenitor Cells in Cerebral Cortex Development. *Developmental Neuroscience,* **30,** 24-32.

Pytliak, M., Vargová, V., Mechírová, V. & Felšöci, M. 2011. Serotonin Receptors - from Molecular Biology to Clinical Applications. *Physiol Res,* **60,** 15-25.

Quartu, M., Serra, M., Boi, M., Ibba, V., Melis, T. & Del Fiacco, M. 2008. Polysialylated-Neural Cell Adhesion Molecule (Psa-Ncam) in the Human Trigeminal Ganglion and Brainstem at Prenatal and Adult Ages. *BMC Neuroscience,* **9,** 108.

Quigley, E. M. M., Wald, A., Fidelholtz, J., Boivin, M., Pecher, E. & Earnest, D. 2006. Safety and Tolerability of Tegaserod in Patients with Chronic Constipation: Pooled Data from Two Phase Iii Studies. *Clinical Gastroenterology and Hepatology,* **4,** 605-613.

Radbruch, A. 2000. Immunofluorescence: Basic Considerations. *Flow Cytometry and Cell Sorting.* Springer.

Radley, J. J. & Jacobs, B. L. 2002. 5-Ht1a Receptor Antagonist Administration Decreases Cell Proliferation in the Dentate Gyrus. *Brain Research,* **955,** 264-267.

Rakic, P. 1985. Limits of Neurogenesis in Primates. *Science,* **227,** 1054-1056.

Rampe, D., Roy, M. L., Dennis, A. & Brown, A. M. 1997. A Mechanism for the Proarrhythmic Effects of Cisapride (Propulsid): High Affinity Blockade of the Human Cardiac Potassium Channel Herg. *FEBS Lett,* **417,** 28-32.

Rao, M. S. & Shetty, A. K. 2004. Efficacy of Doublecortin as a Marker to Analyse the Absolute Number Anddendritic Growth of Newly Generated Neurons in the Adult Dentate Gyrus. *European Journal of Neuroscience,* **19,** 234-246.

Rauscher, F., Robinson, D. & Jens, J. 1998. Improved Maze Learning through Early Music Exposure in Rats. *Neurological Research,* **20,** 427-432.

Ren, K., Ruda, M. & Jacobowitz, D. 1993. Immunohistochemical Localization of Calretinin in the Dorsal Root Ganglion and Spinal Cord of the Rat. *Brain research bulletin,* **31,** 13-22.

Reynolds, G. P., Mason, S. L., Meldrum, A., Keczer, S., Parties, H., Eglen, R. M. & Wong, E. H. F. 1995. 5-Hydroxytryptamine (5-Ht)4 Receptors in Post Mortem Human Brain Tissue: Distribution, Pharmacology and Effects of Neurodegenerative Diseases. *British Journal of Pharmacology,* **114,** 993-998.

Riad, M., Garcia, S., Watkins, K. C., Jodoin, N., Doucet, E., Langlois, X., el Mestikawy, S., Hamon, M. & Descarries, L. 2000. Somatodendritic Localization of 5-Ht1a and Preterminal Axonal Localization of 5-Ht1b Serotonin Receptors in Adult Rat Brain. *J Comp Neurol,* **417**.

Richardson, D. S. & Lichtman, J. W. 2015. Clarifying Tissue Clearing. *Cell,* **162,** 246-257.

Rondé, P., Ansanay, H., Dumuis, A., Miller, R. & Bockaert, J. 1995. Homologous Desensitization of 5-Hydroxytryptamine4 Receptors in Rat Esophagus: Functional and Second Messenger Studies. *Journal of Pharmacology and Experimental Therapeutics,* **272,** 977-983.

Rosenberg, A. B., Roco, C. M., Muscat, R. A., Kuchina, A., Sample, P., Yao, Z., Graybuck, L. T., Peeler, D. J., Mukherjee, S., Chen, W., Pun, S. H., Sellers, D. L., Tasic, B. & Seelig, G. 2018. Single-Cell Profiling of the Developing Mouse Brain and Spinal Cord with Split-Pool Barcoding. *Science (New York, N.Y.),* **360,** 176-182.

Rossi, A., Barraco, A. & Donda, P. 2004. Fluoxetine: A Review on Evidence Based Medicine. *Annals of General Hospital Psychiatry,* **3,** 2.

Rossi, C., Angelucci, A., Costantin, L., Braschi, C., Mazzantini, M., Babbini, F., Fabbri, M. E., Tessarollo, L., Maffei, L., Berardi, N. & Caleo, M. 2006. Brain-Derived Neurotrophic Factor (Bdnf) Is Required for the Enhancement of Hippocampal Neurogenesis Following Environmental Enrichment. *Eur J Neurosci,* **24,** 1850-6.

Rusanescu, G. & Mao, J. 2015. Immature Spinal Cord Neurons Are Dynamic Regulators of Adult Nociceptive Sensitivity. *Journal of cellular and molecular medicine,* **19,** 2352-2364.

Sachs, B. D. & Caron, M. G. 2015. Chronic Fluoxetine Increases Extra-Hippocampal Neurogenesis in Adult Mice. *International Journal of Neuropsychopharmacology,* **18**.

Sadiq, A., Shah, A., Jeschke, M. G., Belo, C., Qasim Hayat, M., Murad, S. & Amini-Nik, S. 2018. The Role of Serotonin During Skin Healing in Post-Thermal Injury. *Int J Mol Sci,* **19**.

Sarkisyan, G. & Hedlund, P. B. 2009. The 5-Ht7 Receptor Is Involved in Allocentric Spatial Memory Information Processing. *Behav Brain Res,* **202,** 26-31.

Sasaki, M., Obata, H., Saito, S. & Goto, F. 2003. Antinociception with Intrathecal Alpha-Methyl-5-Hydroxytryptamine, a 5-Hydroxytryptamine 2a/2c Receptor Agonist, in Two Rat Models of Sustained Pain. *Anesth Analg,* **96,** 1072-1078.

Sawamoto, A., Okuyama, S., Yamamoto, K., Amakura, Y., Yoshimura, M., Nakajima, M. & Furukawa, Y. 2016. 3,5,6,7,8,3',4'-Heptamethoxyflavone, a Citrus Flavonoid, Ameliorates Corticosterone-Induced Depression-Like Behavior and Restores Brain-Derived Neurotrophic Factor Expression, Neurogenesis, and Neuroplasticity in the Hippocampus. *Molecules,* **21,** 541.

Scabia, G., Barone, I., Mainardi, M., Ceccarini, G., Scali, M., Buzzigoli, E., Dattilo, A., Vitti, P., Gastaldelli, A., Santini, F., Pizzorusso, T., Maffei, L. & Maffei, M. 2018. The Antidepressant Fluoxetine Acts on Energy Balance and Leptin Sensitivity Via Bdnf. *Sci Rep,* **8,** 1781.

Seaberg, R. M. & van der Kooy, D. 2002. Adult Rodent Neurogenic Regions: The Ventricular Subependyma Contains Neural Stem Cells, but the Dentate Gyrus Contains Restricted Progenitors. *The Journal of Neuroscience,* **22,** 1784-1793.

Serrats, J., Raurich, A., Vilaró, M. T., Mengod, G. & Cortés, R. 2004. 5-Ht5b Receptor Mrna in the Raphe Nuclei: Coexpression with Serotonin Transporter. *Synapse,* **51,** 102-111.

Smyth, P. G. & Berman, S. A. 2002. Markers of Apoptosis: Methods for Elucidating the Mechanism of Apoptotic Cell Death from the Nervous System. *Biotechniques,* **32,** 648-50, 652, 654 passim.

Sommer, C. 2004. Serotonin in Pain and Analgesia. *Molecular Neurobiology,* **30,** 117-125.

Souza, E. B. D. & Kuyatt, B. L. 1987. Autoradiographic Localization of 3h-Paroxetine-Labeled Serotonin Uptake Sites in Rat Brain. *Synapse,* **1,** 488-496.

Squire, L., Berg, D., Bloom, F. E., du Lac, S., Ghosh, A. & Spitzer, N. C. 2012. *Fundamental Neuroscience*, Academic Press.

Steinbusch, H. W. M. 1981. Distribution of Serotonin-Immunoreactivity in the Central Nervous System of the Rat—Cell Bodies and Terminals. *Neuroscience,* **6,** 557-618.

Steiner, B., Klempin, F., Wang, L., Kott, M., Kettenmann, H. & Kempermann, G. 2006. Type-2 Cells as Link between Glial and Neuronal Lineage in Adult Hippocampal Neurogenesis. *Glia,* **54,** 805-814.

Suwa, B., Bock, N., Preusse, S., Rothenberger, A. & Manzke, T. 2014. Distribution of Serotonin 4(a) Receptors in the Juvenile Rat Brain and Spinal Cord. *Journal of Chemical Neuroanatomy,* **55,** 67-77.

Taber, K. H. & Hurley, R. A. 2014. Volume Transmission in the Brain: Beyond the Synapse. *The Journal of Neuropsychiatry and Clinical Neurosciences,* **26,** iv-4.

Tack, J., Müller-Lissner, S., Bytzer, P., Corinaldesi, R., Chang, L., Viegas, A., Schnekenbuehl, S., Dunger-Baldauf, C. & Rueegg, P. 2005. A Randomised Controlled Trial Assessing the Efficacy and Safety of Repeated Tegaserod Therapy in Women with Irritable Bowel Syndrome with Constipation. *Gut,* **54,** 1707-1713.

Takaki, M., Goto, K. & Kawahara, I. 2014. The 5-Hydroxytryptamine 4 Receptor Agonist-Induced Actions and Enteric Neurogenesis in the Gut. *Journal of neurogastroenterology and motility,* **20,** 17-30.

Takeuchi, Y., Kimura, H., Matsuura, T., Yonezawa, T. & Sano, Y. 1983. Distribution of Serotonergic Neurons in the Central Nervous System: A Peroxidase-Antiperoxidase Study with Anti-Serotonin Antibodies. *Journal of Histochemistry & Cytochemistry,* **31,** 181-185.

Tanaka, K. F., Samuels, B. A. & Hen, R. 2012. Serotonin Receptor Expression Along the Dorsal–Ventral Axis of Mouse Hippocampus. **367,** 2395-2401.

Tauber, S. C., Stadelmann, C., Spreer, A., Brück, W., Nau, R. & Gerber, J. 2005. Increased Expression of Bdnf and Proliferation of Dentate Granule Cells after Bacterial Meningitis. *Journal of Neuropathology & Experimental Neurology,* **64,** 806-815.

Taylor, R. C., Cullen, S. P. & Martin, S. J. 2008. Apoptosis: Controlled Demolition at the Cellular Level. *Nature Reviews Molecular Cell Biology,* **9,** 231-241.

Tecott, L. H., Maricq, A. V. & Julius, D. 1993. Nervous System Distribution of the Serotonin 5-Ht3 Receptor Mrna. **90,** 1430-1434.

Thompson, A. J., Baranzini, S. E., Geurts, J., Hemmer, B. & Ciccarelli, O. 2018. Multiple Sclerosis. *Lancet,* **391,** 1622-1636.

Thompson, A. J. & Lummis, S. C. R. 2006. 5-Ht3 Receptors. *Current pharmaceutical design,* **12,** 3615-3630.

Thor, K. B., Nickolaus, S. & Helke, C. J. 1993. Autoradiographic Localization of 5-Hydroxytryptamine1a, 5-Hydroxytryptamine1b and 5-Hydroxytryptamine1c/2 Binding Sites in the Rat Spinal Cord. *Neuroscience,* **55,** 235-252.

Tong, C. K., Chen, J., Cebrián-Silla, A., Mirzadeh, Z., Obernier, K., Guinto, C. D., Tecott, L. H., García-Verdugo, J. M., Kriegstein, A. & Alvarez-Buylla, A. 2014. Axonal Control of the Adult Neural Stem Cell Niche. *Cell Stem Cell,* **14,** 500-11.

Travagli, R. A. 2009. Nucleus Tractus Solitarii (Nts). *In:* Binder, M. D., Hirokawa, N. & Windhorst, U. (eds.) *Encyclopedia of Neuroscience.* Berlin, Heidelberg: Springer Berlin Heidelberg.

Tung, A., Takase, L., Fornal, C. & Jacobs, B. 2005. Effects of Sleep Deprivation and Recovery Sleep Upon Cell Proliferation in Adult Rat Dentate Gyrus. *Neuroscience,* **134,** 721-3.

Tyce, G. M. 1990. Origin and Metabolism of Serotonin. *Journal of Cardiovascular Pharmacology,* **16,** S1-S7.

van Praag, H., Kempermann, G. & Gage, F. H. 1999. Running Increases Cell Proliferation and Neurogenesis in the Adult Mouse Dentate Gyrus. *Nature Neuroscience,* **2,** 266.

Waeber, C., Sebben, M., Bockaert, J. & Dumuis, A. 1995. Regional Distribution and Ontogeny of 5-Ht4 Binding Sites in Rat Brain. *Behavioural Brain Research,* **73,** 259-262.

Wagstaff, A. J., Frampton, J. E. & Croom, K. F. 2003. Tegaserod. *Drugs,* **63,** 1101-1120.

Wang, D. D. & Bordey, A. 2008. The Astrocyte Odyssey. *Prog Neurobiol,* **86,** 342-67.

Wang, L.-P., Kempermann, G. & Kettenmann, H. 2005. A Subpopulation of Precursor Cells in the Mouse Dentate Gyrus Receives Synaptic Gabaergic Input. *Molecular and Cellular Neuroscience,* **29,** 181-189.

Ward, R. P., Hamblin, M. W., Lachowicz, J. E., Hoffman, B. J., Sibley, D. R. & Dorsa, D. M. 1995. Localization of Serotonin Subtype 6 Receptor Messenger Rna in the Rat Brain by in Situ Hybridization Histochemistry. *Neuroscience,* **64,** 1105-1111.

Weeden, C. S. S., Roberts, J. M., Kamm, A. M. & Kesner, R. P. 2015. The Role of the Ventral Dentate Gyrus in Anxiety-Based Behaviors. *Neurobiology of Learning and Memory,* **118,** 143-149.

Wendeln, A. C., Degenhardt, K., Kaurani, L., Gertig, M., Ulas, T., Jain, G., Wagner, J., Häsler, L. M., Wild, K., Skodras, A., Blank, T., Staszewski, O., Datta, M., Centeno, T. P., Capece, V., Islam, M. R., Kerimoglu, C., Staufenbiel, M., Schultze, J. L., Beyer, M., Prinz, M., Jucker, M., Fischer, A. & Neher, J. J. 2018. Innate Immune Memory in the Brain Shapes Neurological Disease Hallmarks. *Nature,* **556,** 332-338.

Wysowski, D. K., Corken, A., Gallo-Torres, H., Talarico, L. & Rodriguez, E. M. 2001. Postmarketing Reports of Qt Prolongation and Ventricular Arrhythmia in Association with Cisapride and Food and Drug Administration Regulatory Actions11the Views Expressed Are Those of the Authors and Do Not Necessarily Represent Those of, nor Imply Endorsement from, the Food and Drug Administration or the U.S. Government. *The American Journal of Gastroenterology,* **96,** 1698-1703.

Zeidler-Erdely, P. C., Antonini, J. M., Meighan, T. G., Young, S.-H., Eye, T. J., Hammer, M. A. & Erdely, A. 2016. Comparison of Cell Counting Methods in Rodent Pulmonary Toxicity Studies: Automated and Manual Protocols and Considerations for Experimental Design. *Inhalation Toxicology,* **28,** 410-420.

Zeng, C., Pan, F., Jones, L. A., Lim, M. M., Griffin, E. A., Sheline, Y. I., Mintun, M. A., Holtzman, D. M. & Mach, R. H. 2010. Evaluation of 5-Ethynyl-2′-Deoxyuridine Staining as a Sensitive and Reliable Method for Studying Cell Proliferation in the Adult Nervous System. *Brain Research,* **1319,** 21-32.

Zhou, F.-C. & Azmitia, E. C. 1983. Effects of 5,7-Dihydroxytryptamine on Hrp Retrograde Transport from Hippocampus to Midbrain Raphe Nuclei in the Rat. *Brain Research Bulletin,* **10,** 445-451.

Zhou, F. C. & Azmitia, E. C. 1986. Induced Homotypic Sprouting of Serotonergic Fibers in Hippocampus. Ii. An Immunocytochemistry Study. *Brain Research,* **373,** 337-348.

Zhu, Y., Cheng, J., Yin, J., Yang, Y., Guo, J., Zhang, W., Xie, B., Lu, H. & Hao, D. 2020. Effects of Sacral Nerve Electrical Stimulation on 5-Ht and 5-Ht3ar/5-Ht4r Levels in the Colon and Sacral Cord of Acute Spinal Cord Injury Rat Models. *Molecular medicine reports,* **22,** 763-773.